

Cranfield University

Mark Massam

Thermal Characteristics of Grinding Fluids

School of Applied Sciences

Doctor of Philosophy

Cranfield University

School of Applied Sciences

Doctor of Philosophy Thesis

Year 2008

Mark Massam

Thermal Characteristics of Grinding Fluids

Supervisor: Professor D.J. Stephenson
Dr T. Jin

This thesis is submitted in partial fulfilment of the requirements
for the degree of Doctor of Philosophy

© Cranfield University, (2008). All rights reserved. No part of this publication may be reproduced without the written permission of the copyright holder.

TABLE OF CONTENTS

ABSTRACT	i
ACKNOWLEDGEMENTS.....	ii
TABLE OF FIGURES.....	ix
TABLE OF TABLES.....	xv
TABLE OF EQUATIONS.....	xvii

1 Introduction.....	1
1.1 Background.....	1
1.2 Aim.....	3
1.3 Objectives.....	3
1.4 Scope.....	4
1.5 Thesis Structure.....	5

2 Literature Review.....	7
2.1 Introduction.....	7
2.1.1 Historical Background.....	7
2.1.2 High Efficiency Deep Grinding.....	7
2.2 The Role of Cutting Fluids in the Grinding Process.....	10
2.3 Thermal Characteristics of Cutting Fluids.....	11
2.3.1 Cooling.....	12
2.3.1.1 Convection Coefficient.....	13
2.3.1.2 Temperature Measurement.....	16
2.3.1.2.1 PVD Coatings.....	17
2.3.1.2.2 Thermal Imaging Camera.....	18
2.3.1.2.3 Optical Fibre.....	19
2.3.1.2.4 Thermocouples.....	20
2.3.2 Lubrication.....	22
2.3.2.1 Lubrication Testing.....	24

2.3.3 Fluid Misting and Ignition Characteristics	26
2.3.3.1 General Literature on Fluid Ignition.....	26
2.3.3.1.1 Static Electricity.....	28
2.3.3.2 Cutting Fluid Ignition.....	29
2.3.4 Fluid Misting.....	32
2.4 Cutting Fluids.....	33
2.4.1 Introduction.....	33
2.4.2 Neat Oils.....	34
2.4.2.1 Neat Mineral Oils.....	34
2.4.2.2 Vegetable Oils.....	35
2.4.2.3 Organic Ester based Synthetic Neat Oils.....	35
2.4.3 Water Miscible Fluids (Water based Emulsions).....	36
2.4.4 Extreme Pressure (EP) Additives.....	37
2.5 Factors Associated with the Use of Cutting Fluids.....	38
2.5.1 Health and Safety	38
2.5.2 Economic Costs.....	39
2.5.3 Environmental.....	40
2.6 Non Conventional Cooling Media.....	40
2.6.1.1 Cryogenic Cooling.....	41
2.6.1.2 Solid Lubricants.....	41
2.6.1.3 Air / Oil mists.....	42
2.6.1.4 Water.....	42
2.6.1.5 Dry Grinding.....	42
2.7 Cutting Fluid Application.....	43
2.7.1 Coherent Jet Nozzle.....	43
2.7.2 Shoe Nozzles.....	45
2.7.3 Minimum Quantity Lubrication.....	46
2.8 Component and Surface Quality.....	47
2.8.1 Thermal Damage.....	47
2.8.1.1 Grinding Burn.....	47
2.8.2 Residual Stress.....	48

2.8.2.1 Measurement of Residual Stress.....	49
2.9 Summary.....	50
3 Convection Coefficient.....	52
3.1 Introduction.....	52
3.2 The Thermal Model.....	53
3.2.1 Estimation of the Contact and Finish Surface Temperatures.....	55
3.3 Experimental.....	59
3.3.1 Calibration.....	61
3.3.2 Analysis for the Calculation of the Convection Coefficient.....	64
3.3.3 Results and Discussion.....	66
4 Cutting Fluid Evaluation Test Program.....	70
4.1 Introduction.....	70
4.2 Cutting Fluid Lubrication Testing.....	71
4.2.1 Introduction.....	71
4.2.2 Experimental Procedure.....	71
4.2.3 Results.....	72
4.3 Cutting Fluid Misting.....	74
4.3.1 Aim.....	74
4.3.2 Experimental Procedure.....	74
4.3.3 Results.....	77
4.3.3.1 Effect of Fluid Viscosity on Mist Generation.....	78
4.3.3.2 Effect of Agitation Pressure.....	78
4.3.3.3 Effect of Temperature.....	79
4.3.3.4 Effect of Fluid Usage on Misting Performance.....	80
4.3.3.5 Comparative Performance of Cutting Fluids.....	81
4.3.4 Conclusions.....	84
4.4 Cutting Fluid Ignition.....	84
4.4.1 Ignition of Cutting Fluid by Hot Body.....	85
4.4.1.1 Aim.....	85

4.4.1.2	Experimental.....	85
4.4.1.3	Results.....	87
4.4.2	Spark Ignition of Cutting Fluid Evaporate.....	88
4.4.2.1	Aim.....	88
4.4.2.2	Experimental.....	88
4.4.2.3	Correlation Between Spark Energy and Grinding Chip Size.....	90
4.4.2.4	Results.....	93
4.4.3	Spark Ignition of Cutting Fluid Mist.....	95
4.4.3.1	Aim.....	95
4.4.3.2	Experimental.....	96
4.4.3.3	Results.....	97
4.4.4	Conclusions.....	98

5 Grinding Performance.....99

5.1	Introduction.....	99
5.2	High Efficiency Deep Grinding (HEDG).....	99
5.2.1	Experimental.....	99
5.2.2	Results.....	101
5.2.3	Effect of Cutting Fluid Selection on Thermal Damage in HEDG.....	106
5.2.4	Summary.....	107
5.3	Creep Feed Grinding.....	109
5.3.1	Introduction.....	109
5.3.2	Effect of Cutting Fluid Selection on Specific Grinding Energy.....	109
5.3.3	Effect of Cutting Fluid on Surface Quality.....	114
5.3.3.1	Residual Stress.....	115
5.3.3.2	Microstructural Observations.....	117
5.3.4	Summary.....	118

6 Cutting Fluid Application.....119

6.1	Introduction.....	119
6.2	Investigation of Oil Mist Density within the Machine Canopy.....	119

6.2.1 Nozzle Designs.....	119
6.2.2 Measurement of Cutting Fluid Mist in the Machine Canopy.....	120
6.2.3 Test Procedure.....	121
6.2.4 Results.....	123
6.2.4.1 Effect of Nozzle Design on Mist Generation.....	123
6.2.4.2 Effect of Flow Rate and Supply Pressure on Mist Generation.....	124
6.2.4.3 Effect of Grinding Wheel speed on Mist Generation.....	125
6.3 Influence of Nozzle Design on Grinding Performance.....	127
6.3.1 Introduction.....	127
6.3.2 Creep Feed Regime.....	127
6.3.2.1 Results.....	129
6.3.2.2 Barkhausen Noise Measurements.....	131
6.3.3 HEDG Regime.....	134
6.3.3.1 Results.....	134
6.3.3.2 Barkhausen Noise Measurements.....	136
6.4 Summary.....	137

7 Validation of Cutting Fluid Application Strategy.....139

7.1 Introduction.....	139
7.2 Cutting Fluid Selection.....	140
7.3 Sources of Ignition.....	143
7.3.1 Cutting Fluid Application.....	151
7.3.1.1 Cutting Fluid Trough.....	153
7.4 The Cutting Fluid Application Strategy.....	156
7.4.1 Benchmark Tests.....	156
7.4.2 Validation Tests.....	158

8 Conclusions and Recommendations.....162

8.1 Conclusions.....	162
8.2 Contribution to Knowledge.....	163
8.3 Further Work.....	164

References.....	165
Bibliography.....	175
Appendicies.....	176

ABSTRACT

High Efficiency Deep Grinding (HEDG) combines high depths of cut, high grinding wheel speeds with high work piece feed rates to deliver a very high stock removal process that can produce components free of surface damage. High contact temperatures are a characteristic of the process and this produces a mass of hot grinding sparks being ejected from the grinding zone.

Neat oil cutting fluids are typically used in HEDG due to their excellent lubricity, but the high grinding wheel speeds employed leads to high levels of highly volatile cutting fluid mist in the machine canopy. This mist can mix with the hot grinding sparks being ejected from the grinding zone to create a potential fire hazard.

The project aim was to produce a cutting fluid application strategy for the HEDG regime, focusing on establishing the thermal characteristics of cutting fluids in order to determine the optimum cutting fluid for the HEDG process. The cutting fluid application strategy also involved investigating the optimum means by which to apply the cutting fluid, based on minimising amount of cutting fluid used in the process and in reducing the potential fire hazard.

The characteristics that have a thermal impact on the grinding process are the cooling, lubrication, ignition and misting properties of the fluid. A series of tests were established to investigate these properties and therefore allow different fluids to be compared and contrasted for their suitability for the HEDG regime based.

Once an optimal cutting fluid had been established, the project then investigated the optimal method of applying this fluid, with particular reference to the type and design of the nozzle used to apply the fluid to the grinding zone. As part of these trials, a series of benchmark tests were also conducted using long established cutting fluid application techniques to enable the benefits of the new strategy to be evaluated.

The project concluded that high viscosity neat oil ester based cutting fluids were the best fluids to be used in the HEDG regime due to they excellent lubricity and low misting properties coupled to their relatively high resistance to ignition when compared to neat mineral oils. The studies also found that using a high viscosity ester based fluid and then applying it using a coherent jet nozzle, significant reductions in the grinding powder and specific grinding energy could be achieved whilst significantly lowering the amount of mist in the machine, thus reducing the potential fire hazard and the volume of cutting fluid used by the process.

Keywords:

HEDG, Fluid Application, Convection Coefficient, Misting, Fire Hazard

ACKNOWLEDGEMENTS

I wish to express my sincerest thanks to all the staff at Cranfield University who made this research and thesis possible, with particular thanks to the Technicians, Andrew Baldwin and John Hedge, whose knowledge and technical proficiency not only guided me in the right direction, but without whose help and advice none of this work would be possible.

I would also like to thank Dr Ian Walton whose materials and metallographic knowledge was invaluable during this period of research. He also designed the Labview Data acquisition system that was used extensively in the experimental work carried out in this project. I would also like to thank Dr James Kelman of the School of Engineering for his help and assistance with the cutting fluid ignition experiments detailed in chapter 4 of this thesis.

Special thanks are reserved for my two supervisors, Dr Tan Jin and Professor Dave Stephenson, for their enthusiastic support and expert supervision. Dr Tan Jin's help and advice was invaluable in the development of the thermal model used in this thesis and who designed the original inclined thermocouple test rig used extensively in the experimental program carried out in this project.

I would also like to thank Fuchs for the use of their laboratory at the Quality Control and Research Facility at Fuchs Hanley Plant, Stoke on Trent. In particular, I would like to thank Cliff Lea, Paul Littley and Ashley Hurst of Fuchs for their help and assistance in providing their technical knowledge and expertise, which was invaluable in this project.

I would also like to thank the sponsors of this project without whose support and financial contributions this research and thesis would not be possible. The sponsors are:

ESRPC (Engineering and Physical Sciences Research Council)
Holroyd (Grinding Machine Tool Manufacturer),
Castrol, Fuchs (Cutting Fluids),
Saint Gobain (Grinding Wheels)

TABLE OF FIGURES

Chapter 1

Figure 1.1	Fire damage to a grinding machine as a result of cutting fluid ignition.....	2
Figure 1.2	High efficiency deep grinding of a cylindrical component.....	2
Figure 1.3	Edgetek Superabrasive Milling (SAM) and Superabrasive Turning (SAT) Machines.....	5

Chapter 2

Figure 2.1	Relationship Between Specific Material Removal Rate (Q') and Workpiece Temperatures.....	8
Figure 2.2	Relationship Between Specific Material Removal Rate (Q') and Specific Grinding Energy.....	9
Figure 2.3	Partitioning of Thermal Energy in the Grinding Zone.....	12
Figure 2.4	Partitioning of Thermal Energy in the Grinding Zone.....	13
Figure 2.5	Schematic for Measuring the Grinding Temperature using a Thermal Imaging Camera.....	18
Figure 2.6	Optical Fibre and Infrared Pyrometer method of Temperature Measurement.....	19
Figure 2.7	Holes drilled into workpiece to allow the temperature distribution to be measured.....	20
Figure 2.8	Single Pole Thin Film Thermocouple.....	21
Figure 2.9	Two Pole Grindable Thermocouple Technique	22
Figure 2.10	Tribometer developed by Koenig and Vits at the Technical University of Aachen.....	25
Figure 2.11	Visibility inside the Grinding Machine is Severely Obscured by the Cutting Fluid.....	27
Figure 2.12	The Effect of Fluid Support or Nip Blocks in Creep Feed Grinding.....	31
Figure 2.13	Mist Level as a Function of Machine Activity during Milling	33
Figure 2.14	The effect of cutting fluid selection on grinding wheel wear	34
Figure 2-15	Synthesis of Ester Based Synthetic Oils.....	36

Figure 2-16 Active temperature ranges of extreme pressure (EP) additives commonly used in cutting fluids.....	38
Figure 2-17 Crankshaft Manufacturing Costs for a German Automotive Manufacturer.....	39
Figure 2-18 Coherent Jet Nozzle fitted to the Edgetek SAM Machine.....	44
Figure 2-19 Coherent Jet Nozzle.....	44
Figure 2-20 Shoe Nozzle for High Efficiency Grinding.....	46
Figure 2-21 Basic Principle of XRD Residual Stress Measurement.....	50

Chapter 3

Figure 3-1 Inclined Thermocouple Test Rig.....	53
Figure 3-2 Schematic illustration of the grinding process.....	54
Figure 3-3 Relationship between Peclet number and C-Factor.....	57
Figure 3-4 Inclination of the embedded thermocouples to the grind plane.....	59
Figure 3-5 Inclined thermocouple test rig assembled and fitted to the Edgetek SAM Machine.....	61
Figure 3-6 Assembly of the thermocouples within the inclined thermocouple test rig.....	62
Figure 3-7 Temperature response of inclined thermocouple test rig.....	62
Figure 3-8 Relationship between finish surface temperature and measured block temperature.....	63
Figure 3-9 Typical temperature profile for creep feed grinding using a neat oil cutting fluid.....	67
Figure 3-10 Typical temperature profile for creep feed grinding using a water soluble cutting fluid.....	67
Figure 3-11 Predicted Convection Coefficients for Neat Oil Water Based Cutting Fluids	69

Chapter 4

Figure 4-1 Robert Speck Torque Tapping Machine used for Lubrication Testing.....	71
Figure 4-2 Summary of Torque Tapping Results used for Lubrication Testing.....	73
Figure 4-3 Schematic Diagram of Equipment Used to Conduct Oil Misting Tests.....	75

Figure 4-4	Photograph of Equipment used for Oil Misting Tests.....	75
Figure 4-5	Glass test vessel as described by the IP313 standard for the determination of the air release values of oils.....	76
Figure 4-6	Fluid Misting Characteristics of ISO22 and ISO32 Base Stocks.....	78
Figure 4-7	Fluid Misting Characteristics of Fuchs Plantocut 22SR Ester Based Neat Oil.....	79
Figure 4-8	Fluid misting characteristics of Fuchs Plantocut 22SR and Castrol Carecut ES2 Ester Based Neat Cutting Oils.....	79
Figure 4-9	Fluid Misting Characteristics of Used and Un-used Castrol Ilogrind 600SP Neat Mineral Oil Cutting Fluid.....	80
Figure 4-10	Comparative misting performance of cutting fluids.....	82
Figure 4-11	Comparative misting performance of cutting fluids.....	82
Figure 4-12	BOC Transtig AC/DC 375 welding set.....	86
Figure 4-13	Progressive heating of the cutting fluid as it travels down the inclined heated plate.....	86
Figure 4-14	Black carbonised residue remaining in heated channel as a result of the cutting fluid boiling away.....	87
Figure 4-15	Copious amounts of smoke produced when attempting to ignite neat mineral oil cutting fluid with a hot body.....	88
Figure 4-16	Inclined heated plate test rig with Continuum Surelite SL11-10 Nd:YAG laser for testing the ignition characteristics of cutting fluid evaporate.....	89
Figure 4-17	Focusing the laser beam to a point using a 150mm focal length lens in order to simulate a hot grinding spark.....	90
Figure 4-18	Measurement of the laser power using a Laser Power Meter.....	92
Figure 4-19	Grinding swarf generated during cylindrical HEDG grinding at a specific removal rate of 2000.....	92
Figure 4-20	Ignition of the cutting fluid.....	93
Figure 4-21	Spark ignition of cutting fluid evaporate.....	94
Figure 4-22	Test rig to investigate the ignition characteristics of cutting fluid mists..	96
Figure 4-23	Fine cutting fluid mist being injected into the ignition chamber.....	97

Chapter 5

Figure 5-1 Photograph of the Edgetek SAM Machine Set-Up used for HEDG Grinding Trials.....	100
Figure 5-2 Typical power profile for a HEDG grinding test conducted using Castrol Ilogrind 600SP.....	102
Figure 5-3 Effect of cutting fluid selection on specific grinding energy in HEDG...	103
Figure 5-4 Effect of cutting fluid selection on grinding forces in HEDG.....	104
Figure 5-5 Effect of cutting fluid selection on both total and net grind power.....	105
Figure 5-6 Micrographs showing the depths of work piece thermal damage during HEDG.....	108
Figure 5-7 Comparative performance of cutting fluids in creep feed grinding.....	110
Figure 5-8 Comparative performance of cutting fluids in creep feed grinding at high wheel speeds.....	111
Figure 5-9 Effect of cutting fluid selection on specific grinding energy in creep feed grinding.....	112
Figure 5-10 Effect of cutting fluid selection on finish surface temperature in creep feed grinding.....	114
Figure 5-11 X-Ray diffraction machine used to measure surface residual stress of ground components.....	116
Figure 5-12 Effect of cutting fluid selection on residual stress in creep feed grinding.....	117
Figure 5-13 Micrograph showing Microstructure of Component Ground in the Creep Feed Regime.....	118

Chapter 6

Figure 6-1 Nozzle Designs Tested in Cutting Fluid Misting Trials.....	120
Figure 6-2 Formation of cutting fluid mist in the bottom of the SAT Machine.....	121
Figure 6-3 Hund TM Data Tyndallometer mounted in a seal plastic box.....	122
Figure 6-4 Venturi used to pull a constant flow of cutting fluid mist for measurement.....	123
Figure 6-5 Effect of grinding wheel speed on cutting fluid mist generation within the machine canopy.....	125

Figure 6-6	Formation of cutting fluid mist by the action of the grinding wheel.....	126
Figure 6-7	Alignment of the Cutting Fluid Application Nozzles.....	129
Figure 6-8	Influence of nozzle design on both the total grind power and the net grind power for cylindrical creep feed traverse grinding.....	130
Figure 6-9	Influence of nozzle design on specific grinding energy for cylindrical creep feed traverse grinding.....	130
Figure 6-10	Barkhausen noise measurement of cylindrical components.....	132
Figure 6-11	Results of Barkhausen noise measurements of cylindrical components traverse ground in the creep feed regime using different nozzle designs.....	133
Figure 6-12	Influence of nozzle design on both the total grind power and the net grind power for cylindrical HEDG traverse grinding.....	135
Figure 6-13	Influence of nozzle design on specific grinding energy for cylindrical HEDG traverse grinding.....	135
Figure 6-14	Results of Barkhausen noise measurements of cylindrical components traverse ground in the HEDG regime using different nozzle designs.	137

Chapter 7

Figure 7-1	Ball of swarf trapped between right hand coolant nozzle and workpiece.....	144
Figure 7-2	Close-up of ball of swarf that was trapped between right hand nozzle and the workpiece.....	145
Figure 7-3	New fluid application set-up on the Edgetek SAM machine.....	146
Figure 7-4	Comparison of the grind cycle at different points within the cycle.....	147
Figure 7-5	Burn at the left hand end of the workpiece caused by fluid starvation....	148
Figure 7-6	Nip block bolted to the left hand end of the workpiece.....	149
Figure 7-7	The use of nip blocks to eliminate burn at the end of the workpiece, and thus remove a potential source of ignition.....	150
Figure 7-8	Microstructures from workpiece ground without the use of a nip block.....	150
Figure 7-9	Bottom Spark Extinguisher Nozzle Mounted Below the Grinding Zone on the SAT Machine.....	152

Figure 7-10 Mass of Hot Grinding Sparks being Ejected From the Grinding Zone.....	153
Figure 7-11 Cutting Fluid Trough Fitted below the Grinding Zone on the SAM Machine.....	154
Figure 7-12 Comparison of the hot grinding chips underneath the grinding zone....	155
Figure 7-13 Original Cutting Fluid Application Set-up on the Edgetek SAT Machine.....	157
Figure 7-14 Revised Cutting Fluid Application Set-up on the Edgetek SAT Machine.....	158
Figure 7-15 The Effect on the Specific Grinding Energy of Nozzle Size when Operating in the HEDG Regime.....	159
Figure 7-16 Comparison of the Specific Grinding Energy when using the New Cutting Fluid Application Strategy.....	160
Figure 7-17 Comparison of the Total and Net Grind Powers when using the New Cutting Fluid Application Strategy.....	160
Figure 7-18 Comparison the relative mist levels in the machine canopy.....	161

TABLE OF TABLES

Chapter 2

<i>Table 2.1</i>	Comparison of Grinding Parameters and Specific Removal Rates for Different Surface Grinding Regimes.....	8
<i>Table 2.2</i>	Comparison of the values of convection coefficient published by other researchers.....	15
<i>Table 2.3</i>	Typical Thermal and Physical Properties of Cutting Fluids.....	16
<i>Table 2.4</i>	Typical Melting Temperatures of Commonly Used PVD Materials.....	17

Chapter 3

<i>Table 3-1</i>	Constants for calculation of the specific grinding energy when using equation 3-4.....	55
<i>Table 3-2</i>	Cutting Fluids Investigated during Convection Coefficient Experiments.....	60
<i>Table 3-3</i>	Experimental Conditions for Convection Coefficient Experiments.....	60
<i>Table 3-4</i>	Comparison of the Convection Coefficient of Different Cutting Fluids.....	68

Chapter 4

<i>Table 4-1</i>	Cutting Fluids Evaluated during Torque Tapping Trials.....	72
<i>Table 4-2</i>	Fluids Tested during Misting Tests.....	77
<i>Table 4-3</i>	Summary of cutting fluid evaporate spark ignition tests.....	94
<i>Table 4-4</i>	Summary of cutting fluid mist ignition tests.....	97

Chapter 5

<i>Table 5-2</i>	HEDG test grinding conditions.....	99
<i>Table 5-2</i>	Preparatory conditioning cuts used for HEDG grinding trials.....	101
<i>Table 5-3</i>	Fluid delivery pressures and fluid flow rates for HEDG grinding trials.....	101
<i>Table 5-4</i>	Summary of Results from HEDG Grinding Trials.....	103
<i>Table 5-5</i>	Residual Stress Measurements for Creep Feed Grinding Tests.....	115

Chapter 6

Table 6-1 Simulated test grind parameters used to assess the influence of nozzle design and other fluid application parameters on oil mist generation within the machine canopy.....	112
Table 6-2 Effect of nozzle selection on cutting fluid mist generation within the machine canopy.....	124
Table 6-3 Effect of delivery pressure and flow rates on cutting fluid mist generation within the machine canopy.....	124
Table 6-4 Effect of wheel speed on cutting fluid mist generation within the machine canopy. Results for 20 bar delivery pressure.....	126
Table 6-5 Grinding parameters used to assess the influence of nozzle design in creep feed grinding.....	128
Table 6-6 Grinding parameters used to grind reference component used for comparative Barkhausen noise measurements.....	132
Table 6-7 Grinding parameters used to assess the influence of nozzle design in HEDG.....	134

Chapter 7

Table 7-1 Grinding Parameters used for to assess the performance of the cutting fluid trough.....	155
Table 7-2 Grinding Parameters used for the Cutting Fluid Benchmark Tests.....	157

TABLE OF EQUATIONS

Chapter 2

<i>Equation 2.1</i>	13
<i>Equation 2.2</i>	15
<i>Equation 2.3</i>	23
<i>Equation 2.4</i>	23
<i>Equation 2.5</i>	24

Chapter 3

<i>Equation 3-3</i>	53
<i>Equation 3-4</i>	54
<i>Equation 3-5</i>	54
<i>Equation 3-4</i>	55
<i>Equation 3-5</i>	55
<i>Equation 3-6</i>	56
<i>Equation 3-7</i>	56
<i>Equation 3-8</i>	57
<i>Equation 3-9</i>	58
<i>Equation 3-10</i>	58
<i>Equation 3-11</i>	64
<i>Equation 3-12</i>	64
<i>Equation 3-13</i>	65
<i>Equation 3-14</i>	65
<i>Equation 3-15</i>	65
<i>Equation 3-16</i>	65
<i>Equation 3-17</i>	65
<i>Equation 3-18</i>	66
<i>Equation 3-19</i>	66
<i>Equation 3-20</i>	66

Chapter 4

<i>Equation 4-1</i>	91
---------------------------	----

Chapter 5

<i>Equation 5-1</i>	106
---------------------------	-----

Chapter 6

<i>Equation 6-1</i>	127
---------------------------	-----

<i>Equation 6-2</i>	129
---------------------------	-----

<i>Equation 6-3</i>	131
---------------------------	-----

1 Introduction

1.1 Background

“The process of removing material by the use of abrasives is very old. In recent years many papers have appeared on the subject of grinding, and much has been learnt. However, there are still important features which are not clearly understood.”

RS Hahn (1962)

This statement was taken from a paper presented at the 3rd International Machine Tool Design and Research Conference in 1962, and in many ways that statement still holds true today. In more than 40 years since that conference was held, there has been a great deal of research carried out in the field of grinding and abrasive machining, and a great deal has been learned during this period, but with advances in grinding technology, there are still a great many questions to be answered and problems to be solved.

Recent advances in both machine and grinding wheel technology has allowed the development of High Efficiency Deep Grinding (HEDG), a high stock removal abrasive machining process which allows grinding to compete favourably with more traditional stock removal processes such as turning and milling. When applied to the cylindrical grinding process, HEDG technology results in a new process called “Superabrasive Turning”.

Cutting fluids and their application are important in the majority of grinding processes, and the same is true for HEDG. Cutting fluids provide both cooling and lubrication to the grinding zone which helps to control the grinding zone temperature thereby reducing thermal damage to the work piece and grinding wheel wear. Cutting fluids also perform other important functions such as the flushing of grinding swarf and debris from the grinding wheel and grinding zone, as well as corrosion protection of both the workpiece and machine. (Brinksmeier and Brockhoff,1992)

This research project arises from the need to further the understanding of the role of cutting fluids in the grinding process and in particular the HEDG process, where it is well known that the use of neat oil cutting fluids poses a significant fire hazard. This particular project also has real industrial significance, as ignition of the cutting fluid can result in serious and costly damage to the machines (see figure 1.1) as well as posing a serious risk to individuals. Consequently there is a real and immediate need to either eliminate or significantly reduce the risk of cutting fluid ignition.



Figure 1.1 Fire damage to a grinding machine as a result of cutting fluid ignition



Figure 1.2 High Efficiency Deep Grinding of a Cylindrical Component. The hot grinding sparks coupled with high levels of cutting fluid mist pose a significant fire hazard when neat oil cutting fluids are used.

Empirically topics such as likely sources of ignition, sources of excessive heat generation, the flammability of cutting fluids, fluid mists and vapours, all spring to mind when considering measures likely to reduce the fire hazard within a grinding machine. Figure 1.2 shows a typical component (shown bottom right) being machined using the HEDG process, with the subsequent plume of hot grinding sparks being ejected from the grinding zone an obvious candidate as an ignition source.

Measures to reduce the fire hazard may include areas as diverse as cooling and lubrication within the grinding zone to prevent excessive heat generation, or measures to reduce fluid mist and vapours or even the grinding sparks themselves. Also there is a desire to develop cutting fluids that are non flammable or at least less flammable than the ones already in use.

This thesis is therefore concerned with the development of a cutting fluid selection and application strategy based on the particular aspects of fluid selection and application that have either a direct thermal impact on the grinding process, by controlling heat generation for example, or that are affected by the thermal nature of the grinding process, fluid flammability for instance. The following two sections refine this concept into a project aim and a series of objectives.

1.2 Aim

The principal aim of this thesis is to develop a best practice cutting fluid application strategy for the cylindrical High Efficiency Deep Grinding (HEDG) regime. The strategy should produce a robust and reliable process suitable for industrial applications which either eliminates or substantially reduces the risk of cutting fluid ignition.

In order to develop a coherent cutting fluid application strategy for cylindrical HEDG, the project has been split into two main themes which run through the entire project. The two broad themes are:

Cutting Fluid Selection
Cutting Fluid Application

1.3 Objectives

- a. To establish the properties of the cutting fluid which have a thermal impact on the grinding process.
- b. To develop a standardised test program aimed at measuring the above properties.
- c. Use the data from the standardised test program to select the most effective cutting fluid for the cylindrical HEDG process.

- d. To investigate different nozzle designs typically used for fluid application in grinding operations to determine the most effective and efficient method of fluid application.
- e. To minimise the volume of cutting fluid used in the cylindrical grinding process
- f. To reduce the environmental impact of the grinding process attributable to the use of cutting fluids.
- g. To propose a best practice fluid application strategy for the cylindrical HEDG regime.

1.4 Scope

The first part of this thesis reviews previous work on grinding and abrasive machining processes, cutting fluids, their application and their role in the grinding process. Theory is also presented showing the thermal impact of cutting fluids on the grinding process.

Experimental work was predominately undertaken on two superabrasive grinding machines built by Holroyd, the Edgetek SAM surface grinding machine and the Edgetek SAT cylindrical grinding machine (see figure 1.3). The acronyms used to name these machines, SAM and SAT, describe the different processes and stand for Superabrasive Machining and Superabrasive Turning respectively.

Electroplated CBN wheels were used for all grinding trials as they are particularly suited for the HEDG regime, where very high grinding wheel speeds are needed along with grinding wheels exhibiting very high wear resistance characteristics. Furthermore, the SAT and SAM machines were specifically designed for the HEDG process, having very powerful, high speed grinding spindles and cutting fluid delivery systems.

The material used for experimental work was 51CrV4 high alloy steel, which is used extensively for the manufacture of transmission shafts in the automotive industry due to its excellent toughness. This particular material is relatively difficult to machine using conventional cutting processes, making HEDG an attractive manufacturing process for such applications.

A variety of commercially available cutting fluids from a range of different suppliers were tested to allow a representative range of fluids to be compared. It is not the intention to perform a detailed comparison of cutting fluid chemistry, nor is it intended to develop new cutting fluids specifically for the HEDG process, simply to determine which characteristics have the greatest influence on the process and develop a range of standardised tests to allow different fluids to be compared.



*Figure 1.3 Edgetek Superabrasive Milling (SAM) and Superabrasive Turning (SAT) Machines.
 Top left –Edgetek Superabrasive Turning (SAT) Machine
 Top right –Edgetek Superabrasive Turning (SAT) Machine with machine doors open
 Bottom centre – Edgetek Superabrasive Milling (SAM) Machine*

1.5 Thesis Structure

The work carried out during the research project will be presented in this thesis in nine chapters.

Chapter 1, the Introduction provides the background to this research, giving reasons as to why the research was conducted, a list of aims and objectives, and describes the scope and structure of the thesis.

Chapter 2, the Literature Review highlights the main areas of research conducted in grinding and abrasive machining, with particular emphasis on the subject of cutting fluids, their application and their importance in the grinding process.

Chapter 3, Convective Heat Transfer Coefficient of the Cutting Fluid, discusses the thermal modelling of the grinding process, and in particular the convective heat transfer coefficient of the cutting fluid. This chapter also details the experimental work carried out to measure this important thermal attribute of the cutting fluid.

Chapter 4, Cutting Fluid Evaluation Test Program, describes the experimental work carried out in developing and performing a series of screening tests used to determine individual fluid characteristics important in the selection of cutting fluids for different grinding regimes. Screening tests do not by themselves definitively prove a fluid's suitability for a particular process, but provide a simple, cheap and efficient method of establishing a fluid's suitability for any given process. The screening tests presented in this chapter are designed to test fluid lubrication, misting and ignition characteristics.

Chapter 5, Grinding Performance, presents the experimental work conducted with various cutting fluids in both conventional and HEDG regimes. Despite the extensive use of screening tests in cutting fluid development, it has long been understood that the only way to truly test a fluid's effectiveness for any given grinding process is to perform realistic grinding trials using the desired parameters. The results from these grinding trials are correlated with the results from the screening tests presented in chapter four, in order to evaluate the effectiveness of the screening test program.

Chapter 6, Cutting Fluid Application, describes the importance of fluid application in developing a coherent cutting fluid delivery strategy, and discusses the experiments performed to determine the influence of fluid application parameters, such as nozzle design and nozzle position, on both the grinding process and on cutting fluid performance.

Chapter 7, Validation of Cutting Fluid Application Strategy, details the experimental work conducted to produce an optimising cutting fluid application set-up, conducted using the most effective cutting fluid, nozzle design and fluid application parameters determined by experimental work described in earlier chapters. A summary of all the findings of the research is then presented to describe a best practice cutting fluid application strategy based on the thermal characteristics of cutting fluids, the principal aim of the project.

Chapter 8, Conclusions and Recommendations, lists the conclusions that have arisen from the research, and suggestions for areas of further work that would be beneficial in extending the understanding of cutting fluids in abrasive machining process.

2 Literature Review

2.1 Introduction

2.1.1 Historical Background

In 1974 the Grinding Technology Program of research was launched by the Science and Engineering Research Council after it became understood that the experiences of production engineers working within the automotive and aerospace industries during the late 1960's had highlighted there was considerable undeveloped potential for grinding to be developed into a more widely used metal removal process to replace traditional methods such as turning or milling (Challis and Stanton, 1982). Up to that point grinding had been reserved for the fine finishing operations where small material removal rates were employed.

Creep feed grinding, sometimes called abrasive machining, was the result of such research, where the removal of large quantities of material in "one pass" was achievable. It is of considerable value when producing complex shapes and has been used to manufacture parts such as turbine blade roots for approximately 30 years.

By 1979, the creep feed grinding technique was being employed in the deep grinding of twist drill flutes to attain very high specific removal rates on special purpose multi spindle grinding machines employing high stability, high power grinding spindles at high grinding wheel speeds (up to 100m/s). When using high pressure neat oil cutting fluids, maximum specific removal rates of $600\text{mm}^3/\text{mm.s}$ were achievable. Such removal rates were significantly higher than was achievable by conventional flute form milling. (Werner, 1979).

2.1.2 High Efficiency Deep Grinding

The next major development came with the advent of superabrasive grinding wheels. Hard abrasive grains such as diamond and CBN (cubic boron nitride) bonded to a solid hub produced grinding wheels capable of very high metal removal rates without the excessive, uneconomical wear associated with conventional wheels when such high material removal rates were attempted. When used on modern grinding machines designed with greater stiffness for improved accuracy and product consistency, superabrasive wheels enabled the development of High Efficiency Deep Grinding, HEDG, and allowed even greater volumes of material to be removed (Tawakoli, 1993). Depths of cut in HEDG are comparable with creep feed grinding but workpiece feed-rates are far greater, in the range more normally associated with high speed grinding.

Tawakoli (1993) provides a comparison of removal rates for different grinding regimes, with typical grinding parameters employed in surface grinding. This can be seen in table 2.1. Whilst these parameters may not be directly comparable to cylindrical grinding regimes such as superabrasive turning, due to the fact that the contact zone is

significantly smaller in cylindrical grinding (Werner, 1979), the table is useful in showing the relative differences between the different grinding regimes.

Grinding Parameter	Grinding Regime		
	Shallow Cut	Creep Feed	HEDG
Depth of Cut a_e	Low 0.001-0.05mm	High 0.1-30mm	High 0.1-30mm
Workpiece Speed v_w	High 1-30m/min	Low 0.05-0.5m/min	High 0.5-10m/min
Wheel Speed v_s	Low 20-60m/s	Low 20-60m/s	High 80-200m/s
Specific Removal Rate Q_w'	Low 0.1-10mm ³ /mm.s	Low 0.1-10mm ³ /mm.s	High 50-2000mm ³ /mm.s

Table 2.1 Comparison of Grinding Parameters and Specific Removal Rates for Different Surface Grinding Regimes .(Tawakoli, 1993)

All grinding regimes result in large amounts of heat energy being generated within the grinding zone. However, the high removal rates and high wheel speeds used in the HEDG process result in significantly more heat being generated in the grind zone in comparison to conventional grinding regimes. If this heat is not controlled this can lead to thermal damage of the workpiece.(Tawakoli, 1993; Stephenson and Jin, 2003).

The thermal characteristics of the grinding process are dependant on several interacting variables (Stephenson and Jin, 2003). These will be introduced in detail in chapter 3, but it is well known that a general relationship exists between temperature and specific material removal rate. This relationship, which is shown in figure 2.1, shows that either low or high specific removal rates must be employed if the finish workpiece surface temperatures are to be maintained below the burn threshold of the workpiece material. (Tawakoli, 1993; Jin and Rowe, 2001; Jin and Rowe, 2001(a); Jin and Stephenson, 2002; Rowe and Jin, 2001; Stephenson and Jin, 2002).

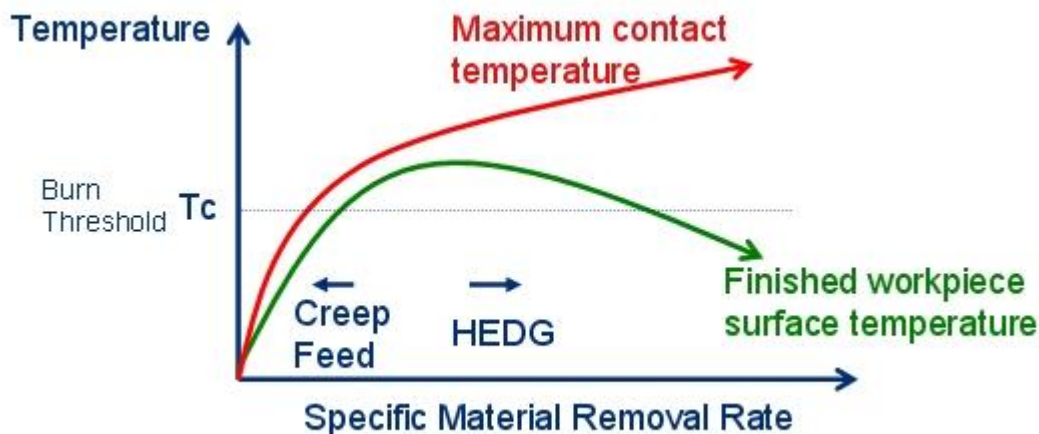


Figure 2.1 Relationship Between Specific Material Removal Rate (Q') and Workpiece Temperature. (Stephenson, 2004)

In HEDG the workpiece finish surface temperature decreases with increasing removal rate despite the fact that the maximum contact temperature within the grinding zone increases. It is also significant that the maximum contact temperature itself does not increase linearly with increasing specific removal rate. Instead, the rate of change of maximum contact temperature decreases at higher specific removal rates. These important characteristics are attributable to two separate mechanisms.

The first mechanism, which is largely responsible for the decreasing workpiece surface temperature at higher specific removal rates, is attributable to the high workpiece feed rates employed in HEDG. In creep feed grinding, the relatively large contact lengths (as a result of the large depths of cut) and the long contact time (as a result of the low workpiece feed rates) result in some of the heat energy flowing into the workpiece. This can result in an accumulation of heat within the workpiece which may ultimately cause thermal damage. Conversely the high feed rates used in HEDG results in heat energy being removed by the ejected metal chips before it is conducted into the workpiece where it could cause thermal damage. (Tawakoli, 1993).

The second mechanism is a result of the relationship between specific grinding energy and the specific material removal rate. Far from being a linear relationship, the specific grinding energy decreases exponentially with increasing specific material removal rate (Jin and Rowe, 2001; Jin and Rowe, 2001a; Rowe and Jin, 2001; Stephenson and Jin, 2002; Stephenson and Jin, 2003). Consequently, the amount of energy needed to remove each unit volume of material reduces significantly as the material removal rate increases. It is this relationship, shown in figure 2.2 that explains the fact that the maximum contact temperature does not increase as rapidly at higher specific removal rates.

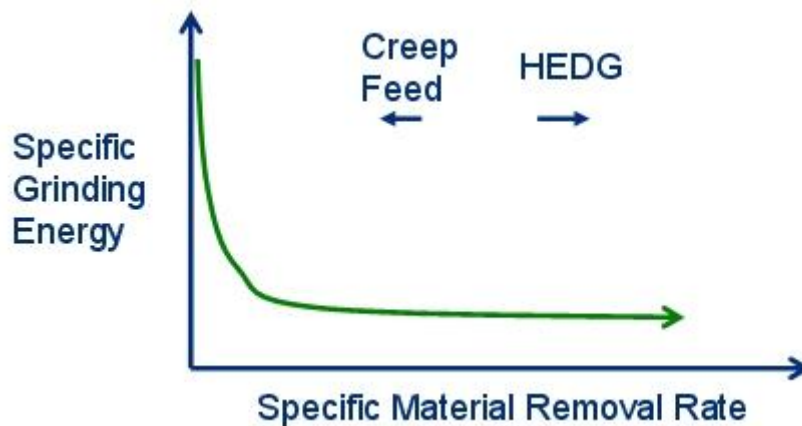


Figure 2.2 Relationship Between Specific Material Removal Rate (Q') and Specific Grinding Energy.

There are several reasons for the relationship seen in figure 2.2. One reason is the greater stress on the abrasive grains at higher specific removal rates. This results in a self sharpening action of the grains (Jin and Rowe, 2001) and promotes a more effective cutting action resulting in larger chip thicknesses and less ploughing and sliding. A second reason is the increased penetration of the abrasive grain into the workpiece. This

improves the geometry of the cutting action (Jin and Rowe, 2001; Jin and Rowe, 2001a). The result is that HEDG is far more efficient than creep feed or shallow cut grinding regimes. (Jin and Rowe, 2001)

The high grinding wheel speeds that are characteristic of HEDG, which are necessary to reduce the chip thickness in order to reduce the cutting forces generated by the process (Tawakoli, 1993), can atomise the cutting fluid leading to high levels of mist within the machine (Campbell, 2001). Neat cutting oils and the mists they produce are flammable, and with the very high grinding zone and chip temperatures associated with the HEDG process, there is obviously a serious risk of ignition.

2.2 The Role of Cutting Fluids in the Grinding Process

As stated both in the introduction and in the previous section, there is a significant fire hazard associated with the use of neat oil cutting fluids in conjunction with the HEDG process. There are also problems, in common with all other grinding regimes where cutting fluids are used, in simply supplying cutting fluids into the arc of contact between the grinding wheel and workpiece, and this in itself can result in an elevated risk of thermal damage to the workpiece surface due to excessive grinding temperatures (Brinksmeier and Heinzl, 1999).

The obvious question that therefore arises is why use neat oil cutting fluids if their use and application is so problematic. Why not use other types of non-flammable cutting fluids or eliminate the use of cutting fluids altogether? In order to answer the second part of this question, we must first look at the role of cutting fluids within the grinding process.

The grinding process is characterised by a relatively large contact area between the workpiece and the grinding wheel coupled with very high friction between the abrasive grains of the grinding wheel and the workpiece when compared to other machining processes (Brinksmeier and Brockhoff, 1997).

Cutting fluids can help to lubricate the grinding zone, thus reducing the friction between the grinding wheel and the workpiece and reducing the amount of frictional heat being generated. They can also help to cool the grinding zone, removing some of the generated heat. Consequently, despite the problems associated with their use and application, cutting fluids have been an integral part of many grinding operations for a considerable length of time. During this time there has been a significant amount of research conducted to improve both the cutting fluids and their application, as they perform several very different but very important functions within the grinding process. Brinksmeier et al (1997) summarises these as follows:

- **Lubrication**

Lubrication of the grinding arc between the grinding wheel and the workpiece reduces the friction forces and thus limits heat generation and grinding wheel wear. Lubrication may also be needed for production tooling such as workrests.

- **Cooling**

Cooling of the grinding wheel and workpiece

- **Corrosion Protection**

Cutting fluids can help to prevent chemical reactions at the newly formed surface of ferrous workpiece materials, and help prevent corrosion of the machine tool structure as a whole.

- **Chip Removal**

Removal of grinding chips out of the grinding area

- **Cleaning**

Cleaning the wheel is important to stop wheel loading, a condition where metal particles become lodged between the abrasive grains of the grinding wheel. (Khudobin, 1970;Tawakoli, 1993; Marinescu and Rowe, 2004)

2.3 Thermal Characteristics of Cutting Fluids

Section 2.2 listed cooling and lubrication as two important functions of the cutting fluid. A cutting fluid's ability to cool the grinding zone, and its ability to reduce heat generation by means of lubrication, are the most obvious attributes of the cutting fluid to have a thermal impact on the grinding process. However, the cutting fluid's misting and ignition characteristics also have a huge impact on the grinding process, especially in the HEDG regime when oil cutting fluids are used, as material removal rates may need to be limited in order to reduce the fire hazard posed by the process.

The characteristics of the cutting fluid that have a thermal impact on the grinding process can therefore be categorised as follows:

- **Cooling Effectiveness**
- **Lubricity**
- **Ignitability**
- **Misting**

These thermal characteristics will be considered in detail in the following sections. Other topics which are not directly associated with the thermal characteristics of cutting fluids will also be discussed in this section where appropriate. For example, the topic of temperature measurement will be discussed in detail when examining the cooling effectiveness of grinding fluids, as one cannot gauge this important fluid attribute without reliably measuring workpiece temperature.

2.3.1 Cooling

The friction between the abrasive grain and the workpiece results in a large amount of thermal energy being generated, and as previously stated, if not controlled it can result in thermal damage to the workpiece (Tawakoli, 1993; Stephenson and Jin, 2003). This thermal energy is distributed or partitioned amongst the four different elements within the grinding zone. These four elements or paths, which are represented graphically in figure 2.3, are as follows:

- **Workpiece**
- **Grinding Wheel**
- **Cutting Fluid (cooling media)**
- **Grinding Chips**

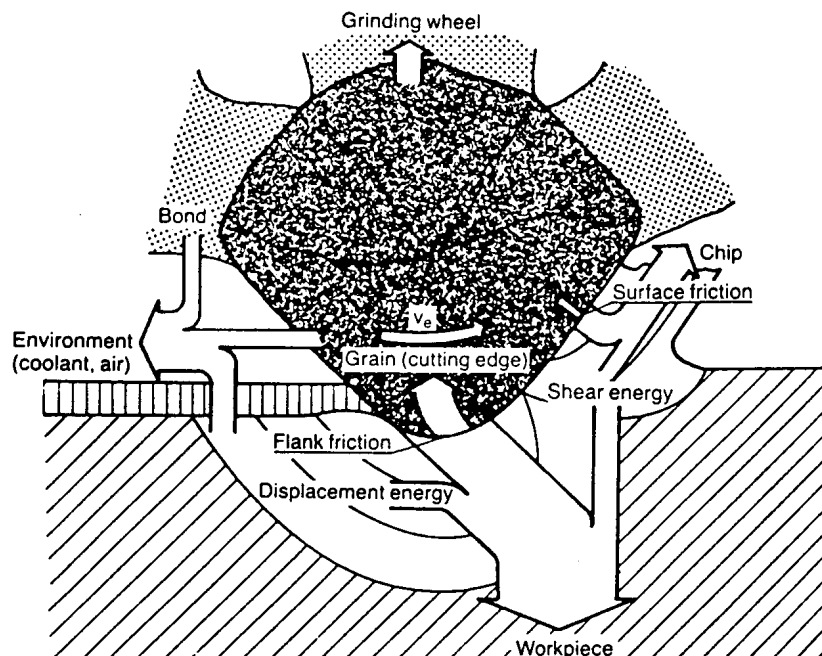


Figure 2.3 Partitioning of Thermal Energy in the Grinding Zone.(Tawakoli, 1993)

The distribution of thermal energy throughout these four paths is not only determined by the thermal properties of the particular elements within the grinding zone, but also on the particular grinding parameters used. Whilst the interrelationships that govern this distribution are complex, it is sufficient at this point simply to understand the basic principles of cooling within the grinding zone, and the concept of energy partitioning. This is best explained graphically and is shown in figure 2.4, whilst the more complex mathematical interrelationships will be covered in greater detail in chapter 3.

Figure 2.4 illustrates the basic principle of considering the grinding process as a thermal process. The total heat flux generated by the process, q_t is divided or split between the four different elements within the grinding zone. Each element has a different amount of

thermal energy entering it, so the heat flux entering the grinding wheel is thus defined as q_s . The same principle applies to the other elements within the grinding zone, the workpiece (q_w), the cutting fluid (q_f) and the chip (q_c). The proportion or ratio of the total thermal energy of the process entering each of the different elements can be calculated, using well established formulae, to give the particular partition ratio. Therefore, amount of the total thermal energy entering the workpiece, for example, is

Equation 2.1

$$q_w = R_w q_t$$

where R_w is the workpiece partition ratio. The same principle applies to all the different elements within the grinding zone. This is the basic principle of partitioning.

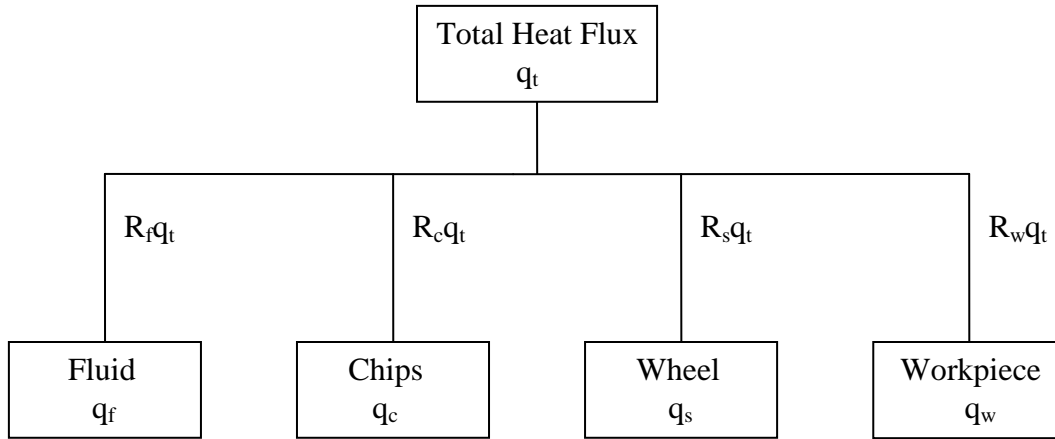


Figure 2.4 Partitioning of Thermal Energy in the Grinding Zone.(Rowe, 2001)

In creep feed grinding cooling by the cutting fluid is of prime importance with more than 90% of the total heat energy generated removed by the cutting fluid (Jin and Stephenson, 2003). In High Efficiency Deep Grinding however, the very high contact temperatures that are characteristic of this aggressive process can lead to a condition where fluid film boiling occurs, and as a result, the cooling effectiveness of the fluid is reduced to almost zero (Andrew and Howes, 1985; Ohishi and Furukawa, 1985; Howes, 1990). Instead HEDG relies on high workpiece feed rates to ensure heat energy is removed by the grinding chips.(Tawakoli, 1993)

2.3.1.1 Convection Coefficient

The measure of a cutting fluids ability to cool the grinding zone is defined as the convection heat transfer coefficient (h_f), or convection coefficient for short. Under

certain grinding conditions, convective cooling can be a major mechanism for the removal of heat energy from the grinding zone, and can therefore be important in reducing the possibility of thermal damage in the workpiece. It is therefore an important variable in determining the amount or ratio of the total heat generated in the grinding zone that is removed by, or partitioned to, the cutting fluid.

Several attempts have been made to measure or calculate the convection coefficient from grinding data and these are summarised in table 2.2. It can be seen that there is a wide variance in the values published by different researchers. This is partly attributable to the different process parameters used, but also due to the different methods used to establish these values. Kim et al (1997) measured the temperature rise in the workpiece when creep feed grinding. A triangular heat source model was then used to predict the temperature response using different values of the fluid convection coefficient to match the predicted temperature response to the measured temperature response established during the creep feed grinding trials.

Lavine (1988) on the other hand divided the total heat generated during the grinding process into two parts, the energy entering the workpiece and the energy entering a solid composite consisting of the grinding wheel and the grinding fluid. The energy removed by the chips was not explicitly considered. Lavine (1988) then calculated the energy entering these two bodies and by assigning suitable values of convection coefficient to oil and water, the maximum surface temperatures predicted using this method showed “remarkably good” agreement with the grinding zone temperature published by other researchers.

Okuyama et al (1993) and Ohishi et al (1985) both built special test rigs in an attempt to measure the convection coefficient. The rig used by Okuyama et al (1993) measured the temperature distribution along a piece of copper wire mounted vertically within a block, which was heated (by a coil heater) at one end, and cooled at the other by cutting fluid being applied to a rotating grinding wheel. This allowed the average heat transfer coefficient from the top surface of the copper wire to be calculated. Using this method Okuyama et al (1993) established values of approximately $120\text{kW/m}^2\text{K}$ for water based cutting fluids at grinding wheel speeds of 30m/s .

Ohishi et al (1985) used a slightly different method as they heated small copper cylinders and put the cylinders horizontally in the flow of cutting fluid at 5 different locations. By measuring the temperature change in the copper cylinders, values of convection coefficient up to $14.4\text{kW/m}^2\text{K}$ were found, but these values are significantly lower than the values published by Okuyama et al (1993). Unfortunately Ohishi et al (1985) were not explicit about what type of cutting fluid and grinding wheel speeds they used for these tests.

All this leads to a certain degree of uncertainty over the true value of this very important parameter. What is certain is the fact that the convection coefficient of the cutting fluid is very difficult to measure (Jin and Stephenson, 2003a; Ohishi and Furukawa, 1985)

Source of Data	Kim (1997)	Kim (1997)	Lavine (1988)	Lavine (1988)	Lavine (1988)	Lavine (1988)
Grinding Regime	Creep	Creep	Shallow Cut	Shallow Cut	Creep	Creep
Grinding Mode	Down Grinding	Up Grinding	Down Grinding	Down Grinding	Down Grinding	Down Grinding
Wheel Diameter (mm)	350	350	200	200	200	200
Wheel speed (m/s)	30	30	20	20	20	20
Wheel Type	Alumina	Alumina	Alumina	Alumina	Alumina	Alumina
Depth of Cut (mm)	0.5	0.5	0.01	0.01	1	1
Work speed (mm/s)	5	5	100	100	1	1
Cutting Fluid	Emulsion	Emulsion	Emulsion	Oil	Emulsion	Oil
h_f (W/m ² K)	15000	20000	410000	130000	260000	40000

Table 2.2 Comparison of the values of convection coefficient published by other researchers. (Jin and Stephenson 2003a)

The main difficulty in measuring the convection coefficient arises from the fact that it is not determined solely by the thermal properties of the cutting fluid, but also on the grinding parameters used in the process. The simplest way of illustrating this is to look at the simple “fluid wheel” mathematical model described by both Rowe (2001a) and Jin et al (2002) to calculate this parameter. This particular model assumes that a layer of cutting fluid travels through the grinding zone at the grinding wheel speed, driven through by the hydrodynamic action of the grinding wheel, and covers practically the entire contact zone, including all the space between the abrasive grains. (Rowe, 2001a; Rowe and Morgan, 1991)

The convection coefficient can then be estimated from:

Equation 2.2

$$h_f := 0.94\beta \cdot \left(\sqrt{\frac{v_s}{l_c}} \right) \quad (\text{Jin and Stephenson, 2002; Rowe, 2001a})$$

where:

- h_f = convection coefficient of the cutting fluid
- v_s = grinding wheel speed
- l_c = grinding arc of contact
- β = thermal property of the cutting fluid.

Whilst this model does not take into account the porosity of the grinding wheel, which is known to influence the cooling effectiveness of the cutting fluid (Andrew and Howes, 1985; Jin and Stephenson, 2003a), it is useful for demonstrating how grinding parameters such as the grinding wheel speed and the depth of cut (which affects the grinding arc of contact) help determine the convection coefficient of the cutting fluid.

Whilst the convection coefficient may not solely be determined by the thermal properties of the cutting fluid, it can be seen from equation 2.2 that it is proportional to them. Typical values of the thermal properties of different cutting fluids can be seen in table 2.3. and it can be seen from these values that water based cutting fluids (emulsion) offer far greater levels of cooling than neat oil fluids, due to their high thermal property (β) which is attributable to their high water content, typically 90% or more. One would therefore assume that water based cutting fluids would be preferable to neat oils cutting fluids, especially in creep feed grinding, where, as stated earlier, over 90% of the heat is removed by the fluid (Jin and Stephenson, 2003).

Material	k(W/mK)	ρ (kg/m ³)	c(J/kgK)	β (J/mKs ^{1/2})	$\alpha \times 10^{-6}$ m ² /s
Mineral Oil	0.14	900	2100	514	0.7
Emulsion	0.56	1000	4200	1534	0.145

Table 2.3 Typical Thermal and Physical Properties of Cutting Fluids.(Jin and Stephenson, 2003a)

where:

k = thermal conductivity

ρ = mass density

c = specific heat capacity

β = thermal property (kpc)^{1/2}

α = thermal diffusivity

However, it is important to realise that neat oil cutting fluids offer far greater levels of lubrication (Malkin, 1989), a subject that will be covered in more detail later. Consequently despite the fact that oil is less effective at removing heat from the grinding zone, less heat is generated in the first place. This poses the classical quandary of which cutting fluid should be used? Should a water based cutting fluid be used to remove a larger percentage of a larger generated heat load, or should a neat oil based cutting fluid be used which removes a smaller percentage of a much reduced heat load? One of the aims of this thesis is to answer this question.

2.3.1.2 Temperature Measurement

Although temperature measurement is an aside to the main subjects of cooling and the convection coefficient of the cutting fluid, it is useful at this point to discuss the subject of temperature measurement. An important feature of all the different methods used to establish the cooling effectiveness of cutting fluids is the ability to accurately measure the grinding temperature. It is therefore convenient to cover this topic at this point, as it

is of fundamental importance if one wants to compare and contrast the performance of different fluids. The following sections will cover the different methods used to measure grinding temperature.

2.3.1.2.1 PVD Coatings

The physically vapour deposited (PVD) film method has been used successfully in both surface (Kato and Fujii, 1997; Kato and Fujii, 2000) and cylindrical grinding (Comley and Stephenson, 2004) to measure the workpiece temperature in grinding. A single material with a precise and known melting point is vapour deposited on a polished internal surface of a split workpiece. The split workpiece is then clamped together and the grinding test performed. Once the grinding test is complete, the workpiece can be split, and the depth to which the PVD coating has melted can be measured using a microscope.

Repeating the grinding tests using the same grinding parameters, but using different PVD materials with different melting temperatures, allows the temperature at different depths within the workpiece to be established. Thus a temperature profile within the workpiece for the grinding parameters employed can be established.

PVD Coating Material	Symbol	Melt Temperature (°K)	Melt Temperature (°C)
Germanium	Ge	1211	938
Antimony	Sb	904	631
Tellurium	Te	723	450
Zinc	Zn	693	420
Lead	Pb	601	328
Bismuth	Bi	545	272
Indium	In	429	156
Bi-Pb Alloy ⁽¹⁾	Bi-Pb	399	126
Rose Alloy ⁽²⁾	Rose	370	97
Anatomical Alloy ⁽³⁾	Anatomical	334	61

Table 2.4 Typical Melting Temperatures of Commonly Used PVD Materials. (Kato and Fujii, 2000; Comley and Stephenson, 2004; Komanduri and Hou, 2001)

Composition by weight: (1) Bi = 55.5%, Pb = 44.5%; (2) Bi = 50%, Pb = 28%, Sn = 22% ; (3) Bi = 53.5%, Pb = 17%, Sn = 19%, In = 10.5%

This technique is however of limited value when one wants to measure the grind temperature to ascertain the convection coefficient of a variety of different cutting fluids. To obtain realistic values of the convection coefficient, grinding parameters need to be selected with care to ensure the process does not cause either fluid film boiling or nucleate boiling of the cutting fluid under investigation, both of which can significantly affect the magnitude of the convection coefficient (Andrew and Howes, 1985).

When neat oil cutting fluids are used, a number of the coatings listed in table 2.4 could be used to develop a temperature profile within the grind zone, which could then be

used to establish the convection coefficient, as the boiling point of these fluids is typically in the range of 300-320°C (Yasui and Tsukuda, 1983; Rowe, 2001a; Jin and Stephenson, 2003a; Howes, 1990), but may increase above this depending on the pressure in the contact zone.

For water based fluids however, only the “Anatomical Alloy” (Kato and Fujii, 2000) is significantly below the 100-130°C boiling point of the cutting fluid (Yasui and Tsukuda, 1983; Rowe, 2001a; Jin and Stephenson, 2003a; Howes, 1990) making it virtually impossible to develop a reliable temperature profile within the workpiece.

2.3.1.2.2 Thermal Imaging Camera

A thermal imaging camera has been used to measure the workpiece temperature distribution in surface grinding (see figure 2.5), a technique that allows a graphical real-time image of the heat distribution to be obtained (Hwang and Chandrasekar, 2002). The major disadvantage with this method is, however, that the camera only records heat radiated from the side of the workpiece facing the thermal imaging camera, and cannot measure actual contact temperature within the grind zone, as the view will always be obscured (Batako and Rowe, 2005). Furthermore the cutting fluids under test, which will inevitably splash all round the work area, could interfere with the thermal radiation observed by the thermal imaging camera. This could lead to inaccuracies in the temperature readings, with the consequent repercussions on the accuracy of any convection coefficient data derived from these thermal measurements. Finally the temperature distribution on the observed surface may not be representative of the distribution throughout the whole workpiece, and this again can lead to uncertainty over the reliability of the measurements (Batako and Rowe, 2005).

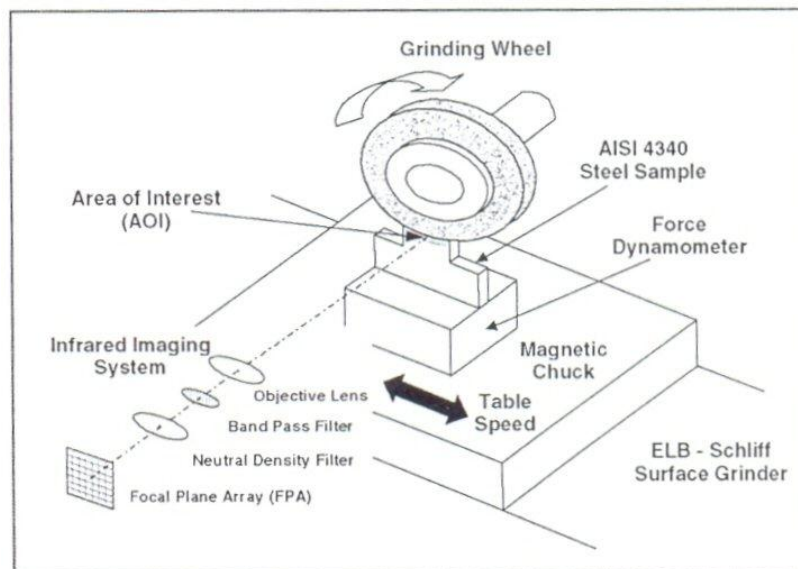
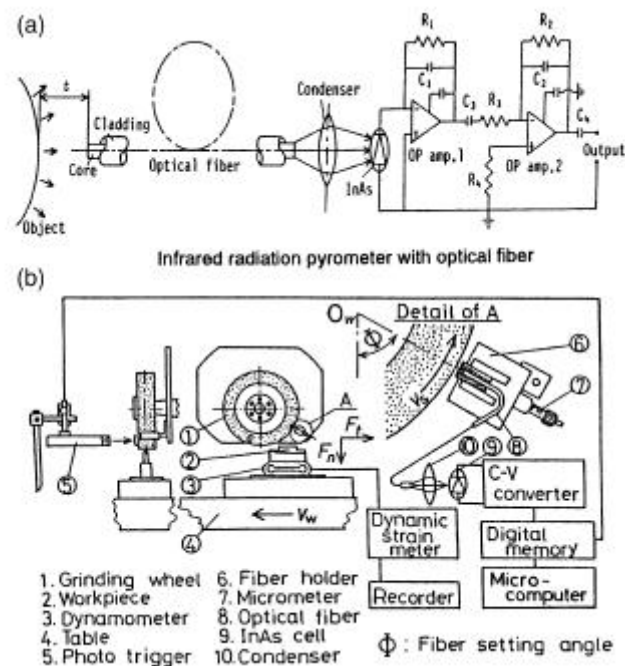


Figure 2.5 Schematic for Measuring the Grinding Temperature using a Thermal Imaging Camera (Hwang and Chandrasekar, 2002).

2.3.1.2.3 Optical Fibre

Infrared radiation pyrometers have been used to measure both infrared energy radiated from the active cutting grains of a grinding wheel (Ueda and Tanaka, 1993) and the grinding temperature in surface grinding (Ueda and Hosokawa, 1986; Xu and Malkin, 2001). An optical fibre is mounted to accept infrared radiation from the target area which is then transmitted via an LED to the infrared detector. There it is converted to an electrical signal which can then be passed, via some signal processing system to a computer (See figure 2.6)



a) Schematic of infrared pyrometer used by Ueda et al (1993) and

b) Experimental grinding set-up

Figure 2.6 Optical Fibre and Infrared Pyrometer method of Temperature Measurement.(Ueda and Tanaka, 1993).

When measuring the temperature of active cutting grains, the optical fibre observes the grinding wheel after it has passed through the grinding zone (see figure 2.6(b)). There is therefore a time delay (measured in milliseconds) between cutting and measurement during which the cutting grains cool. This effect needs to be considered and compensated for (Ueda and Tanaka, 1993), and, unless done correctly, it can be a source of inaccuracy within the measurements.

Measuring the workpiece temperature with this method requires the optical fibre to be mounted in a small blind hole drilled from the underside of the workpiece which extends almost to the ground surface. When the grinding wheel passes over the top of the hole, the infrared detector can detect the radiation emitted from the bottom of the hole. (Ueda and Hosokawa, 1986; Xu and Malkin, 2001)

In order to prevent damage to the fibre optic, which is both relatively expensive and fragile, a small “safety layer” must be maintained between the ground surface and the sensor. As a result, this method cannot provide direct contact temperatures, the contact temperature being extrapolated from the temperature measurements (Batako and Rowe, 2005), and, as before, unless done correctly, it can be a source of inaccuracy within the measurements.

2.3.1.2.4 Thermocouples.

Thermocouples are probably the most obvious choice for temperature measurement due to their simplicity and relatively low cost, and consequently have been used in a number of different ways. One method employed is to use either a single or multiple thermocouples mounted below the workpiece surface to determine the effect of grinding parameters on workpiece temperature. If multiple thermocouples are inserted into holes drilled at increasing distances from the ground surface the temperature distribution within the workpiece can be measured (see figure 2.7), with the average surface temperature being calculated by extrapolation (Tawakoli, 1993). Similarly this method can also be used to measure the contact zone temperature, with holes precisely drilled in a pre-determined arc corresponding to the arc of contact of the grinding wheel. A test grind can then be performed with the wheel stopping a short distance (typically 0.1mm) away from the thermocouples to prevent damage. This allows the temperatures very close to the contact zone to be measured (Tawakoli, 1993).

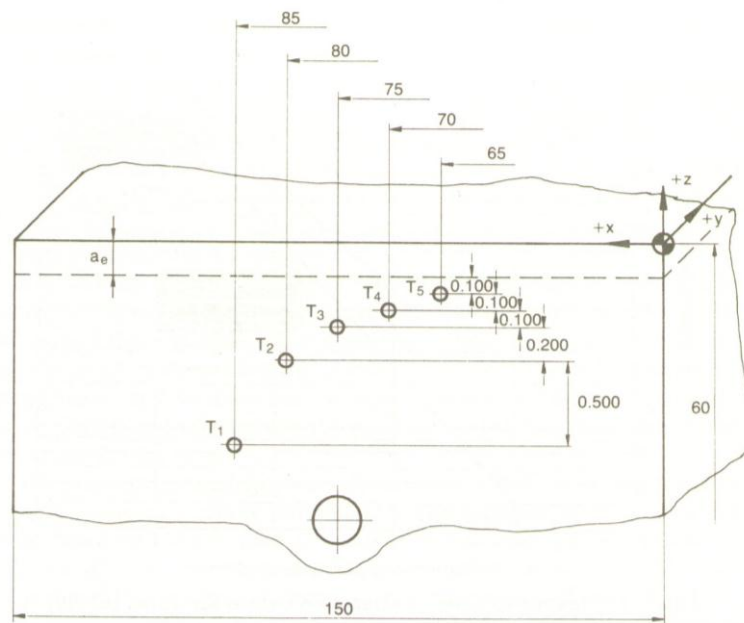


Figure 2.7 Holes drilled into workpiece to allow the temperature distribution to be measured. (Tawakoli, 1993)

Both these methods have the advantage that standard, calibrated thermocouples can be used. These methods are also unaffected by the application cutting fluids, but, as with the fibre optical system described earlier, contact temperatures must be determined by extrapolation (Black and Rowe, 1995). This poses particular problems in HEDG, where the feed rates and contact temperatures are high. The temperature gradient in the material between thermocouple and the ground surface may be steep and non-linear which can result in errors in the extrapolation (Batako and Rowe, 2005). The hole in the workpiece used to mount the thermocouple also affects the temperature measurements, as the volume of heated material is reduced, and this may cause the measured temperature to be artificially high (Black and Rowe, 1995).

An alternative is to use thin film thermocouples, either single or two pole, inserted within a split workpiece and exposed to the ground surface. Such thermocouples can also be inserted into a grinding wheel but this adds to complexity of the system as the signals need to be extracted using high speed slip rings which can be a source of electrical noise (Batako and Rowe, 2005).

Single pole thermocouples, as seen in figure 2.8, are single foil strips, typically 10-15 μ m thick, insulated from the bulk workpiece material, which are then smeared onto the workpiece surface during grinding process, thus creating the measuring junction. Consequently actual contact temperature is measured (Batako and Rowe, 2005). and there is no need for extrapolation. This technique however does require calibration (Black and Rowe, 1995) and the thermocouples are effectively destroyed by the grinding process and need to be replaced. There are also problems associated with maintaining a good measuring junction which can break down, particularly under wet grinding conditions, as can the insulation between the thermocouple and bulk workpiece material (Batako and Rowe, 2005)

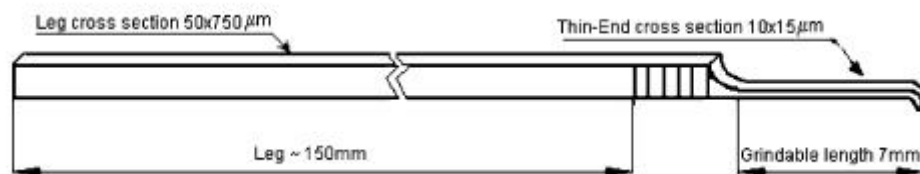


Figure 2.8 Single Pole Thin Film Thermocouple. (Batako and Rowe, 2005)

Two pole thermocouples, as seen in figure 2.9, exposed at the workpiece surface as before, can also be employed. Typically these are made from standard commercially available thermocouples, but the junction between the two thermocouple legs is split and a thin layer of insulation placed between them. This creates a new “grindable” thermocouple which can then be inserted into a split workpiece as before. Once again, very thin thermocouples can be used, typically 50 μ m thick, so as to minimise any temperature distortions around the thermocouple.

During the grind, the junction between the two poles of the thermocouple is recreated and the contact temperature measured (Black and Rowe, 1995). This technique overcomes the calibration issues of the single pole technique (Black and Rowe, 1995;

Batako and Rowe, 2005), but is more difficult to assemble than the single pole method due to the multiple layers of thin mica insulation and fragile nature of the foil elements of the thermocouple. These additional layers also increase its physical size. (Batako and Rowe, 2005)

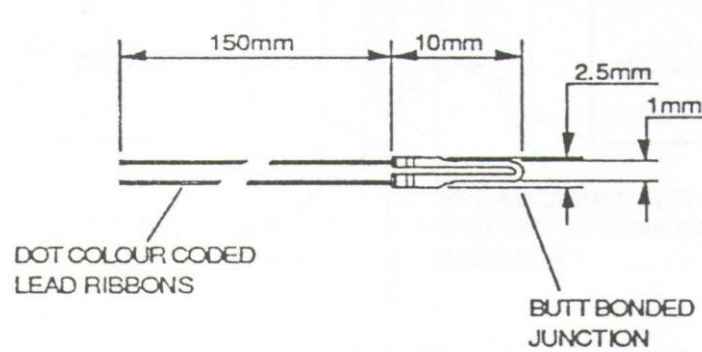


Figure 2.9 Two Pole Grindable Thermocouple Technique (Black and Rowe, 1995).

As stated previously, cooling is not the only thermal characteristic of the cutting fluid, and it is to these other thermal characteristics that attention will now turn.

2.3.2 Lubrication

The next thermal characteristic of the cutting fluid to be discussed is lubrication. When grinding, material is removed by a large number of different cutting edges. Each cutting edge has an indeterminate shape, but each cutting edge is in contact with the workpiece, albeit with a very small contact area. This results in conditions where there is a lot of friction between the grinding wheel and the workpiece, associated with rubbing and sticking friction. The use of a lubricant between the grinding wheel and the workpiece significantly reduces these frictional forces and reduces wheel wear. (Marinescu and Rowe, 2004)

In order to understand the role of lubrication in the grinding process, and the thermal impact fluid lubricity has on the grinding process, it is important to understand the concept of specific grinding energy and its relationship with grinding forces.

The specific grinding energy is defined as the energy per unit volume of material removed (Andrew and Howes, 1985; Shaw, 1996) and for a grinding process it is a measure of process efficiency. An abrasive process is said to be efficient when material is removed rapidly with low power consumption and thus processes that give rise to a low specific grinding energy are considered to be efficient, whereas processes that give rise to a high specific grinding energy are considered to be inefficient (Marinescu and Rowe, 2004).

Specific energy is calculated by

$$\text{Specific Grinding Energy} = \text{Net Machining Power} \div \text{Rate of Material Removal}$$

In mathematical notation this is described as follows:

Equation 2.3

$$e_c = P_{net} \div Q_w$$

Equation 2.3 can be re-written

Equation 2.4

$$e_c = (F_t \cdot v_s) \div (b_w \cdot a_e \cdot v_w) \quad (\text{Marinescu and Rowe, 2004})$$

Where:

e_c = specific grinding energy

F_t = tangential force

v_s = grinding wheel speed

b_w = grinding wheel width

a_e = depth of cut

v_w = work piece feed rate

Equation 2.4 shows the specific grinding energy is proportional to the tangential grinding force (F_t). Many factors affect the tangential force, including the workpiece material, condition of the grinding wheel, size of grinding chips produced, dressing parameters when conventional abrasives are employed, along with the type and quantity of any cutting fluid employed and how effectively it is applied.

However, it is well known that lubrication reduces the friction between the grinding wheel and workpiece (Brinksmeier and Heinzl, 1999). The reduction in the grinding forces is associated with a reduction in both the forces associated with chip formation, and the waste forces associated with ploughing. As a consequence of the reduction of grinding force, the specific grinding energy of the process is also reduced, as the specific grinding energy is proportional to the tangential grinding force (see equation 2.4).

The amount of thermal energy (the total heat flux) generated by the grinding process can be calculated using the specific grinding energy, a relationship which can be seen in equation 2.5. It is therefore quite clear that lubrication reduces the grinding zone temperature (Brinksmeier and Brockhoff, 1997; Malkin, 1989) and can therefore reduce the likelihood of thermal damage for any given set of grinding conditions (Malkin, 1989). In HEDG, where fluid film boiling can occur, prevents the cutting fluid from cooling the grinding zone, the reduction in heat generation due to improved lubrication gives neat oil based cutting fluids a significant advantage over water based fluids (Jin and Stephenson, 2002a; Stephenson and Laine, 2001).

Equation 2.5

$$q_t = e_c \cdot a_e \cdot v_w / l_c \quad (\text{Jin and Stephenson, 2003})$$

Where

q_t = total heat flux
 e_c = specific grinding energy
 a_e = depth of cut
 v_w = workpiece feedrate
 l_c = arc of contact

The fluid film boiling effect inhibits the cooling action of a cutting fluid once a threshold temperature has been reached (Andrew and Howes, 1985; Ohishi and Furukawa, 1985; Howes, 1990), does not prevent lubrication of the contact zone, as it is known that lubricants can lubricate whilst in their vapour phase (Williams and Tabor, 1977). If certain extreme pressure (EP) additives are used, sulphur for example, the high contact temperatures that are characteristic of the HEDG process, actually assist the lubrication process, by activating and promoting the chemical reactions between the EP additive and workpiece that result in a high load carrying film being generated between the workpiece and tool (Kajdas, 1989).

2.3.2.1 Lubrication Testing

In grinding, there are a number of different variables that ultimately determine grinding performance. For example, grinding forces and the specific grinding energy are not simply determined by workpiece material, depth of cut and grinding wheel speed, but other factors such as the specification and condition of the grinding wheel.

The condition of a grinding wheel varies over time as it becomes progressively worn, or if the active surface of the grinding wheel becomes clogged by debris in a process referred to as wheel loading (Khudobin, 1970; Tawakoli, 1993; Marinescu and Rowe, 2004). If conventional, vitrified or metal bonded grinding wheels are used, the dressing parameters, dressing frequency and the condition of the dressing tool will all influence the condition of the grinding wheel, and thus the grinding process. Furthermore, no two grinding wheels can ever be identical even when manufactured to the same specification, as the abrasives grains are randomly orientated and distributed over the active surface of the wheel.

These sources of variance makes it very difficult to formulate a standardised grinding test to determine cutting fluid lubricity, and whilst continuous dressing has been proposed as a possible solution to this problem (Howes, 1990), it is a technique that cannot be applied to electroplated superabrasive grinding wheels used in the HEDG process, as they are not dressed during normal use.

The literature revealed that simply measuring the coefficient of friction obtained from two sliding surfaces lubricated by a fluid is not a particularly meaningful test when applied to machining and grinding processes. This is because the contact conditions between the chip and tool (abrasive grain in grinding) are very different from those of more conventional lubricated sliding surfaces (Williams and Tabor, 1977).

Therefore the lubricity of a fluid is usually tested by means of a Tribometer, an instrument designed to replicate the friction couple under investigation. It does this by not only replicating the materials, but also the contact type in question and the type of contact the two materials form. The use of a Tribometer allows a number of different fluids to be compared, quickly, efficiently and cost effectively (Marinescu and Rowe, 2004).

A number of quite different Tribometer's are used to test the performance of lubricants and include the Timkin method (ASTM D 2782-88 "*Measurement of the EP Properties of Lubricating Fluids (Timkin Method)*" 1988), Falex Pin and Vee method (ASTM D 3233-93 "*Measurement of the EP Properties of Lubricating Fluids (Falex Pin and Vee Block Method)*" 1993) and the Four Ball method ("*Measurement of the EP Properties of Lubricating Fluids (Four Ball Method)*" 1988). (Belluco and DeChiffre, 2001) Unfortunately, there is general agreement that these tests offer poor correlation with real cutting processes (Belluco and DeChiffre, 2001; De Chiffre, 1978), though the four ball tests can provide "useful information on the possible mechanisms of the lubricating behaviour of the fluids relevant to grinding" (Cholakov and Rowe, 1992).

More sophisticated and representative Tribometers have been developed in order to better simulate the contact and materials found in grinding. The "Falex Block on Ring" method has been modified to include a CBN electroplated ring to simulate the grinding wheel (Yamanaka and Hayama, 1998), and Koenig and Vits (Marinescu and Rowe, 2004) developed a Tribometer specially designed for the comparative testing of grinding fluids. This Tribometer is shown in Figure 2.10.

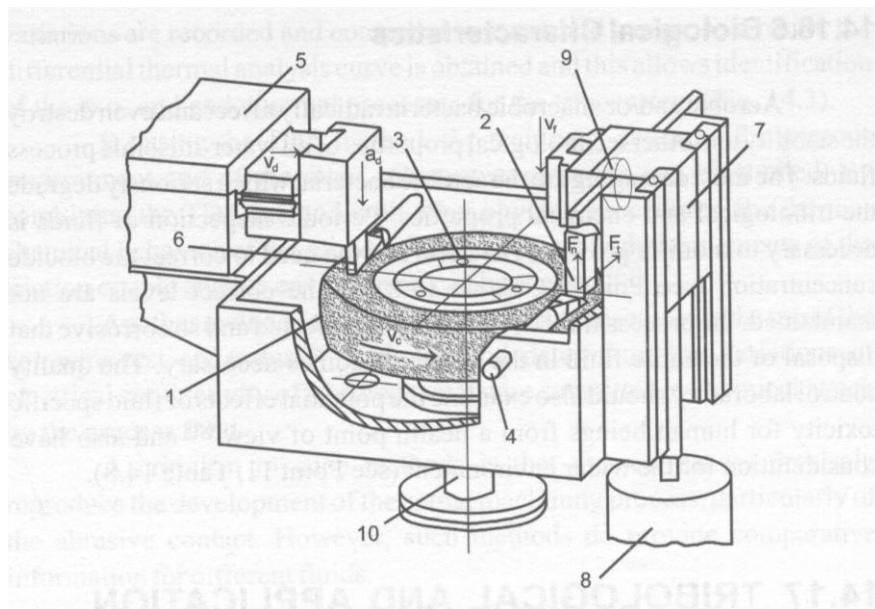


Figure 2.10 Tribometer developed by Koenig and Vits at the Technical University of Aachen (Marinescu and Rowe, 2004).

- (1) grinding wheel, (2) workpiece, (3) balancing washer, (4) fluid inlet,
- (5) dresser, (6) dressing tool, (7) infeed slide, (8) motor, (9) load cell
- (10) main spindle

Unfortunately, the author did not have access to these more sophisticated designs of Tribometer, so a different testing method needed to be selected. The literature revealed a number of alternative methods for testing the lubricity of cutting fluids. Blanchard (1974) investigated several different test methods including lathe plain turning tests, drill life test, drilling force test and tapping torque test and found that a torque tapping test was the most suitable test for comparing both neat oil and water based cutting fluids. DeChiffe (2000), who compared tool life, cutting force (drilling, reaming and tapping) and surface finish test, also found that cutting force tests (torque tapping) offered a relatively low cost and repeatable method for evaluating the performance of cutting fluids.

As a consequence of these findings, torque force (torque tapping) tests were selected as the method to evaluate the lubricity of different cutting fluids, and these results are presented in chapter four.

2.3.3 Fluid Misting and Ignition Characteristics

There are two more thermal characteristics of the cutting fluid that whilst less obvious, they can still impose limitations on the grinding process. These are the ignition and misting characteristics of the cutting fluid. Whilst at first glance these would not appear to be thermal characteristics, the achievable removal rates for any given process may need to be limited in order to reduce the fire hazard if neat oil cutting fluids are used.

2.3.3.1 General Literature on Fluid Ignition

Whilst it is well known that the use of neat oil cutting fluids in grinding poses a fire hazard (Malkin, 1989) and that a fine mist existing within grinding machine canopies, produced when high pressure cutting fluids come into contact with the grinding wheel, also presents a fire hazard (Campbell, 2001), no detailed research into the combustion and ignition of cutting fluids could be found.

It is therefore important to identify the probable sources of cutting fluid ignition during the HEDG process when neat oil cutting fluids were used in order to eliminate or significantly reduce the likelihood of ignition. Unfortunately owing to the volume of cutting fluid typically applied during grinding and the fact that the machines are totally enclosed, effective viewing of the grinding process is seriously inhibited (see figure 2.11). This fact and the unpredictable nature of ignition, definitive identification of the ignition source was virtually impossible and may be one explanation for the lack of detailed literature on the subject

More general ignition and combustion research does provide useful information on the ignition process and likely causes of ignition in the context of grinding. Flammable fluids ignite can when they come into contact with hot surfaces and is a common cause of industrial fires (Bennett and Ballal, 2003). The temperature of a hot surface is not the only factor which determines whether a fluid will ignite. The time a fluid is exposed to the heat source also plays an important role. Exposure to any given temperature for a

short time may not lead to ignition, whilst exposure to a lower temperature for a longer period of time may well lead to ignition (Fisher, 2000). This phenomenon is referred to as residence time, and a cutting fluids ability to withstand an elevated workpiece temperature will therefore be influenced not only by the workpiece temperature and the fluid flow rate.

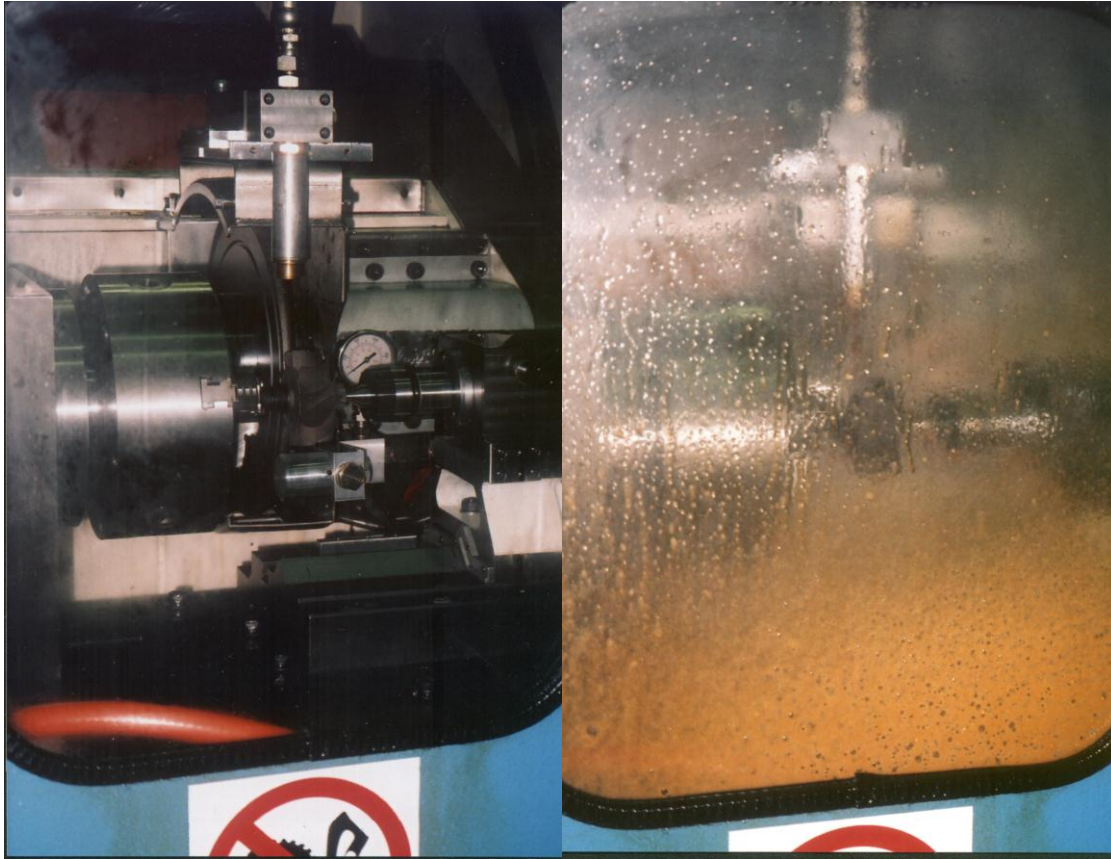


Figure 2.11 *Visibility inside the Grinding Machine is Severely Obscured by the Cutting Fluid.*

The Edgetek SAT Machine. Images show the difference between no fluid (left) and fluid (right) being applied to the grinding zone.

Unfortunately conventional, commonly used and quoted ignition point or flash point tests such as Pensky-Martens Test (IP34/82 : BS2000: Part 34: 1982) and the Cleveland Open Cup Test (IP36/84 : BS4689 : 1971), fail to consider the flow aspect of the ignition process as the fluid is held within a cup whilst it is heated. As a result the ignition point temperatures obtained from such tests may be of limited value. Consequently a new series of tests to determine the ignition characteristics of different cutting fluids are presented in chapter four.

Another possible ignition source, mentioned briefly earlier in this section, was the cutting fluid mist, as it is well known that oil mists can ignite well below their flashpoints (Bowen and Shirvill, 1994; Bowen and Shirvill, 1994a; Maragkos and Bowen, 2002) and that the potential fire hazard is determined largely by the droplet size

with smaller droplets igniting more readily than larger droplets. (Bowen and Shirvill, 1994; Bowen and Shirvill, 1994a).

Unfortunately, accidentally produced fluid mists, such as those found within a grinding machine canopy do not have a defined droplet size, but instead contain a distribution of different droplet sizes and these distributions are notoriously difficult to measure (Bowen and Shirvill, 1994; Bowen and Shirvill, 1994a). This means that developing a model or tool which predicts when cutting fluid mist ignition could occur based on the grinding parameters to be employed, or for that matter, a monitoring system that measures the cutting fluid mist level in the machine canopy to determine whether a pre-determined mist threshold level has been reached, would in practice be very difficult to develop.

This was demonstrated by Zhong et al (2002) when trying to develop a predictive model for aerosol generation in cylindrical grinding when trying to predict the air quality in machine shops. The error between the mist levels predicted by the model and the actual mist measurements taken during verification experiments were in the order of 10-50% (Chen and Liang, 2002).

The most obvious source of ignition in grinding are the grinding sparks which are clearly visible in figure 1.2. Empirically, one would think that these sparks would ignite either the cutting fluid bulk or the cutting fluid mist. However Suzuki et al (1992) attempted to ignite an atomised gasoline and air mixture with grinding sparks. Whilst the results show such a mixture could be ignited by this method, the probability was low as only 3 out of 40 tests conducted under a variety of different test conditions (different grit size grinding wheels, workpiece material, wheel speeds, etc) resulted in ignition despite the fact that the grinding sparks were significantly hotter (approximately 1000°C or higher) than the flashpoint of gasoline. These results show how difficult it is to ignite a mist or aerosol of flammable fluid with grinding sparks. Tests were also conducted to ignite both liquid gasoline and light oil with grinding sparks and found that the bulk fluid could not be ignited by grinding sparks. These findings help to explain why cutting fluid ignition is, thankfully, relatively infrequent.

2.3.3.1.1 *Static Electricity*

Another potential ignition source is static electricity, which is an issue for many manufacturing sectors and its ability to be the source of fire and explosions should not be underestimated. It is however very unpredictable and difficult to detect but the hazards posed by electrostatic ignition can be identified and controlled. Hearn (2003) states that there are five conditions which need to be met for an electrostatic charge to be an ignition hazard.

- Sensitive flammable atmosphere
- Generation of electrostatic charge
- Accumulation of charge
- Electrostatic discharge
- Sufficient discharge energy

Clearly a sensitive flammable atmosphere is already present within the confines of the grinding machine when neat oil is used as a cutting fluid; otherwise there would not be a fire hazard in the first place.

An electrostatic charge can be generated in many different ways. The rate of charge generation can be very difficult to predict, but the sources of generation are well understood. Electrostatic charge is generated during operations where rapid and energetic movement occurs and /or where there is contact and separation of solid surfaces (Hearn, 2003). The following are potential electrostatic charge generation mechanisms within the grinding process (Hearn, 2003).

- The contact and separation of solid surfaces
- Flow / movement of liquids
- Production of mists or aerosols
- Charging by induction in an electric field

It should be noted that the movement of personnel can also generate an electrical charge if their footwear or the flooring are insulated, but as we are specifically looking at in-process sources of ignition this particular source will not be considered.

Flammable hydrocarbon vapours are extremely sensitive to spark discharge ignition, needing only between 0.2-2mJ of discharge energy for ignition (Hearn, 2003). This is a very small amount of energy and with standard light oils exhibiting relatively high evaporation loss characteristics there is clearly a potential for ignition if sufficient vapours are present within the machine canopy. Hydrocarbon droplets of a larger size generally associated with mists require significantly higher discharge energy for ignition, typically between 1-1000mJ of energy (Hearn, 2003).

The accumulation of charge is more difficult to access. However, the accumulation of electrical charge is easily eliminated by ensuring the all the relevant machine components are electrically bonded. Such electrical bonding totally eliminates the risk of ignition by electrostatic discharge, as it removes one of the five key elements, listed earlier, necessary for an electrostatic discharge to occur. Consequently, the earth bonding on both the SAT and the SAM machines was tested very early in the project, and found to be more than adequate. Without any possible accumulation of electrical charge, static discharge was not a possible cause of the machine fires experienced at Cranfield.

2.3.3.2 Cutting Fluid Ignition

Putting the more general literature on combustion and ignition of fluids and fuels into context, it is possible to determine the likely sources of ignition associated with the use of neat oil cutting fluid in grinding and in particular HEDG. Five different ignition sources can be identified when the general concepts of ignition are put into context:

- Cutting fluid mist / vapour combining with hot grinding sparks
- Cutting fluid mist / vapour combining with a hot body
- Ignition caused by elevated workpiece temperature
- Ignition caused by elevated workpiece temperature caused by poor fluid application
- Electrostatic discharge.

The last point in this list, electrostatic discharge is worth mentioning first, as whilst it was eliminated as an ignition source on the machines at Cranfield, in situations where the machine bonding is not adequate, static discharge could still potentially be a problem. In these circumstances, electrical bonding on the machines in question should always be checked and rectified to the appropriate standard. Once the machine bonding is rectified, electrostatic discharge can be totally eliminated as an ignition source.

Two of the other items in the list of possible sources of cutting fluid ignition are as a result of elevated workpiece temperature. It is valuable to discuss possible reasons why the workpiece temperature should be sufficiently raised so as to cause a potential fire hazard.

It is well known that prolonged and excessive grinding zone temperatures, where the thermal energy created by the grinding process is too great to be removed by the cutting fluid, grinding wheel and grinding chip, results in elevated body temperature. There are a number of different causes which include poor selection of process parameters such as depth of cut and feed-rate, inappropriate grinding wheel speed, poor grinding wheel selection.

Whilst these factors may result in excessive workpiece temperatures during the development stages of a process, clearly under normal everyday process conditions, the workpiece temperature cannot normally be sufficiently high as to cause ignition of the cutting fluid otherwise the cutting fluid would ignite during every cycle of the process, and the process would simply be unviable.

Another, more likely cause is the build-up of grinding swarf on the grinding wheel due to inadequate scrubbing and / or cleaning, machine failures such as jamming of the workpiece, cutting fluid delivery failure, or failure in the machine control system. Excessively worn or stripped grinding wheels and the subsequent rise in frictional heat generation will also result in excessive body temperature which can ultimately lead to spontaneous ignition of the cutting oil.

Unfortunately, this particular type source of ignition can never be totally eliminated when oil based fluids are used. Errors in machine set-up, errors in the selection of process parameters or worn grinding wheels would normally manifest themselves before fluid ignition occurs with evidence of workpiece burn if the workpiece was manufactured from steel. Other materials however, such as Inconel, are far more resilient to thermal stress and damage, and ignition could occur before standard quality control procedures detected a problem.

Machine failures are also difficult to prevent, and whilst a sensor may stop a grinding process if the cutting fluid fails, failure of the control system due to fluctuations in the electrical supply for example, are far more difficult to control. Under these circumstances, therefore, a non flammable fluid, or at least one exhibiting a high resistance to ignition, is essential.

Another possible cause of excessive workpiece temperature is attributable to poor fluid application. Whilst under normal circumstances this should not be a problem under certain conditions (for example if the cutting fluid stream is masked by the workpiece or fixture) mainly observed at the end of the workpiece, the flow of cutting fluid to the grinding zone can be reduced as a result of the workpiece geometry (see figure 2.12).

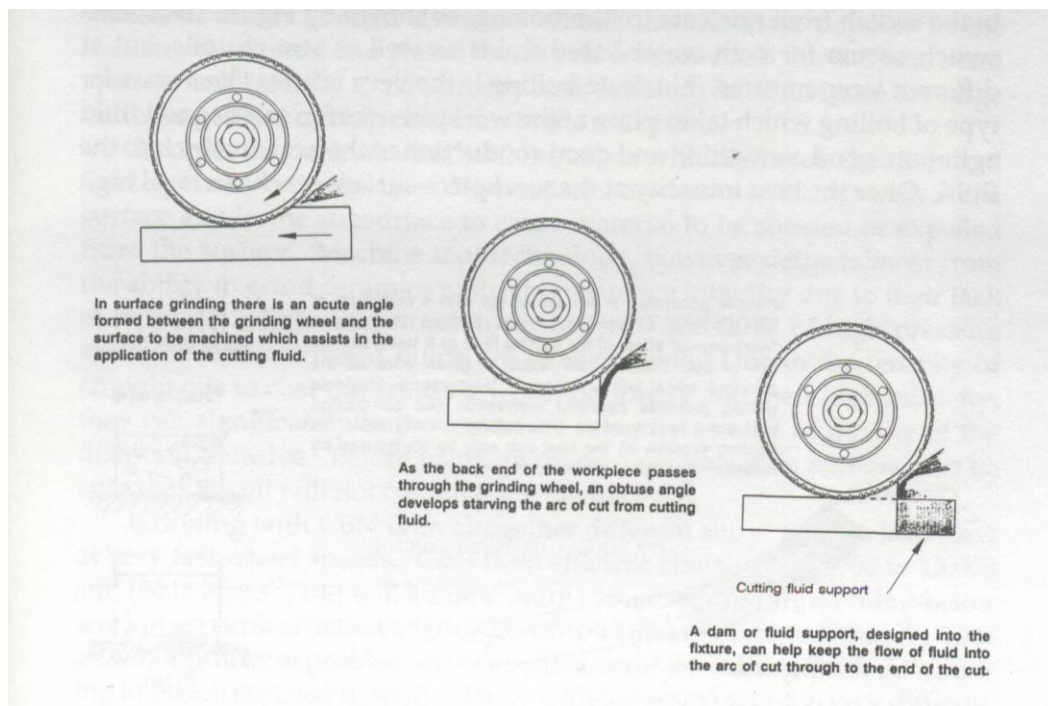


Figure 2.12 The Effect of Fluid Support or Nip Blocks in Creep Feed Grinding (Silliman and Perich, 1992)

Under normal grinding conditions the cutting fluid is pointed at the wheel and forms a “pool” slightly in front of the grinding zone. Secondly the wedge formed by work piece and wheel helps to focus the fluid into the grinding zone. At the end of a cut when surface grinding, or the end of the component in some traverse grinding applications, helical gear grinding for example, fluid is prevented from forming a pool by the edge of the component, as there is no workpiece material to constrain or focus it. As a result there is less fluid within the grinding zone, resulting in less lubrication and increased grinding zone temperatures. These increased grinding zone temperatures could potentially be a source of ignition.

2.3.4 Fluid Misting

The literature presented in the previous sections highlighted the significance of fluid mists in increasing the likelihood of fluid ignition within the grinding zone. Reducing cutting fluid mist is important if the probability of cutting fluid ignition is to be reduced.

Much of the literature surrounding cutting fluid mist is not aimed at a reduction in the fire hazards mists, but in reducing the health hazards associated with these mists. In recent years a raft of new legislation in both the United States and Europe called for reductions in the mist (airborne droplets or aerosols) created by machine tools using cutting fluids. In 1998 the United States, for example, reduced the recommended permissible mist limit in an operator's breathing space from $5\text{mg}/\text{m}^3$ to an equivalent of $0.5\text{mg}/\text{m}^3$ total particulate mass. (NIOSH, 1998).

In order to achieve a reduction in the mist exposure, two main mechanisms were proposed. The first, the use of a machine ventilated canopy or enclosure (Johnston and White, 1995; Dasch and Ang, 2001) which obviously forms a barrier coupled between the operator and the mist, does reduce the mist in the machine operator's breathing space, but does little to prevent the mist being generated in the first place. Another mechanism proposed was the use of polymer anti-misting additives, which whilst very effective at reducing the mist level – up to 70-90% in the some circumstances (Dasch and Ang, 2001), these additives do deteriorate with use, and therefore need constant replenishment (Dasch and Ang, 2001).

The literature did, however, reveal some important factors that influence the amount of mist generated in the machine. The base oil can have a significant influence, with more volatile fluids of comparable viscosities producing more mist than less volatile base oils (Dasch and Ang, 2002; Dasch and Ang, 2001).

Furthermore Dasch et al (2002) reported that both synthetic neat cutting oils along with water based cutting fluids produced significantly less mist than neat mineral oils. The fact that water based cutting fluids produced such low levels of mist was attributed to the fact that unlike neat mineral oils that contain 100% oil, water based fluids only contain approximately 5- 10% oil, the rest being water.

When investigating the mist generated during a milling process, Dasch et al (2002) found that mist is generated when the cutting fluid impacts on the tool and the workpiece, and also found there was a small increase in fluid mist as the fluid velocity increased. This in itself is not surprising, as the faster the fluid velocity, the greater the impact on the tool and workpiece.

However Dasch (2002) found the most significant contribution to the mist level was from the centrifugal spin off of fluid droplets (typically greater than 20 micron in size) from the milling tool (see figure 2.13). It was found that the mist level was related to the square of the tool speed, so was influenced by both the spindle speed and the milling tool diameter.

Figure 2.13 also shows a slight increase in the mist level during the machining process and Dasch et al (2002) attributed this to the possibility that cutting fluid was being evaporated. It then re-condensed as it cooled for form larger particles (typically less than 1 micron is size) which were then detectable by the aerosol monitor used in the tests.

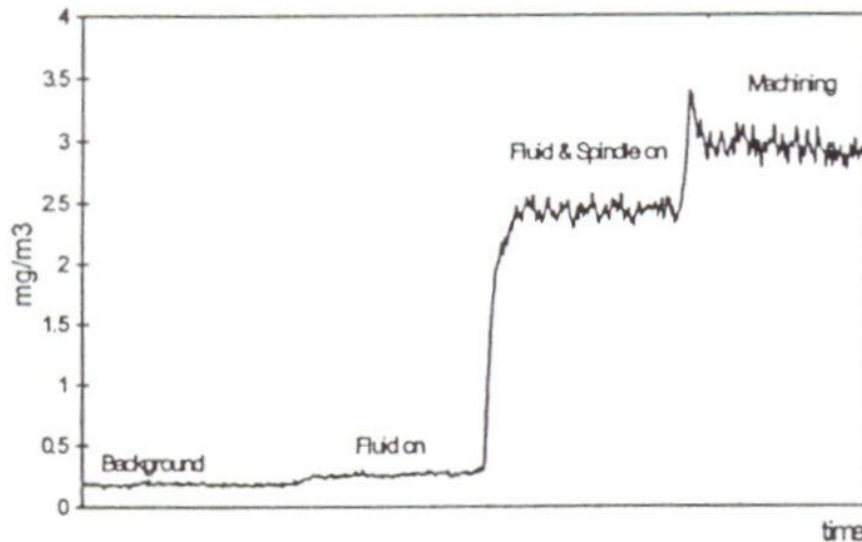


Figure 2.13 Mist Level as a Function of Machine Activity during Milling (Dasch and Ang, 2002)

Mist measurements were taken when face milling aluminium using a water based cutting fluid – 5% concentration.

Whilst none of this literature is specifically aimed at reducing the mist level in a grinding machine in order to reduce the potential fire hazard, the literature presented does give valuable information into some of the factors that influence the mist generation process. Now that the four thermal characteristics of cutting fluids have been discussed, attention will now turn to the cutting fluids themselves.

2.4 Cutting Fluids

2.4.1 Introduction

There are basically three different types of cutting fluids used in the grinding process, neat mineral oils (sometimes referred to as straight oils), water based cutting fluids (sometimes referred to as soluble oils or emulsions), and synthetic neat oils. All have different advantages and disadvantages, and the following sections will give a brief overview of all these types of fluid.

2.4.2 Neat Oils

2.4.2.1 Neat Mineral Oils

Neat mineral oils have been used extensively in previously published research on the HEDG process (Stephenson and Laine, 2001; Jin and Stephenson, 2003; Stephenson and Jin, 2002) and are generally recommended for the HEDG due to their excellent lubricity (Tawakoli, 1993; Jin and Stephenson, 2002a; Stephenson and Laine, 2001). Their use is less than satisfactory because of pollution and safety considerations as their use may present a fire hazard (Malkin, 1989), however, neat oils have been found to increase grinding wheel life by up to 50 times.

Neat oils also offer certain advantages over water based cutting fluids in most grinding regimes because of their excellent lubrication characteristics as, with the “notable exception of creep feed grinding, cooling by grinding fluids appears to be generally ineffective in lowering the peak temperature within the grinding zone”(Malkin, 1989). The high lubricity of cutting fluids reduces wheel wear (see figure 2.14) which in turn helps to reduce the grinding forces and as a consequence the grinding zone temperature and the likelihood of thermal damage is reduced in comparison to water based cutting fluids.

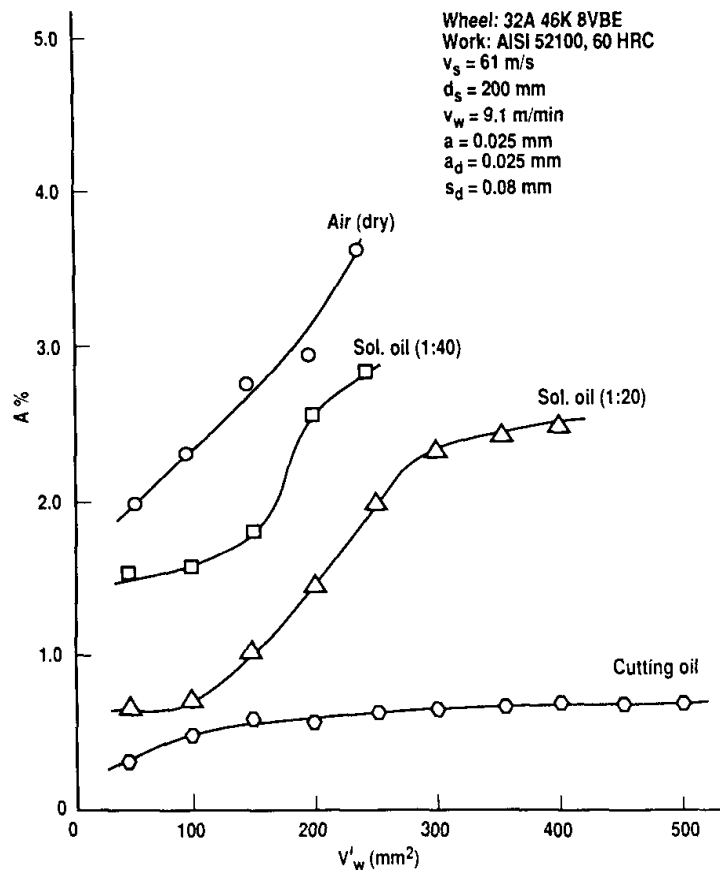


Figure 2.14 The effect of cutting fluid selection on grinding wheel wear (Malkin, 1989)

The graph shows the accumulated wear flat area ($A\%$) versus the accumulated material removal per unit width (V'_w) for an aluminium oxide grinding wheel used in a straight plunge grinding operation.

Mineral oil cutting fluids are a mixture of liquid hydrocarbon molecules obtained from refining and distilling crude oil. Mineral oil cutting fluids contain a wide range of hydrocarbon molecules of various different molecular and specific weights, along with impurities such as sulphur, oxygen and nitrogen compounds. The composition of the base oil is a major factor in determining important properties of cutting fluid including viscosity, lubricity and service life (Marinescu and Rowe, 2004). Mineral oil cutting fluids have excellent lubricity but they are far less efficient at cooling when compared to water based cutting fluids.

Neat oil cutting fluids are also “CBN” friendly, an important factor when using superabrasive grinding wheels. The water in water soluble cutting fluids has a tendency to react with CBN, promoting grinding wheel wear (Carius, 1990; Malkin, 1989). Since neat oil cutting fluids contain no water, there is no such problem.

Neat oil cutting fluids, in common with water soluble cutting fluids tend to contain EP additives to enhance the performance in the high pressure contact conditions found in cutting and grinding. These will be discussed later in section 2.4.6

2.4.2.2 Vegetable Oils

Neat mineral oils are not the only type of neat oil cutting fluid available. Vegetable oils are increasingly being promoted as an “environmentally friendly option”, but there is general agreement within industry that they are simply not suitable for grinding applications.

This appears to be borne out by findings by Suda et al (2002) who found that whilst these types of fluids may be biodegradable, their performance in two different standard lubrication tests was poorer than ester based synthetic products. Furthermore Suda et al (2002) found that the vegetable oil tested, performed poorly in an oxidation stability test in comparison to ester based cutting fluids, which means the useful service life and storage life of these fluids is questionable.

2.4.2.3 Organic Ester based Synthetic Neat Oils

Ester based synthetic neat oils can be considered as relatively new products aimed at applications where mineral oils are less than satisfactory (Marinescu and Rowe, 2004). Ester based fluids are manufactured by synthesising acid with alcohol, a reaction which produces the organic ester and water (see figure 2.15). This, however, is not a one way operation, and in the presence of water, esters can revert back to the base elements of acid and alcohol. (Bock, 2004)

This deterioration can ultimately determine the service and storage life of the fluid and the change in acidity of the fluid must be monitored to ensure that it is still in good condition. Such deterioration is especially important in processes where cutting fluid usage is minimised as fluid consumption is low. In these situations the cutting fluid must remain stable for long periods of time (Suda and Yokota, 2002).

In general organic ester based neat oils offer good thermal, oxidation and lubrication stability, and whilst relatively expensive, costing approximately 10 times more than mineral oils (Marinescu and Rowe, 2004), ester based fluids offer a good compromise between cost and performance when compared to other types of synthetic neat oils such as silicon based compounds and halogenated organic compounds, which can be between 20 and 250 times more costly in comparison to mineral oils (Marinescu and Rowe, 2004). However, it should be noted that recent, well publicised increases in the cost of oil, which have reduced the cost differential between neat mineral oil and organic ester lubricants.

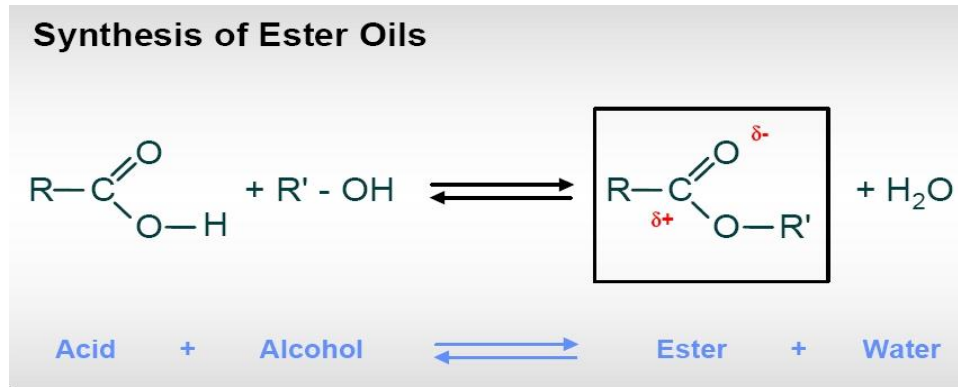


Figure 2-15 Synthesis of Ester Based Synthetic Oils (Bock, 2004)

2.4.3 Water Miscible Fluids (Water based Emulsions)

An emulsion is a suspension of oil droplets in water made by blending the oil with emulsifying agents or other materials. The high specific heat capacity, high thermal conductivity, and high heat of vaporisation makes these types of fluid the most effective cooling media known (Silliman and Perich, 1992). Water miscible fluids offer less rust control and corrosion inhibition than neat oil cutting fluids (mineral oil or synthetic) due to the introduction of water, though these fluids may contain anti-corrosion additives which can prevent the onset of any corrosive activity for almost one week (Silliman and Perich, 1992).

The viscosity of water based fluids is extremely low, almost equal to water, and as a result, its inherent film strength and lubricity are substantially lower than neat cutting oils resulting in higher abrasive wear of the grinding wheel. The shortcomings of water based fluids in heavy grinding operations such as thread and crush grinding, where wheel form must be maintained, has long been known (Silliman and Perich, 1992).

There is a further problem associated with the use of water based fluids in conjunction with CBN grinding wheels as there is a tendency for CBN to react with high temperature water (Carius, 1990; Malkin, 1989). This can result in accelerated breakdown of the abrasive CBN grits and the subsequent reduction in wheel life.

Partly due to their relatively low initial costs, water soluble cutting fluids have far greater acceptance in industry. However, whilst they may be considered as being

acceptable for most grinding applications, the poor lubrication properties of water based cutting fluids result in higher grinding forces, higher specific grinding energy and higher grinding wheel wear. Even the very best, heavily lubricated emulsions still require approximately 20-25% more grind power in comparison to neat oils with lubrication additives, which can result in greater thermal stress in the workpiece.

Water based cutting fluid systems require constant monitoring if their performance is to be maintained, and this can prove expensive, though in practice this rarely happens. The concentration of the emulsion varies over time, and requires frequent checking and replenishment as the water evaporates. Bacteriological activity is also a problem, which not only poses a health and safety risk, a subject that will be discussed later, but actually reduces the performance of the fluid. Hallet et al (1998) reported that this deterioration of fluid performance could lead to grinding burn, if the biocide level in the fluid was too low. On the other hand, oil based fluid systems are generally considered to be maintenance free, though as will be shown later on in this thesis, this is not strictly true. However, neat oil cutting fluid systems are much less maintenance intensive than water based cutting fluids.

The performance of the water based fluids can also vary with local water supply, with additional antifoam additives needed if the water is soft, or additional anti-corrosion additives needed if the water is hard.

2.4.4 Extreme Pressure (EP) Additives

In order to enhance the lubrication performance of cutting fluids, extreme pressure (EP) additives are extensively used in both neat oil and water soluble cutting fluids to provide tougher more stable solid film lubrication. This is achieved by a chemical reaction between the EP additive and the highly reactive, freshly machined surface which results in a high load carrying film being generated between the workpiece and tool that prevents welding of the surfaces (Kajdas, 1989), effects lower cutting / grinding forces, reduces chip thickness and improves surface finish (Silliman and Perich, 1992).

The high localised temperatures found in machining and grinding operations helps to activate and promote this process, but the very high temperatures found in HEDG mean that EP activated cutting fluids containing reactive sulphur, chlorine or phosphorous components are preferred over fluids containing milder EP additives such as fatty acids or soaps, which are more suited to less severe operations (Kajdas, 1989). The activation temperatures of different EP additive types can be seen in figure 2.16.

Chlorinated paraffin extreme pressure additives have been extensively used in metalworking fluids for a number years, though their use is becoming increasingly unpopular due to environmental, and health and safety concerns. As a result, their use is being restricted and many cutting fluids are now employing alternative EP additives such as sulphur, phosphorous and sometimes esters (Jones, 2004).

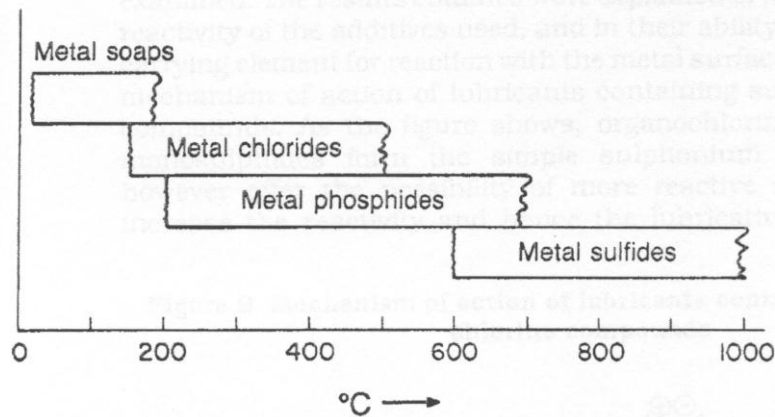


Figure 2.16 Active temperature ranges of extreme pressure (EP) additives commonly used in cutting fluids. (Kajdas, 1989)

2.5 Factors Associated with the Use of Cutting Fluids

2.5.1 Health and Safety

The use of cutting fluids in material removal processes can pose significant health and safety risks. Any cutting fluid that generates a mist, whether it be water or oil based, may cause respiratory ailments such as chronic bronchitis, occupational asthma and loss of lung function (Sutherland and Kulur, 2000). Prolonged exposure may cause cancer of the oesophagus, stomach, pancreas, larynx, colon and rectum (Gunter and Sutherland, 1999). It is for this reason that there are strict limits on the amount of mist a machine operator can be exposed to. In the UK these limits stood at 3mg/m^3 for oil based cutting fluids and 1mg/m^3 for water based cutting fluids (Health and Safety Executive, 2002) but at the time of writing it understood these limits are under review.

There is also a serious hazard of skin dermatitis when water based fluid systems are used (Howes and Tonshoff, 1991) and they are always susceptible to bacteriological activity that can be potentially damaging to health (Horner, 2003; Coughlin and Williams, 1992). Water based fluid systems therefore require the use of anti-bacterial agents that require frequent checks and possible replenishment, with the subsequent impact on full life cycle costs.

It was however a very serious fire hazard that was one of the principal motivations for this research project. Both Cranfield University and Holroyd have witnessed a number of machine fires associated with the use of neat oil with HEDG. This fire hazard continues to be of great concern not only because of the serious risk to personal safety, but it also prevents greater acceptance of HEDG within industry.

2.5.2 Economic Costs

Cutting fluids represent a significant proportion of the total manufacturing costs, with surveys showing that between 7%-17% (Klocke and Eisenblatter, 1997) of the total production costs are attributable to the use of cutting fluids when the cost of purchase, maintenance and waste disposal are taken into consideration. Some suggest that the cost is even higher, nearly 20% (Brinksmeier and Brockhoff, 1997) and whilst these figures may be reasonably old, both sets of results were published in 1997, it is clear there are significant costs associated with the use of cutting fluids.

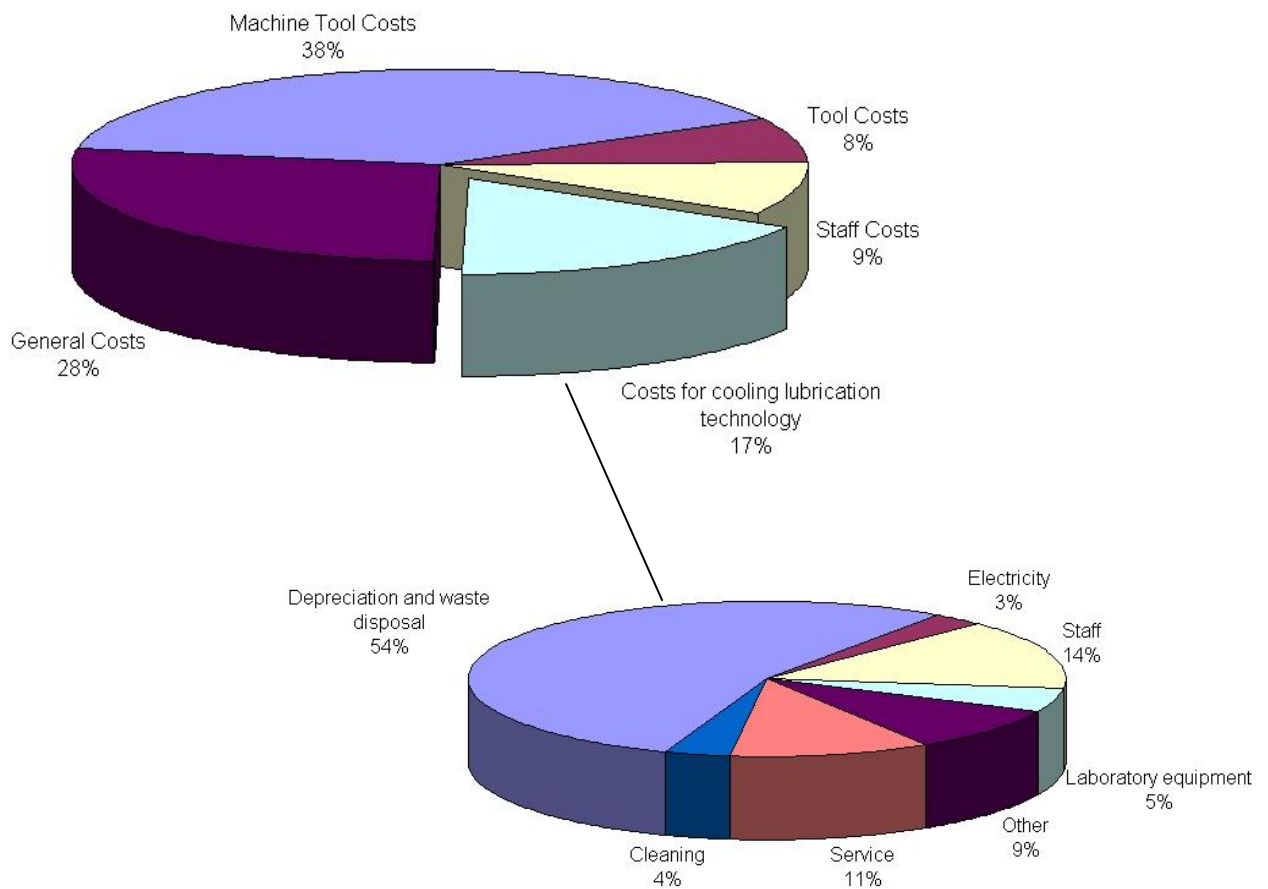


Figure 2-17 Crankshaft Manufacturing Costs for a German Automotive Manufacturer (Brinksmeier and Brockhoff, 1997)

The uppermost pie chart, shows the total manufacturing cost breakdown for a German automotive manufacturer, whilst the second pie chart (bottom left) gives the cost breakdown associated with the use of cutting fluids.

2.5.3 Environmental

In recent years the environmental impact of all lubricants, which obviously includes cutting fluids, has led to a raft of legislation being introduced aimed at minimising any potential ecological damage. For instance European legislation has forced the removal of nitrite from cutting fluids as well as short chain chlorinated paraffin's which were used for as extreme pressure additives (Bartz, 2001).

However, legislation is not the only factor forcing both the manufacturers and end users of cutting fluids to investigate what impact cutting fluids have on the environment. Bartz (1998) lists a total of five drivers which are:

- 1) Environmental Facts
- 2) Public Awareness
- 3) Government Directives and Regulations
- 4) Globalisation of Markets
- 5) Economic Incentives

Environmental facts and public awareness of these facts go hand in hand in putting pressure on companies to adopt more environmentally conscious policies. Government legislation on the other hand tends to force companies to reduce the toxicity of all waste including cutting fluids being returned to the environment and to increase the biodegradability of their waste products (Bartz 1998).

In recent years a number of environmentally friendly biodegradable cutting fluids have been introduced into the market. A biodegradable cutting fluid is one where micro-organisms can ingest and metabolise the fluid and essentially return it to nature. However, for total biodegradability to be achieved all the components of the fluid need to be completely broken down. If one or more components of the fluid cannot be broken down, then it is considered to be only partially biodegradable (Bartz 1998).

The biodegradability of a cutting fluid can be measured, but unfortunately several different standards and testing methods exist to generate the required data. This can lead to some confusion over what "biodegradability" actually means. However, an International Standard – ISO 15380 does exist, and this standard stipulates that at least 60% of the major components of the cutting fluid, for example the base fluid used to manufacture the cutting fluid has biodegraded after 28 days (Battersby, 2004).

2.6 Non Conventional Cooling Media

In recent years there have been studies carried out to test more exotic methods of cooling and/or lubricating the grinding zone. Cryogenic cooling fluids, solid lubricants and compressed air have all been proposed and used to varying degrees of success. All have limitations when applied to HEDG. The following is a brief list of these methods and some of the limitations.

2.6.1.1 Cryogenic Cooling

As the name suggests this involves applying super cooled nitrogen to the grinding zone to control the workpiece temperature but unfortunately this technique can adversely affect the accuracy of the grinding machine. The super cooled nitrogen being applied to the workpiece can set up large thermal gradients with the machine structure and consequently seriously impair the dimensional accuracy and stability of the machine tool. The cost of liquid nitrogen also makes the process uneconomical for normal grinding processes (Paul and Chattopadhyay, 1995) and there are problems associated with grinding wheel wear and the subsequent reduction in wheel life due to the low lubrication properties of liquid nitrogen.

2.6.1.2 Solid Lubricants

Solid lubricants such as graphite and molybdenum disulphide have been suggested as possible alternatives to cutting fluids as way of providing lubricant to the grinding zone. Shaji et al (2002, 2003) attempted to use graphite as a lubricant and whilst finding that this offered good lubrication properties there were problems associated with wheel loading as there was no mechanism for flushing away grinding debris and cleaning / scrubbing the grinding wheel.

In an attempt to overcome these problems, Jarleton (2003) conducted an investigation into the use of molybdenum disulphide solid lubricant in conjunction with conventional cutting fluids (neat oil and a water based cutting fluids) applied purely for the purposes of cleaning the grinding wheel.

Whilst Jarleton (2003) did conclude that solid lubricants were preferable to water based cutting fluids for both the shallow cut and HEDG regimes, their use resulted in a reduction in the specific grinding energy as well as a reduction in the grinding power, he found their use was more problematic in the creep feed regime as there was a significant rise in the workpiece temperature. This may have been attributable to the fact the both the grinding power and the specific grinding energy increased when solid lubricants were used in the creep feed regime. However since over 90% of the thermal energy is removed by the fluid in creep feed grinding, the fact that solid lubricants offer little or no cooling probably explains the significant rise in the workpiece temperature.

Jarleton (2003) also found there was no significant difference in the specific grinding energy or grinding power when solid lubricants were used in comparison to conventional neat oil cutting fluids for the shallow cut, creep feed or the HEDG regimes. This result is, however, hardly surprising when one considers that the neat oil cutting fluid used for these particular investigations contained extreme pressure additives specifically designed to activate at the temperatures found in the grinding zone and would have therefore formed stable solid film lubricants in the grinding zone.

Furthermore Jarleton (1993) showed that all the benefits attributable to the use of solid lubricants in comparison to water based cutting fluids were equally valid when neat oil cutting fluids were used without the increase in surface roughness that was experienced when using solid lubricants during these investigations.

2.6.1.3 Air / Oil mists

This technique is more normally associated with cutting operations such as some milling and precision diamond turning operations, but it also has been used in some grinding operations. A very light, low viscosity lubricant is normally used which readily atomises to a fine air / oil mist that can be directed very precisely to the cutting or grinding interface. The technique has been used with some success for small material removal rates, but lubrication is not sufficient when higher material removal rates are employed.

There is an additional problem associated with air / oil mists which is the deliberate atomisation of light cutting oils. This can produce an extremely volatile atmosphere within the machine which can ignite when in contact with hot surfaces or grinding sparks. There are also health and safety risks associated with the use of air / oil mists, a subject that was discussed in section 2.5.1.

2.6.1.4 Water

Since cooling is an important function of the cutting fluid, pure water (as opposed to water based emulsions) has occasionally been used. Water however offers very poor lubrication which can lead to excessive wheel wear, and excessive workpiece temperatures especially at higher material removal rates. Secondly, pure water will corrode ferrous workpieces and it can also quickly corrode the machine structure of the grinding machine leading to increased maintenance costs.

2.6.1.5 Dry Grinding

Dry machining and grinding processes have for some time been seen as potentially ecologically friendly and economical manufacturing processes where cutting fluids are not used. Future environmental and occupation health and safety legislation coupled with the increasing costs of waste disposal makes dry machining an attractive proposition, and in time industry may be compelled to implement dry processes (Sreejith and Ngoi, 2000).

Dry machining or cutting processes are the most common, often using special self lubricating coatings applied to the cutting tools (Byrne and Dornfeld, 2003) to minimise friction and thus heat generation. Salmon (2000) refers to the example of Daimler Benz where a 16% cost saving was achieved by dry machining. Whilst this may have been a conventional metalworking process, it still generated considerable excitement within the industry and the cost saving is often quoted.

There are however significant disadvantages with dry grinding such as the higher contact temperatures, higher grinding forces and lower wheel life attributable to the lack of lubricant and the resultant increase in thermal wear, dust generation and a lack of corrosion protection for both machined ferrous surfaces and possibly even the machine structure (Salmon, 2000). In truth cutting fluids are a vital ingredient in the majority of grinding operations, and the heavy machining nature of HEDG means the use of cutting fluids are indispensable.

2.7 Cutting Fluid Application

Cutting fluids have traditionally been applied in “a lot help a lot” manner despite the fact that only a small fraction of the cutting fluid actually penetrates the grinding contact zone and performs “useful work” (Brinksmeier and Brockhoff, 1997). In many industrial applications, cutting fluid is applied to the cutting zone using a wide variety of different designs with varying degrees of sophistication. The “bent pipe” approach is quite common, consisting of nothing more than an open section of pipe bent in such a way as to direct the fluid stream towards the grinding zone. Various designs of fabricated rectangular nozzle are also common, usually in the form of a “slit” nozzle, whereby the nozzle aperture is relatively narrow in comparison to the overall width, designed in an attempt to produce a relatively flat stream of cutting fluid to cover the active surface of the grinding wheel.

Applying the cutting fluid through the grinding wheel has also been proposed (Graham and Whiston, 1978; Sun and Xu, 2002), and whilst such an approach appears to work relatively well in reducing the grinding zone temperature in creep feed grinding thereby allowing higher material removal rates to be achieved (Sun and Xu, 2002), there are two major practical considerations which make through wheel fluid application difficult to apply in industrial applications. The first of these is the cleanliness of the cutting fluid. If the fluid is poorly filtered, then the grinding wheel itself can become clogged and the system will cease to function altogether (Graham and Whiston, 1978). This is a particular problem when using conventional grinding wheels, but the problem is also applicable to superabrasive grinding wheels if the ports in the grinding wheel are relatively small. Secondly, and perhaps more importantly when considering the HEDG regime, through wheel fluid application tends to produce disproportionately high levels of cutting fluid mist (Graham and Whiston, 1978).

Irani and Bauer (2005) performed an extensive review of the many different types of cutting fluid application methods and divided them into common and uncommon methods. Irani and Bauer (2005) describe two different common method of fluid application, the first is the coherent jet nozzle the second being the shoe nozzle, and these will be discussed separately below.

2.7.1 Coherent Jet Nozzle

The coherent jet nozzle (Cui, 1995) produces a highly coherent, laminar stream of cutting fluid that can be accurately focused toward the grinding zone. This is shown in figure 2-18, and it is important, for if the cutting fluid is to be effective in cooling and lubricating the grinding zone it is essential that it is directed properly into the grinding zone (Webster and Cui, 1995).

The design of the coherent jet nozzle is fundamental in producing a highly coherent, laminar stream of cutting fluid. The internal shape of the nozzle should have a high contraction ratio from inlet to outlet as shown in figure 2-19. The internal surfaces of the nozzle, past which the cutting fluid flows, should be smooth and concave and the nozzle aperture should have sharp corners Irani and Bauer (2005).

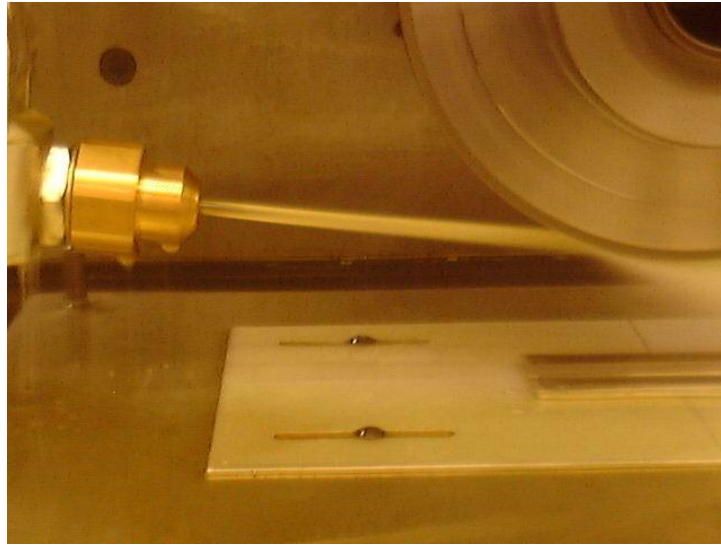


Figure 2-18 Coherent Jet Nozzle fitted to the Edgetek SAM Machine (Courtesy of Cranfield University)

Whilst it is relatively easy to produce round nozzles to this design, it is also possible to make rectangular coherent jet nozzles designed to provide a wider coverage of the active surface of the grinding wheel. However, manufacturing these nozzles is more complex, and as a result it is normal to produce either a large single round nozzle to provide sufficient coverage, or to use a number of smaller nozzles (Irani and Bauer, 2005).

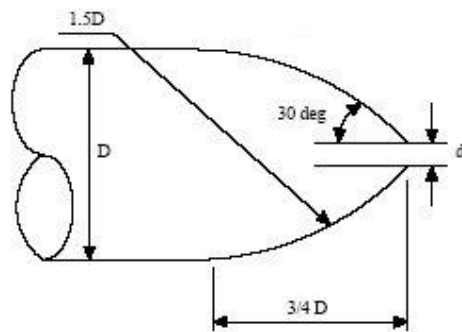


Figure 2-19 Coherent Jet Nozzle (Cui 1995; Webster and Cui, 1995)

Over recent years, these particular nozzles have become increasingly popular due to their high performance in a variety of conditions in both academic, but perhaps more importantly, industrial applications where the simplicity and robustness of the design makes them relatively easy to implement. An important factor in this is the fact that the effectiveness of the nozzle is relatively insensitive to the angle at which the fluid is applied to the grinding wheel thus simplifying machine set-up (Webster and Cui, 1995).

Furthermore, because the jet is highly coherent, it can still apply cutting fluid accurately to the grinding zone even when positioned a relatively large distance, over 300mm, from the grinding zone (Webster and Cui, 1995). This is an extremely important factor

when selecting cutting fluid nozzles, as in many industrial applications, such as camshaft and crankshaft grinding for example, a large amount of tooling is used to clamp and hold the component. There may also be a significant number of gauges used for in-process measurement of the part. The ability to be able to position the nozzle a significant distance from the grinding zone is an important consideration, as this may significantly simplify the design of the tooling and gauging used on the machine.

However, the use of a coherent jet nozzle does not guarantee a highly laminar stream of cutting fluid will be applied to the grinding zone. If the pipe work used to connect the nozzle to the cutting fluid delivery system has a number of changes in bore diameter, or there are a number of elbows used in the system, it can have an adverse effect on the coherency of the jet. It is important to minimise any elbows and any changes in diameter in the pipe work used in the supply line to these nozzles, and if necessary flow conditioners can be used. These can make a significant improvement to the uniformity of flow and thus the coherency of the jet.

2.7.2 Shoe Nozzles

A shoe nozzle is a low pressure method of applying cutting fluid to the grinding zone, an attractive proposition as high pressure pumps can be extremely costly. A shoe nozzle fits over the grinding wheel and covers not only the active surface of the grinding wheel, but also both side walls of the wheel (Brinksmeier and Heinzl, 2000). Very low pressure cutting fluid is then supplied to the shoe nozzle where it is applied directly to the grinding wheel, effectively coating the wheel with a layer of cutting fluid. The fluid is then accelerated up to the wheel speed by the grinding wheel itself as it travels through the nozzle. The cutting fluid then exits the shoe nozzle, clinging to the surface of the grinding wheel whilst travelling at circumferential wheel velocity before entering the grinding zone (Klocke and Baus, 2000).

Shoe nozzles have been proven to be very effective as they can maximise the amount of cutting fluid entering the grinding zone, whilst minimising the total amount of cutting fluid used (Klocke and Baus, 2000). However, it is important to note that the amount of fluid supplied to the shoe nozzle is largely determined by the closeness of the fit between shoe nozzle and the grinding wheel. If the gap between the shoe nozzle and the grinding wheel is large, fluid flow rates can be very high.

Furthermore, unless the gap between shoe nozzle exit point and the grinding zone is kept to a minimum, the grinding fluid can be spun off the grinding wheel because of the centrifugal force. This can result in a reduction in the amount of fluid entering the grinding zone, and an increase in the mist level within the machine.

There are many different designs of shoe nozzle. Ramesh and Yeo (2001) developed a shoe nozzle with 3 adjustable orifice jets to improve the cutting fluid application when grinding with CBN grinding wheels and this is shown in figure 2-20. The first jet disrupts the air curtain surrounding the grinding wheel, with the second orifice supplying the cutting fluid which coats the grinding wheel surface. The third orifice sends cutting fluid directly into the grinding zone. Tests performed with this nozzle

showed a 40-60% reduction in the grinding forces and an improvement in the surface finish in comparison with a conventional coolant application set-up.

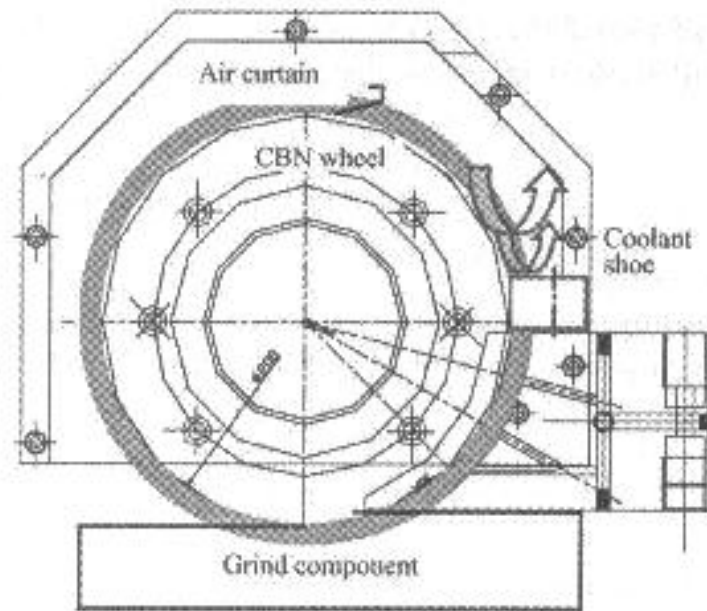


Figure 2-20 Shoe Nozzle for High Efficiency Grinding (Ramesh and Yeo, 2001)

2.7.3 Minimum Quantity Lubrication

No discussion of cutting fluid application would be complete without considering the concept of minimum quantity lubrication, or MQL as it is more commonly known. It is often considered simply as a method of applying cutting fluid as an air/ oil mist to the tool / workpiece interface as discussed previously in section 2.6.1.3. However, this is not a fair reflection of MQL, as it is a philosophy of applying just enough lubricant to the grinding zone (or tool / workpiece interface in cutting processes) to ensure proper lubrication.

Shoe nozzles have been proposed as a suitable method for applying minimum quantity lubrication in grinding operations (Klocke and Baus, 2000; Klocke and Beck, 2000), but air oil mist have also been used, supplying 0.5ml/min of cutting fluid to the grinding zone (Brinksmeier and Brockhoff, 1997) albeit when grinding at very low specific removal rates, typically less than 15mm³/mm.s.

It is typical in many grinding operations to apply significant volumes of cutting fluid. Flow rates of tens if not hundreds of litres per minute are common even though it is well known that only a small proportion of this ever enters the grinding zone. When using a CBN grinding wheel in conjunction with a shoe nozzle, Klocke and Beck (2000) states that only flows of less than 0.5l/min per mm of grinding wheel width can be forced onto the grinding zone. If the cutting fluid delivery rate is higher than this, the extra cutting fluid does not enter the grinding zone, but flows unused past the contact point. Flows exceeding 0.5l/min per mm of grinding wheel width merely acts as a parasitic loss, not

only due from a fluid delivery system perspective, but also due to an increase in the normal grinding force.

2.8 Component and Surface Quality

Thermal damage and its avoidance is an important theme running throughout this thesis. This topic and the more widely understood aspects of workpiece quality, such as the achievement and maintenance of predetermined dimensional, form and surface finish tolerances will be discussed in the following sections.

2.8.1 Thermal Damage

It is well known that excessive heat generation in the workpiece surface of a ground component, caused by improper or abusive grinding conditions, may result in thermal damage to the workpiece. Poor selection and application of cutting fluids also play an important role in determining whether thermal damage occurs (Howes and Gupta, 1990).

Thermal damage of the workpiece surface includes “burn”, a general term to describe several different types of damage caused by high temperatures and the formation of tensile residual stresses (McCormack and Rowe, 2001).

2.8.1.1 Grinding Burn

Excessive workpiece temperature during grinding can cause the formation of surface oxidation and subsurface metallurgical changes. These changes fall in to three categories (McCormack and Rowe, 2001).

- Surface Oxidation
- Re-hardening Burn
- Overtempering / Temper Burn

McCormack and Rowe (2001) provide a very thorough examination of the different categories of workpiece burn which is summarised in the following paragraphs.

Surface oxidation is the discolouration of the workpiece surface similar to the temper colours produced during standard heat treatment processes, though the temper colours are produced at quite different temperatures. The thickness and colour of the oxide layer is determined by both time and temperature and, for normal grinding wheel speeds, are higher than one would find in standard heat treatment. This is because the workpiece is exposed to high temperatures for a significantly shorter time period, typically a few milliseconds, in comparison to standard heat treatment.

The presence of a slight oxide layer, which can be removed by polishing, may or may not be detrimental to the reliability of the workpiece, and will depend on the exact

function of the finished component. If the workpiece is a critical component, surface oxidation is unacceptable as it may be associated with more profound subsurface metallurgical and tensile residual stress problems.

Re-hardening burn occurs if the workpiece material has already been hardened and tempered. When a grinding wheel passes over the workpiece, the surface layers are subjected to rapid heating and then cooling. If the grinding temperature is sufficiently high to allow the formation of austenite, when the wheel has passed, the surface cools rapidly at a rate faster than the critical cooling rate of the material which results in the rehardening. The rapid cooling is a combination of bulk cooling from the workpiece, and depending on the fluid application strategy employed, the quenching action of the fluid (Walton and Stephenson, 2006).

The cooling can be so fast, that there is insufficient time for transformation to any phase but martensite which is not controlled by diffusion but is driven by the cooling action. Rehardening may result in the formation of untempered martensite (UTM) or white layer which is extremely brittle and may reduce the service life of the component (Shaw and Vyas, 1994)

In less severe grinding operations, one where the grinding temperature exceeds the original tempering temperature of the previously hardened workpiece material, but is insufficiently high as to cause a phase transformation in the material, then overtempering or “temper burn” will occur. This will cause the surface layer of the workpiece to be softened, and this can lead to a reduction in the wear resistance of the component (McCormack and Rowe, 2001).

2.8.2 Residual Stress

Compressive residual stresses have a beneficial effect on the fatigue life of dynamically loaded components which can be significantly reduced if micro-cracks and or tensile residual stresses are present. (Snoeys and Leuven, 1978)

Residual stress is defined as the stress which would exist on an elastic body if all the external load, acceleration or gravitational forces were removed (Heindlhofer, 1948). Residual stress in grinding is brought about either as a result of thermal expansion or contraction during the process or as a result of the load exerted on the workpiece surface by the grinding wheel. Both cause permanent deformation of the material and as a result the residual stress persists at room temperature (Heindlhofer, 1948) and can therefore be measured. Residual stresses in the workpiece surface layer affect the service life of the component, with tensile residual stresses tending to promote micro cracking of the workpiece surface layer and a subsequent reduction in service life.

Balart and Bouzina et al (2004) describes the different thermo-mechanical effects which generate residual stress in the workpiece as a result of the grinding process as follows:

- 1 **Mechanical deformation.** Loads from the grinding wheel result in plastic deformation of the workpiece surface giving rises to compressive residual stresses.
- 2 **Thermally induced plastic deformation.** High temperatures in the contact zone can rapidly heat the surface layers of the workpiece. The surface layers are however constrained by the bulk material and the grinding wheel which results in stresses being generated. If these stresses exceed the yield point of the workpiece material (which reduces significantly with increasing temperature) then plastic deformation occurs. On cooling, the expanded surface layer contracts which results in the generation of tensile residual stresses.
- 3 **Phase transformations in Hardened Steels.** Quenched and tempered steels have a tempered martensite microstructure. During grinding the workpiece surface is exposed to a steep temperature gradient, which can cause over-tempering or tempered burn at temperatures below the austenitising temperature if the material. Alternatively, rehardening burn can occur if the grinding temperature exceeds the austenitising temperature, where austenite forms and then transforms to untempered martensite when the workpiece surface is rapidly quenched by the cutting fluid. Both phase transformations involve rapid volume changes, resulting in tensile stresses in the overtempered martensite layer or compressive stresses in the untempered martensite layer.

2.8.2.1 Measurement of Residual Stress

A common method of measuring residual stress is by X-Ray diffraction (XRD) which works on the principle that parallel sets of planes in any given crystalline structure can be used as diffraction grating in much the same way that fine parallel line on a surface can be used to diffract light (Dowdell and Jerabek, 1943). The actual spacing between the planes in the crystalline structure is determined by chemical composition and physical conditions such as temperature and stress. It is possible to control all other effects on the plane spacing except that caused by stress, and therefore a unique linear correlation can be established between the distance between the planes of a crystal and the residual stress or strain. (Heindlhofer, 1948)

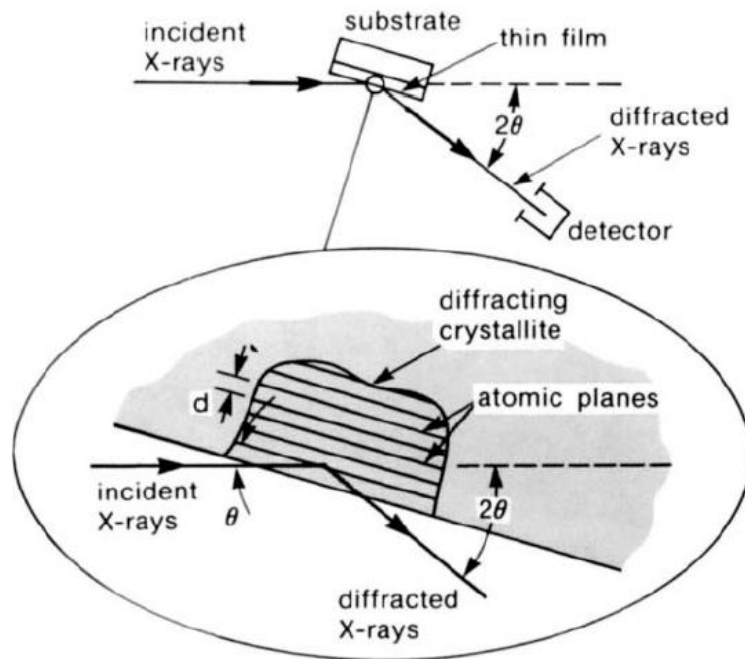


Figure 2-21 Basic Principle of XRD Residual Stress Measurement.(Brundle and Evans, 1992)

2.9 Summary

In order to compare the relative performance of different cutting fluids for use with the High Efficiency Deep Grinding process, it was important to first identify the attributes of the cutting fluid which had a thermal impact on the grinding process.

A cutting fluids ability to remove heat and its ability to reduce heat generation by means of it lubricity are the most obvious attributes that have an impact on the grinding process. However, the cutting fluid misting and ignition characteristics also have a huge impact on the grinding process, especially in the HEDG regime when oil cutting fluids are used, as the material removal rates may need to be limited in order to reduce the fire hazard posed by the process.

The attributes of the fluid that impact on the grinding process are:

Convection Coefficient (cooling effectiveness)
Lubricity
Ignitability
Misting

Once these attributes were established a program of standardised comparative tests needed to be developed in order to allow fair and unbiased comparison between different fluids.

The test program consists of the following tests:

Convection Coefficient

Fluid Ignition

Fluid Misting

Fluid Lubrication

Grinding Performance

These tests, and the results generated by these tests will be discussed in the following chapters, starting with the tests to establish the convection coefficient of different cutting fluids which are presented in chapter 3.

3 Convection Coefficient

3.1 Introduction

The convective heat transfer coefficient of a cutting fluid, or convection coefficient for short, is the measure of a cutting fluids ability to remove heat from the grinding zone. Accurate values of this parameter are therefore hugely important if we want to calculate how much of the total heat energy generated by the grinding process is removed by, or partitioned to, the cutting fluid and subsequently calculate how much energy enters the workpiece, as the amount of heat energy entering the workpiece in large part determines the likelihood of any thermal damage.

Accurate values of the convection coefficient are also important if one wishes to compare the cooling effectiveness of different cutting fluids and if one wants to reliably model the grinding process. Modelling such a difficult and complex multivariable process such as grinding is extremely valuable, as not only does it allow the impact of process variable changes to be assessed, but such a model can also be used as an online monitoring system. Monitoring a single, easily measurable parameter such as grinding power can be used to detect problems within the process at an early stage, thus reducing potentially costly scrap and rework.

Unfortunately, as stated previously, the measurement of the convection coefficient is not simply a matter of measuring the thermal properties, the thermal conductivity for example, of the cutting fluid in question. Other factors such as grinding wheel speed and depth of cut also play an important part in determining this vital process parameter. These will be discussed in greater detail later in this chapter.

It has proved extremely difficult to obtain precise values of the convection coefficient, and even an order of magnitude estimation has proved to be troublesome (Jin and Stephenson, 2003a). A theoretical study on the subject published by Jin et al proposing that the magnitude of the convection coefficient should be significantly higher than had previously been thought (Jin and Stephenson, 2003a), but this study lacked good independent experimental data to corroborate these findings.

In order to correct this, a special inclined thermocouple test rig was designed at Cranfield University to measure the amount of heat energy entering the workpiece, and thus indirectly establish the convection coefficient of the cutting fluid with the specific aim of validating the high values of convection coefficient that were predicted. The design of this test rig is shown in figure 3-1, and was assembled and used in a series of grinding trials aimed at establishing this vital parameter for a range of different cutting fluids.

Before discussing the experimental aspects regarding the “measurement” of the convection coefficient, a thermal model of the grinding process will be presented to show the mathematical relationships in the grinding process and thus show the

importance of this parameter within grinding and thus put this body of work into context.

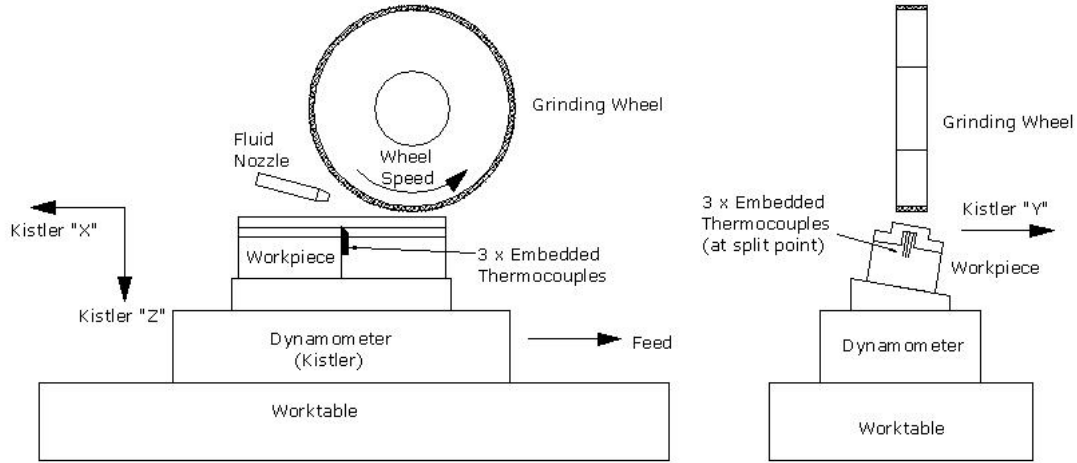


Figure 3-1 Inclined Thermocouple Test Rig

3.2 The Thermal Model

The literature review introduced some important elements of the thermal model such as energy partitioning and the convection coefficient of the cutting fluid. The concept of considering grinding as a thermal process is important in putting the principle of a cutting fluid application strategy, based upon the thermal characteristics of the cutting fluid, into context. Consequently the thermal model is a vital tool used throughout this project in helping to determine the direct thermal impact of different cutting fluids. The following section is therefore dedicated to showing, step by step, the mathematical relationships which are used in the modelling process.

The first step in the thermal model is to calculate the thermal property of the cutting fluid which is given by (Rowe, 2001):

Equation 3-1

$$\beta := \sqrt{(k \cdot \rho \cdot c)}$$

where:

- β = thermal property of the cutting fluid
- k = thermal conductivity of the cutting fluid
- ρ = mass density of the cutting fluid
- c = specific heat capacity of the cutting fluid

The arc length of the grinding contact is calculated by equation 3-2 (Andrew and Howes, 1985)

Equation 3-2

$$l_c := \sqrt{(a \cdot D)}$$

where:

a = depth of cut

D = grinding wheel diameter

as shown in figure 3-2. Using these equations and the grinding wheel speed, the convection coefficient can be calculated using the simple fluid wheel model introduced in the literature review. (Jin and Stephenson, 2003)

Equation 3-3

$$h_f := 0.94\beta \cdot \left(\sqrt{\frac{V_s}{l_c}} \right)$$

where:

h_f = convection coefficient of the grinding fluid

β = thermal property of the grinding fluid

v_s = grinding wheel speed

l_c = contact length of the grinding arc

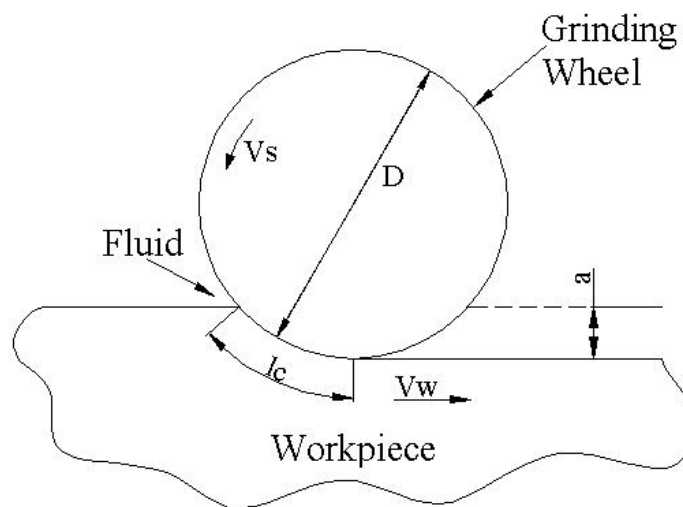


Figure 3-2 Schematic illustration of the grinding process.

3.2.1 Estimation of the Contact and Finish Surface Temperatures

If no experimental data is available to calculate the specific grinding energy, it can be estimated using the following equation (Stephenson and Jin, 2003)

Equation 3-4

$$e_c = A \times Q'_w{}^{-t} \text{ J/mm}^3$$

Where A and t are constants based on the material, grinding wheel speeds and specific removal rates employed in the grinding process. Typical values for A and t when grinding steel with a CBN grinding wheel are shown in table 3-1.

Workpiece/ Abrasive	A	T	$v_s(\text{m/s})$
Steel/CBN	70	0.25-0.4	100~150

Table 3-1 Constants for calculation of the specific grinding energy when using equation 3-4.
(Stephenson and Jin, 2003)

This particular equation is very important in HEDG, as it shows that the specific grinding energy, a measure of process efficiency, decreases exponentially with increasing specific removal rate. This relationship was first introduced in figure 2.2. As a consequence, process efficiency improves at higher specific removal rates, as less energy is required to remove each unit volume of material.

The preferred method of calculating the specific grinding energy is, however, to use real experimental values of net grind power. These are values of grind power with the influence of the cutting fluid removed. If grind power data is available, the specific grinding energy can be calculated using the following equation (Stephenson and Jin, 2002)

Equation 3-5

$$e_c = P_{\text{net}} / (v_w \cdot b \cdot a)$$

where:

e_c = specific grinding energy

P_{net} = net grind power

v_w = workpiece feedrate

b = width of grinding wheel

a = depth of cut

It is important at this point to make the distinction between total grind power and net grind power and the significance of this difference. Total grind power is the amount of power drawn by the grinding spindle during grinding. This measured value comprises

not only the power drawn by the spindle motor to remove material from the workpiece, but also the power consumed by the hydrodynamic flow of cutting fluid between the wheel and workpiece. In order to establish the power consumed in removing material, the net grind power, the influence of the grinding fluid must be removed. (Jin and Stephenson, 2002)

Special spark out tests are performed which determine the power consumed by the hydrodynamic flow of the cutting fluid. The test simulates the contact geometry of the real grinding process, but without removing any material from the workpiece. The spark out procedure involves running the grinding wheel at the prescribed grinding wheel speed and cutting fluid delivery parameters for several seconds along a stationary, preformed arc within the workpiece.

The preformed arc within the workpiece is generated using the same depth of cut as the real grind conditions. Therefore, when the workpiece is stationary, no material is removed. Consequently the power consumed by the cutting fluid flow within the grinding zone can be determined.

Once the specific grinding energy is known, the total heat flux generated by the grinding process can be calculated by: (Stephenson and Jin, 2003)

Equation 3-6

$$q_t := e_c \cdot a \cdot \frac{V_w}{l_c}$$

where:

q_t = total heat flux generated by the grinding process

a = depth of cut

v_w = workpiece feedrate

l_c = contact length of grinding arc

The next step in the thermal model is to calculate the amount of energy partitioned to both the grinding wheel and the workpiece. The wheel/work partition ratio R_{ws} is calculated by (Hahn, 1962)

Equation 3-7

$$R_{ws} := \left[1 + \frac{(0.97 \cdot K_g)}{\beta \cdot \sqrt{(r_o \cdot V_s)}} \right]^{-1}$$

where:

R_{ws} = wheel / workpiece partition ratio
 K_g = thermal conductivity of the abrasive grains
 β = thermal property of the workpiece
 r_o = grain wear flat radius
 v_s = grinding wheel speed

The conduction factor of the workpiece which helps to determine the amount of thermal energy partitioned to the work piece is calculated by (Jin and Stephenson, 2003a)

Equation 3-8

$$h_w := \frac{\beta}{c} \cdot \sqrt{\left(\frac{V_w}{l_c} \right)}$$

where:

h_w = conduction factor of the work piece
 β = thermal property of the work piece material
 c = a constant determined by the process parameters
 v_w = workpiece feedrate
 l_c = contact length of grinding arc

The C constant is calculated using the circular arc contact heat source model for deep grinding (Jin and Rowe, 2001; Rowe and Jin, 2001). Alternatively, if both the Peclet number, a function of the material removal rate and the thermal characteristics of the work piece material, and the contact angle of the grinding process are known, values of the C-factor can be established from figure 3-3

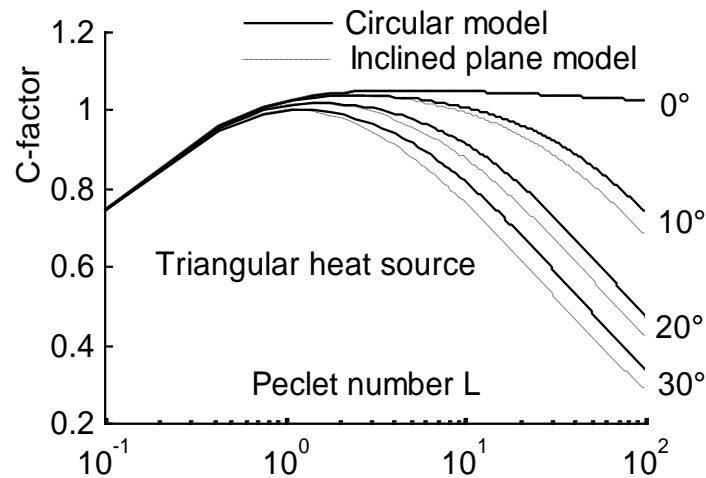


Figure 3-3 Relationship between Peclet number and C-Factor.

The maximum contact temperature is calculated by (Jin and Stephenson, 2003a)

Equation 3-9

$$T_{\max} := T_o + \left[\frac{q_t - q_{ch}}{\left(\frac{h_w}{R_{ws}} \right) + h_f} \right] \quad T_{\max} < T_b \quad \text{or} \quad T_{\max} := T_o + \left[\frac{q_t - q_{ch}}{\left(\frac{h_w}{R_{ws}} \right)} \right] \quad T_{\max} > T_b$$

where:

T_o = ambient temperature,

q_t = total heat flux

q_{ch} = energy removed by the grinding chips

h_w = workpiece conduction factor

h_f = convection coefficient of the grinding fluid

R_{ws} = work/wheel partition ratio

T_{\max} = maximum contact temperature

T_b = threshold for film boiling

The amount of energy removed by the grinding chip is calculated as follows (Rowe and Jin, 2001; Rowe, 2001a; Stephenson and Jin, 2003):

Equation 3-10

$$q_{ch} := e_{ch} \cdot \frac{(a \cdot V_w)}{lc}$$

where:

q_{ch} = heat flux entering the grinding chips

e_{ch} = limiting chip energy

a = depth of cut

v_w = workpiece feedrate

lc = contact length of grinding arc

The thermal model demonstrates some important principles in grinding. Equation 3-10 shows the amount of heat energy (q_{ch}) removed by the grinding chips is proportional to the work speed (v_w). It therefore follows that at low workpiece feed rates, such as those employed in creep feed grinding, the amount of heat energy removed by the ejected grinding chips will be almost negligible, and is therefore usually ignored (Jin and Stephenson, 2002).

However, as the workpiece feedrate increases, the amount of energy removed by the grinding chips increases, so that at high work speeds the energy removed by the grinding chips can be very large. It is this mathematical relationship that helps explain the distinctive HEDG curve shown in figure 2-1 with the surface finish temperature decreasing at very high specific removal rates.

The thermal model also shows the importance of having accurate values of the convection coefficient of the cutting fluid. Without reliable values, whether they be estimated or obtained from actual experimental data, accurate prediction of the maximum grinding zone temperatures becomes impossible.

3.3 Experimental

Experiments were conducted on the straight surface grinding (SAM) machine using the inclined thermocouple test rig described earlier and shown in Figure 3-1. Essentially, the test rig consists of three Omega Type C02- K cement on K type thermocouples sandwiched in a split sensor block with a sacrificial sample mounted over the top. The split sensor block and the sacrificial sample all manufactured from the same material, in this case 51CrV4. All mating surfaces on the test rig and sacrificial samples were fine ground to get the best surface finish achievable in order to provide the best possible thermal contact.

The Omega thermocouples, which are 10 μ m thick, were selected for their fast response time, typically between 2-5 milliseconds. The response time, or “time constant”, being the time required to reach 63.2% of an instantaneous temperature change.

The whole assembly was then inclined at an angle of 12° in relation to the grinding wheel. This effectively positions the thermocouples at increasing distances from the ground surface, once material has been removed from the sacrificial sample as a result of a plain grinding pass (see figure 3-4). This allows the temperatures at different depths from the ground surface to be measured. The sacrificial samples were 104mm long in the grind direction and 20mm wide.

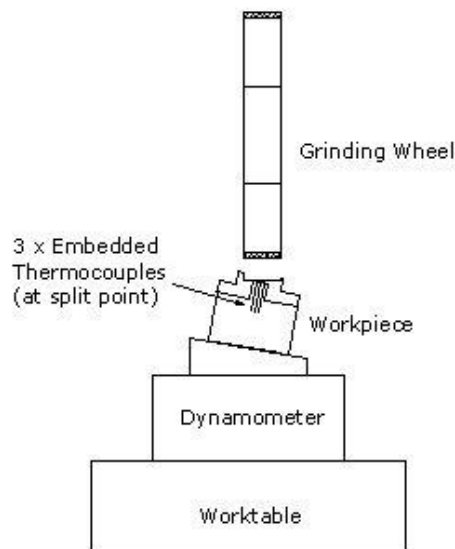


Figure 3-4 Inclination of the embedded thermocouples to the grind plane.

The data from both the thermocouples and a Hall Effect transducer measuring the grind power was collected using a National Instruments PCI6036E data acquisition system with dedicated Labview software at a sampling rate of 1000Hz, and collected data for 30 seconds during each run. The grind power was monitored to allow the specific grinding energy to be calculated. The temperature within the workpiece was measured to allow the heat flux entering the workpiece to be established.

Comparative tests were conducted using the neat oils, ester based synthetic and water-based emulsion fluids listed in table 3-2, the data sheets for which are included in appendix 1. Tests were conducted at two different grinding wheel speeds, each at two different fluid delivery pressures (and hence flows) in order to establish the effect of these parameters on the performance of the fluid. The grind parameters and fluid delivery ranges are shown in table 3-3

Fluid	Description
Castrol Ilogrind 600SP	Neat Mineral Oil with EP additives. 9.8cst. @ 40°C
Castrol ES1	Ester Based Fully Saturated Neat Oil. 27cst. @ 40°C
Fuchs Plantocut 22SR	Ester Based Partially Saturated Neat Oil. 22cst. @ 40°C
Fuchs Plantocut 40SR	Ester Based Partially Saturated Neat Oil. 40cst. @ 40°C
Prolong Ultracut 1	Water Soluble EP Activated Cutting Fluid @ 10%
Quakercool 2772LF	Water Soluble Polymer Based Cutting Fluid @ 7%
Castrol Hysol XH	Water Soluble EP Activated Cutting Fluid @ 7%

Table 3-2 Cutting Fluids Investigated during Convection Coefficient Experiments

Grinding Conditions	
Grinding Machine	Edgetek five-axis CNC grinder
Grinding Mode	Surface down-grinding
Wheel	Electroplated CBN, B252, diameter: 200mm, width: 15mm wide
Wheel Speed	50m/s
Depth of cut	0.4mm
Worktable Speed	1mm/s
Cutting fluid	See Table 3-2
Work piece material	Low Alloy Steel – 51CrV4
Number of Repeats	4

Table 3-3 Experimental Conditions for Convection Coefficient Experiments

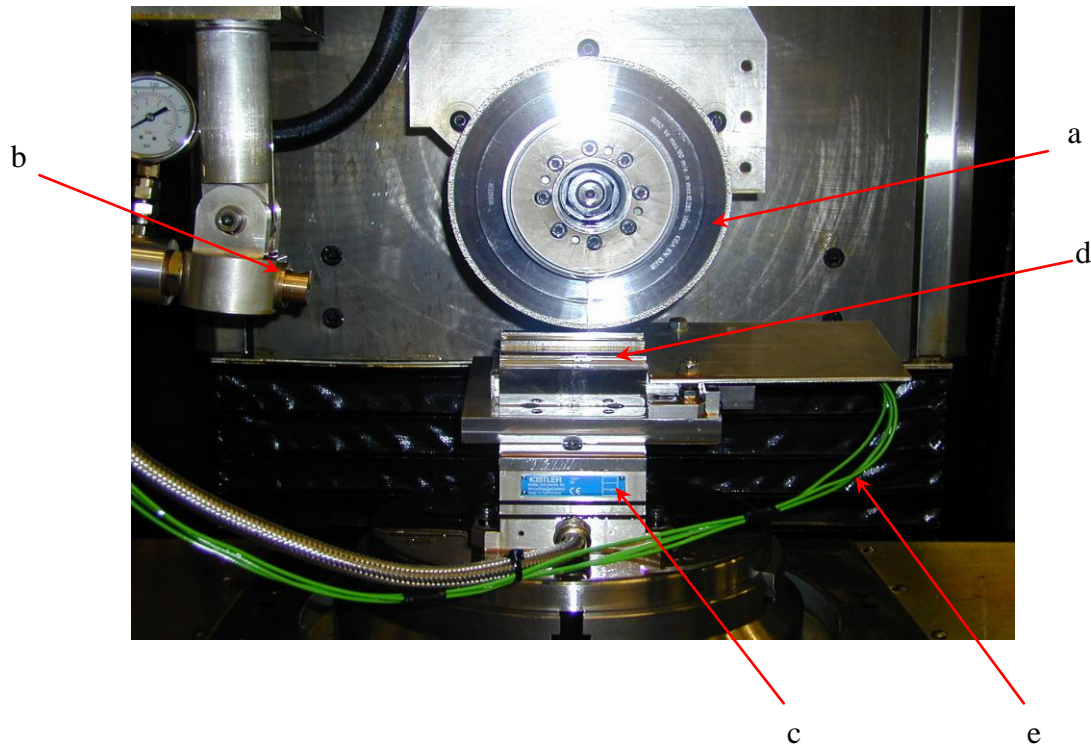


Figure 3-5 Inclined thermocouple test rig assembled and fitted to the Edgetek SAM Machine

- a) grinding wheel
- b) coolant nozzle
- c) dynamometer
- d) inclined thermocouple test rig
- e) thermocouple compensating cable

3.3.1 Calibration

Figure 3-6 shows the layer of mica used to insulate the thermocouple from the bulk material of the workpiece. The mica and the layers of adhesive used to attach the thermocouples have a significantly different thermal conductivity than the surrounding material and that of the sacrificial workpiece mounted over the top of the thermocouples. In order to obtain accurate surface temperature measurements needed when calculating the convection coefficient (see equation 3.20), the test rig needed to be calibrated. This then allows the finish surface temperature to be extrapolated from the temperatures measurements recorded by the embedded thermocouples measurements in the body of the test rig.

The calibration procedure was fairly simple. A water based cutting fluid was heated in a glass vessel with the temperature measured using a calibrated, hand held Omega HH506RA digital thermometer with a calibrated K type thermocouple. The cutting fluid was continually stirred in order to ensure a consistent temperature throughout.

The cutting fluid was then carefully and steadily poured onto the surface of a pre-ground sample mounted over the top of the thermocouples. The distance between the pre-ground surface of the sample and the thermocouples was measured and recorded. The temperature rise measured by the embedded thermocouples within the test rig

recorded using the same National Instruments data acquisition system detailed earlier. Data was recorded at 1000 samples per second for a total of 60 seconds by which time the temperature within the test rig had reached steady state conditions.

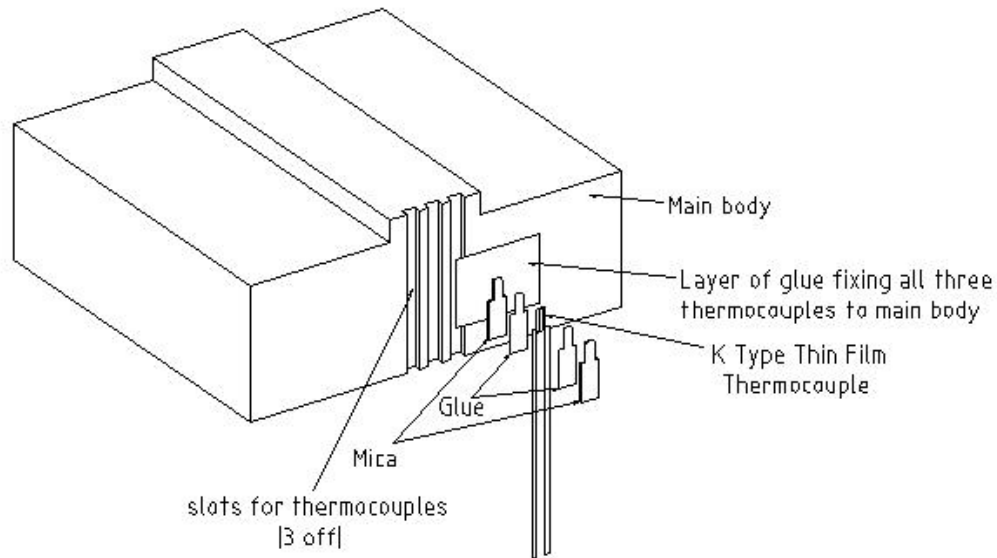


Figure 3-6 Assembly of the thermocouples within the inclined thermocouple test rig

Figure shows the layers of mica and glue surrounding the thermocouple in the inclined thermocouple test rig assembled which act as layers of insulation. These layers alter the thermal conductivity of test rig and need to be taken consideration.

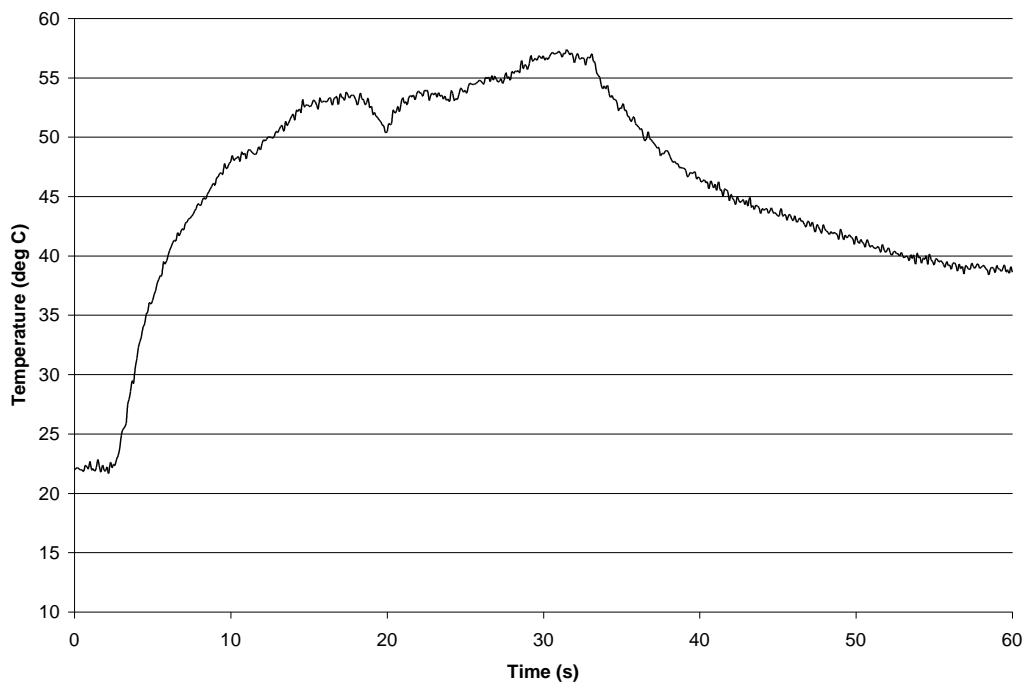


Figure 3-7 Temperature response of inclined thermocouple test rig.

Response to application of preheated cutting fluid, at a known (measured) temperature. Although the fluid being poured over the test rig is over 70°C, the temperature measured by the embedded thermocouples reaches an average steady state temperature of 57°C after approximately 30 seconds.

The tests were repeated with the cutting fluid heated at a variety of different temperatures to allow a temperature response profile to be developed over a temperature range representative of the grinding temperatures predicted by thermal modelling.

Variations in ambient temperature were taken into consideration by measuring the block temperature with the digital thermometer prior to each test run.

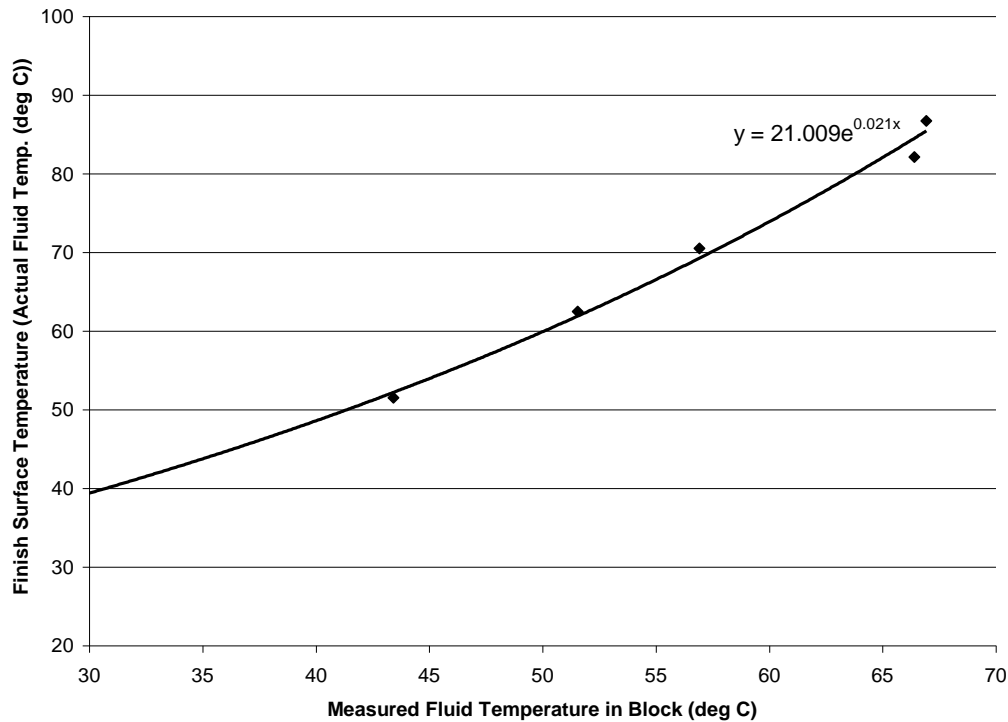


Figure 3-8 Relationship between finish surface temperature and measured block temperature.

This is the relationship between the fluid temperature which is poured onto the workpiece (actual measured fluid temperature) and measured block temperature as measured by embedded thermocouples within the test rig.

Knowing the relationship between finish surface temperature and measured block temperature as measured by the embedded thermocouples allows the finish surface temperatures to be extrapolated accurately from the embedded thermocouple data gathered during test grinds.

Additional grinding tests performed using specially prepared samples with thermocouples mounted as close to the finish surface as possible showed excellent correlation between the actual finish surface temperature and the finish surface temperature extrapolated from the measurements recorded using the embedded thermocouples in the body of the test rig. Despite difficulties in mounting thermocouples just below the grind surface, these tests showed that there was only 2°C difference between these measurements and those calculated by extrapolating from the embedded thermocouples.

3.3.2 Analysis for the calculation of the convection coefficient.

The first step of the analysis for calculating the convection coefficient is to calculate the specific grinding energy from measured values of net grinding power using equation 3-5 stated earlier, and shown again for simplicity.

Equation 3-11

$$e_c = P_{net} / (v_w \cdot b \cdot a) \quad (\text{Stephenson and Jin, 2002})$$

where:

e_c = specific grinding energy

P_{net} = net grind power

v_w = workpiece feedrate

b = width of grinding wheel

a = depth of cut

Next, the total heat flux (q_t) generated by the grinding process is calculated:

Equation 3-12

$$q_t = P_{net} / \text{Grind Area} \quad (\text{Rowe, 2001a})$$

where:

$\text{Grind Area} = b \cdot l_c$

and:

b = width of grinding wheel

l_c = length of contact

The next step is to calculate the heat flux entering the workpiece. As stated previously, the thermocouple test rig contains three separate thermocouples. Once the test rig is inclined, the thermocouples are effectively placed at increasing depths from the finish surface, and consequently measure the temperature at increasing depths from the finish ground surface. Because of the very low feed rates used in creep feed grinding conditions, the heat flux can be considered to be linear, in other words, it has reached steady state conditions. The heat flux entering the workpiece can therefore be determined using Fouriers Law.

Equation 3-13

$$q_w = -k ((T_3 - T_1) / \delta z)$$

where :

q_w = heat flux entering the work piece

k = thermal conductivity of the work piece

T_3 , T_2 and T_1 are the measured temperatures from the thermocouples

δz = differential height between the thermocouples

Thermal conductivity of the work piece material (51CrV₄) = 42W/mK (Stephenson and Jin, 2003)

The differential depth of the thermocouples in relation to the ground surface can be calculated using basic trigonometry. The test rig is inclined at an angle of 12°, so the vertical distances between the thermocouples is given by:

Equation 3-14

$$\delta z = 8 \sin 12^\circ = 1.66\text{mm}$$

between thermocouples 1 and 3.

or:

$$\delta z = 4 \sin 12^\circ = 0.83\text{mm}$$

between thermocouples 1 and 2 or 2 and 3.

Calculation of the partition ratios is the next stage of the analysis

Equation 3-15

$$1 = R_w + R_s + R_{ch} + R_f$$

Equation 3-16

$$q_t = q_w + q_s + q_{ch} + q_f$$

Equation 3-17

$$R_w = q_w / q_t \quad (\text{Rowe, 2001})$$

Equation 3-18

$$R_s = R_w((1 - R_{ws}) - 1) \quad (\text{Jin and Stephenson, 2003})$$

Knowing the total heat flux and the grinding wheel partition ratio (R_s), the heat flux entering the grinding wheel (q_s) can be calculated:

Equation 3-19

$$q_s = R_s * q_t$$

Assuming the energy removed by the grinding chips is negligible for creep feed grinding conditions ($q_{ch} = 0$) (Jin and Stephenson, 2002), the convection coefficient of the cutting fluid (h_f) is given by:

Equation 3-20

$$h_f = (q_t - q_w - q_s) / (T_s - T_o)$$

where:

h_f = convection coefficient of the cutting fluid

q_t = total heat flux

q_w = heat flux entering the work piece

q_s = heat flux entering the grinding wheel

T_o = ambient temperature

T_s = measured finish surface temperature

3.3.3 Results and Discussion

Figure 3-9 and figure 3-10 show typical measurements obtained during the convection coefficient grinding trials. Both figures show the temperature measurements from the three embedded thermocouples within the test rig body, with thermocouple 1 being closest to the surface, thermocouple 3 being the furthest from the finish ground surface. Also shown is the spindle power output – a 0-10V analogue output signal from a hall effect transducer monitoring the grinding spindle power.

The higher lubrication offered by neat oil is clearly shown by the lower spindle power measured using the hall effect transducer fitted to the wheel spindle drive. The lower spindle power gives rise to a lower specific grinding energy value for the process. When using a neat oil at 5 bar and a wheel speed of 50m/s for example, the specific grinding energy was less than half that for a water based emulsion, 89.7J/mm² for the oil and 103.5J/mm² for the water based fluid. The increase in lubrication results in less heat generation within the grinding zone, with the total heat flux (q_t) significantly lower when oil is used (4011700W/m² when oil is used, 4630068W/m² with the water based

fluid) This trend is continued throughout the results, and clearly shows the benefits of oil especially in HEDG where lubrication is of key importance.

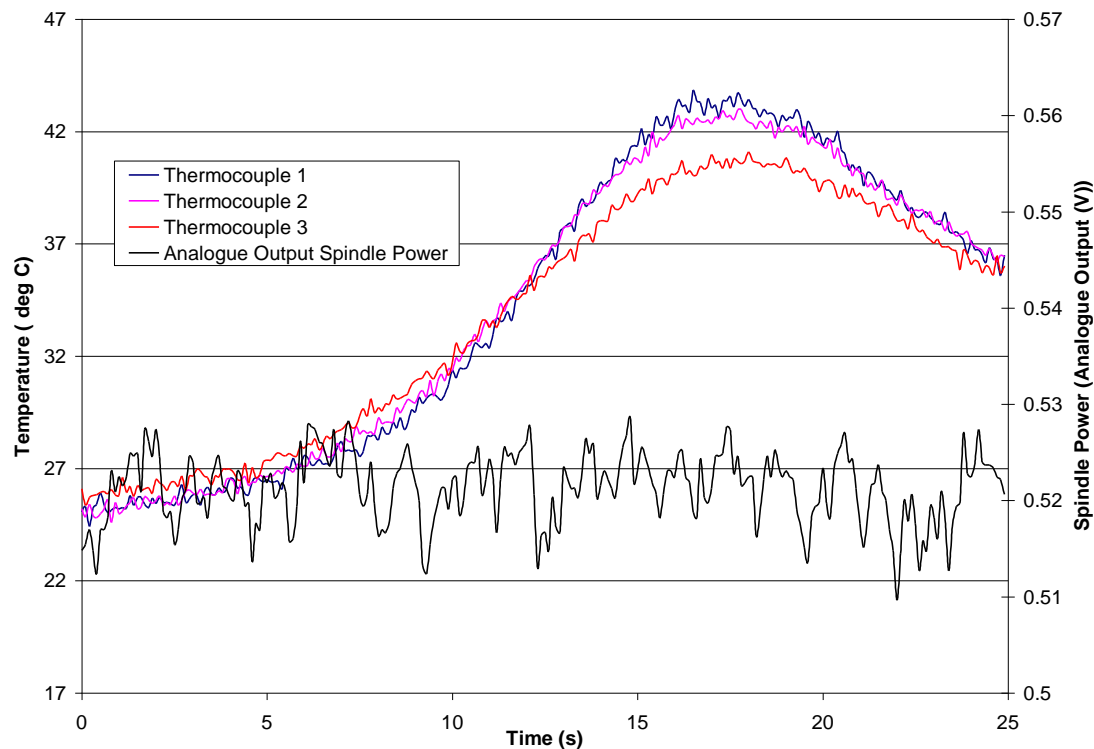


Figure 3-9 Typical temperature profile for creep feed grinding using a neat oil cutting fluid.

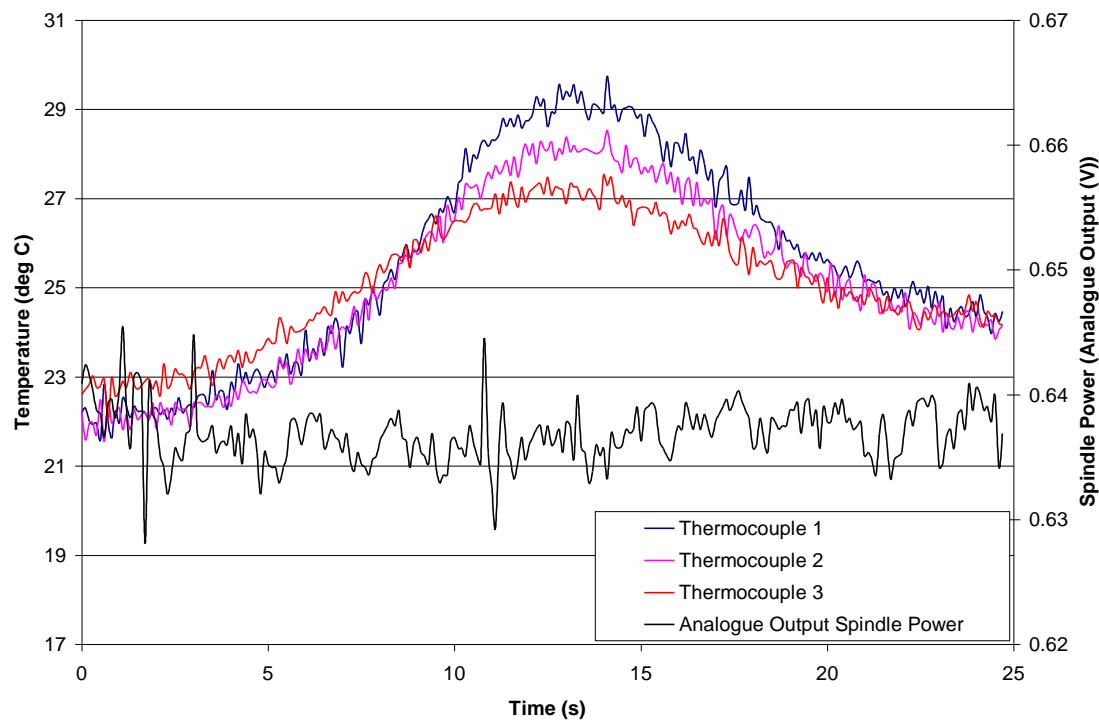


Figure 3-10 Typical temperature profile for creep feed grinding using a water soluble cutting fluid.

Conversely these results also show the much higher level of cooling offered by water-based fluids, immediately apparent from figure 3-9 and figure 3-10. These clearly show higher work piece temperatures with oil despite significantly lower heat generation. The maximum measured temperature, as measured by the embedded thermocouples is in excess of 43⁰C when oil is used and less than 30⁰C with the water based fluid. This is attributable to the fact that when creep-feed grinding, over 90% of the heat energy can be removed by the cutting fluid, so the convection coefficient becomes important.

Comparative tests were conducted on a number of different cutting fluids under strictly controlled grinding condition, and theses results are shown in table 3.4. The results show substantially higher convection coefficients (h_f) for the water based fluid, $h_f = 258911 \text{ W/m}^2\text{K}$ (Hysol @ 7%) as opposed to $h_f = 97728.14 \text{ W/m}^2\text{K}$ for oil (Illogrind) when grinding at 50m/s, 5 Bar delivery pressure. The higher convection coefficient results in far more heat energy being removed by the cutting fluid (by convection) from the grinding zone. As a result, far less heat energy enters the work piece (heat-flux into work piece $q_w = 161533 \text{ W/m}^2$ for oil, 25654 W/m^2 for water) which results in the lower measured temperatures seen in figure 3-10. The better convective cooling properties of water based fluids, as demonstrated by their higher convection coefficients, clearly demonstrate the value of these types of fluid for conventional grinding when fluid boiling is not a problem.

Fluid	SGE (J/mm ³)	Total Heat Flux (q_t) (W/m ²)	R_f	H_f (W/m ² K)
Illogrind 600SP	89.7	4011700	0.93	97728+/- 3.2%
Castrol ES1	82.6	3695364	0.83	71257 +/- 1%
Hysol XH @ 7%	103.5	4630068	0.99	258911 +/- 4.4%
Plantocut 22SR	85.7	3831508	0.84	56742 +/-2.1%
Prolong Ultracut 1	94.9	57291	0.97	271503+/-3.4%
Prolong AFTM	82.9	3701906	0.89	68899 +/-2.5%

Table 3-4 Comparison of the convection coefficient of different cutting fluids

Note: The results for Fuchs Plantocut 40SR and Quakercool 2772LF are not presented, as there was a fault with the thermocouple test rig due to ingress of cutting fluid. However, the power measurements were unaffected, and the results for these trials are shown in chapter 5 – Grinding Performance.

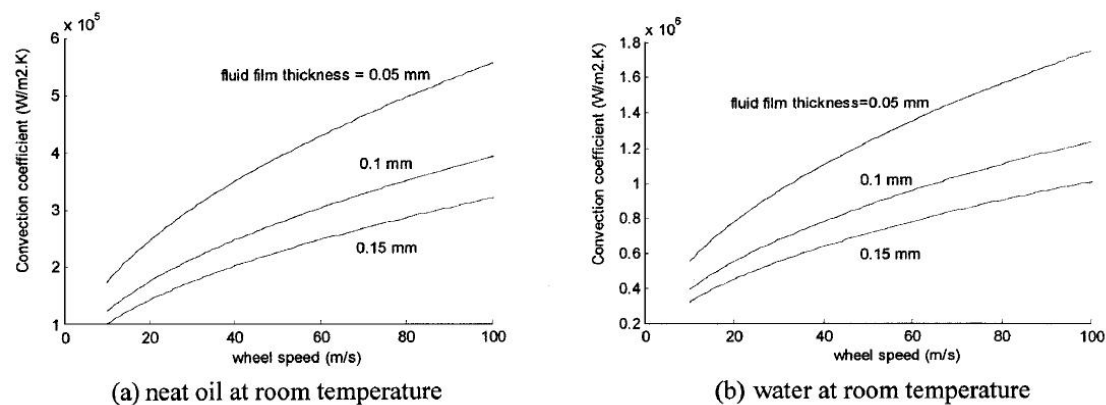


Figure 3-11 Predicted Convection Coefficients for Neat Oil Water Based Cutting Fluids (Jin and Stephenson, 2003a)

The magnitude of the convection coefficients show reasonable correlation with those predicted by Jin and Stephenson et al (2003a) and shown in figure 3-11 which are taken from this paper, and this is significant, as the results published by Jin and Stephenson (2003a) were much higher than those published by other researchers. The higher values of h_f measured by the inclined channel test rig can be attributable to a number of different factors.

Film thickness for example has a significant effect on the convection coefficient as is clearly shown in figure 3-11. The film thickness is the thickness of the fluid film in the contact zone between the workpiece and the grinding wheel. It is impossible to measure this parameter directly, but it is known to be influenced by a number of different parameters including the porosity of the grinding wheel, or in the case of superabrasive grinding wheels, the size of the abrasive grains. There could therefore be significant difference between the film thickness used in the thermal model by Jin and Stephenson et al (2003a) and these convection coefficient experiments. The thermal properties of the fluid also play a significant role in determining the convection coefficient, and these can change with both pressure and temperature.

Furthermore the values of convection coefficient obtained from the inclined thermocouple test rig were highly sensitive to changes in the grinding power, as this is used to calculate the total heat flux generated by the grinding process as shown in equation 3-12. For example, a 5% error in the measured grinding power could result in a 5% increase in the value of convection coefficient. The measured grinding power can be influenced by a number of factors including variations in the workpiece material, the hydrodynamic effect caused by the cutting fluid, and perhaps most importantly variations in the condition of the grinding wheel. Whilst every effort was made to minimise these variations, including using the same grinding wheel for all the tests, and monitoring the condition of this wheel by performing a standardised test using a standard cutting fluid (Castrol Ilogrind 600SP) to check whether there had been any significant change in the grinding wheel condition, it was impossible to completely remove these potential sources of error from the system.

4. Cutting Fluid Evaluation Test Program

4.1 Introduction

The aim of this chapter is to describe the series of screening tests used to evaluate individual attributes of the cutting fluid that are of particular importance in the grinding process, especially HEDG. Screening tests are relatively simple and cost effective tests designed to allow quick comparative tests to be conducted on different fluid formulations. Such tests are used extensively in industry for new product development in order to test particular fluid attributes.

The screening test program conducted during this test the following cutting fluid attributes.

- Lubrication
- Fluid Misting
- Fluid Ignition

The literature presented in chapter two clearly shows the importance of lubrication in the grinding process, and particularly in HEDG. Lubrication is vital in reducing the amount of heat generated in the grinding zone (Brinksmeier and Brockhoff, 1997), and is therefore an obvious thermal characteristic of the cutting fluid.

Fluid ignition and misting characteristics are less self evident as thermal characteristics, but it is important to understand that material removal rates, particularly in HEDG, may need to be limited in order to minimise the risk of ignition. The literature shows that high levels of oil mist in an atmosphere increases the risk of ignition, and that fluids can ignite below their flashpoint when these fluids form mists. It is important to understand that the material removal rates may need to be limited in order to reduce the risk of fire when oil cutting fluids are used, particularly in HEDG.

Selecting a fluid that has a greater resistance to ignition and reducing the level of mist and volatile fractions around the grind zone is therefore important in reducing the risk of ignition if neat oil cutting fluids are used in the grinding process. This will therefore reduce the need to place artificial restrictions on the material removal rates placed on the process by the cutting fluid.

This chapter aims to show how a series of tests have been designed to measure these important fluid attributes and use the data to help to determine the most effective cutting fluid for use in the grinding process.

4.2 Cutting Fluid Lubrication Testing

4.2.1 Introduction

In grinding, there are a number of different variables that determine the grinding process. Grinding forces and the specific grinding energy are not simply determined by workpiece material, depth of cut and wheel speed, but other factors such as the condition of the grinding wheel.

A simpler and more reliable method with far fewer variables was therefore needed to perform comparative cutting fluid lubricity tests. The literature presented in section 2.3.2.2 showed that torque tapping test is a quick, simple and reliable method of evaluating different cutting fluids.

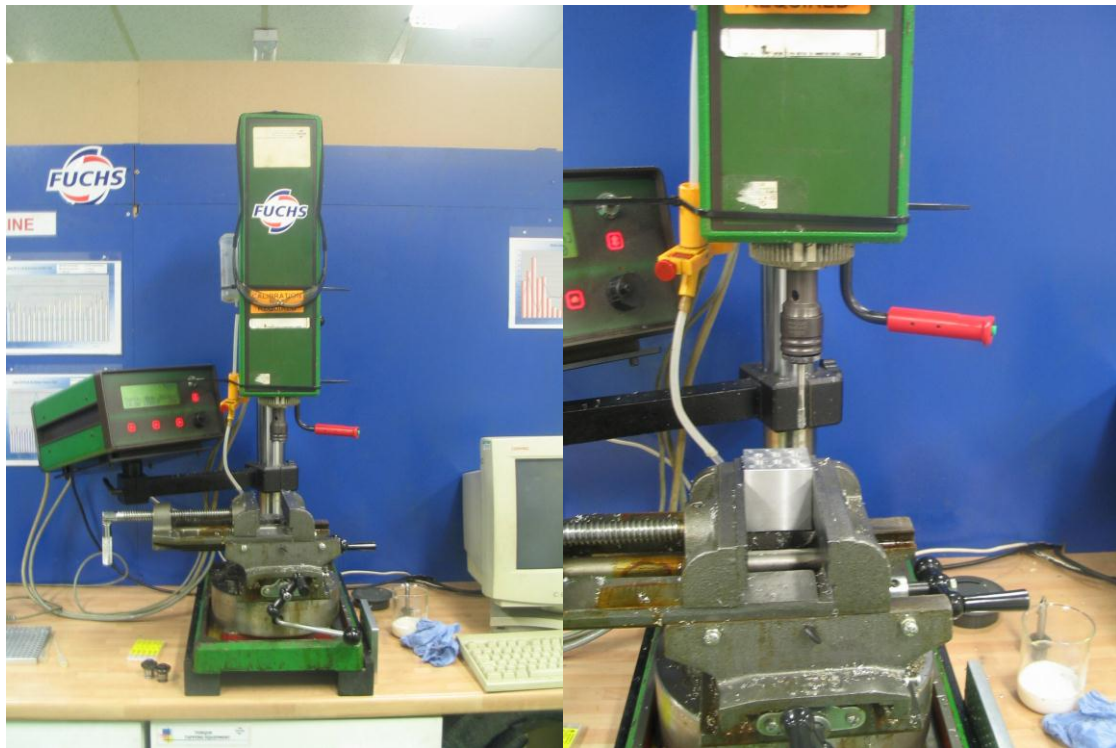


Figure 4-1 Robert Speck Torque Tapping Machine used for Lubrication Testing.

4.2.2 Experimental Procedure.

Torque tapping tests were conducted on a Robert Speck torque tapping machine, seen in figure 4-1, courtesy of Fuchs Petrolub UK Ltd. The machine was fitted with an online computer based tapping force measurement system allowing force measurements to be recorded.

DIN 376 M6 x 1,0 pitch taps were used for all the torque tapping tests and the holes in the sample were pre-drilled and then reamed to Ø5mm in accordance with BS1157: 1975. Reaming the holes helped to maintain both dimensional and surface finish consistency.

Aluminium was selected as the sample material as it is much easier to machine than the 51CrV4 high alloy steel used for the grinding trials. Whilst use of 51CrV4 would have been more representative, aluminium was used to minimise the possibility of tool breakage and also because there was a limited amount of torque available from the torque tapping machine.

Each sample had a series of predrilled blind holes allowing each hole to be filled with the same amount of cutting fluid prior to each test, thus ensuring consistent fluid application. All samples were manufactured from a single piece of aluminium bar to minimise variance attributable to material inconsistency.

Four individual runs were conducted for each of the fluids listed in table 4-1, with a new tap being used for each different fluid.

As the machine was not calibrated, all the tests were performed over the course of a single afternoon reducing any errors associated with time dependant drift. Furthermore, as the machine was not calibrated, the output from the torque tapping machine was not converted to an actual torque as this could be misleading. Instead the results are presented as a series of normalised measurements, where the analogue output of the torque tapping machine was modified by simply multiplying the data set acquired from the tests by a constant (300) to aid presentation and analysis.

Fluid	Description
Castrol Ilogrind 600SP	Neat Mineral Oil with EP additives. 9.8cst. @ 40°C
Castrol ES1	Ester Based Fully Saturated Neat Oil. 27cst. @ 40°C
Fuchs Plantocut 22SR	Ester Based Partially Saturated Neat Oil. 22cst. @ 40°C
Fuchs Plantocut 40SR	Ester Based Partially Saturated Neat Oil. 40cst. @ 40°C
Prolong Ultracut 1	Water Soluble EP Activated Cutting Fluid @ 10%
Quakercool 2772LF	Water Soluble Polymer Based Cutting Fluid @ 7%
Castrol Hysol XH	Water Soluble EP Activated Cutting Fluid @ 7%

Table 4-1 Cutting Fluids Evaluated during Torque Tapping Trials.

4.2.3 Results.

A summary of the results is shown in figure 4.2 which clearly shows that the use of a neat oil cutting fluid significantly reduces the torque tapping force. This is clearly attributable to the increased lubricity of neat oil cutting fluids over water soluble fluids.

Another interesting point raised by the results in the effect of extreme pressure additives. Fluids containing a chlorine based EP additive provided the lowest torque force measurements for each fluid type (water soluble and neat oil). In fact Castrol Ilogrind 600SP produced the lowest torque force measurement when treated with the

Prolong AFTM chlorinated paraffin additive, and was significantly lower than the untreated Ilogrind 600SP.

This result is very good at showing the effect of different EP additives, as although Ilogrind contains EP additives, sulphur and phosphorous based, the addition of a chlorine based EP additive showed significant improvements. This is attributable to the different activation temperatures of the different EP additives which are shown in figure 2.16 within the literature survey.

The ester based cutting fluids all displayed good lubrication characteristics with the slightly less viscous fluids performing marginally better than the Fuchs 40SR, with no significant difference between fully saturated (Castrol Carecut ES1) and partially saturated products (Fuchs 40SR and 22SR).

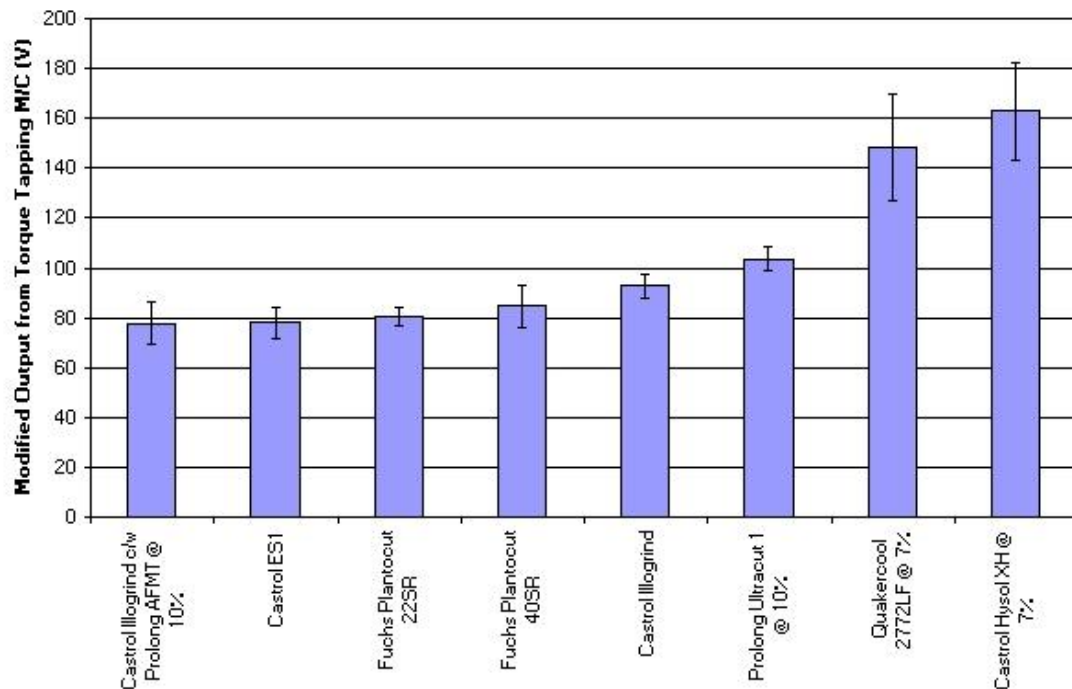


Figure 4-2 Summary of Torque Tapping Results used for Lubrication Testing

The graph shows the average normalised measurements for the torque tapping tests for each of the different cutting fluids. Error bars show the maximum and minimum values of the normalised measurements.

The ester based cutting fluids all displayed good lubrication characteristics with the lower viscosity fluids performing marginally better than the high viscosity Fuchs 40SR, with no significant difference between fully saturated (Castrol Carecut ES1) and partially saturated ester based product (Fuchs 22SR). However, there will be a more rapid deterioration in lubrication performance with the partially saturated ester based products over time, as it is known that fully saturated ester based fluids have a longer life than partially saturated ester based fluids.

4.3 Cutting Fluid Misting

4.3.1 Aim

An important theme throughout this thesis has been the importance of reducing fluid misting in the machine canopy in order to reduce the fire hazard when neat oil cutting fluids are used in HEDG.

The reduction of cutting fluid mist is split into two main areas. The first area, an investigation into chemical means of mist reduction by appropriate selection of the cutting fluids will be covered in the following sections. The second area, an investigation into mechanical means of mist reduction by improving cutting fluid application will be covered in chapter six.

The aim of the fluid misting tests was to develop a simple method of comparing the oil misting characteristics of different cutting fluids, and then use the test to determine which cutting fluids produced the least amount of mist.

The literature shows that high levels of oil mist in an atmosphere increases the risk of ignition, and that fluids can ignite below their flashpoint when these fluids form mists. Reducing the level of mist around the grind zone is therefore important in reducing the risk of ignition if neat oil cutting fluids are used in the grinding process.

The data has been used to help determine the most effective fluid for the grinding process, as fluids that produce less mist will help reduce the amount of mist produced in the grinding machine.

4.3.2 Experimental Procedure

Tests were conducted on equipment originally designed to measure the air release value of oils, a measure of an oils ability to release entrapped air in accordance with IP313/77 (BS 2000-313:2001). This equipment, manufactured by Stanhope Seta and shown in appendix 5, was adapted to allow oil mist to be collected and measured allowing comparative tests to be performed on different oils. A schematic of the test equipment can be seen in figure 4.3, with the actual layout shown in figure 4.4. These tests were performed at Fuchs Petrolub UK's laboratory facilities in Stock on Trent.

Oil is placed into the glass test vessel (figure 4.5) of the air release apparatus and heated to the required temperature by passing water, pre-heated to the required temperature by a Grant Instruments re-circulating water bath, through a water jacket that surrounds the test chamber. A calibrated thermocouple is used to test that the oil sample is at the required temperature prior to the tests being run.

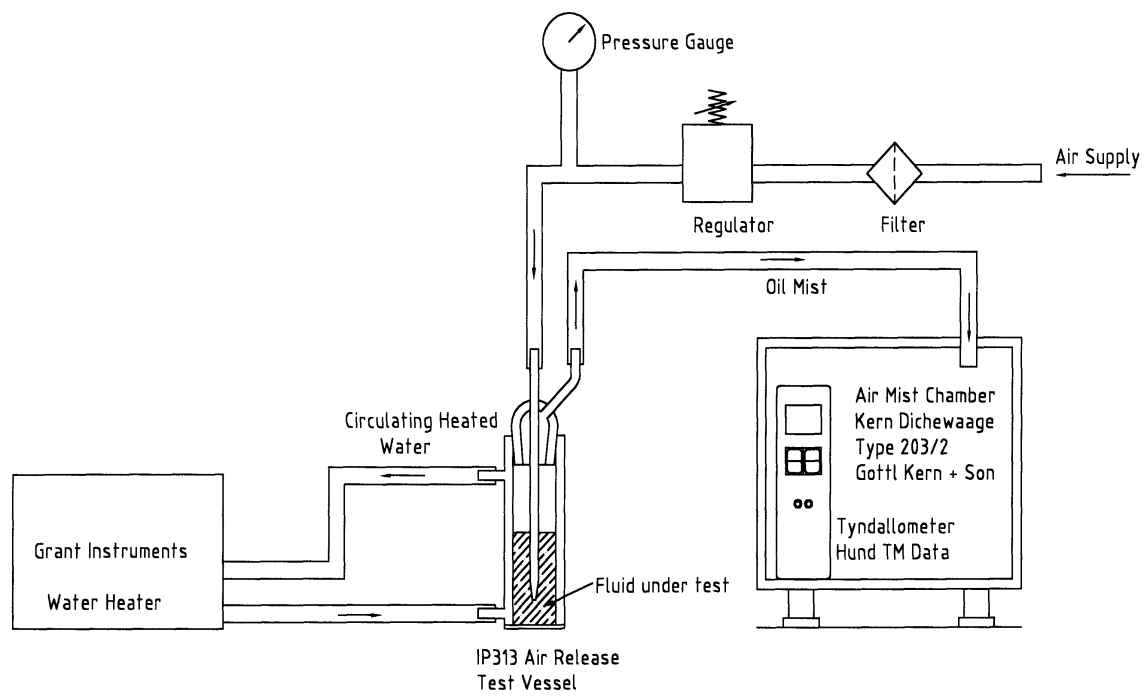
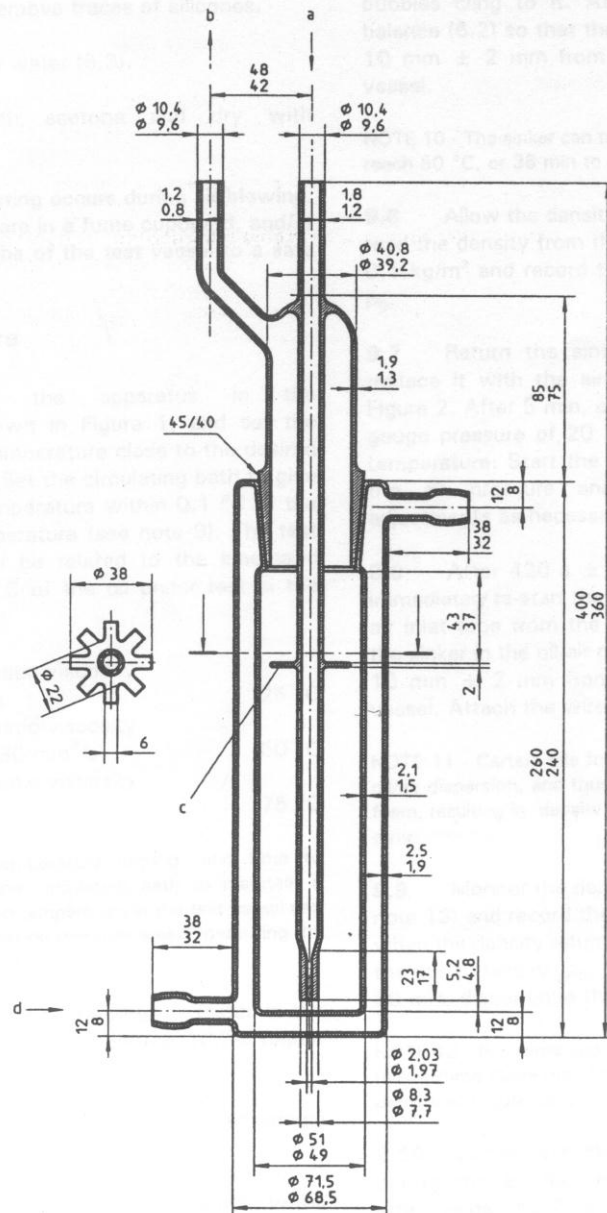


Figure 4-3 Schematic Diagram of Equipment Used to Conduct Oil Misting Tests



Figure 4-4 Photograph of Equipment used for Oil Misting Tests

Dimensions in millimetres



- a Air inlet
- b Air outlet
- c Baffle plate
- d Circulating fluid in
- e Circulating fluid out

Figure 4-5 Glass test vessel as described by the IP313 standard for the determination of the air release values of oils. (BS 2000-313:2001)

To ensure consistency, the same volume of each cutting fluid was tested each time. This was achieved by filling the glass test vessel up to a pre-scribed line 115mm above the bottom of the vessel, so a constant volume of 0.191 litres of cutting fluid was tested.

Compressed air then pumped at low pressure (20&40mBar) into the chamber containing the oil sample under test and the particle emission from the fluid is passed into a collecting chamber where it is measured using an optical device called a Tyndallometer, named after its inventor. A Tyndallometer works on the principle of light scatter to measure the mass concentration of dust and aerosol distributions (http://www.osti.gov/energycitations/product.biblio.jsp?osti_id=6442985). It does this by measuring the intensity of the light scattered at an angle from an incident beam by the dust or aerosol cloud (<http://www.maden.hacettepe.edu.tr/dmmrt/dmmrt660.html>). Mist density measurements displayed on the Tyndallometer are recorded at regular intervals during the test.

To minimise any cross contamination between fluids when changing from one cutting fluid and the next, the test vessel was thoroughly cleaned with a solvent cleaner and then acetone and allowed to dry between each series of tests.

The mineral and ester based cutting fluids listed in table 4-2 were tested, but aqueous fluids were not as they produce mists containing mainly water. Only a small percentage of the total mist generated by aqueous fluids is the concentrate. (Health and Safety Executive, 2002; Yue and Michalec, 1999)

Fluid	Comments
New Castrol Ilogrind 600SP	Unused Neat Mineral Oil. 9.8 cst @ 40°C with Polymer Anti-Mist Additives
Used Castrol Ilogrind 600SP	Used Neat Mineral Oil. 9.8 cst @ 40°C with Polymer Anti-Mist Additives
Used Castrol ES1	Ester Based Fully Saturated Neat Oil. 27cst. @ 40°C
New Castrol ES2	Ester Based Fully Saturated Neat Oil 8.8 cst @ 40°C
Fuchs Plantocut 22SR	Ester Based Partially Saturated Neat Oil. 22cst. @ 40°C with Polymer Anti-mist Additives
Fuchs Plantocut 40SR	Ester Based Partially Saturated Neat Oil. 40cst. @ 40°C with Polymer Anti-mist Additives
Fuchs ISO-22	ISO-22 Base Stock. 22cst @ 40°C
Fuchs ISO-32	ISO-32 Base Stock. 32cst @ 40°C

Table 4-2 Fluids Tested during Misting Tests.

4.3.3 Results

In conducting these experiments a large amount of data was collected. To ensure clarity the pertinent data have been separated and used to demonstrate important relationships in isolation. Once these relationships have been shown, then the comparative performance of the cutting fluids tested will be examined.

4.3.3.1 Effect of Fluid Viscosity on Mist Generation.

The easiest way of looking at the effect of viscosity was to perform misting tests on two ISO base oils. Such base fluids are the building blocks of many lubricating oils, and are blended together with different additives packages to give a lubricating oil of the correct viscosity and performance characteristics.

These base stocks fluids contain no anti-misting additives, nor any other performance enhancing additive which may influence the misting characteristics, and are therefore useful in helping to evaluate the effect of fluid viscosity on mist generation.

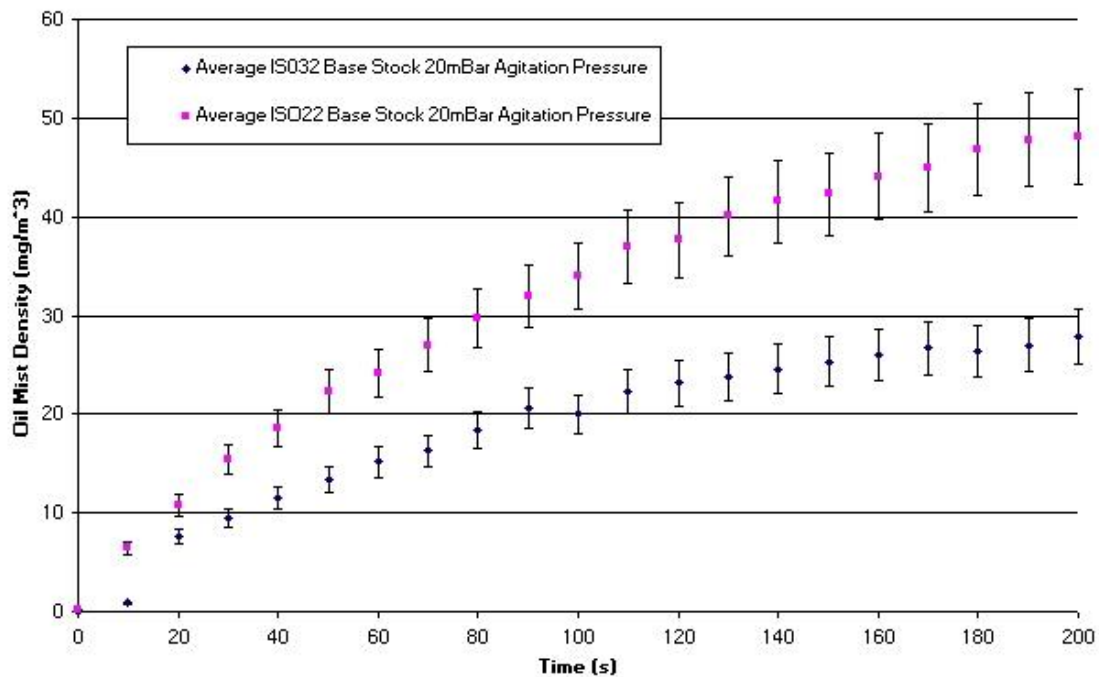


Figure 4-6 Fluid Misting Characteristics of ISO22 and ISO32 Base Stocks.

Tests performed at 50°C, 20mBar Agitation Pressure.

It is clear from figure 4-6 that the higher viscosity oil (ISO32) produces less mist under these test conditions, and supports the statement by Malkin (1989) that higher viscosity oils produce less mist.

4.3.3.2 Effect of Agitation Pressure

Tests were performed at a constant temperature of 50°C, with two different supply or agitation pressures, 20 and 40mBar. Figure 4-7 shows there is a significant increase in the amount of mist generated when the agitation pressure is increased, due to the increase in energy being applied to the system.

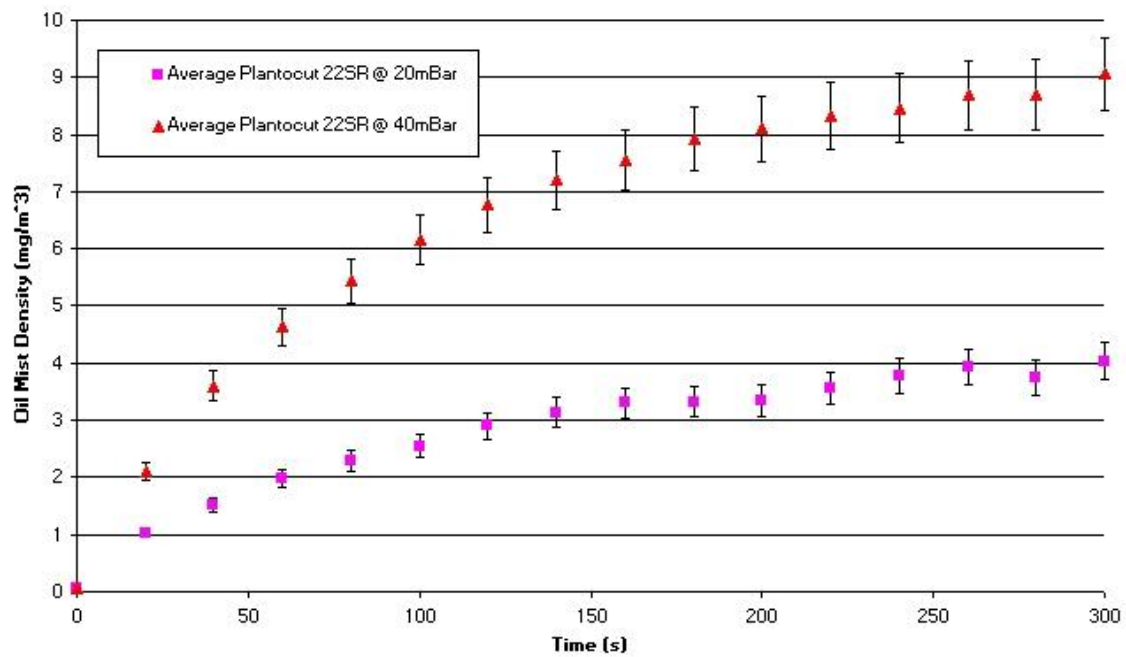


Figure 4-7 Fluid Misting Characteristics of Fuchs Plantocut Ester Based Neat Cutting Oils.
Tests performed at 50°C, and at two different agitation pressures, 20 & 40mBar.

4.3.3.3 Effect of Temperature

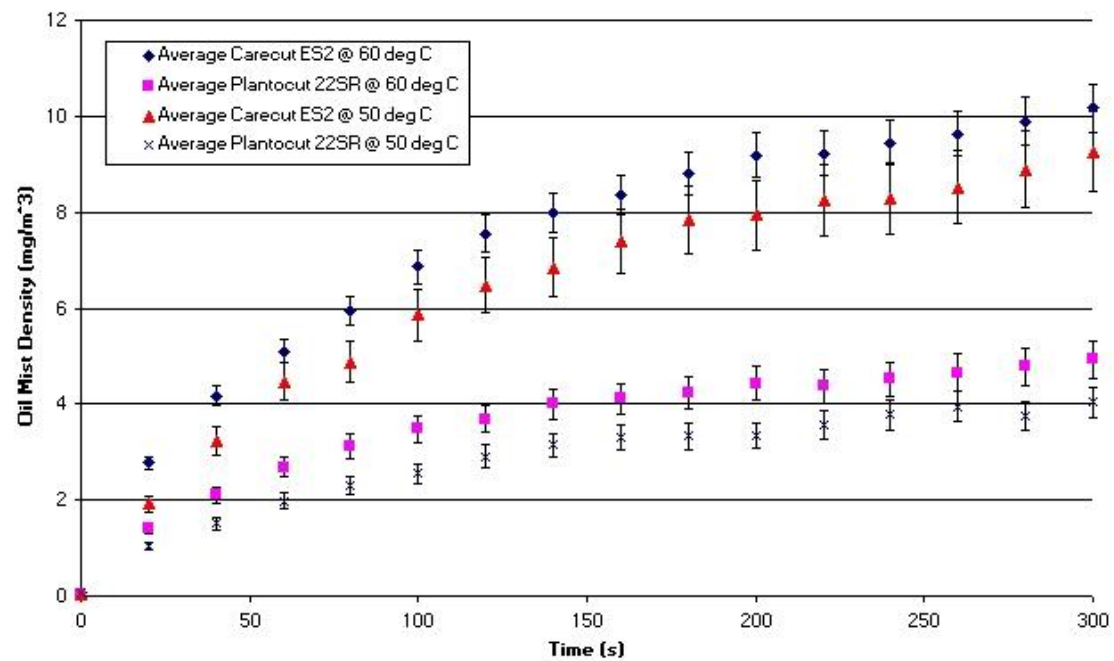


Figure 4-8 Fluid misting characteristics of Fuchs Plantocut 22SR and Castrol Carecut ES2 Ester Based Neat Cutting Oils.

Tests performed at 20mBar agitation pressure, and at two different temperatures, 50 & 60°C.

Tests were performed at a constant agitation pressure of 20mBar, at two different oil temperatures, 50°C and 60°C. Figure 4-8 shows that there is a significant increase in the amount of mist generated when the oil temperature is increased.

Both Horner (Horner, 2003) and Thornburg et al (2000) observed this phenomenon in metal cutting, where both the cutting tool and workpiece can get very hot, and attributed the increase in mist level to an increase in the evaporation loss (Horner,2003; Thornburg and Leith, 2000) with subsequent condensation forming the mist (Thornburg and Leith, 2000). This process can extend beyond the cutting operation and continue in other parts of the machine, and in particular where cutting fluids are in contact with hot swarf. (Horner, 2003)

4.3.3.4 Effect of Fluid Usage on Misting Performance

Figure 4-9 shows the stark difference between the misting performance between a used and un-used mineral oil that contains polymer based anti-misting additives. The used fluid was taken from the clarifier system used to supply the Edgetek SAM and Edgetek SAT machines at Cranfield University and has had been in use for approximately 4 years when the sample was taken. The unused Ilogrind 600SP sample was taken from a new barrel of oil.

Whilst there may be small variances between different batches of the same fluid, the basic composition of the fluid has not changed in the four years between the used and unused fluids were manufactured (Castrol (UK) Ltd: private correspondence, 2005).

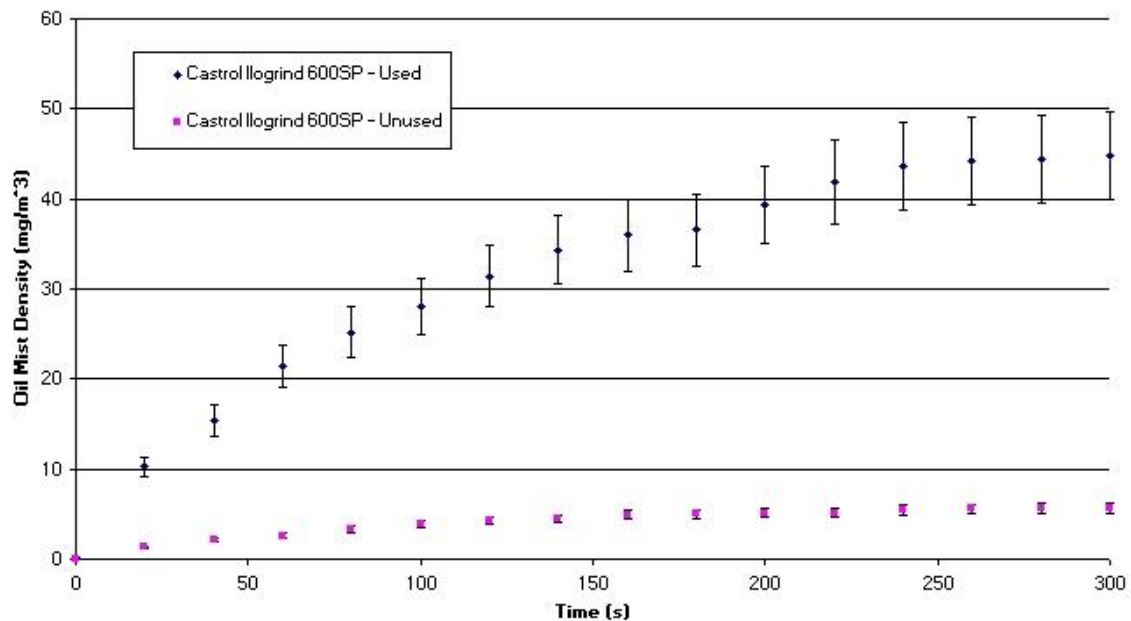


Figure 4-9 Fluid Misting Characteristics of Used and Un-used Castrol Ilogrind 600SP Neat Mineral Oil Cutting Fluid.

Tests performed at 50°C, 20mBar Agitation Pressure. This fluid contains Polymer Based Anti-misting Additives.

Whilst there is inevitably some contamination of the used oil with other fluids, attributable to fluid changes undertaken on the Edgetek machines in the course of the experimental work which takes place on these machines, this is undoubtedly less than is suffered in the majority of industrial systems which are renowned for their abuse.

The most likely explanation for the significantly higher mist generated by the used Ilogrind is the degradation of the anti-misting additives. These additives are long chain, high molecular weight polymer molecules, which attract smaller lighter molecules toward them due to Van der Waals forces. It is well known that these long chain molecules are shear sensitive, which means that they are easily torn apart when shear forces such as those found in the grinding zone and fluid pumping systems (Kalhan and Twining, 1998; Kalhan and Twining, 2000), are applied to the molecules. Consequently, the anti-mist molecules are chopped up into a series of smaller, lighter molecules, with a subsequent drop in anti-misting performance.

Gulari and Manke et al (1995) observed this degradation in mist performance when testing polymer anti-mist additives in neat oil cutting fluids and correlated this increase with a decrease in the molecular weight of the polymer additive. This problem is not restricted to neat oil cuttings fluid, Turchin and Byers (2000) also observed this phenomenon when testing water soluble cutting fluids

This has important ramifications if neat oil cutting fluids are used containing anti-mist additives. If the performance of a fluid is to be maintained, then the condition of such polymer additives must be checked and replenished as necessary. This is contrary to the usual assumption that neat oil cutting fluid systems are maintenance free.

4.3.3.5 Comparative Performance of Cutting Fluids

Figure 4-10 shows all the comparative results for the different cutting fluids when tested at a temperature of 50°C and an agitation pressure of 20mBar. The error bars have been omitted for clarity, but it is clear that the used Ilogrind 600SP produces the by far the most mist under these conditions. When a key aim is to reduce the level of mist within the machine in order to reduce the potential fire hazard, this is clearly a poor result.

Figure 4-11 is a comparison of all the different cutting fluids with the exception of the used Ilogrind 600SP, again when tested at a temperature of 50°C and an agitation pressure of 20mBar. It is clear that the unused ester based cutting fluids (Fuchs 40SR, Fuchs 22SR) performed significantly better than the unused neat mineral oil (Castrol Ilogrind 600SP). It is also clear that the amount of mist generated reduced with increasing viscosity, with the Fuchs 40SR producing less mist than the 22SR, mirroring the trend shown with the ISO base oils in section 4.3.3.1.

The unused Castrol Ilogrind 600SP performed well, as it produced the third lowest mist level despite its low viscosity. However, its performance reduces dramatically with use due to the shear stability of the polymer anti-mist additives. This effect is clear in both figures 4-9 and 4-10

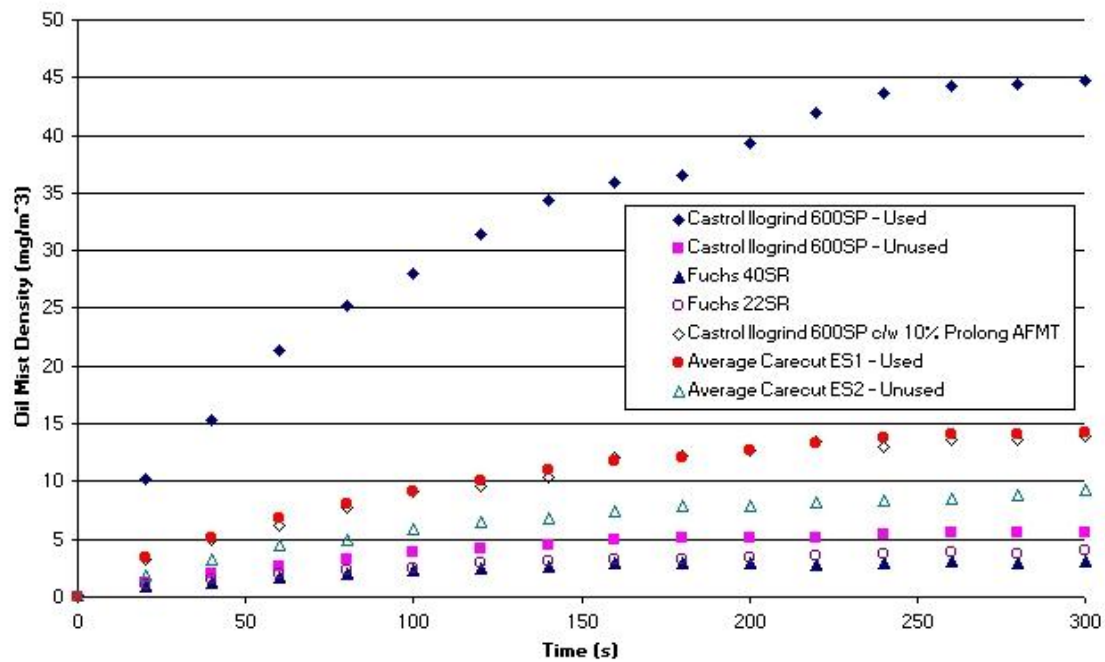


Figure 4-10 Comparative misting performance of cutting fluids.

Tests performed at 50°C, 20mBar agitation pressure. Error bars not shown for clarity. The fluids are unused unless otherwise stated.

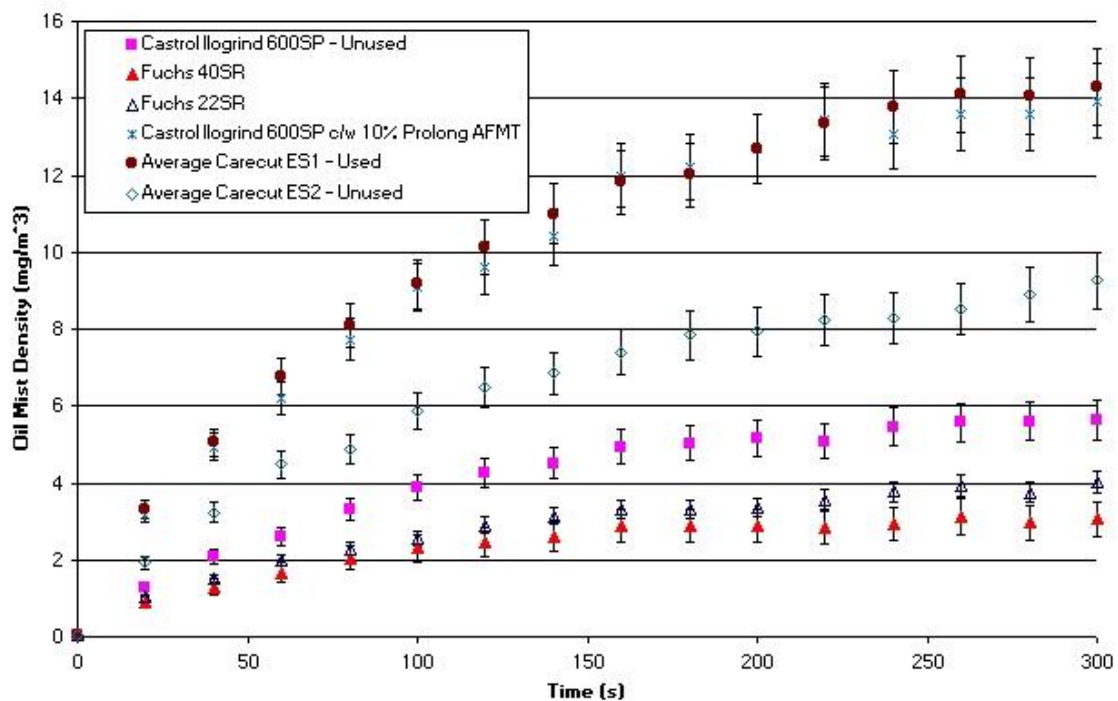


Figure 4-11 Comparative misting performance of cutting fluids.

Tests performed at 50°C, 20mBar agitation pressure. Used Ilogrind 600SP Neat Mineral Oil is not shown for clarity. The fluids are unused unless otherwise stated.

It is important to note however, that both the Fuchs products contain similar anti-mist additives to the Castrol Ilogrind product, so its performance too will degrade over time and thus produce greater levels of mist, all be it from a lower starting lower point.

Neither Castrol ester based products, the Carecut ES1 and ES2, contain anti-mist additives so are not susceptible to degradation of polymer additives. Both these products are fully saturated products, meaning the base stocks are of a higher quality or grade than the Fuchs ester based products. This said however, there is a price premium to be paid for these products.

The Carecut ES2 product therefore performed very well, producing the fourth lowest mist levels of all the fluids tested, despite having the lowest viscosity, and an absence of any anti-mist additives.

One would expect the Carecut ES1 product therefore to produce even lower levels of mist than the ES2 product as a result of its higher viscosity. This was not in fact the case. It is important however to note that this fluid had been used on a previous project, and unfortunately an unused sample was unavailable. The higher misting level is attributable to two factors.

- This particular fluid had previously been used in the large coolant clarifier system at Cranfield University, one that usually contained used Ilogrind 600SP. Whilst every care is taken when changing cutting fluids to clean the system out, some cross contamination is inevitable, and there will have been a small percentage of used Ilogrind 600SP within this sample.
- This particular fluid was over four years old when tested, and whilst this fluid is a fully saturated product, which gives the fluid a prolonged life over non-saturated product, some deterioration and oxidation of the fluid over this time is inevitable. This said however, used Castrol ES1 produced substantially less mist than used Castrol Ilogrind 600SP, and it is reasonable to expect unused ES1 to produce less mist than unused Carecut ES2.

In all the ester based fluids performed significantly better than neat mineral oil cutting fluids as they produced less mist. This is attributable to a more defined molecular weight distribution than found in neat mineral oils. Neat mineral oil fluids are blended from a wide range of different viscosity base stocks to achieve a fluid with the desired performance characteristics and attributes. As a result, their molecular weight distribution is far less defined, the fluid containing a wide range of lighter and heavier fractions. Consequently, synthetic fluids have lower evaporation loss (Horner, 2003) and lower volatility for fluid of a given viscosity as both are largely determined by molecular size and structure (Jackson, 1989), with lighter fractions both more volatile and prone to evaporation.

Prolong AFTM performed poorly in these tests, with the resultant fluid producing significantly higher levels of mist than the base fluid that it was applied to. The AFTM treatment was added at a concentration of 10% into unused Ilogrind 600SP neat mineral

oil, yet the resultant fluid produced more than twice the amount of mist after 300seconds.

It is doubtful that this loss of performance is attributable to a dilution of the anti-mist additives in the Ilogrind 600SP, as polymer anti-mist additives are generally used at very low concentrations (typically 1%) otherwise they affect the viscosity of the fluid. A far more likely explanation is that whilst the viscosity of the AFTM additive is quite high (approximately 40cst @ 40°C), the fluid contains many lighter fractions that are easily released from the bulk fluid to form the mist.

4.3.4 Conclusions

Some interesting conclusions can be drawn from these misting tests

- Ester based fluids produce less mist than neat mineral oil fluids.
- Higher viscosity fluids tend to generate less mist.
- The shear stability of polymer additives reduces their performance with use, resulting in higher levels of mist being produced.
- Fluids containing anti-mist additives should not be used in HEDG, but instead better quality base fluids are preferred which have no need for anti-mist additives thus reducing the deterioration of mist performance over time.
- Cutting fluid temperature should be kept as low as possible.
- Mechanical agitation should be reduced as much as possible.

4.4 Cutting Fluid Ignition

The literature revealed the fluids exhibit a characteristic known as residence time, whereby a cutting fluid exposed to a specific heat source may or may not ignite depending on the time the fluid is exposed to the heat source. Clearly therefore, flow is an important variable when testing cutting fluids for grinding applications. As standard flashpoint tests fail to consider the residence time, as the body of fluid under test is stationary, two special test rigs were designed and built by the author to allow more representative testing to be carried out. The first, an inclined channel test rig was designed to test the following ignition characteristics.

- Ignition of cutting fluid by a hot body
- Spark ignition of evaporate caused by a hot body

The second test rig was designed to test

- Spark ignition of cutting fluid mist

In practice, it proved impossible to design a test rig to precisely simulate the conditions which occur within the grinding zone, Cutting fluid speed, for example, is almost impossible to replicate if one wants to make a test rig designed to fit onto a work bench, when cutting fluid speeds of approximately 150m/s are common place in HEDG.

However the tests described in the sections are more representative of the grinding process than standard flashpoint tests.

4.4.1 Ignition of Cutting Fluid by Hot Body

4.4.1.1 Aim

The aim of this particular test was to establish whether a simple heat source, which may be a workpiece where the temperature is elevated due to poor selection of process parameters or a badly worn grinding wheel for example, could ignite bulk cutting fluid. In these tests, the cutting fluid is exposed to a heated body, but no external ignition source, such as a grinding spark, is introduced.

4.4.1.2 Experimental

The cutting fluids under tests are supplied to an inclined heated channel test which consists of a heated stainless steel plate inclined at 3° to ensure the fluid flows at a constant speed over the heated plate, with the fluid taking 8 seconds to travel the full length of the heated plate.

The heated plate has an 8mm wide x 2.2mm deep oil groove machined in its upper surface which ensures the cutting fluids flow in a controlled and consistent manner down the heated plate. A simple dam formed at the top of the heated channel ensures that the cutting oil can only flow down the pre-machined oil groove.

Cutting fluid is supplied to the inclined heated plate from a pressurised reservoir via a feed block. The reservoir is pressurised using either nitrogen or carbon dioxide (CO₂) used to prevent any unwanted ignition within the reservoir. The gas is supplied from a standard gas bottle via a pressure regulator set, which is set to a pressure of 10PSI. Such a low pressure is normal in these types so as to prevent the nitrogen or carbon dioxide gas diffusing into the cutting fluid and thus influencing the results.

The flow of cutting fluid supplied to the inclined heated plate is carefully controlled by means of a flow control valve and measured using a F & P Precision Bore Flowrate fitted with a No.3F – 3/8 – 20.5/81 tube, and allows a cutting fluid film of constant thickness to be maintained in the oil groove.

The inclined heated plate is heated by passing a very large direct electrical current through it. The plate is connecting via 2 large brass contact blocks to a large DC power supply, in this case a BOC Transtig AC/DC 375 welding set (see figure 4-12). The current flowing through the inclined heated plate can be varied on the welding set, and consequently the temperature of the plate and thus any cutting fluid running down it, can be varied. As the cutting fluid flows down the inclined heated plate, the fluid gets progressively hotter the further it travels down the heated plate. This effect can be seen in figure 4-13.



Figure 4-12 BOC Transtig AC/DC 375 welding set.

This was used as a large DC power supply to provide the current used to heat the incline plate.

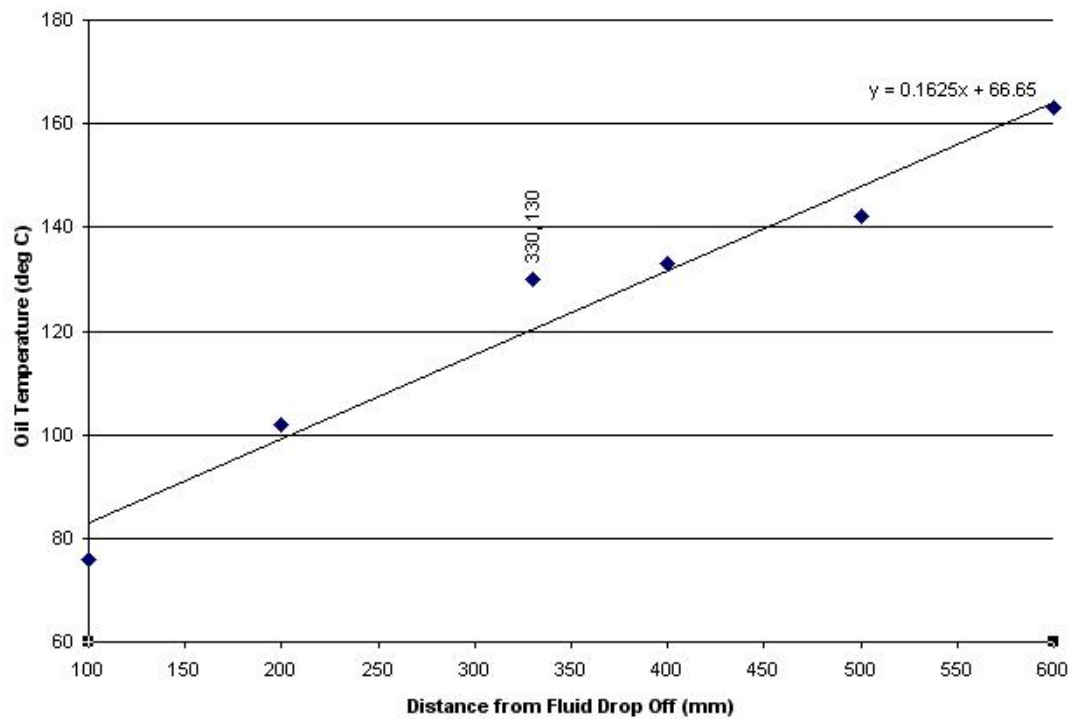


Figure 4-13 Progressive heating of the cutting fluid as it travels down the inclined heated plate.

In this particular case the fluid has reached a temperature of 130°C by the time it had travelled 330mm from the fluid drop of point.

4.4.1.3 Results

Attempts were made to ignite a neat mineral oil (Castrol Ilogrind 600SP) and an ester based neat cutting oil (Fuchs 40SR) by this method but both attempts were unsuccessful.

When either cutting fluid was exposed to a hot heat source of sufficiently high temperature, the cutting fluid simply boiled away, producing copious amounts of smoke in the process, leaving behind a black carbonised residue on the heated plate (see figure 4.14). Figure 4-15 shows this the large amounts of smoke being generated as the cutting fluid boils off, in this instance; the fluid in question is a neat mineral oil cutting fluid (Castrol Ilogrind 600SP).

Increasing the temperature of the heated channel failed to result in cutting fluid ignition, with increasing channel temperatures simply causing the cutting fluid to evaporate closer to the fluid drop off point.

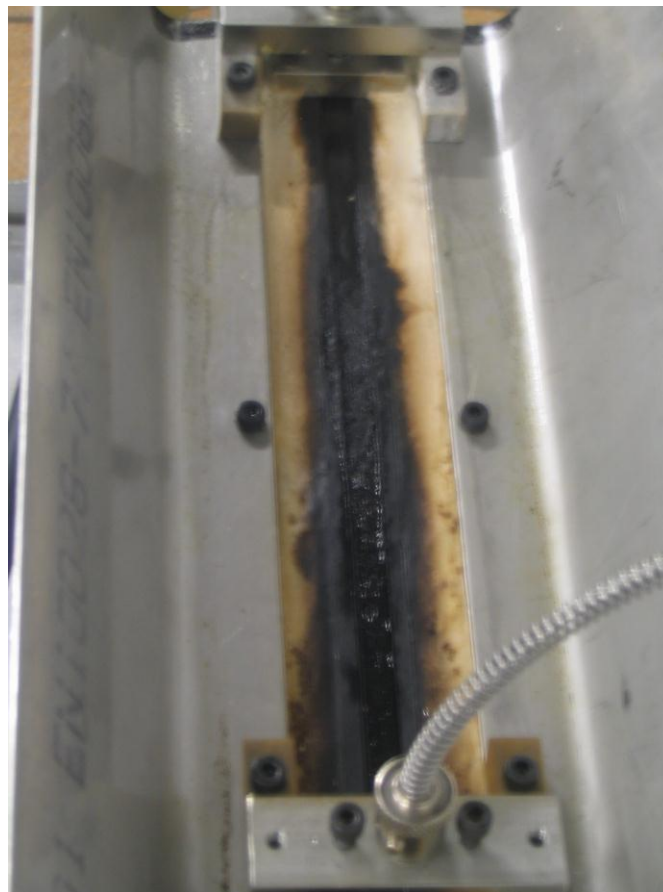


Figure 4-14 Black carbonised residue remaining in heated channel as a result of the cutting fluid boiling away.



Figure 4-15 Copious amounts of smoke produced when attempting to ignite neat mineral oil cutting fluid with a hot body.

4.4.2 Spark Ignition of Cutting Fluid Evaporate

4.4.2.1 Aim

The aim of these tests was to determine whether exposure to a heat source would increase the likelihood of cutting fluid ignition when an external ignition source such as a grinding spark was present. Furthermore, by testing a range of different cutting fluids, different fluids could be ranked according to their susceptibility / resistance to this form of ignition.

4.4.2.2 Experimental

These tests were similar to those conducted to test the ignition characteristics of cutting fluids when exposed to a hot body described in the previous section. They differed only by the fact that a laser was introduced to create a spark to ignite any evaporate / volatile fractions released from the cutting fluid as a consequence of exposure to a heat source.

A Continuum Surelite SL11-10, 532nm wavelength, Nd:YAG laser was used as an energy source as the laser beam can be focused to a point in order to simulate a hot grinding spark. The overall set-up of the laser and inclined heated plate test rig is shown in figure 4-16.

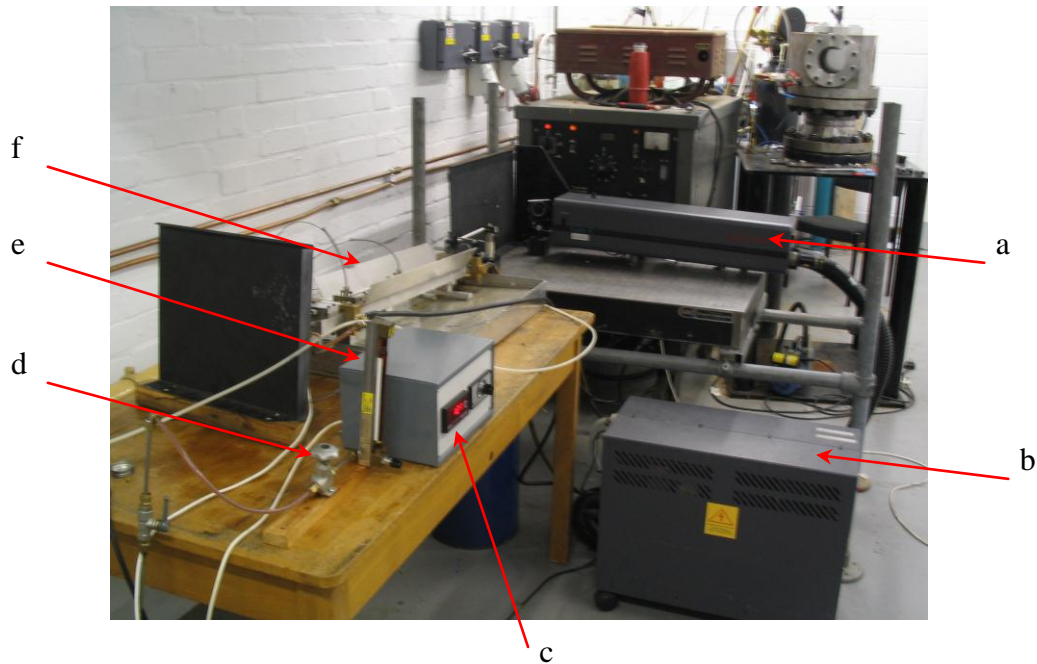


Figure 4-16 Inclined heated plate test rig with Continuum Surelite SL11-10 Nd:YAG laser for testing the ignition characteristics of cutting fluid evaporate.

Note also BOC Transtig welder in the background.

- a) Surelite ND-YAG laser
- b) Laser control box and power supply
- c) Digital Thermometer (not used during experiments)
- d) Flow regulator
- e) F+P precision bore flowmeter
- f) Inclined channel test rig

Figure 4-17 shows a close up of the Surelite laser, a 532nm mirror and the 150mm focal length lens used to direct and focus the laser beam respectively. The 532nm mirror is used to reflect the laser beam through 90° so it travels straight down the centre of the inclined heated plate. The 150mm focal length lens focuses the beam to a point 19mm above the heated plate, 145mm from the end. The Surelite laser trigger frequency was set to 10Hz, which translates to 10 lasers pulses per second.

The temperature of the cutting fluid was again measured using a hand held Omega HH506RA digital thermometer with a calibrated K type thermocouple (fig 3.6).

Temperature measurements were taken at a point 330mm from the fluid drop off point, this point was selected as it was sufficiently far removed from the laser focus point so as not to interfere with the laser in any way, but more importantly, it was sufficiently far from the point of ignition for personal safety reasons. Although this was not the point at which the laser was focused, and that the fluid is significantly cooler than at the point of ignition, consistently measuring the different cutting fluids at the same point does allow fair comparisons to be made.

To illustrate this point, if one refers to the example shown in figure 4-13, the measured fluid temperature was 130°C when measured at a point 330mm from the fluid drop off

point, the fluid was over 160°C when it had reached a point 600mm from the fluid drop off point. If the fluid ignited when the measured temperature was 130°C, then the actual temperature of the fluid would actually have been much closer to 160°C when the fluid evaporated ignited. However, measuring the exact temperature of the fluid at the exact point of ignition was not possible for safety reasons. Instead great care was taken to ensure the test rig was set up correctly to ensure consistency between the tests, and the fluid temperature was measured at the same point to allow fair comparisons to be made.

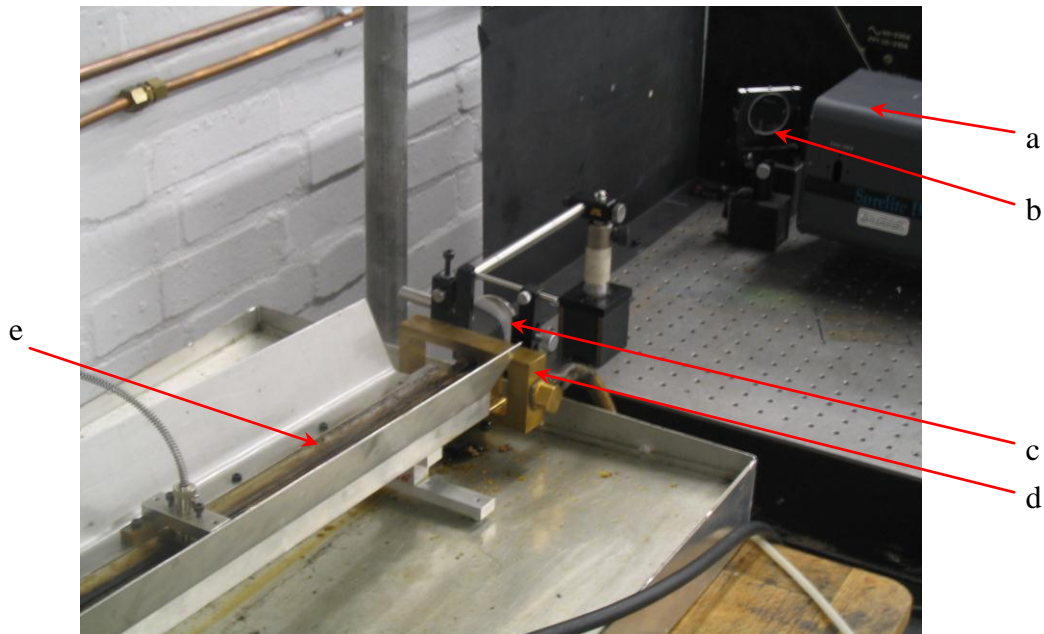


Figure 4-17 *Focusing the laser beam to a point using a 150mm focal length lens in order to simulate a hot grinding spark.*

- a) *Surelite Nd-YAG Laser*
- b) *532nm Mirror*
- c) *150mm focal length lens*
- d) *Electrical contact*
- e) *Inclined heated plate*

4.4.2.3 Correlation Between Spark Energy and Grinding Chip Size.

Throughout the tests, the laser was set to a power setting of 1.35KV. The actual laser power was measured using an Ophir Optronics Ltd Model AN2/E Laser Power Meter (see figure 4-18) to allow the laser power, and the subsequent ignition spark energy, to be correlated to an actual grinding chip size. The measured laser power was 150mJ and according to Jin et al (Jin and Stephenson, 2003), the limiting chip energy can be estimated from:

Equation 4-1

$$e_{ch} = \rho c T_{ch} \quad (\text{Jin and Stephenson, 2003})$$

Where :

E_{ch} = limiting chip energy (J/mm³)

T_{ch} = chip temperature (°C)

ρ = workpiece material density (Kg/m³)

c = specific heat capacity (J/KgK)

If we assume the workpiece material is 51CrV4, and estimating the chip temperature is close to the melting temperature of the material (1500°C) (Jin and Stephenson, 2003)

$$T_{ch} = 1500^{\circ}\text{C}$$

$$\rho = 7770 \text{ Kg/m}^3$$

$$c = 460 \text{ J/KgK}$$

Then:

$$\text{Limiting chip energy} = 5.36 \text{ J/mm}^3$$

Using the measured laser power of 150mJ

$$\text{Chip volume} = \text{chip energy} / \text{limiting chip energy}$$

$$= 150 \text{ mJ} / 5.36 \text{ J/mm}^3$$

$$\text{Chip volume} = 0.028 \text{ mm}^3$$

Assuming the chip is a cube, the chip size would be:

$$\text{Chip size} = \text{chip volume}^{1/3} \text{ mm}$$

$$\text{Chip size} = 0.028^{1/3} \text{ mm}$$

$$\text{Chip size} = 304 \mu\text{m} \times 304 \mu\text{m} \times 304 \mu\text{m}$$

Whilst this may seem excessively large in conventional grinding, extremely large pieces of grinding swarf have been witnessed when HEDG is employed, and particularly in cylindrical HEDG. The grinding swarf shown in figure (4-19) was not a single grinding chip, but a knotted mass of small chips and very fine metal strands or threads more typical of conventional turning operations. This swarf was found on the worktable, just below the grinding area and shows that very large pieces of hot material can be ejected from the grinding zone and could be a potential ignition source.

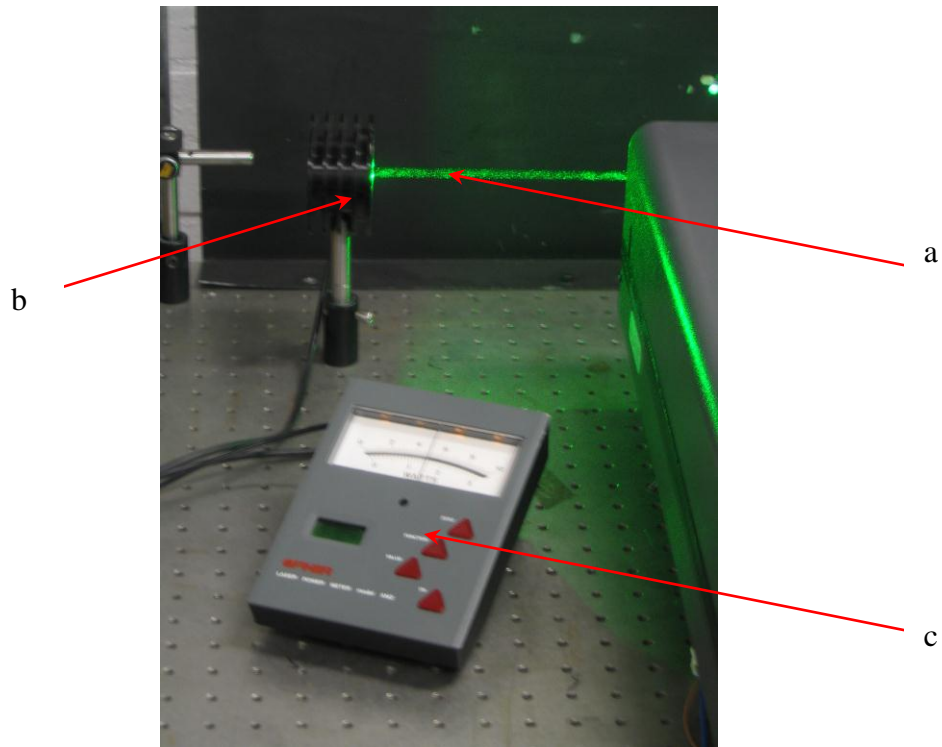


Figure 4-18 Measurement of the laser power using a Laser Power Meter.

- a) Laser Beam
- b) Ophir Optronics Ltd Model AN2/E Laser Power - Detector
- c) Ophir Optronics Ltd Model AN2/E Laser Power Meter

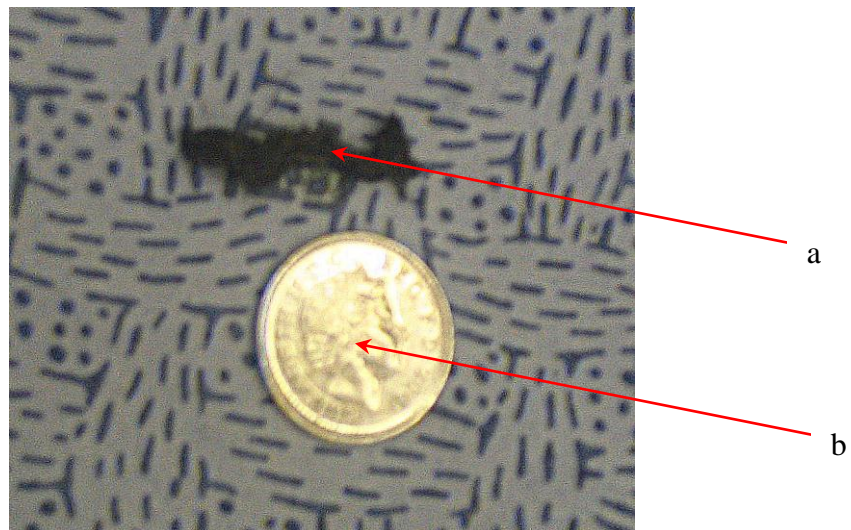


Figure 4-19 Grinding swarf generated during cylindrical HEDG grinding at a specific removal rate of 2000.

- a) Grinding Swarf
- b) 10 pence piece

Note, a 10 pence piece is included for reference purposes ($\varnothing 24.5\text{mm}$)

4.4.2.4 Results

Figure 4-20 shows a typical ignition of cutting fluid evaporate when a spark is used as an ignition source. Although the laser is focused in free space above the channel, when the cutting fluid evaporant is ignited the flame spreads quickly to the bulk fluid. Carbon Dioxide or Nitrogen gas is then used to put out the fire.

Figure 4-21 shows a typical series of tests used to establish the ignition characteristics of a cutting fluid. The first six tests in the particular sequence shown were used to find the temperature at which the cutting fluid ignites. The remaining tests are designed to define the transition temperature, the temperature below which the cutting fluid fails to ignite, above which ignition will occur.

In practice, there is no single transition temperature, rather a fuzzy band or range of temperatures where ignition may or may not occur. In the example shown in figure 4-21, ignition occurred at 173°C and 174°C and yet failed to ignite 176°C. The remaining tests are therefore used to narrow the temperature range between the ignition and non-ignition regions.

When summarising the results in table 4-3, ignition tests in the transition band are used to define the threshold temperatures, but are not included in the table for clarity purposes. Furthermore, a 10% tolerance band based on the nominal threshold temperature is calculated, with any tests conducted at a temperature either above or below this tolerance band being omitted as being outside the area of interest.



Figure 4-20 Ignition of the cutting fluid.

Once the cutting fluid evaporate has been ignited with a spark, the flame spreads to the bulk fluid.

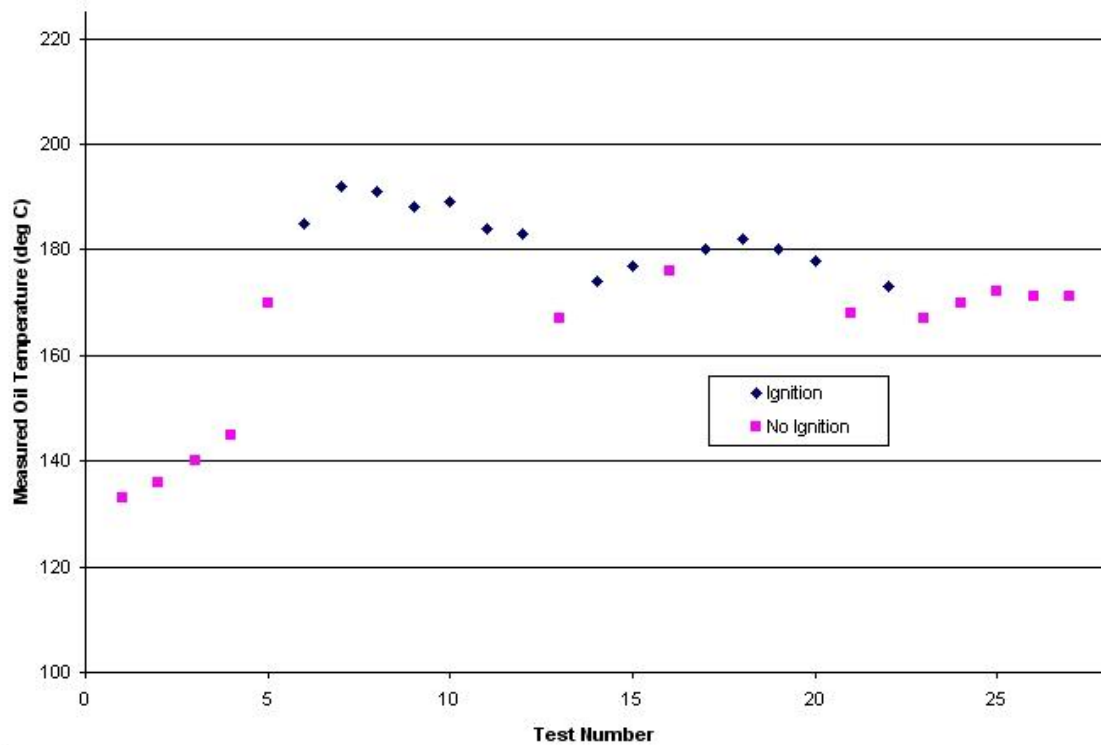


Figure 4-21 Spark ignition of cutting fluid evaporate.

Results for Ilogrind 600SP c/w Prolong AFMT @ 10%. Oil temperature measured at 330mm from fluid drop off point.

For the example shown in figure 4-21, the first four tests are omitted from the summary table, as all were conducted at a temperature lower than the nominal threshold temperature (175°C – 10%)

Fluid	Temperature (°C)		No. of Tests	Ignition Frequency	Closed Cup Flashpoint (°C)
Fuchs 40SR	Above	185	9	9 from 9	216
	Below	183	6	0 from 6	
Fuchs 22SR	Above	178	11	11 from 11	215
	Below	176	7	0 from 7	
Castrol ES1	Above	213	8	7 from 8	240
	Below	211	7	0 from 7	
Used Castrol Ilogrind 600SP	Above	125	7	7 from 7	>130
	Below	124.5	6	0 from 6	
Unused Castrol Ilogrind 600SP	Above	127	7	7 from 7	>130
	Below	123	6	0 from 6	
Unused Ilogrind c/w Prolong AFTM @ 10%	Above	177	12	12 from 12	135 open cup
	Below	172	7	7 from 7	

Table 4-3 Summary of cutting fluid evaporate spark ignition tests.

The summary of results in table 4-3 shows the neat mineral oil (Castrol Ilogrind 600SP) ignited at a significantly lower temperature than all the ester based neat cutting oils. The results for the Fuchs 22SR and Fuchs 40SR products show that for fluids from the same product family, lower viscosity fluids will ignite when exposed to a lower temperature than their higher viscosity counter parts. The results also show that the fully saturated ester based cutting oil, the Castrol ES1 product, had the greatest resistance to ignition, needing to be raised to a temperature in excess of 210°C, at the point of temperature measurement, before ignition of the evaporate was realised. The fully saturated ester based product therefore performed better than the partially saturated Fuchs 22SR and 40SR products.

One interesting result was the similarity in performance between the used and un-used neat mineral oil. Despite a significant deterioration in the levels of mist generated by used Ilogrind shown in section 4.3.3.4 of this chapter, there was no significant difference in the temperature at which the used and unused samples could be ignited. It is interesting to note however, that the threshold between ignition and non ignition far more defined for the used sample of Ilogrind 600SP. The most likely explanation for this would be the loss, due to evaporation over time, of the lighter fractions from the cutting fluid.

As a general rule, there is good correlation between the inclined heated channel ignition tests and the standard flashpoint results published in the manufacturer's data sheet. The exception to this is when the neat mineral oil (Castrol Ilogrind 600SP) is mixed with the Prolong AFMT additive. Despite having very similar flashpoints, when combined the resultant fluid ignited only when the fluid had been raised to a significantly higher temperature. The most probable explanation for this is that the Prolong AFMT additive has a very long residence time, a factor not considered in normal flashpoint tests.

This particular result therefore demonstrates the usefulness of this type of ignition testing when evaluating cutting fluids, as it allows the influence of both the residence time the fluid volatility to be accessed simultaneously in one, relatively simple test. This type of test provides a single output – the “ignition temperature”, which allows different cutting fluids, with different flashpoint, residence time and volatility characteristics to be compared, both easily and fairly, in a more meaningful and representative manner.

4.4.3 Spark Ignition of Cutting Fluid Mist

4.4.3.1 Aim

The literature surrounding the ignition of fluids showed that fluid can ignite well below their flashpoints. It is therefore important to understand the ignition behaviour of cutting fluid mists and like the previous section of the ignition of cutting fluid evaporate, rank different cutting fluids according to their susceptibility / resistance to this form of ignition.

4.4.3.2 Experimental

A second test rig was designed in order to perform spark ignition tests on cutting fluid mists. A large aluminium ignition chamber was designed and constructed in order to control any flame that resulted when attempting to ignite a cutting fluid mist with the aid of a spark.

The cutting fluid mist was generated by a Delavan No.4 type WDA hollow cone spray nozzle mounted into a special heated nozzle block mounted at the end of the ignition chamber. The nozzle block was heated using 3 x 200w cartridge heaters both to allow the cutting fluid to mist more readily, but also to assist with ignition. The temperature of the heated nozzle block was measured using a K type thermocouple connected to a digital temperature display and controlled by adjusting the supply voltage to the cartridge heaters by means of a Claude Lyons 240vac 15amp variac.

The laser described in section 4.4.2 was again used to simulate a hot grinding spark ignition source, and focused at a distance 120mm from the end of the spray nozzle.

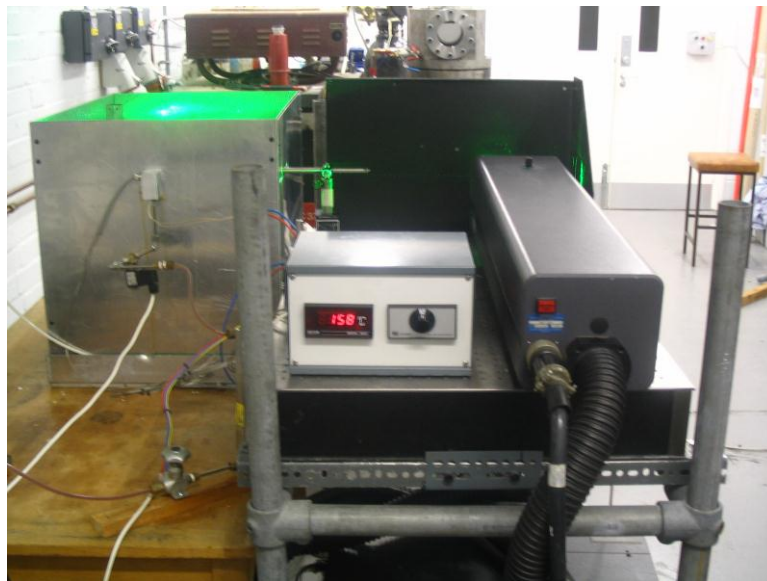


Figure 4-22 Test rig to investigate the ignition characteristics of cutting fluid mists.

Left of picture is the aluminium ignition chamber. Note, the green light being emitted from the ignition chamber is a result of the laser beam being diffracted by the cutting fluid mist. On the right of the photo is the Surelite ND:YAG laser and in the centre, the digital temperature display showing the temperature of the heated nozzle block.



Figure 4-23 Fine cutting fluid mist being injected into the ignition chamber (left).

Notice also the lens used to focus the laser beam on the left hand side of picture. The photo on the right shows ignition of the cutting fluid mist.

4.4.3.3 Results

Fluid	Temperature (°C)		No. of Tests	Ignition Frequency	Closed Cup Flashpoint (°C)
Fuchs 40SR	Could not ignite. Fluid boiled off at c.340°C.				216
Fuchs 22SR	Could not ignite. Reached maximum rig temperature of 390°C				215
Castrol ES1	Above	340	19	8 from 19	240
	Below	340	14	0 from 14	
Unused Castrol Ilogrind 600SP	Above	130	29	29 from 29	>130
	Below	120	17	4 from 17	
Used Castrol Ilogrind 600SP	Random ignition behaviour. Fluid may or may not ignite in range 168 - 288°C				>130
Unused Ilogrind c/w Prolong AFTM @10%	Above	216	18	9 from 18	135 (open cup)
	Below	213	21	4 from 21	

Table 4-4 Summary of cutting fluid mist ignition tests.

Table 4-4 summarises the results from the spark ignition tests of cutting fluid mist. The results clearly show that the ester based cutting fluids tested needed to be raised to a significantly higher temperature than their neat mineral oil counterparts before ignition would occur, if in fact they could be ignited at all.

The results shown in table 4-4 largely reflect the results found when testing the ignition characteristics of cutting fluid evaporate described in section 4.4.2. However, the temperature at which the cutting fluid will ignite is far less defined. This is attributable to the fact that when attempting to ignite the cutting fluid mist, ignition will not only depend on cutting fluid temperature, but also on there being the correct mixture (fluid mist and air mix) in the correct place at the correct time.

Another interesting result was the ignition characteristics of the used Castrol Ilogrind 600SP. As stated previously, this particular fluid was taken from the coolant clarifier system in the High Performance Machinery Laboratory at Cranfield University, where it has been used for the past four years. Consequently, it has undergone the inevitable deterioration and contamination over this time. As a result, this particular fluid exhibited almost random ignition characteristics, as it would or would not ignite during tests at almost identical temperatures anywhere in the range 168 to 288°C.

This almost random ignition behaviour may account in some part for the apparently random ignition of the cutting fluid witnessed on grinding machines. Several researchers at Cranfield have witnessed cutting fluid fires when repeating tests that have already been performed with identical process parameters (feedrate, depth of cut, grinding wheel speed etc.) for no apparent reason. The fact that the cutting fluid being used during these tests exhibits almost random ignition behaviour may explain this phenomenon.

4.4.4 Conclusions

The most significant finding of the ignition tests is that in both the cutting fluid evaporate and the cutting fluid mist trials, the ester based cutting fluids tested were more resistant to ignition as they needed to be raised to a significantly higher temperature in comparison to their neat oil counterparts before ignition occurred. As a result, the use of ester based cutting fluids such as those tested should significantly reduce the fire hazard within the grinding machine.

5 Grinding Performance

5.1 Introduction

The cutting fluid performance evaluation test program, presented in chapter four, was developed to assess the attributes of cutting fluids that have a thermal impact on the grinding process. These tests were designed to complement existing industry standard tests used in the development and control of metalworking fluids. These tests however, like the ones performed by the manufacturers, only give an indication of a fluid suitability for any given process. There is only one way to definitively assess how a fluid will perform in any particular application, and that is to test it in the actual operation for which it is intended. (Hunz, 1984)

5.2 High Efficiency Deep Grinding (HEDG)

5.2.1 Experimental

HEDG grinding trials were conducted on an Edgetek SAM 5 axis computer numerically controlled (CNC) grinding machine to allow the performance of the cutting fluids listed in table 3-2 to be compared. Similar grinding conditions were maintained throughout the test program to allow fair comparisons to be made. Table 5-1 gives the test conditions for the comparative trials, with the actual machine set-up shown in figure 5-1.

HEDG Test Conditions	
Grinding Machine	Edgetek SAM – 5 Axis Surface Grinding Machine
Grinding Mode	Down Grinding
Workpiece	Dimensions : 3mm wide x 100mm long Material : 51CrV4 Hardness : 59Rc
Grinding Parameters	Wheelspeed : 146m/s Workpiece Feedrate : 125mm/s Depth of Cut : 4mm Specific Removal Rate : 500mm ² /s
Grinding Wheel	Electroplated CBN wheel, B252 grit Diameter : 200mm Width : 15mm
Fluid Delivery	Nozzle Pressure: See table 5-3 RH Nozzle : 4mm coherent jet nozzle LH Nozzle : 3mm coherent jet nozzle
Grinding Fluids	See Table 3-2

Table 5-1 HEDG test grinding conditions

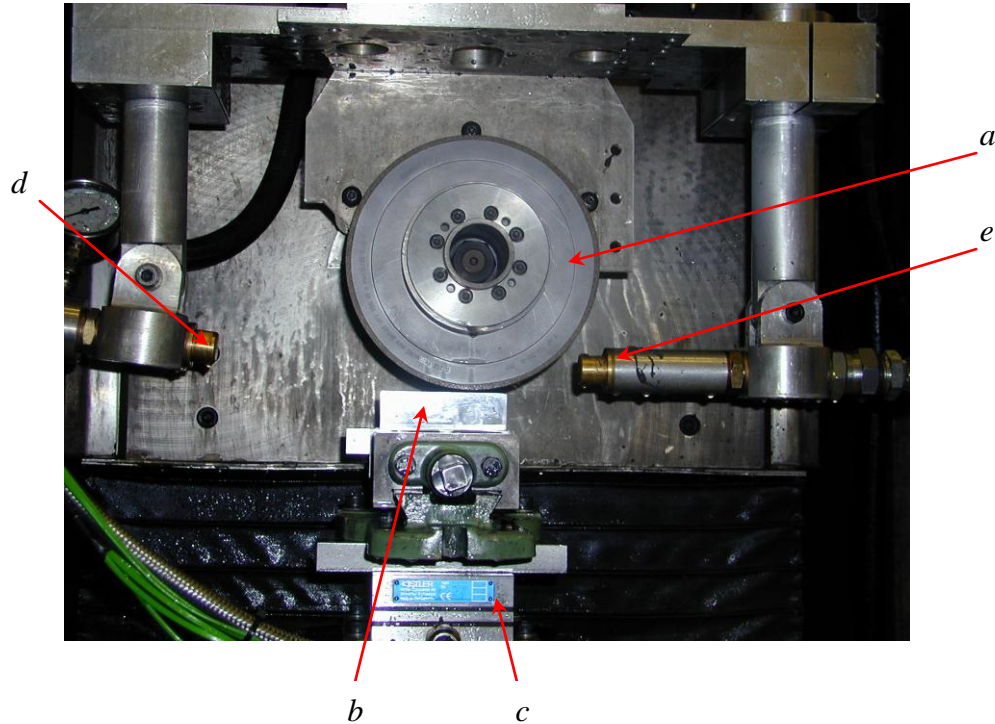


Figure 5-1 Photograph of the Edgetek SAM Machine Set-Up used for HEDG Grinding Trials

- a) Grinding wheel
- b) Workpiece
- c) Kistler dynamometer
- d) Main coolant nozzle (left hand nozzle)
- e) Spark arresting nozzle (right hand nozzle)

Grinding power was measured using a hall effect transducer (see appendix 2) connected to a National Instruments PCI6036E data acquisition system with dedicated Labview software. Data was recorded at 5000 samples per second for 5 seconds. The influence of the cutting fluid was measured by conducting a “spark out” cut, where the steady state wheel power is measured whilst the grinding wheel rotates along a stationary pre-cut grinding arc in the workpiece. The specific grinding energy was calculated for each of the different cutting fluids tested (equation 3-10)

Normal and tangential grinding forces were also measured using a Kistler type 9257BA dynamometer connected to a PC equipped with Dynoware data acquisition software. Tests were repeated five times for each cutting fluid to allow variance to be assessed.

The condition of the grinding wheel was maintained as far as was practicable by using a different section of the wheel for each of the different grinding fluids. A newly re-plated grinding wheel was selected, and by physically turning the grinding wheel around coupled with a combination of wheel spacers, 5 individual 3mm wide tracks could be used across the full 15mm width of the grinding wheel. Furthermore, an identical sequence of conditioning cuts was taken at 146m/s, 125mm/s feedrate before any recordings were made. This sequence is shown in table 5.2.

Depth of Preparation Cut	Number of Cuts
1mm cut	2
2mm cut	1
3mm cut	1
4mm cut	2

Table 5-2 Preparatory conditioning cuts used for HEDG grinding trials

Since more than 5 different fluids were evaluated the remaining fluids were tested using wheel tracks previously used in conjunction with the ester based cutting fluids, where wheel wear from either attrition (Silliman and Perich, 1992) and / or the possible damage caused by the tendency of CBN to react with water (Malkin, 1989; Carius, 1990), was likely to be less than those wheel tracks used to test water based fluids. Furthermore, the number of preparation cuts were minimised to simply 1 x 2mm cut and 1 x 3mm cut in order to ensure any additional wheel wear was minimised.

The nozzle pressure was nominally set to 5 Bar for all tests by adjusting a pressure regulator on the main “coolant” pump. However, this was not always attainable due to limitations of the fluid delivery system, and in these cases the pressure regulator was adjusted to give the maximum pressure attainable at the nozzle. The actual nozzle pressures can be seen in table 5-3 along with the resultant flow-rates.

Fluid	Nozzle Pressure (Bar)	Flow Rate (l/min)
Castrol Ilogrind 600SP	4.5*	29
Castrol ES1	5	27
Castrol Hysol XH @ 7%	5	28
Castrol Ilogrind c/w Prolong AFTM@ 10%	4.5*	29
Fuchs 22SR	5	26
Fuchs 40SR	1.8*	18
Prolong Ultracut 1 @ 10%	5	27
Quakercool 2772LF @ 7%	5	29

Table 5-3 Fluid delivery pressures and fluid flow rates for HEDG grinding trials

(* maximum nozzle pressure attainable due to limitations of the fluid delivery system)

5.2.2 Results

Figure 5-2 shows a typical power trace recorded using the Labview data acquisition system when conducting a HEDG test grind using Castrol Ilogrind 600SP. The profile shows the high power requirements of HEDG, but due to the high feed rates employed, the entire test is completed in just over one second.

The effect of cutting fluid selection on the average specific grinding energy under HEDG conditions is shown in figure 5-3 and summarised in table 5-4. The results clearly show that the neat oil cutting fluids, whether they are straight mineral oil or ester based synthetic fluids, gave rise to significantly lower levels of specific grinding energy in comparison to water miscible cutting fluids.

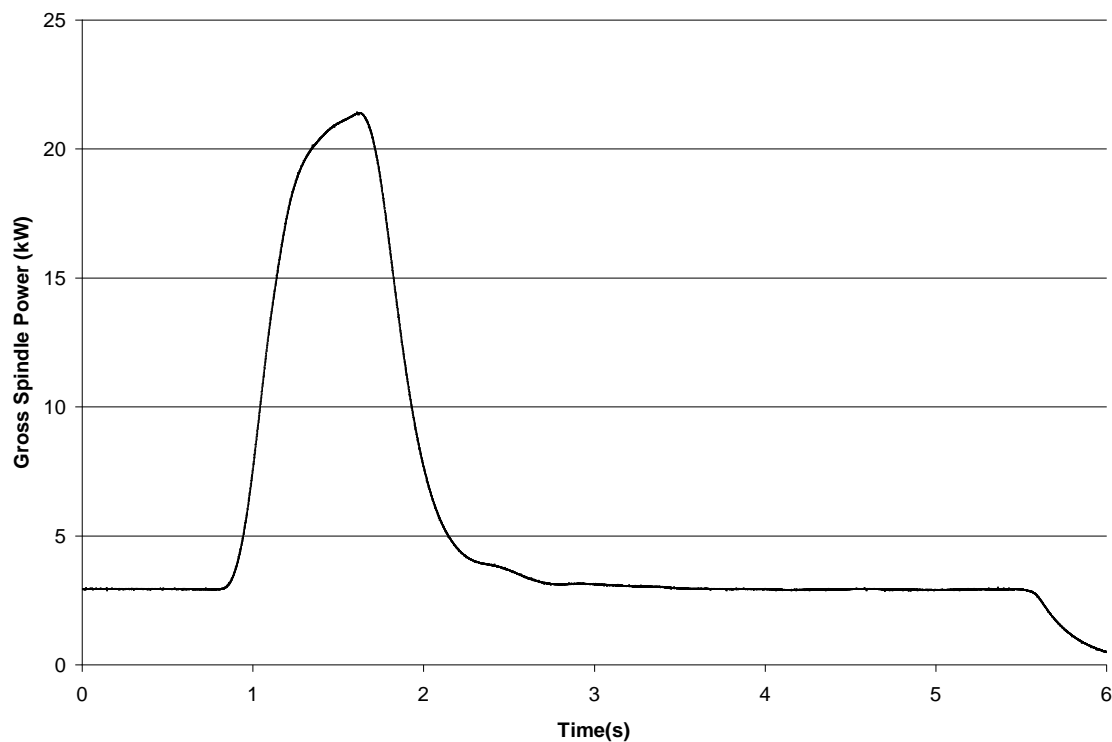


Figure 5-2 Typical power profile for a HEDG grinding test conducted using Castrol Ilogrind 600SP

The effect of cutting fluid selection on the average specific grinding energy under HEDG conditions is shown in figure 5-3 and summarised in table 5-4. The results clearly show that the neat oil cutting fluids, whether they are straight mineral oil or ester based synthetic fluids, gave rise to significantly lower levels of specific grinding energy in comparison to water miscible cutting fluids.

The lower levels of specific grinding energy when grinding with neat oil cutting fluids is attributable to a reduction in the tangential grinding force (see equation 2-4) as a result of improved lubrication within the grinding zone, as all the other grinding parameters remained constant. When using Fuchs 40SR for example, the average specific grinding energy was 3J/mm^3 lower when the same tests were performed using Castrol Hysol XH @7%, a reduction of 21.6%. In fact figure 5-4 shows that not only was the tangential grinding force reduced, but there was also reduction in the normal grinding force. The normal grinding force is usually attributable to the sliding action of dulled grains (or wear flats) rubbing against the workpiece without removing any material (Malkin, 1989). Empirically one would think that increasing the lubricity of the cutting fluid would reduce the wasted energy associated with the sliding action of any dulled abrasive grains, and this is clearly borne out by the reduction in normal forces when using neat oil cutting fluids in comparison to water soluble products.

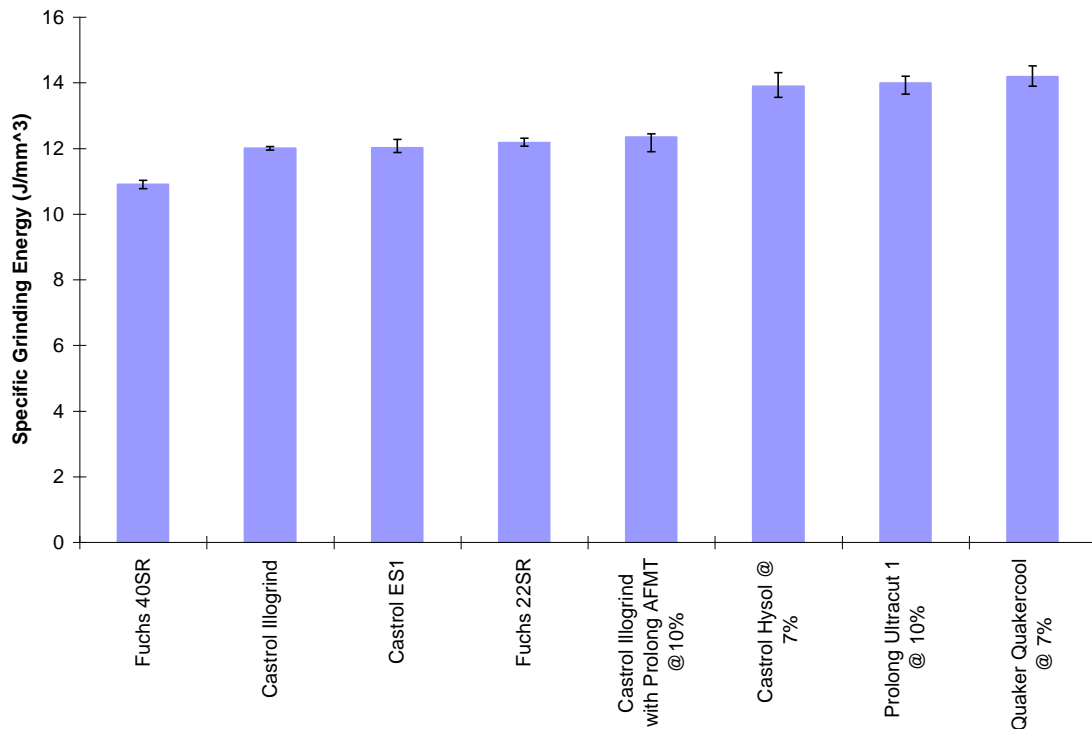


Figure 5-3 Effect of cutting fluid selection on specific grinding energy in HEDG.

(The graph shows the average specific grinding energy calculated from the test results, with the error bars depicting the maximum and minimum values of specific grinding energy for each grinding condition.)

Fluid	Average SGE (J/mm ³)	Average Total Power (kW)	Average Net Grind Power (kW)	Estimated Finish Surface Temperature (°C)
Fuchs 40SR	10.9	19.2	16.4	890
Castrol Ilogrind 600SP	12.0	21.5	18.0	1070
Castrol ES1	12.0	21.8	18.0	1070
Fuchs 22SR	12.2	22.5	18.3	1095
Ilogrind c/w Prolong AFTM @ 10%	12.4	22.1	18.4	1125
Castrol Hysol @ 7%	13.9	25.3	21.3	1370
Prolong Ultracut 1 @ 10%	14.0	25.1	20.1	1380
Quakercool 2772LF @ 7%	14.2	25.7	20.8	1415

Table 5-4. Summary of Results from HEDG Grinding Trials.

(Grinding Parameters : $Q'=500$, $v_s=146\text{m/s}$, $v_w=124\text{mm/s}$, $a_e=4\text{mm}$)

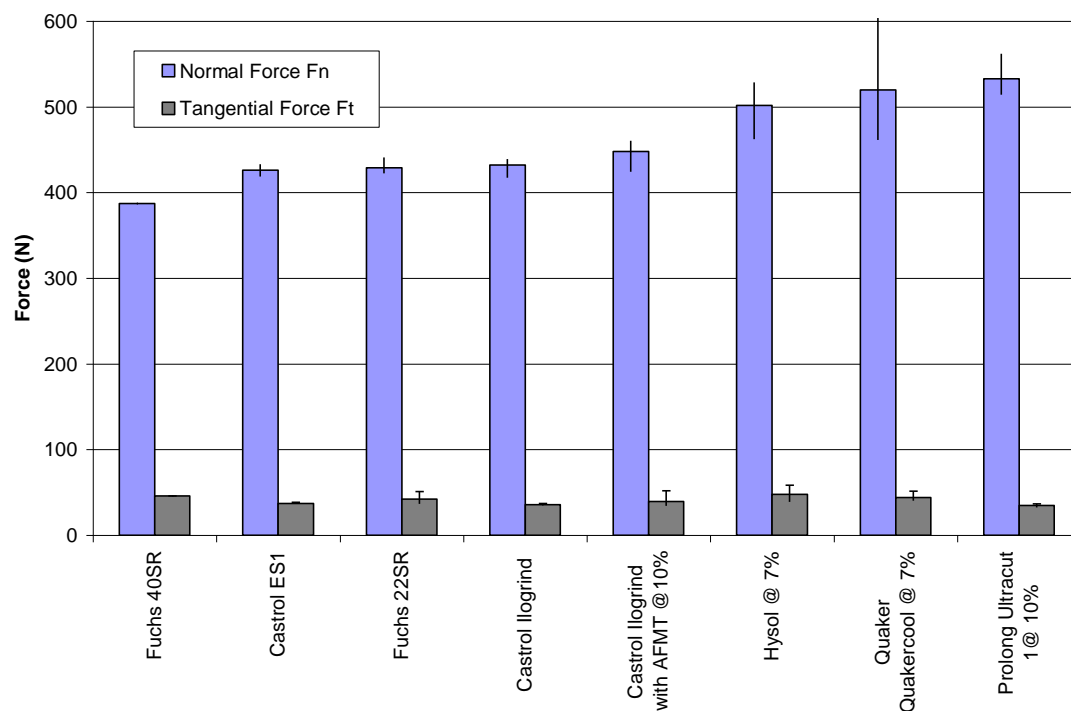


Figure 5-4 Effect of cutting fluid selection on grinding forces in HEDG.

(The graph shows the average normal and tangential grinding forces calculated from the test results, with the error bars depicting the maximum and minimum values of each force for each grinding condition.)

The average values of specific grinding energy derived from the experimental data were used to estimate the finish surface temperature for all grinding conditions using the thermal model presented in chapter three. These are shown in table 5-4. The convection coefficient of the cutting fluid was assumed to be zero as the workpiece surface temperatures, as witnessed by the presence of white layer observed on all of the work pieces when conducting microstructural observations (presented later in section 5.2.3) was clearly above the fluid burn out temperature of both oil and water soluble cutting fluids. The formation of white layer, which is a layer of untempered martensite, must mean the workpiece surface had been raised above a minimum temperature of approximately 760°C for the necessary phase transformation to occur (Walton and Stephenson, 2006). Under such high temperature conditions the cooling ability of the fluid is reduced to almost zero (Andrew and Howes, 1985).

The use of neat oil cutting fluids also gave rise to the lowest grinding powers (see figure 5-5), both in terms of the net grind power (the power required to actually remove material) and the total grind power. This is hugely significant, as all grinding machines have a finite amount of available grinding power to perform the particular grinding process. This is determined by the grinding spindle / drive design and by reducing the grinding power for any given material removal rate, higher material removal rates can be achieved whilst operating within the constraints of the machine.

In the case of the Edgetek SAM machine, which has a grinding power of 27kW, the 24.7% reduction (6.38kW) in the total grinding power between the tests performed using the Fuchs 40SR and Quakercool 2772LF represents an increase of nearly 24% in available grinding power for additional material removal. Furthermore, for any set of process parameters and subsequent material removal rate, the reduction in the power requirements of the process results in a reduction in the carbon footprint of the process with all the associated environmental and cost benefits this entails.

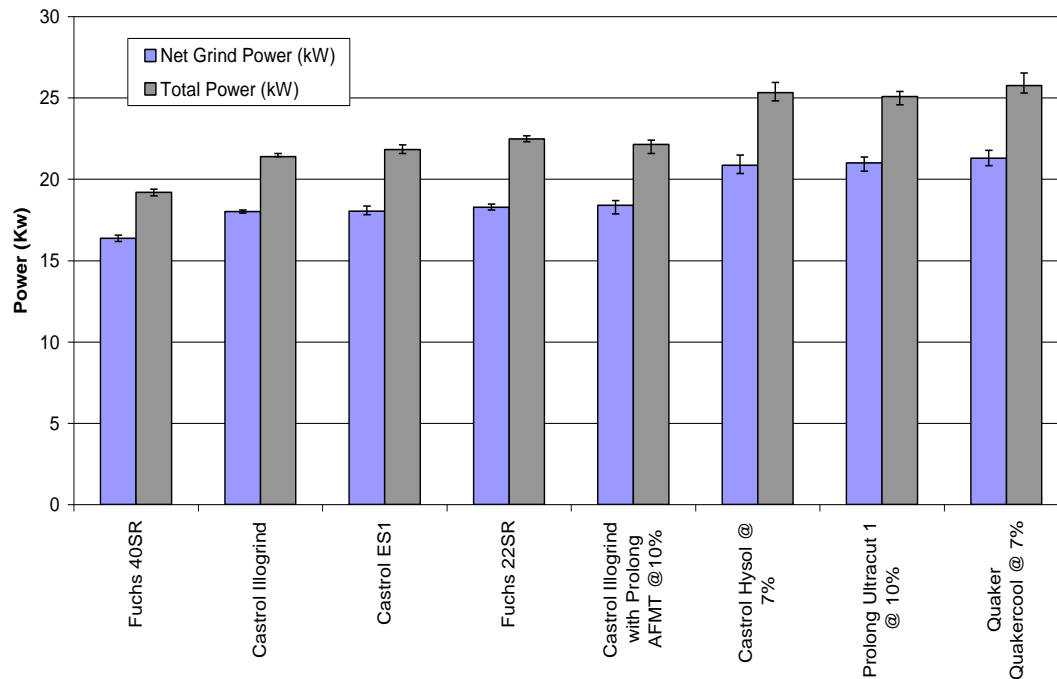


Figure 5-5 Effect of cutting fluid selection on both total and net grind power.

(The graph shows the average grinding power (both total and net) calculated from the test results, with the error bars depicting the maximum and minimum values of grinding power for each grinding condition.)

All the water based cutting fluids tested offered the least amount of lubrication as demonstrated by the higher specific grinding energies recorded from these tests. This result was not surprising as water based fluids are generally poorer than oil based cutting fluids, especially in high pressure, elastohydrodynamic contacts where both the low viscosity and the very low pressure-viscosity coefficient prevent satisfactory formation of elastohydrodynamic separating films. (Ratoi and Spikes, 1999) Elastohydrodynamic lubrication is a development of hydrodynamic lubrication to take into account the elastic deflection of the contact surfaces. Film thicknesses are much smaller than in conventional hydrodynamic lubrication and under these conditions a continuous film can only be achieved through elastic deformation of the contact surfaces. (Marinescu and Rowe, 2004)

The use of the highest viscosity ester based neat oil cutting fluid, Fuchs Plantocut 40SR, resulted in the lowest specific grinding energy, lowest grinding forces, lowest grinding

power and lowest workpiece finish surface temperature compared to any other fluid tested despite the relatively small amount of fluid being applied as a result of the limitations of the fluid delivery system. The penetrating ability of such a high viscosity fluid was a concern prior to the tests, but proved not to be a problem despite the high grinding wheel and workpiece speeds employed during the tests.

5.2.3 Effect of Cutting Fluid Selection on Thermal Damage in HEDG.

Minimising the depth of any thermal damage within the workpiece is of key importance in this project. Whilst HEDG may be a roughing operation, and that any thermal damage which could affect the surface life of the component will normally be removed by subsequent finishing operations, it is important to minimise the amount of stock which needs to be removed as finishing operations are typically slow, low material removal rate types of processes. Removing large amounts of material during finishing operations in order to remove large depths of thermal damage from the workpiece as a consequence of the roughing operation obviously reduces the cost effectiveness of the entire process chain, and may also have implications on the final tolerances, surface texture and surface topography that can be achieved.

Equation 5-1 shows that the amount of heat energy generated within the grinding zone is reduced when the specific grinding energy is reduced. Consequently any thermal damage within the workpiece will also be reduced or even eliminated. This effect can be seen in the micrographs taken of the different samples ground using different cutting fluids (see figure 5-6). This shows that the specific grinding energy was reduced from 13.9 J/mm³ to 10.9 J/mm³ when using Fuchs 40SR rather than Hysol XH water miscible cutting fluid, and consequently the depth of thermal damage, as witness by white layer in the work piece was reduced from approximately 315µm (figure 5-6a) to approximately 150µm (figure 5-6d).

Equation 5-1

$$q_t = e_c \cdot a_e \cdot v_w / l_c \quad (\text{Stephenson and Jin, 2003})$$

Where

q_t = total heat flux
 e_c = specific grinding energy
 a_e = depth of cut
 v_w = work piece feed rate
 l_c = arc of contact

The reduction in white layer also corresponds with a decrease in the finish surface temperature calculated using the thermal model described in chapter 3. The calculated values of finish surface temperature can be seen in figure 5-6 and table 5-4 and show that for Fuchs 40SR a finish surface temperature of 910°C was calculated with the finish surface temperature increasing to 1370°C for the water soluble cutting fluid, Hysol XH.

This increase in finish surface temperature corresponds to the increase in the depth of thermal damage from 150 μ m to 315 μ m.

Similar findings were in fact reported by Liu et al (Liu and Abe, 1994) who found higher viscosity oils performed better than lower viscosity oils in preventing workpiece thermal damage during severe creep feed grinding operations. Since HEDG can be considered as an extension of creep feed grinding (Tawakoli, 1993; Klocke and Brinksmeier, 1997) it is logical that higher viscosity oils are more suitable for the HEDG process.

It is also important to note that reducing the temperature in the grinding zone also has the obvious beneficial effect of reducing the potential fire hazard within the grinding machine when neat oil cutting fluids are used. In the examples of Fuchs 40SR and Quakercool 2772LF, a drop of 3J/mm³ in the specific grinding energy resulted in a 360°C reduction in the estimated finish surface temperature. The reason for this is that when grinding above the fluid burn out threshold, for any given set of grinding parameters (e.g. feedrate, depth of cut, wheel speed etc.) the main factor in controlling the amount of heat generated is the reduction of the frictional forces.

This effect can clearly be seen if one looks at the mathematical relationships between the tangential grinding force, specific grinding energy and the thermal energy generated by the process. Equation 2.4 shows the specific grinding energy is directly proportional to the tangential grinding force. Equation 2.5 shows the total thermal energy produced by the grinding process is directly proportional to the specific grinding energy. If the tangential grinding force can therefore be reduced, it follows that the total thermal energy generated by the process is also reduced.

5.2.4 Summary

In general the ester based cutting fluids tested performed as well as if not better than Castrol Ilogrind 600SP, the neat mineral oil with sulphur based EP additives. The higher viscosity oils provided the highest levels of lubrication giving rise to the lowest grind power, lowest specific grinding energy, lowest grind forces and least amount of thermal damage within the work piece.

Water based cutting fluids are not suitable for HEDG due to their low lubricity. Their use results in higher levels of specific grinding energy, higher grinding forces, higher grinding powers (both net and total), increased finish surface temperatures with the subsequent effect on higher levels of thermal damage.

Whilst the use of neat oil based cutting fluids in HEDG clearly has certain benefits, their use is not without problems as their use still poses a significant fire hazard. However the results presented in chapter 4 show ester based neat cutting oils produce significantly lower levels of mist and are significantly less flammable than their neat mineral oil counterparts. Any strategy for cutting fluid application in HEDG will need to take these factors into account in order to minimise the fire hazard, a subject that will be discussed in chapter 7.

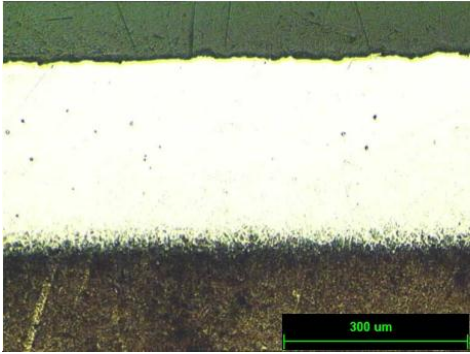
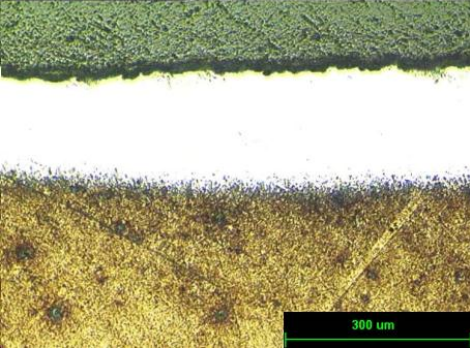
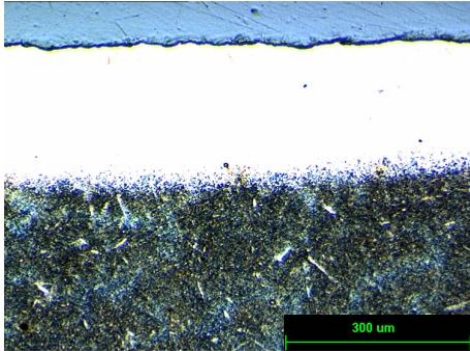
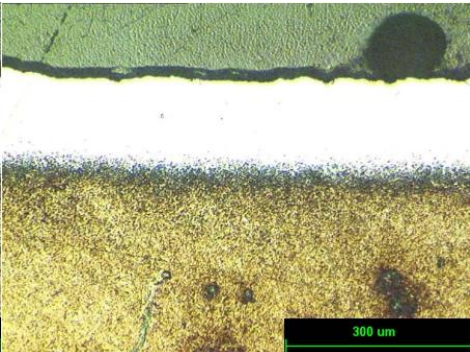
	Cutting Fluid : Hysol XH
	Average specific grinding energy : 13.90 J/mm ³
	Depth of white layer : 315μm
	Estimated finish surface temperature : 1370°C
	Cutting Fluid : Fuchs 22SR
	Average specific grinding energy : 12.18 J/mm ³
	Depth of white layer : 240μm
	Estimated finish surface temperature : 1100°C
	Cutting Fluid : Castrol Ilogrind 600SP
	Average specific grinding energy : 12.01 J/mm ³
	Depth of white layer : 220μm
	Estimated finish surface temperature : 1070°C
	Cutting Fluid : Fuchs 40SR
	Average specific grinding energy : 10.90 J/mm ³
	Depth of white layer : 152μm
	Estimated finish surface temperature : 910°C

Figure 5-6 Micrographs showing the depths of workpiece thermal damage during HEDG.

Note: Marker size on all micrographs - 300μm

5.3 Creep Feed Grinding

5.3.1 Introduction

Chapter three outlined the experimental work conducted in investigating the convection heat transfer coefficient of cutting fluids. The cooling ability of cutting fluids is not however the only consideration when selecting a cutting fluid in creep feed grinding. In this section other aspects of the cutting fluid's influence within the creep feed grinding regime will be presented. The data presented in this section was collected whilst performing the experimental work described in chapter three.

5.3.2 Effect of Cutting Fluid Selection on Specific Grinding Energy

Figure 5.7 shows that, with the exception of the Quakercool 2772LF water soluble cutting fluid, which will be discussed further in the next paragraph, the specific grinding energy is lower when a neat oil cutting fluid is used in creep feed grinding in comparison to a water soluble cutting fluid. This is attributable to the greater lubricity of the neat oil which reduces the grinding forces, thus lowering the specific grinding energy as previously stated in section 5.22, with its commensurate effect of reducing the total amount of heat energy generated by the process.

The somewhat surprising performance of the Quakercool 2772LF water soluble cutting fluid in delivering both high levels of lubricity as demonstrated by the low levels of specific grinding energy coupled with the high values of convection coefficient presented in chapter 3, would appear to make this fluid ideal for creep feed grinding applications. The enhanced lubricity of this product comes from the use of synthetic polymer lubrication additives rather than mineral oils conventionally used in water soluble fluids.

However, it is known that polymer molecules degrade over time due to the high shear forces found in grinding, and section 4.3.3.4 in chapter four clearly showed that such deterioration has an adverse effect on cutting fluid performance, by showing how the misting performance of a neat oil cutting fluid deteriorated over time due to the degradation of the polymer anti-mist additive. Therefore questions arise over the long term performance of this particular fluid, which could not be tested or answered fully due to time constraints within the project.

However, a more arduous grinding environment was produced by increasing the grinding wheel speed and the fluid delivery pressure whilst keeping other grinding parameters constant. Tests were performed using a selection of fluids and figure 5.8 shows how these changed the specific grinding energy within the creep feed grinding regime. Whilst such high grinding wheel speeds are not normally associated with creep feed grinding, they can and are used in practice, for instance to achieve the desired workpiece surface finish.

The results show that neat oil cutting fluids produced the lowest levels of specific grinding energy as one would expect due to the improved lubricity of neat oil cutting

fluid. The Quakercool 2772LF polymer synthetic cutting fluid gave rise to one of the highest levels of specific grinding energy, with its performance being more consistent with the other water soluble cutting fluids. This suggested that whilst this particular fluid may work relatively well at relatively modest removal rates and wheel speeds, over a wider range of grinding parameters the performance would be similar to other water based cutting fluids, and its exceptionally good performance seen in figure 5-7 may have been a less representative result. Overall, it is reasonable to state from both sets of results that the use of neat oil cutting fluids consistently gives rise to the lowest levels of specific grinding energy due to their higher lubricity.

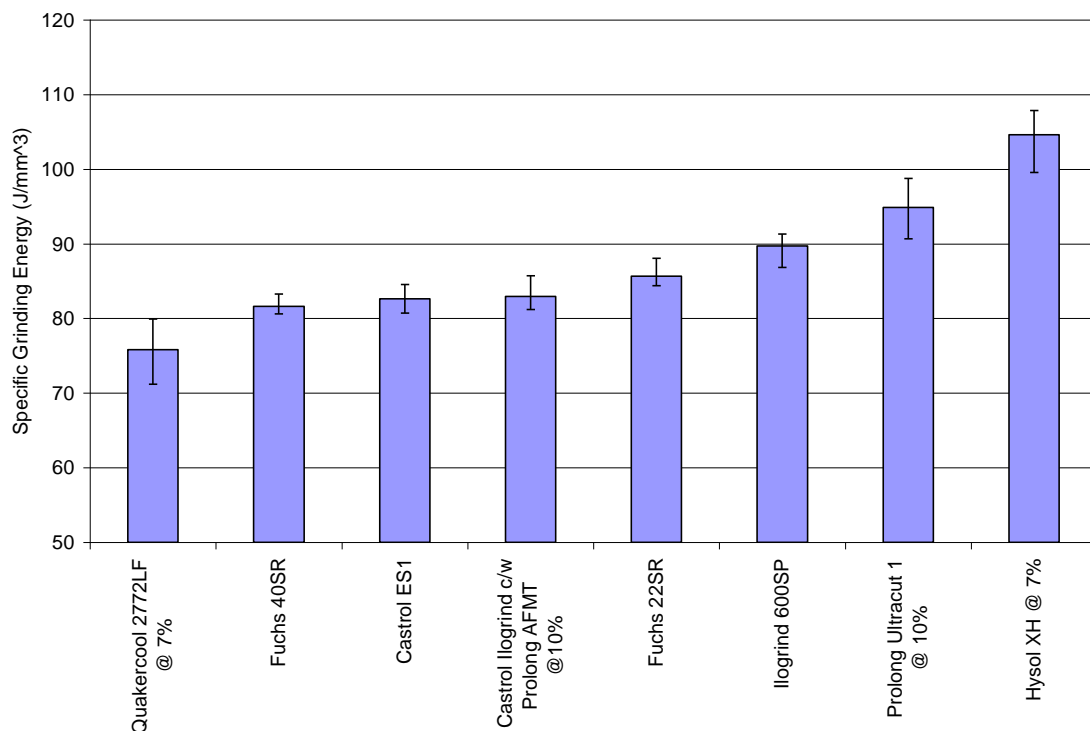


Figure 5-7 Comparative performance of cutting fluids in creep feed grinding.

(Graph shows average values of specific grinding energy when different cutting fluids are used. Tests performed at 50m/s grinding wheel speed. 5 Bar pump pressure, 0,4mm depth of cut, 1mm/s feedrate, B252 grinding wheel. Error bars show maximum and minimum values of specific grinding energy calculated from the experimental data).

Figure 5.9 shows the effect of cutting fluid selection on the specific grinding energy over a wider range of specific removal rates in creep feed grinding. Tests were performed using the same creep feed set-up as previously described, but the specific removal rate was increased by increasing the workpiece feedrate. The feedrate was increased from 1mm/s to 20mm/s whilst maintaining the depth of cut at 0,4mm to give a commensurate increase in specific removal rate from $0.4\text{mm}^3/\text{mm.s}$ to $8\text{mm}^3/\text{mm.s}$. Tests were repeated four times for each set of grinding conditions to allow average values to be determined. The results clearly show that the use of a neat oil cutting fluid

in creep feed grinding consistently gives rise to lower levels of specific grinding energy in comparison to water soluble products, as the specific removal rate increases.

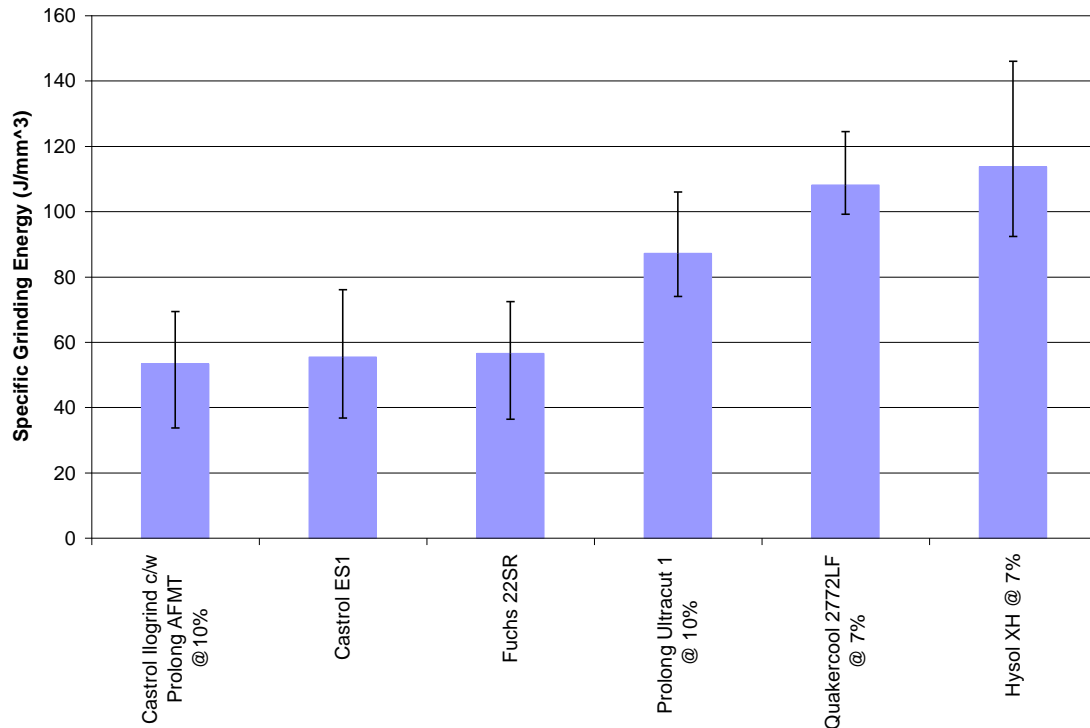


Figure 5-8 Comparative performance of cutting fluids in creep feed grinding at high wheel speeds.

(Graph shows average values of specific grinding energy when different cutting fluids are used. Tests performed at 146m/s grinding wheel speed. 10 Bar pump pressure, 0,4mm depth of cut, 1mm/s feedrate, B252 grinding wheel. Error bars show maximum and minimum values of specific grinding energy calculated from the experimental data).

Unlike the HEDG regime, the creep feed trials were all performed at very modest material removal rates in order to ensure the burn-out limit of the cutting fluids were not exceeded. This was originally done so that the convection coefficients of the cutting fluids could be measured. As a result, and in contrast to the HEDG regime described earlier where a reduction in specific energy resulted in a decrease in workpiece finish surface temperature, the complete opposite occurred during the creep feed grinding trials with the lowest finish surface temperature being measured when using water soluble fluids, despite the higher levels of specific grinding energy associated with their use.

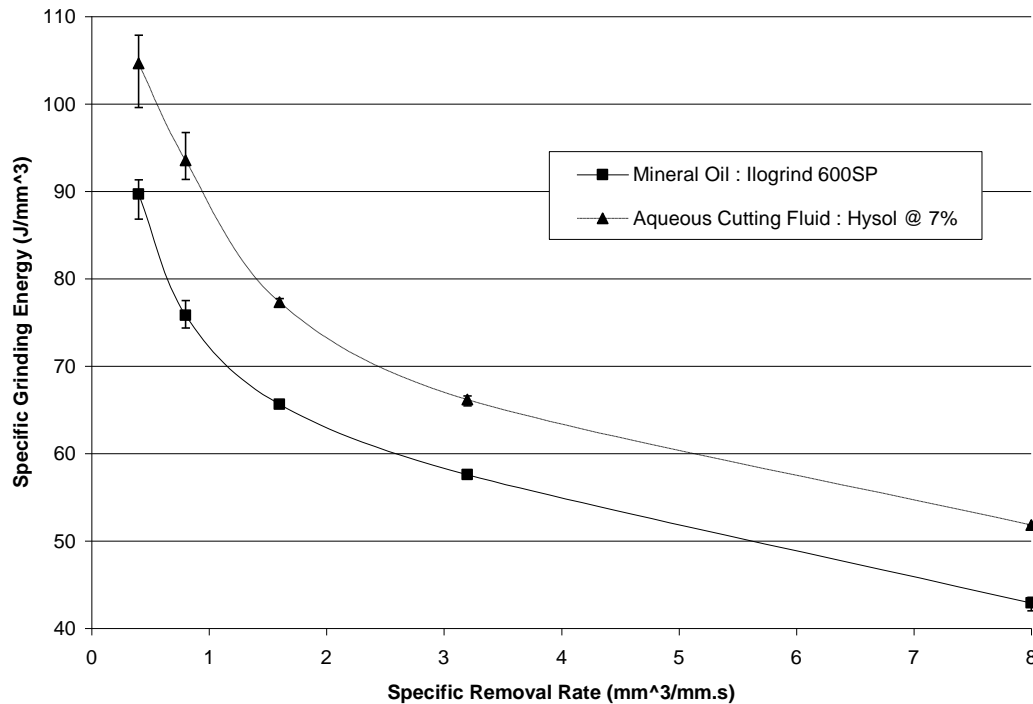


Figure 5-9 Effect of cutting fluid selection on specific grinding energy in creep feed grinding.

(Graph shows average values of specific grinding energy and the effect of increasing the specific removal rate (Q') when different cutting fluids are used. Tests performed at 50m/s grinding wheel speed, 5Bar pump pressure, 0.4mm depth of cut, B252 grinding wheel. Error bars show maximum and minimum values of specific grinding energy calculated from the experimental data).

To illustrate this, the finish surface temperature when grinding with Castrol Ilogrind was 64.6°C as opposed to 38.6°C when using Castrol Hysol XH, despite an increase in specific grinding energy from 89.7 to 104.6 J/mm³, with the commensurate increase in the total heat flux generated by the grinding process, increasing from 401170W/m² to 4630068W/m². This was an increase of over 15% when grinding at wheel speed of 50m/s, 0.4mm depth of cut, 1mm/s feedrate with the fluid being delivered at a pump pressure of 5 bar.

This reversal is attributable to the cooling action of the grinding fluid within the grinding zone. Table 3.5 shows the convection heat transfer coefficients (convection coefficient) for the various cutting fluids tested during this project, and clearly shows that the convection coefficients are far higher for water based cutting fluids than for neat oil cutting fluid. Consequently, the cooling action of cutting fluid is far greater for water based cutting fluids.

As a result a far greater proportion of the total heat energy is removed by, or partitioned to, the cutting fluid. For the grinding parameters in question, the average cutting fluid partition ratio was 0.93 when using the neat mineral oil cutting fluid (Castrol Ilogrind) which increases to an average of almost 0.99 when Castrol Hysol XH water soluble cutting fluid was used. In other words, the water soluble cutting fluid removed almost

99% of all the heat generated within the grinding zone, with the neat mineral oil only 93%. This explains the fact that despite more thermal energy being generated by the grinding process, the workpiece finish surface temperature remains significantly lower when water based cutting fluids are used in creep feed grinding due to the change in thermal energy partitioning. In other words, when water based cutting fluids are used, just over 1% of the total thermal energy generated by the process enters the grinding wheel and workpiece combined (the energy entering the grinding chips is negligible in creep feed grinding due to the low workpiece feed rates employed), whereas 7% of the total thermal energy enters the grinding wheel and workpiece combined when neat oil cutting fluids are used. As the wheel / work partition ratio (see equation 3-7) is effectively constant for any given set of grinding conditions, it is easy to understand why the workpiece temperature was 26°C higher Castol Ilogrind, a neat oil cutting fluid was used.

Empirically one would therefore think that water based cutting fluids are the most appropriate for the creep feed grinding regime due to the higher convection coefficients of the fluid and consequently their enhanced cooling ability over neat oil products. In fact Ye and Pearce (1984) found that water based were indeed superior to neat oil cutting fluids when creep feed grinding a nickel based alloy with an induced porosity grinding wheel as there was an increased likelihood of workpiece burn when using neat oil fluids, which could in turn result in reduced material removal rates (Ye and Pearce, 1984).

However Andrew and Howes (1985) reported that Hassell found the opposite was true and that higher material removal rates were achievable when using a neat oil cutting fluid when creep feed grinding hardened tool steel. Whilst the workpiece material changed, the other important factor was the wheel specification, as Hassell used a dense (low porosity) fine grain grinding wheel. Andrew and Howes (1985) point to the most likely explanation for this apparent contradiction being the reduction in wheel porosity which may have had more of an effect on the fluid application when using water based rather than a neat oil cutting fluid. Their conclusion was that highly porous grinding wheels are more necessary when water based cutting fluids are used in high stock removal grinding processes.

Grinding trials performed by Bell (2005) at Cranfield University using a superabrasive grinding wheel, tend to support this argument. By their very nature, superabrasive grinding wheels are not porous like their conventional counter parts, and by following Andrews and Howes (1985) reasoning, neat oil cutting fluids should permit higher material removal rates to be achieved before the onset of thermal damage. Figure 5-9 shows the results of the test performed by Bell (2005) on the Edgetek SAT machine, and clearly show that higher material removal rates were indeed achievable when using neat oil cutting fluids, as there was a sharp increase in finish surface temperature, at a specific removal rate of approximately $25\text{mm}^3/\text{mm.s}$ when using a water soluble cutting fluid, due to fluid burnout. This sharp increase in finish surface temperature, from less than 100°C to almost 1000°C would have almost certainly resulted in thermal damage to the workpiece, as the threshold for thermal damage for the particular material in question (51CrV4) is approximately 400°C (Stephenson and Jin, 2002)

Whilst quality of this data suffers from the fact that only one test was performed for each grinding condition, making any assessment of variance impossible, these tests do confirm Hassel's observation (Andrew and Howes, 1985) that higher removal rates are possible when using neat oil cutting fluids in creep feed grinding when using a grinding wheel of low porosity.

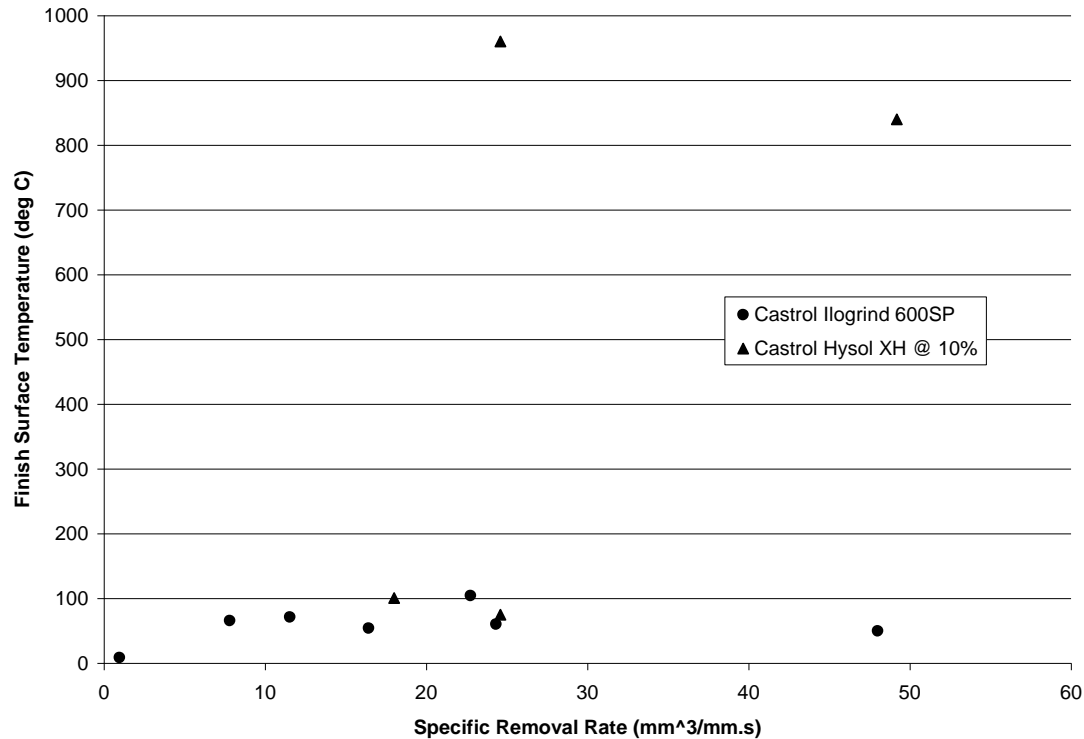


Figure 5-10 *Effect of cutting fluid selection on finish surface temperature in creep feed grinding (Bell, 2005)*

(Graph shows values of finish surface temperature calculated using experimental data at increasing specific removal rates for both a neat oil cutting fluid (Castrol Ilogrind 600SP) and a water soluble product (Castrol Hysol XH). Workpiece material 51CrV4, 1mm DOC, 150m/s wheel speed, B252 CBN grinding wheel, 10Bar Nozzle Pressure).

5.3.3 Effect of Cutting Fluid on Surface Quality

Cutting fluids play an import role in determining the surface quality of the workpiece, such as residual stress and the presence of any thermal damage. In conventional grinding regimes these are of particular importance, as these operations are often used as finishing processes. In order to determine the influence of the cutting fluid on the surface quality the following measurements / tests were performed.

- Residual Stress
- Microstructural Observations

5.3.3.1 Residual Stress

Surface residual stress measurements were conducted using a Siemens X-Ray diffraction machine at Cranfield University which can be seen in figure 5.10. As previously stated in the literature review, X-Ray diffraction works on the principle that parallel sets of planes in any given crystalline structure can be used as a diffraction grating, in a similar way as fine parallel lines on a surface can be used to diffract light (Dowdell and Jerabek, 1943). The actual spacing between the planes in the crystalline structure is determined by chemical composition and physical conditions such as temperature and stress. It is possible to control all other effects on the plane spacing except that caused by stress, and therefore a unique linear correlation can be established between the distance between the planes of a crystal and the residual stress or strain (Heindlhofer, 1948).

Fluid	Vs (m/s)	Vf (mm/s)	DOC (mm)	Pump Pressure (Bar)	Normal Stress (MPa)	Sheer Stress (MPa)
Illogrind 600SP	50	1	0.4	5	-295 +/- 17	-39+/-4
Hysol XH @ 7%	50	1	0.4	5	-229 +/- 14	46+/-3
Quakercool @ 7%	50	1	0.4	5	-258 +/-15	38 +/- 4
Fuchs 22SR	50	1	0.4	5	-297 +/- 15	26+/-4
Fuchs 40SR	50	1	0.4	5	-317 +/-16	22 +/- 4
Castrol ES1	50	1	0.4	5	-320 +/-16	26 +/- 4
Illogrind with AFMT @ 10%	50	1	0.4	5	-452 +/- 19	26+/-4
Hysol XH @ 7%	50	2	0.4	5	-258 +/- 15	45+/- 4
Hysol XH @ 7%	50	4	0.4	5	-233 +/- 15	49 +/- 4
Hysol XH @ 7%	50	8	0.4	5	-194 +/- 15	61 +/- 4
Hysol XH @ 7%	50	20	0.4	5	-149 +/-14	66+/-3
Illogrind 600SP	50	2	0.4	5	-488 +/- 21	-7 +/-5
Illogrind 600SP	50	4	0.4	5	-244 +/- 15	-45+/-4
Illogrind 600SP	50	8	0.4	5	-476 +/- 21	-3+/-5
Illogrind 600SP	50	20	0.4	5	-478 +/- 22	-12 +/-5

Table 5-5 Residual Stress Measurements for Creep Feed Grinding Tests.

The residual stress results presented in table 5-5 and figure 5-11 show clearly that the use of neat oil cutting fluids produced surfaces that contained far higher levels of compressive residual stress than their water based counterparts when ground in the creep feed regime, and this increase may be useful in enhancing the service life of the component (Chen and Rowe, 2000). The higher levels of compressive stress are not attributable to any thermal effect, as during the creep feed grinding trials the finish surface temperature was typically less than 70°C even when neat cutting oils were used. This is far lower than 400°C, the threshold temperature for 51CrV4 above which microstructural changes in the material occur (Stephenson and Jin, 2002).

Instead these compressive residual stresses were formed due to Hertzian compression and shear forces produced by the abrasive grains during the grinding process. These mechanical forces cause permanent plastic deformation of the work piece surface (Chen and Rowe, 2000).

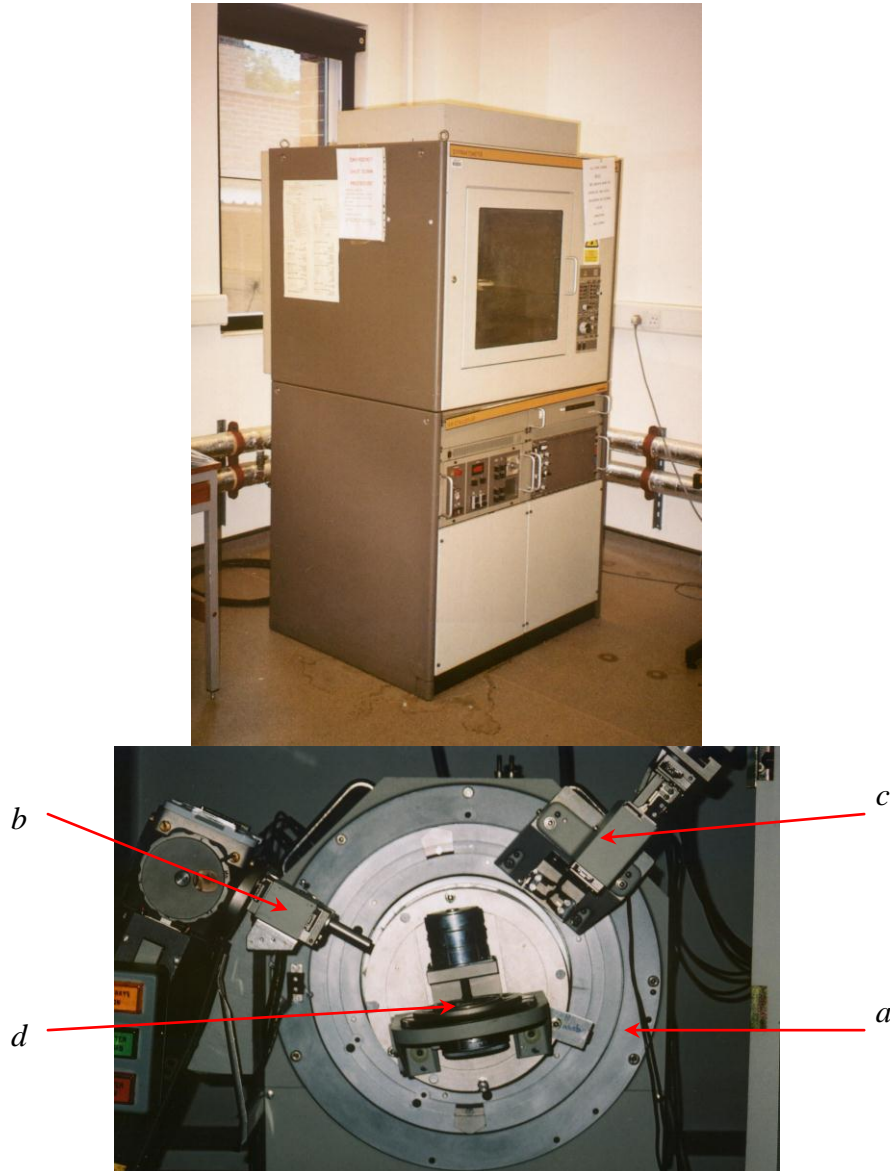


Figure 5-11 X-Ray diffraction machine used to measure surface residual stress of ground components.

- a) headstock*
- b) X-Ray tube*
- c) X Ray receiver*
- d) Sample under test*

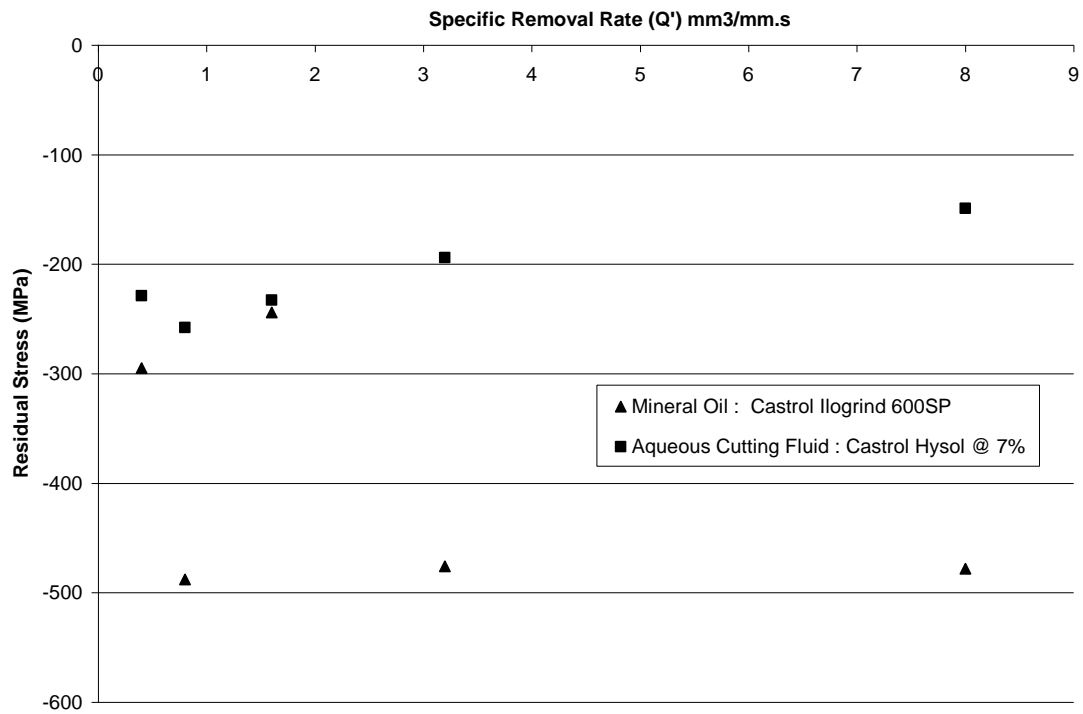


Figure 5-12 Effect of cutting fluid selection on residual stress in creep feed grinding.

(Results for Increasing Specific Removal Rate (Q') at 50m/s Grinding Wheel Speed, 5Bar Pump Pressure, 0.4mm Depth of Cut, B252 Grinding Wheel, Increasing Feedrate). Errors are shown in table 5-5

5.3.3.2 Microstructural Observations.

The measurement of surface residual stress only gives a partial insight into the residual stress profile within the workpiece. Surface compressive residual stresses can occur in thermally damaged components. If a phase transformation of the material has occurred, which is followed by rehardening as the workpiece cools, the surface layer will consist of untempered martensite (white layer), whilst the sub-layer has been tempered. Since the untempered martensite has a greater lattice volume than the tempered martensite, compressive residual stress can be measured at the surface, whilst the subsurface contains tensile residual stresses (Chen and Rowe, 2000).

Therefore in order to definitively ascertain whether any thermal damage had occurred in the workpiece, microstructural observations were performed on all the components ground in the creep feed regime. A typical micrograph is shown in figure 5-12.

Microstructural observations revealed that there was no significant change in the microstructure of components ground in the creep feed regime when different cutting fluids were used. This was not unexpected however, due to the low temperatures measured during the grinding process, as the critical temperature below which no thermal damage would occur for 51CrV4 is typically 400°C (Stephenson and Jin, 2002).

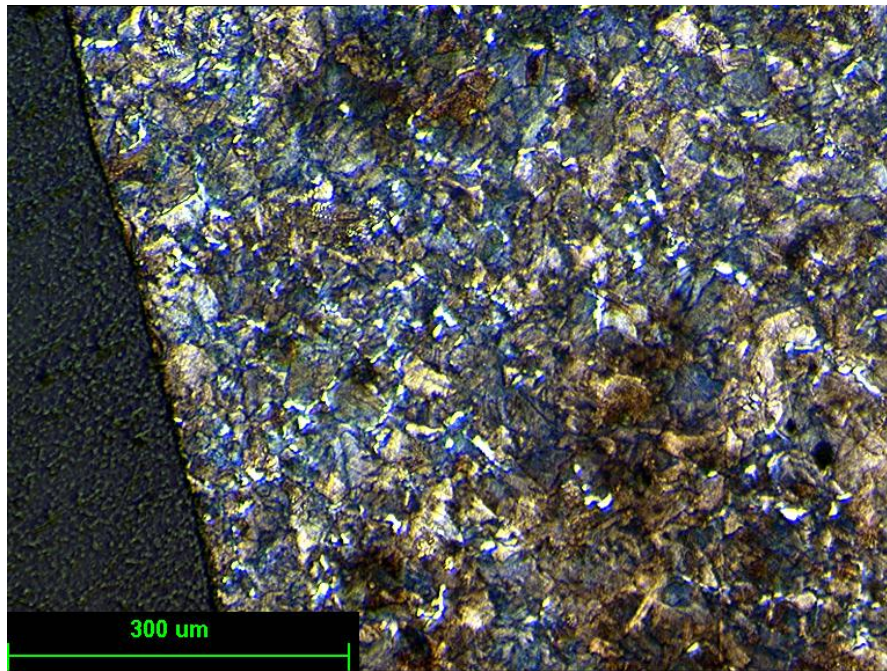


Figure 5-13 Micrograph showing microstructure of component ground in the creep feed regime. (Sample taken from component ground using Castrol ES1, 50m/s wheel speed, 1mm/s feedrate, 0,5mm depth of cut, 5 bar pump pressure).

5.3.4 Summary

The use of neat oil grinding fluids resulted in the lowest levels of specific grinding energy during these grinds. However, owing to the lower values of convection coefficient of the fluid, finish surface temperatures were significantly higher in comparison to components ground using water soluble products. Despite this fact, higher specific removal rates are achievable when using neat oil cutting fluids with superabrasive grinding wheels in the creep feed regime. This is important, as in some circumstances, higher material removal rates are achievable with water based cutting fluids. A good example of this is the VIPER grind process, which uses extremely porous grinding wheels and a high pressure cutting fluid supply to force fluid into the grinding wheel. The key difference with superabrasive grinding wheels is the porosity of the wheel. Superabrasive grinding wheels are simply not porous, and consequently the cutting fluid cannot be forced into the grinding wheel as in the VIPER process. This very important difference explains why water based cutting fluids do not perform as well as neat oil based cutting fluids, in terms of highest material removal rates, when creep feed grinding with superabrasive grinding wheels.

The use of neat oil cutting fluids also produces surfaces with higher compressive residual stress than those generated with water soluble cutting fluids, and this can have a beneficial effect on the service life of the component.

6 Cutting Fluid Application

6.1 Introduction

An important aspect of this project was to determine the optimum method of applying the cutting fluid, not only to optimise the grinding process itself, but also to minimise the fire hazard.

The findings in chapter five, grinding performance showed that for the HEDG grinding process, non-flammable water based fluids were inadequate. If neat oil cutting fluids are to be used, other means and measures need to be considered. Reducing cutting fluid mist and reducing grinding zone temperatures are key elements if the fire hazard is to be significantly reduced.

As stated in chapter four, the reduction of cutting fluid mist is split into two main areas. The first area was to investigate chemical means of mist reduction by appropriate selection of cutting fluids. The second was to investigate mechanical means of mist reduction by improving cutting fluid application.

It is in this second area, improving cutting fluid application, that attention will now be focused.

6.2 Investigation of Oil Mist Density within the Machine Canopy

In order to understand the influence of nozzle design and other fluid application parameters, such as delivery pressure and fluid flow rate, on the generation of cutting fluid mist within the machine canopy, a series of comparative tests were performed using different commonly used nozzle designs.

6.2.1 Nozzle Designs.

The effect on cutting fluid mist within the machine canopy of four different nozzle designs was tested. These are listed below and shown in figure 6-1.

- Coherent Jet Nozzle (after Cui (1995))
- Coherent Rectangular Nozzle (after Cui (1995))
- Shoe Nozzle (after Ramesh and Yeo (2001) see appendix 8)
- Flat Jet Spray Nozzle (Lechler part no. 652.361.16.00.00.0)

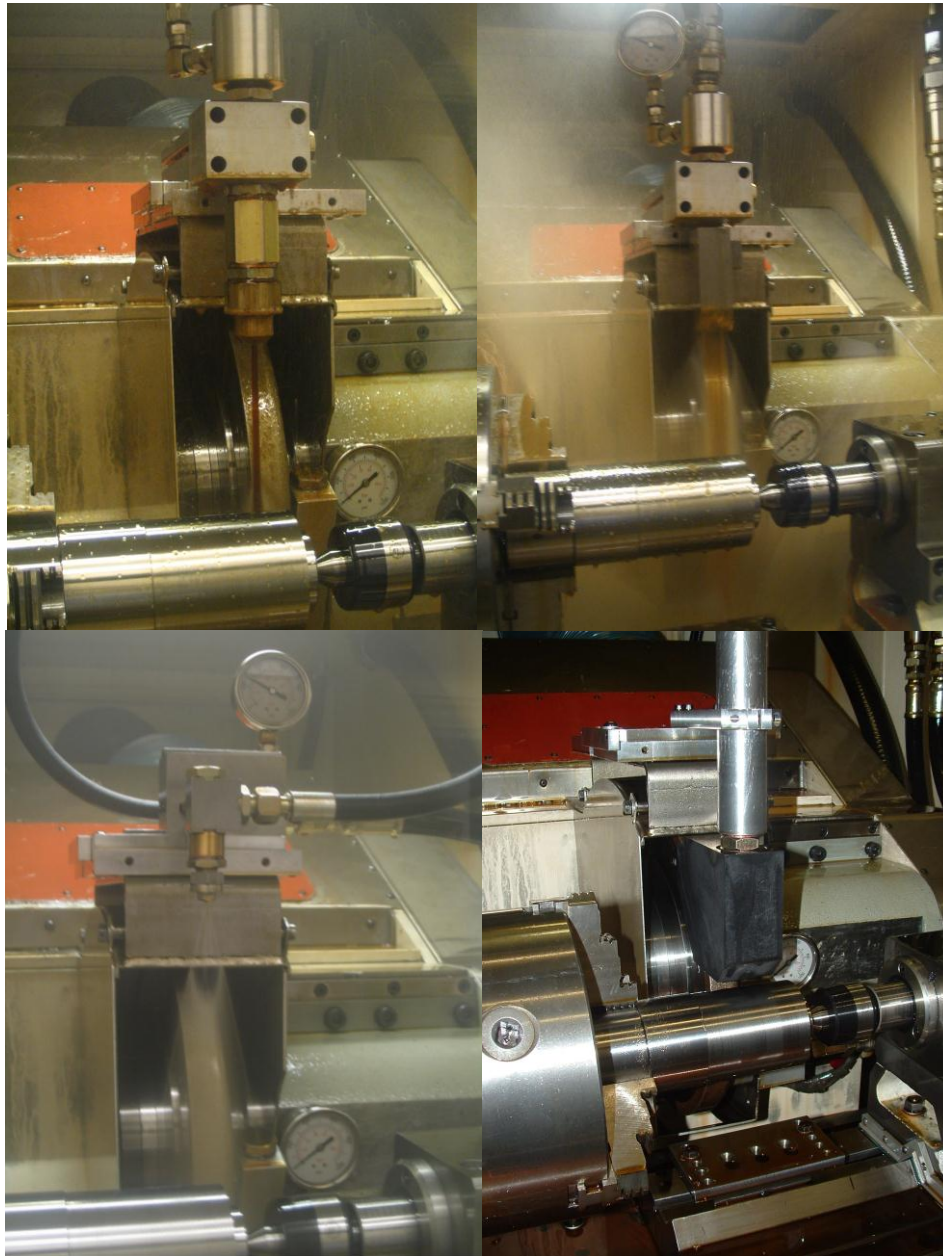


Figure 6-1 Nozzle Designs Tested in Cutting Fluid Misting Trials.

Ø5mm coherent Jet Nozzle (Top Left), Coherent Rectangular (Top Right), Lechler Spray Nozzle (Bottom Left) and Shoe Nozzle (Bottom Right)

6.2.2 Measurement of Cutting Fluid Mist in the Machine Canopy

The Tyndallometer used to perform the cutting fluid screening tests detailed in chapter four was used to measure the cutting fluid mist level within the machine canopy of the Edgetek SAT cylindrical grinding machine. Due to the limited range of this instrument and the high levels of mist, which are clearly visible within the machine canopy (see figure 6.2), the Tyndallometer could not be mounted within the machine canopy.



Figure 6-2 Formation of cutting fluid mist in the bottom of the SAT Machine.

Photograph taken moments after the flow of fluid has been started. Within seconds, this mist permeates throughout the machine. These mist levels are much higher than the saturation point of the Tyndallometer precluding its use inside the machine.

The Tyndallometer was therefore mounted in a sealed plastic box mounted outside the machine canopy and a small amount of air / oil mist was drawn from inside the machine into the plastic box where the oil mist density could be measured.

A Ø40mm hole was pre-drilled in the sealed box and a length of hose, of the same diameter, was used to connect the sealed box to a similar hole in the machine canopy. Custom flanges were used to ensure the pipe sealed correctly at both ends to minimise external contamination. A venturi was then used to create a slight vacuum in the sealed box in order to pull a constant flow of air through into the seal box which contained the Tyndallometer allowing the mist level within the machine canopy to be measured. This arrangement is shown in figure 6.3 with the venturi shown in figure 6.4

6.2.3 Test Procedure

A pre-ground Ø77mm workpiece was placed in the machine and a cylindrical traverse grind cycle, which removed no material, was performed. A simulated cycle was selected to create a controlled and constant testing regime which would allow fair comparisons between different nozzles to be made. The simulated grind cycle was performed three times for each set-up to allow mean values and variance to be calculated. The simulated test grind parameters are shown in table 6-1 unless otherwise stated.

Measurement of the mist density within the machine canopy was then recorded manually every 10 seconds from the Tyndallometer display which started from the moment the grinding cycle was initiated (pressing cycle start) to allow the effect of different nozzle designs to be evaluated.

Simulated Test Grind Conditions	
Grinding Machine	Edgetek SAT – 3 Axis Cylindrical Grinding Machine
Grinding Mode	Up Grinding
Workpiece	Dimensions : Ø77mm Material : 51CrV4 Hardness : 59Rc
Grinding Parameters	Wheelspeed : 50m/s Workpiece Speed : 10rpm Depth of Cut : 0.0mm Cross Traverse Speed : 30mm/min Specific Removal Rate : 0mm ³ /mm.s
Grinding Wheel	Electroplated CBN wheel, B213 grit Diameter : 350mm Width : 30mm Wheel Drawing : 300 HP 700-350-30 (see appendix 3)
Fluid Delivery	Top Nozzle : Various Bottom Nozzle : None
Grinding Fluids	Castrol Ilogrind 600SP Neat Mineral Oil
Number of Repeats	3

Table 6-1 Simulated test grind parameters used to assess the influence of nozzle design and other fluid application parameters on oil mist generation within the machine canopy.

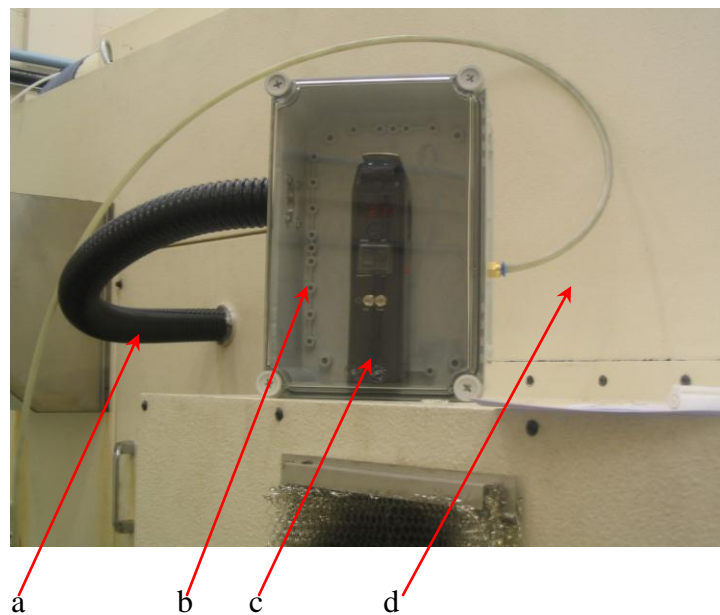


Figure 6-3 Hund TM Data Tyndallometer mounted in a seal plastic box.

A Ø40mm black hose is used to connect the Tyndallometer to the hole cut in the machine canopy. A Ø6mm clear nylon pipe is connected to a venturi that draws a constant flow of mist from the machine.

- a) Black hose used to draw mist from the machine canopy
- b) Sealed Plastic Box
- c) Hund TM Data Tyndallometer
- d) Machine Canopy

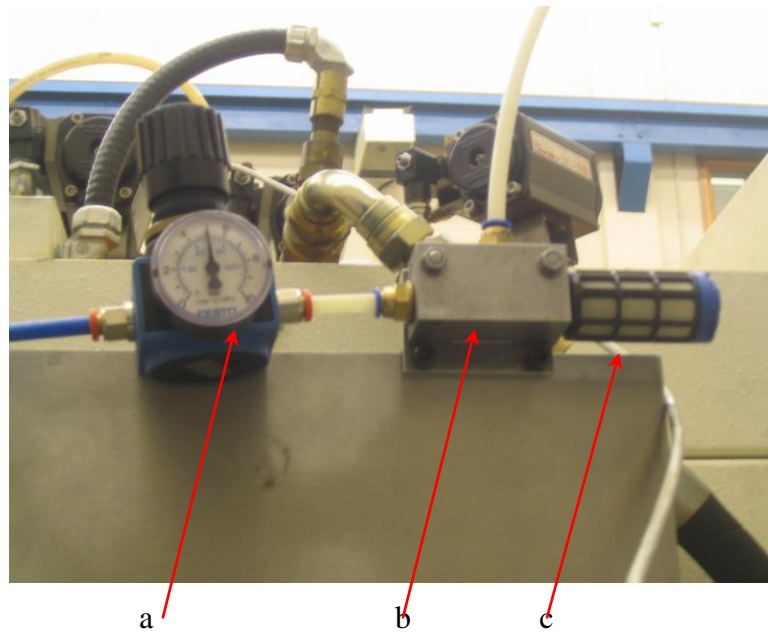


Figure 6-4 Venturi used to pull a constant flow of cutting fluid mist for measurement.

Venturi used to pull a constant flow of cutting fluid mist from the machine canopy though to the Tyndallometer where it can be measured. Pressure regulator maintained at 5 bar for all tests performed to ensure consistency.

- a) Pneumatic pressure regulator with integral pressure gauge*
- b) Venturi*
- c) Pneumatic solenoid*

6.2.4 Results

6.2.4.1 Effect of Nozzle Design on Mist Generation

The results in table 6-2 show the relative oil mist density within the machine canopy for typical creep feed grinding conditions. Throughout these particular tests, the pump pressure was maintained at a constant pressure as far as was practicable so that any influence in the mist levels within the machine canopy caused by variations in delivery pressure was minimised. The exception to this was the shoe nozzle.

Jet and spray nozzles are typically designed to operate at relatively high pressures in order to focus the cutting fluid to the desired area of the grinding zone. Conversely, shoe nozzles are low pressure devices and are typically used to coat the grinding wheel with cutting fluid. The supply pressure was therefore minimised when using the shoe nozzle in order to minimise the fluid flow rate, the conventional approach for this type of nozzle. The resultant mist levels are therefore more representative of what one would typically expect in normal grinding conditions.

The shoe nozzle produced the lowest levels of mist, both in terms of actual mist generated and the mist generated per unit flow of cutting fluid. Conversely, the spray nozzle produces significantly higher levels of mist per unit flow of cutting fluid. Since

the aim of the cutting fluid application strategy is to minimise mist generation in order to reduce the inherent fire hazard, the spray nozzles are clearly inadequate for this purpose.

Nozzle	Pressure (Bar)	Flow (l/min)	Mist after 70 seconds (mg/m ³)	Deviation	Mist / Flow (mg.min/m ³ /l)
Spray Nozzle	8 (min attainable)	3	16.4	13%	5.5
G0,75 0.9 x 20mm Rectangular	7.5	32	16.4	6%	0.5
G0,75 5mm Round	7.5	35	36.3	1.4%	1.0
Shoe Nozzle	5	50	13.5	4%	0.27

Table 6-2 Effect of nozzle selection on cutting fluid mist generation within the machine canopy.

Results for 30m/s wheel speed, 10rpm work speed. Cutting fluid : Castrol Ilogrind 600SP.

6.2.4.2 Effect of Flow Rate and Supply Pressure on Mist Generation

Leaving aside any variance between the different nozzles, (i.e. between 2mm and 5mm round nozzles) which may be attributable to simple random variations such as internal surface finish etc, table 6-3 shows that for any given nozzle design, increasing the nozzle pressure increases the amount of mist generated.

Nozzle	Pressure (Bar)	Flow (l/min)	Mist after 70 seconds (mg/m ³)	Deviation	Mist / Flow (mg.min/m ³ /l)
G0.375 2mm Round	20	10	25.8	4.5%	2.6
G0.375 2mm Round	7.5	5	13.9	28%	2.8
G0.375 5mm Round	20	46	22.9	3%	0.5
G0.375 5mm Round	7.5	28	5.8	7.2%	0.2

Table 6-3 Effect of delivery pressure and flow rates on cutting fluid mist generation within the machine canopy.

Results for 30m/s wheel speed, 10rpm work speed. Cutting fluid: Castrol Ilogrind 600SP.

The increase in oil mist density is a result of the increase in the volume of cutting fluid being applied, as the fluid flow rate increases with increases in fluid delivery pressure. This is shown by the fact that the values of mist per unit flow (mist / flow) of cutting

fluid do not change significantly between low and high delivery pressures (and thus low and high cutting fluid flow rates). Consequently, for any given nozzle aperture, pump pressures should be minimised in order to minimise the resultant fluid flow rate, and thus to minimise the resultant cutting fluid mist within the machine canopy.

6.2.4.3 Effect of Grinding Wheel speed on Mist Generation

Figure 6-5 shows the effect of increasing the grinding wheel speed on fluid mist generation within the machine canopy. The effect of the grinding wheel speed has a far greater effect on the oil mist density within the machine than either the nozzle design (see table 6-2) or changes in the fluid delivery pressure (see table 6-3). The grinding wheel essentially acts as a large oil mist generator, an effect of which can be seen clearly in figure 6-6.

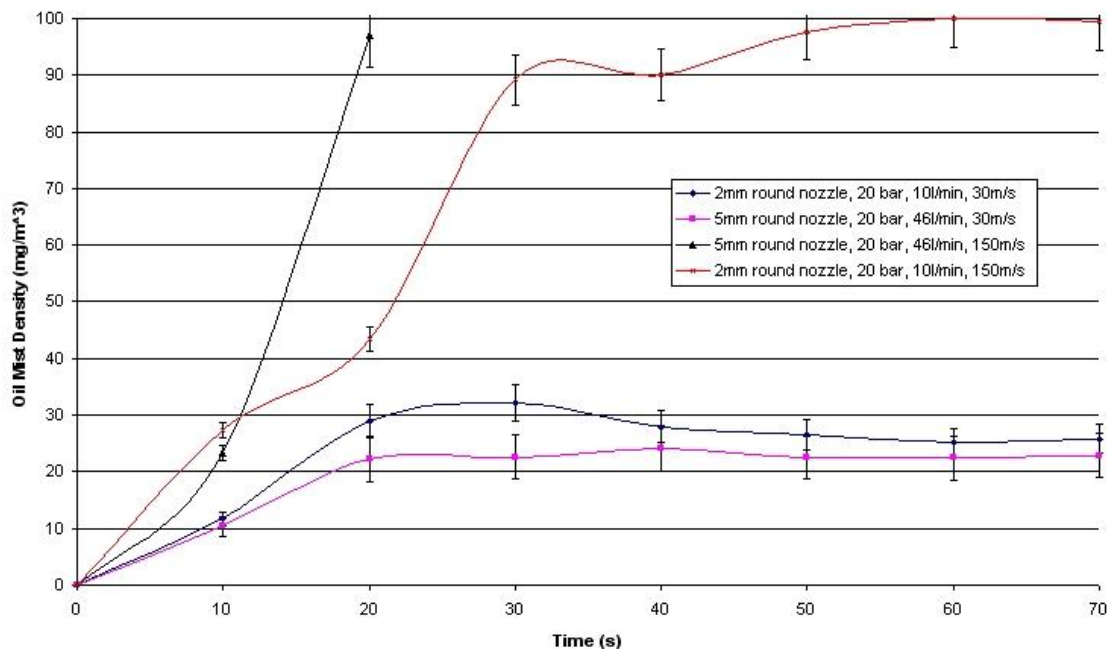


Figure 6-5 Effect of grinding wheel speed on cutting fluid mist generation within the machine canopy.

Cutting fluid : Castrol Ilogrind 600SP.

Unfortunately, high grinding wheel speeds are essential in HEDG in order to reduce the chip thickness and lower the grinding forces. In other grinding regimes, surface finish may be important, which again may determine what grinding wheel speed is selected. Minimising the grinding wheel speed in order to minimise cutting fluid mist may not therefore be an option.

Nozzle	Flow (l/min)	Wheelspeed (m/s)	Mist after 20 seconds (mg/m ³)	Deviation	Mist / Flow (mg.min/m ³ /l)
G0.375 2mm Round	10	30	29.3	3%	2.9
G0.375 2mm Round	10	150	43.32	1%	4.3
G0.375 5mm Round	46	30	22.1	3.7%	0.5
G0.375 5mm Round	46	150	96.58	2%	2.1

Table 6-4 Effect of wheel speed on cutting fluid mist generation within the machine canopy. Results for 20 bar delivery pressure.

Cutting fluid : Castrol Ilogrind 600SP.

Figure 6-5 shows the benefit of reducing the fluid flow rate when operating at high grinding wheel speeds. This is more clearly shown by the values of mist generation per unit flow rate displayed in table 6-4. Whilst there is undoubtedly a significant increase in mist generated when using the 2mm round nozzle, where the mist generation per unit flow almost doubles from 2.9 to 4.3 mg.min/m³/l, when the wheel speed is increased from 30 to 150m/s, the increase is far larger for the 5mm round nozzle. With the 5mm round nozzle, the increase in mist generation per unit flow increases over four fold, increasing from 0.5 to 2.1 mg.min/m³/l. for the same increase in grinding wheel speed. This increase is attributable to the higher fluid flow with the 5mm nozzle.

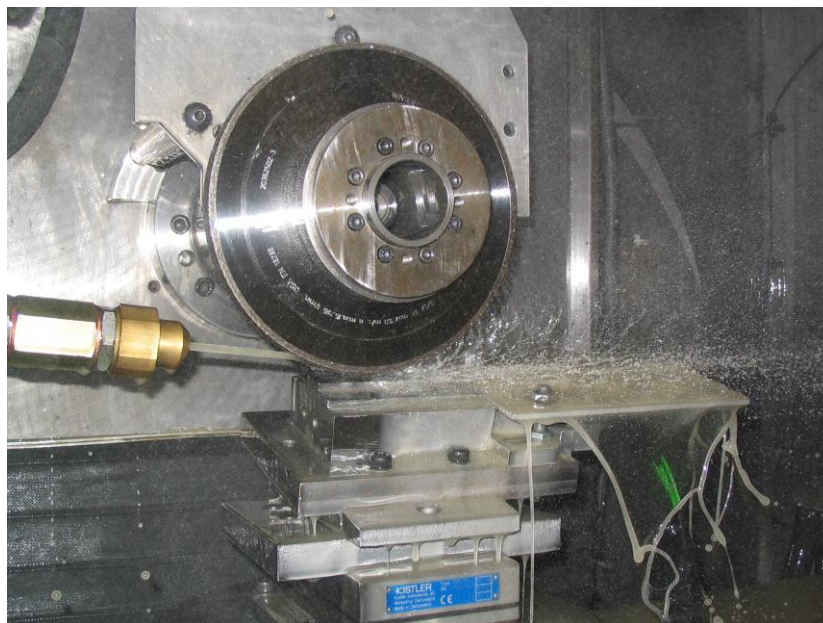


Figure 6-6 Formation of cutting fluid mist by the action of the grinding wheel.

With the grinding wheel rotating at 2000rpm, the formation of a mist can be clearly observed. The mist is formed by a variety of different droplet sizes. Cutting fluid: Castrol ES1

6.3 Influence of Nozzle Design on Grinding Performance

6.3.1 Introduction

As a result of the relatively poor performance of the spray nozzle in the misting tests detailed in the previous section on the effect of nozzle design within the machine canopy, comparative cylindrical traverse grinding trials in both the Creep and HEDG regimes were conducted using coherent rectangular, coherent round and shoe nozzles on the Edgetek SAT machine in order to ascertain the influence of the nozzle design on the grinding process.

Cylindrical traverse grinding operations were selected in preference to a plunge grinding operation, as the main focus of the project was to investigate the new process of superabrasive turning as described in chapter one, in other words the cylindrical HEDG traverse grinding regime.

Grinding power was measured using a Load Controls Inc. Model UPC Hall Effect Transducer (see appendix 2) installed on the SAT machine and National Instruments PCI6036E data acquisition system with dedicated Labview software for data acquisition. Data was recorded at 1000 samples per second for 30 seconds. Test grinds were repeated three times to allow mean values and variance to be calculated.

The influence of the cutting fluid was measured by conducting a “spark out” cut, where the steady state grinding wheel power is measured whilst the wheel and workpiece rotate at the prescribed speeds whilst in contact, and the cross traverse and in-feed axes remain stationary.

6.3.2 Creep Feed Regime

Table 6-5 details the grinding parameters used to evaluate the effect of different nozzle designs on grinding performance in creep feed grinding. For creep feed grinding, a specific removal rate (Q') of approximately 20 was used, which was calculated using equation 6-1.

Equation 6-1

$$Q' = \frac{(\pi.D.N)}{60} \cdot a_e$$

where Q' = specific removal rate ($\text{mm}^3/\text{mm.s}$)
 D = work piece diameter (mm)
 N = rotational speed (rpm)
 a_e = depth of cut (mm)

The apertures of the coherent rectangular and the coherent round nozzles were matched as far as was practicable so that when operated at the same supply pressure, both nozzle

designs would provide similar fluid flow rates. This was to allow fair comparisons to be made.

The position of both the rectangular and round nozzles was set so that the jet of cutting fluid was focused toward the leading edge of the grinding wheel, slightly before the grinding wheel entered the grinding zone (see figure 6-7). This is the conventional way to set up this type of nozzle.

Creep Feed Grinding Test Conditions	
Grinding Machine	Edgetek SAT – 3 Axis Cylindrical Grinding Machine
Grinding Mode	Up Grinding
Workpiece	Dimensions : Ø79mm Material : 51CrV4 Hardness : 59Rc
Grinding Parameters	Wheel speed : 50m/s Work piece Speed : 10rpm Depth of Cut : 0.5mm Cross Traverse Speed : 30mm/min Specific Removal Rate : 4mm ³ /mm.s
Grinding Wheel	Electroplated CBN wheel, B213 grit Diameter : 350mm Width : 30mm Wheel Drawing : 300 HP 700-350-30 (see appendix 3)
Fluid Delivery	Pump Pressure: 15 bar Top Nozzle : a) Ø5mm coherent jet nozzle. 6 Bar Pump Pressure, 32l/min b) 0.9mm x 20mm coherent rectangular nozzle. 6 Bar Pump Pressure, 30l/min c) Shoe nozzle 7.5 Bar Pump Pressure, 19l/min Bottom Nozzle : None
Grinding Fluids	Castrol Ilogrind 600SP Neat Mineral Oil
Number of Repeats	3

Table 6-5 Grinding parameters used to assess the influence of nozzle design in creep feed grinding.

The exception to this was again the shoe nozzle for the reasons stated earlier. The shoe nozzle was set-up so as to minimise the fluid flow rate with the pressure being adjusted to the minimum attainable pressure on the supply pump. It should be noted that the shoe nozzle was in fact modified after the tests detailed in section 6.2 in order to restrict the flow, which was deemed to be excessive at 50l/min at a supply pressure of 5bar. Consequently, the fluid flow rate dropped to 19l/min at a supply pressure of 7.5bar.

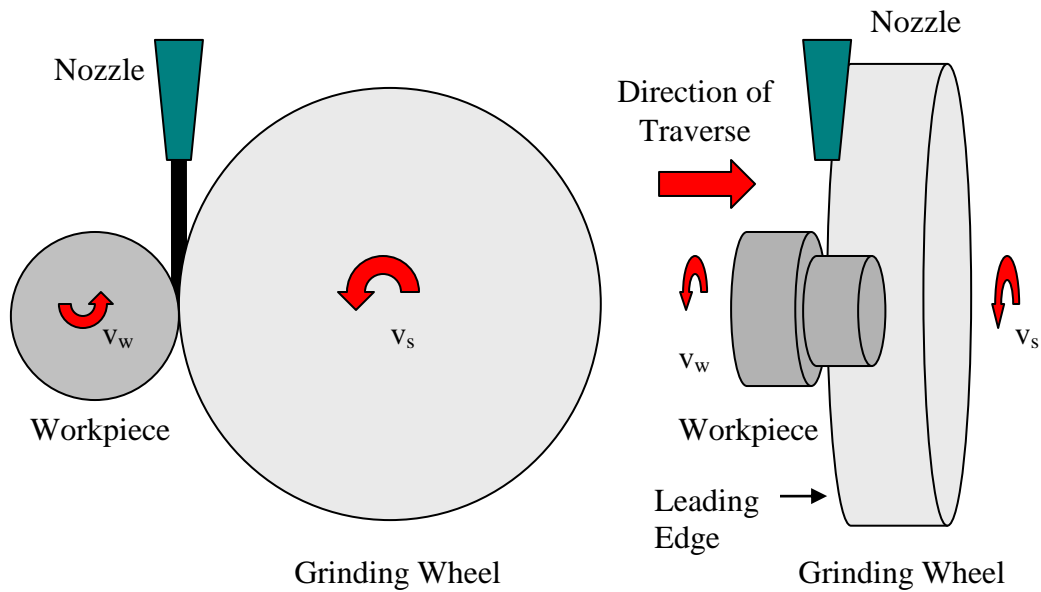


Figure 6-7 Alignment of the Cutting Fluid Application Nozzles.

Both the rectangular and round coherent nozzles were adjusted so that the cutting fluid hit the grinding wheel slightly ahead of the grind zone, and toward the leading edge of the grinding wheel.

6.3.2.1 Results

The use of the shoe nozzle resulted in the lowest net “grind” power (figure 6-8) and consequently the lowest specific grinding energy (figure 6-9) for all the different nozzles tested under similar creep feed grinding conditions. This was despite the high total power measured during tests. This is attributable to the differences in the fluid velocity between the shoe nozzle and both the rectangular and round nozzles.

The mean cutting fluid velocity exiting both the rectangular and round nozzle, which was calculated using equation 6-2, was very similar, being 27.7m/s and 27.2m/s respectively. When using a shoe nozzle however, the fluid velocity is effectively zero (Andrew and Howes, 1985), thus despite having the lowest flow rate and the lowest grind power, the use of the shoe nozzle resulted in the highest total power, the extra power being required to accelerate the cutting fluid to grinding wheel speed.

Equation 6-2

$$Q = AV \quad (\text{Granet, 1996})$$

therefore $V = Q / A$

where $V = \text{mean fluid velocity}$
 $Q = \text{volume rate of flow}$
 $A = \text{aperture area}$

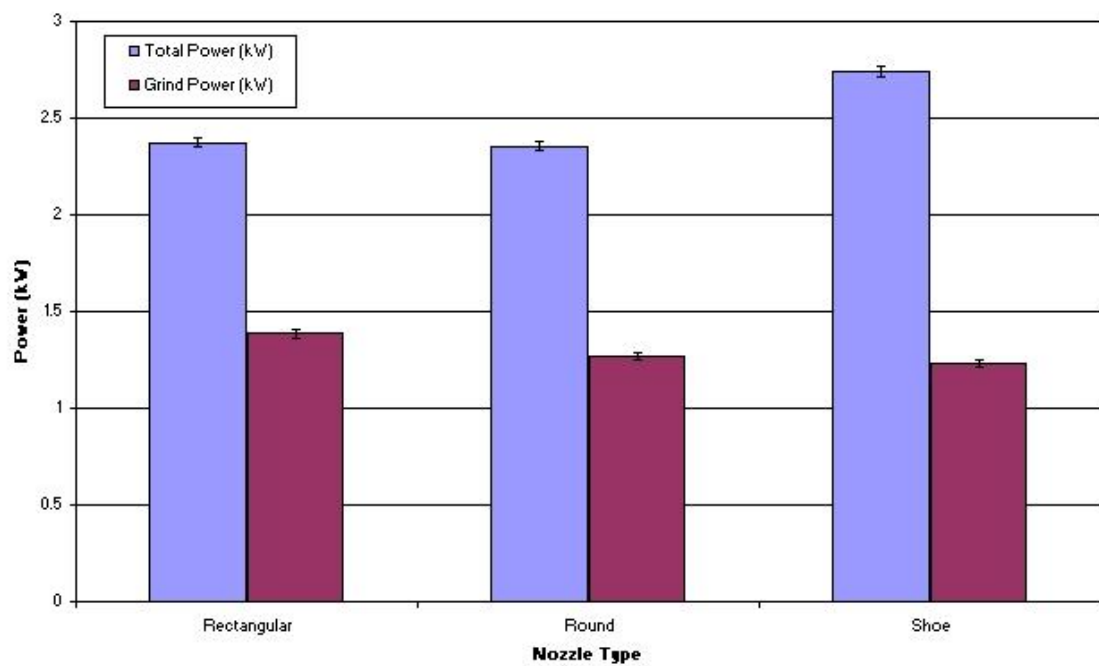


Figure 6-8 Influence of nozzle design on both the total grind power and the net grind power for cylindrical creep feed traverse grinding.

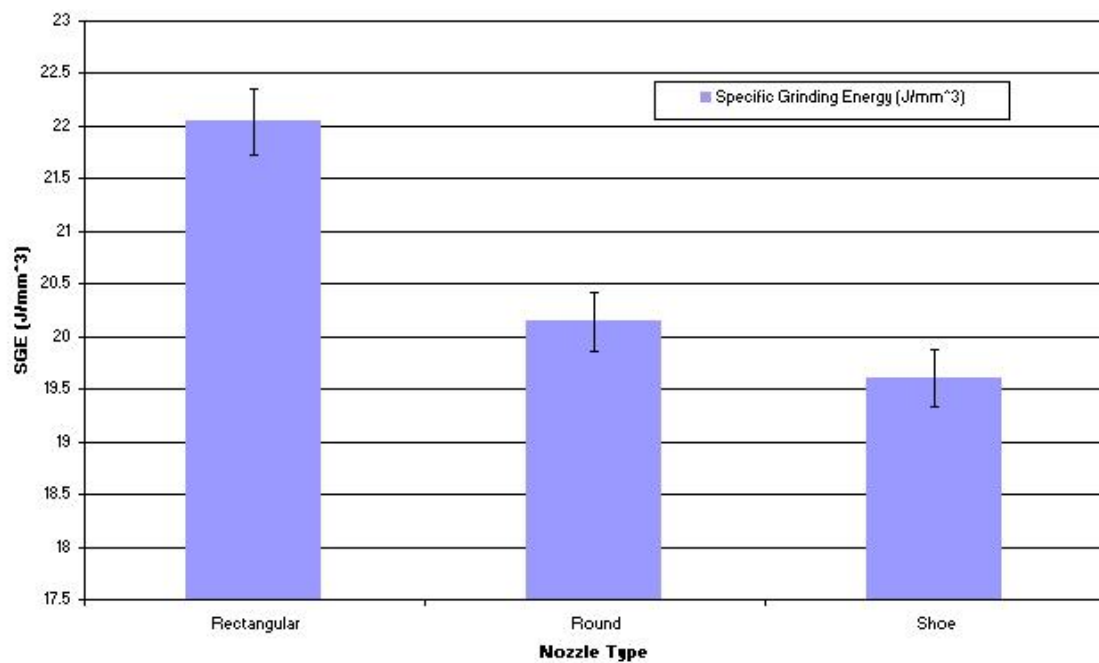


Figure 6-9 Influence of nozzle design on specific grinding energy for cylindrical creep feed traverse grinding.

However, the low specific grinding energy results, witnessed when using a shoe nozzle during these tests, must have been as a consequence of a reduction in the tangential grinding force (see equation 2.4) attributable to improved fluid application when using this type of nozzle, as all the other parameters remained constant.

It can also be inferred that the amount of heat energy generated in the grinding zone must be also lower. Equation 6-3 shows that the amount of thermal energy generated by the grinding process (q_t) is proportional to the specific grinding energy (e_c). As the thermal energy generated by the grinding zone is distributed or partitioned to the four different elements of the grinding process (see figure 2-4), a reduction in the total thermal energy (q_t) as signified by a reduction on the specific grinding energy, it follows that there must be a reduction in the amount thermal energy entering the workpiece. This is because the wheel/work partition ratio (R_{ws}) is fixed both by the process parameters and the relative thermal properties of the grinding wheels and the workpiece (see equation 3-7). Therefore comparatively low levels of specific grinding energy signify a reduced likelihood of thermal damage to the workpiece. Reducing the grinding zone temperature also has the obvious beneficial effect of reducing the potential fire hazard within the grinding machine.

Equation 6-3

$$q_t = e_c \cdot a_e \cdot v_w / l_c \quad (\text{Stephenson and Jin, 2003})$$

Where

$$\begin{aligned} q_t &= \text{total heat flux} \\ e_c &= \text{specific grinding energy} \\ a_e &= \text{depth of cut} \\ v_w &= \text{work piece feedrate} \\ l_c &= \text{arc of contact} \end{aligned}$$

6.3.2.2 Barkhausen Noise Measurements.

Barkhausen noise measurements were taken to establish whether there were any significant differences in the metallurgical properties of components ground using different fluid application nozzles. The components were placed on a custom test bed, where they could be rotated at constant speed via the motorised headstock. Stresstech Rollscan 200 equipment used in conjunction with ViewScan software was then used to take Barkhausen noise measurements around the periphery of the component. This set-up can be seen in figure 6-10. Barkhausen noise measurements were taken every one degree of rotation at constant magnetisation and gain settings.

A reference component was also prepared which was ground extremely conservatively to ensure no thermally dependant metallurgical changes occurred within in the workpiece, and yet have a comparable surface finish to the test components as it is known that surface finish affects the Barkhausen noise response. The grinding parameters used to prepare the reference component can be seen in table 6-6

Reference Component Grinding Parameters	
Grinding Machine	Edgetek SAT – 3 Axis Cylindrical Grinding Machine
Grinding Mode	Up Grinding
Workpiece	Dimensions : Ø79mm Material : 51CrV4 Hardness : 59Rc
Grinding Parameters	Wheelspeed : 50m/s Workpiece Speed : 10rpm Depth of Cut : 0.1mm Cross Traverse Speed : 30mm/min Specific Removal Rate : 20mm ³ /mm.s
Grinding Wheel	Electroplated CBN wheel, B213 grit Diameter : 350mm Width : 30mm Wheel Drawing : 300 HP 700-350-30 (see appendix 3)
Fluid Delivery	Shoe nozzle 7.5 Bar Pump Pressure, 19l/min Bottom Nozzle : None
Grinding Fluids	Castrol Ilogrind 600SP Neat Mineral Oil
Number of Repeats	3

Table 6-6 Grinding parameters used to grind reference component used for comparative Barkhausen noise measurements.

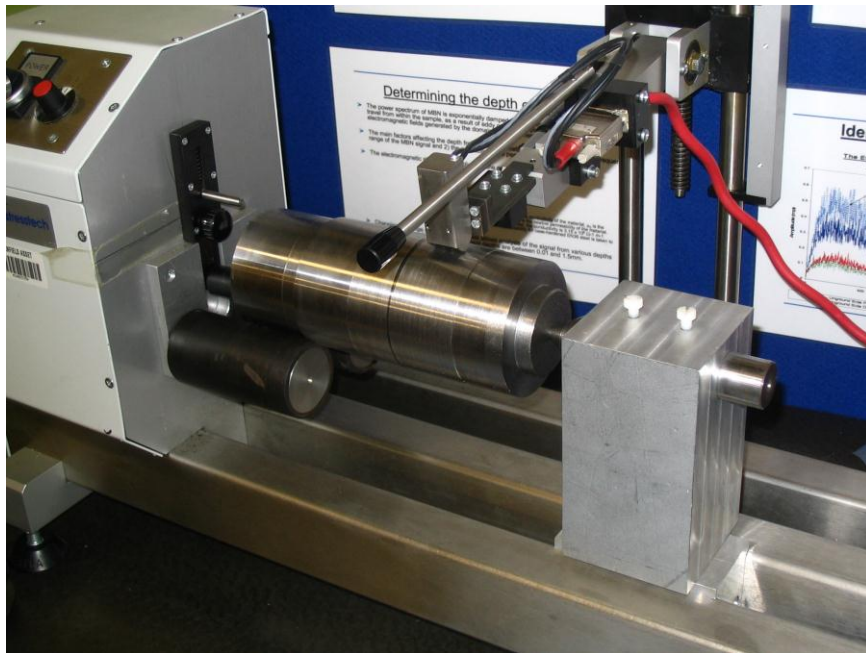


Figure 6-10 Barkhausen noise measurement of cylindrical components.

Figure 6-11 shows the results of the Barkhausen noise measurements for the components ground using different nozzle designs along with the reference component for comparison purposes. It clearly shows that there was no significant difference in the Barkhausen noise response, as indicated by changes in the Mp value, between components ground using different nozzle designs, or with the reference component indicating there is no significant differences or changes in the metallurgical properties of the components.

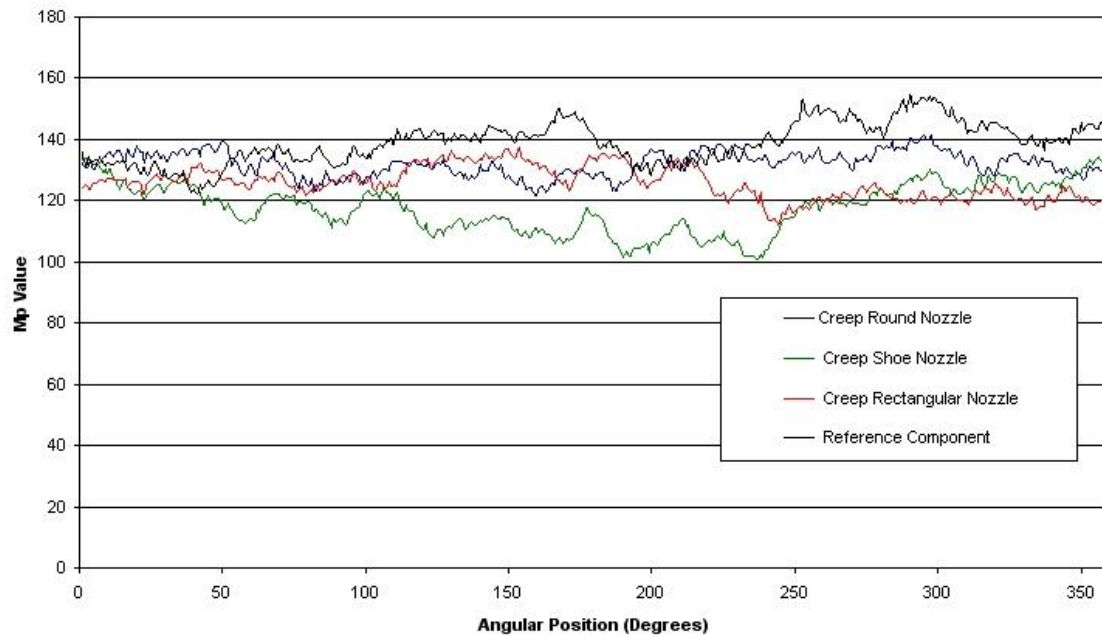


Figure 6-11 Results of Barkhausen noise measurements of cylindrical components traverse ground in the creep feed regime using different nozzle designs.

These results indicate that not only did the finish surface temperatures not exceed the temperature threshold, approximately 400°C for 51CrV4 (Stephenson and Jin, 2002), at which metallurgical changes within the material would occur, but also they also indicate that the contact temperature during the grind could not have exceeded 300°C, the fluid burn out limit for neat cutting oils.

In creep feed grinding, over 90% of the total heat generated is removed by the cutting fluid, and it is this mechanism that ultimately controls workpiece temperature. In the creep feed regime, the point at which the cutting fluid burn out limit is reached is characterised by a massive increase in the contact temperature. Since the creep feed regime employs very low workpiece speeds, this thermal energy cannot be removed by the grinding chips (as is the case in HEDG), but instead is conducted into both the grinding wheel but most importantly the workpiece, where it caused thermal damage.

6.3.3 HEDG Regime

The same experimental procedure as the creep feed grinding tests detailed in section 6.3.2 was followed for the HEDG regime tests with the obvious exception of the grinding parameters which are shown in table 6-7

HEDG Test Conditions	
Grinding Machine	Edgetek SAT – 3 Axis Cylindrical Grinding Machine
Grinding Mode	Up Grinding
Workpiece	Dimensions : Ø79mm Material : 51CrV4 Hardness : 59Rc
Grinding Parameters	Wheel speed : 150m/s Work piece Speed : 1000rpm Depth of Cut : 0.5mm Cross Traverse Speed : 100mm/min Specific Removal Rate : c.2000mm ³ /mm.s
Grinding Wheel	Electroplated CBN wheel, B213 grit Diameter : 350mm Width : 30mm Wheel Drawing : 300 HP 700-350-30 (see appendix 3)
Fluid Delivery	Pump Pressure: 15 bar a) Ø5mm coherent jet nozzle. 6 Bar Pump Pressure, 32l/min b) 0.9mm x 20mm coherent rectangular nozzle. 6 Bar Pump Pressure, 30l/min c) Shoe nozzle 7.5 Bar Pump Pressure, 19l/min Bottom Nozzle : None
Grinding Fluids	Castrol Ilogrind 600SP Neat Mineral Oil
Number of Repeats	3

Table 6-7 Grinding parameters used to assess the influence of nozzle design in HEDG.

6.3.3.1 Results

In contrast to the creep feed grinding tests, when conducting cylindrical HEDG traverse grinding, the use of round and rectangular coherent nozzles resulted in lower net grinding powers (see figure 6-12) and consequently lower specific grinding energies (see figure 6-13) than the shoe nozzle under similar process conditions.

As with the creep feed grinding regime, the low specific grinding energies witnessed were as a consequence of a reduction in the tangential grinding force (see equation 2.4) as a result of improved fluid application, but in this instance it was attributable to the use of the rectangular and round coherent nozzles, as all the other parameters remained constant. It can also be reiterated that the amount of heat energy generated in the grinding zone must also be lower (see equation 6-3) and thus the likely-hood of thermal damage to the workpiece is reduced, and as with the creep feed grinding trials, reducing the grinding zone temperature has the obvious beneficial effect of reducing the potential fire hazard within the grinding machine

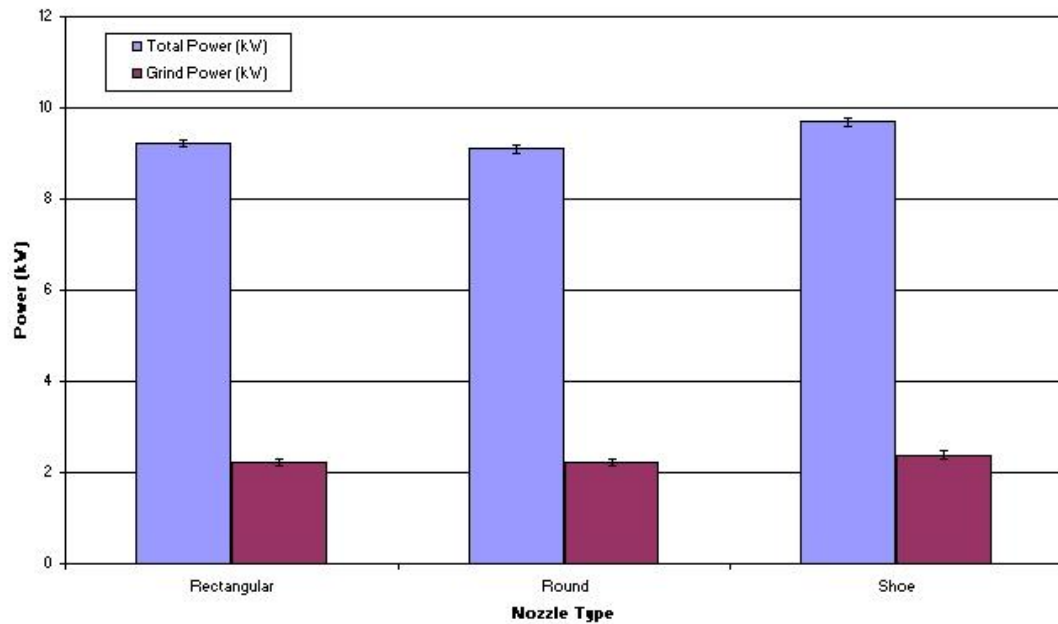


Figure 6-12 Influence of nozzle design on both the total grind power and the net grind power for cylindrical HEDG traverse grinding.

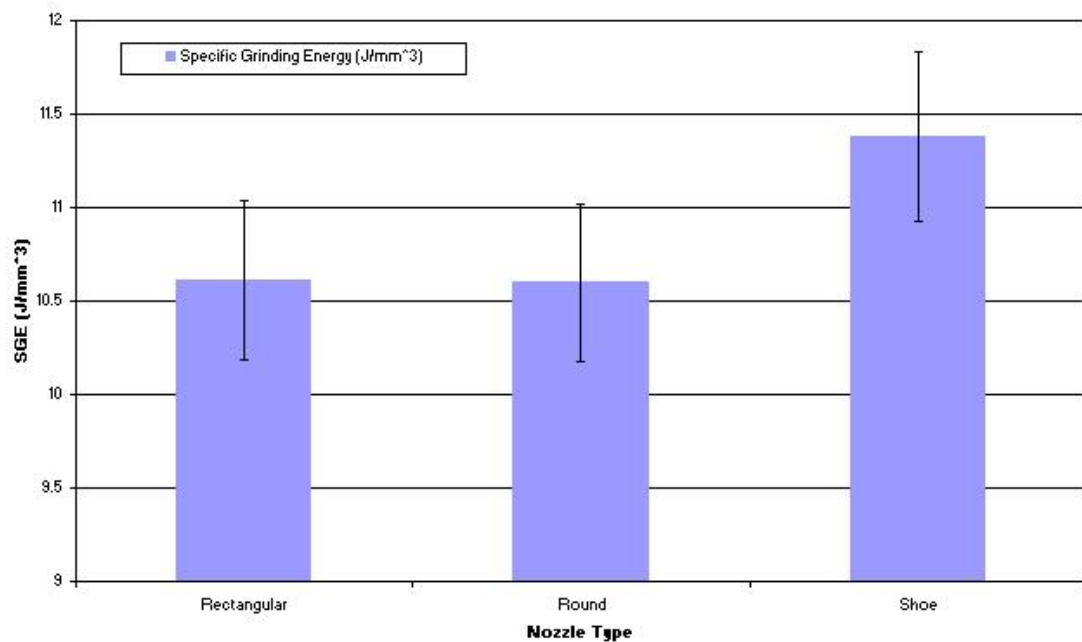


Figure 6-13 Influence of nozzle design on specific grinding energy for cylindrical HEDG traverse grinding.

One possible explanation for this reversal in the performance of the different nozzle designs between creep feed and HEDG regimes is that the increase in grinding wheel speed in the HEDG regime results in more cutting fluid being spun off the grinding

wheel when using the shoe nozzle, with the consequent reduction in the amount of fluid entering the grinding zone for lubrication purposes.

Due to the bulky nature of the coolant shoe, which can clearly be seen in figure 6-1, the shoe was positioned 50mm above the grinding wheel centreline. This allowed the component, nominally 80mm in diameter (40mm radius) to pass under the shoe nozzle with a clearance of approximately 10mm, when the grinding wheel advanced to contact the component. As a result, the cutting fluid that is “attached” to the grinding wheel has to pass through a relatively large arc before entering the grinding zone, whilst being subjected to a significant centrifugal force as a result of the high grinding wheel speed. Obviously, the high centrifugal force will want to throw the cutting fluid from the periphery of the grinding wheel.

This spin off effect was to some extent witnessed when conducting the misting trials detailed in section 6.2. When conducting tests with the shoe nozzle at a grinding wheel speed of 30m/s, the average relative mist level within the machine canopy reached 13.7mg/m^3 after 70 seconds. When the grinding wheel speed was increased to 150m/s, the relative mist level exceeded 100mg/m^3 , the saturation limit of the Tyndallometer, in less than 20 seconds. When operating a 5mm round nozzle at 150m/s (refer to table 6-4), which delivered similar amounts of cutting fluid as the unmodified shoe nozzle, the relative mist level was measured at 96.58mg/m^3 mist level after 20 seconds. Whilst this was close to the saturation limit of the Tyndallometer, the oil mist density certainly did not exceed it, despite the fact that when the same nozzle was operated at 30m/s, it resulted in a mean relative oil mist density of 22.1mg/m^3 after 70 seconds, significantly higher than the level of mist experienced when using the shoe nozzle under similar conditions.

6.3.3.2 Barkhausen Noise Measurements

As with the creep feed grinding trials, Barkhausen noise measurements were taken to establish whether there was any significant differences in the metallurgical properties of components ground using the different nozzle designs within the cylindrical HEDG traverse grinding regime. The set-up of the Barkhausen noise equipment was the same as that used for the creep feed grinding trials described in 6.3.2.2.

Figure 6-14 shows the results of these tests and, as for the tests conducted in the creep feed regime, they show there is no significant difference in the Barkhausen noise response, as indicated by changes in the Mp value, either between components ground using different nozzle designs or with the reference component. This indicates that there are no significant changes or differences in the metallurgical properties of the components.

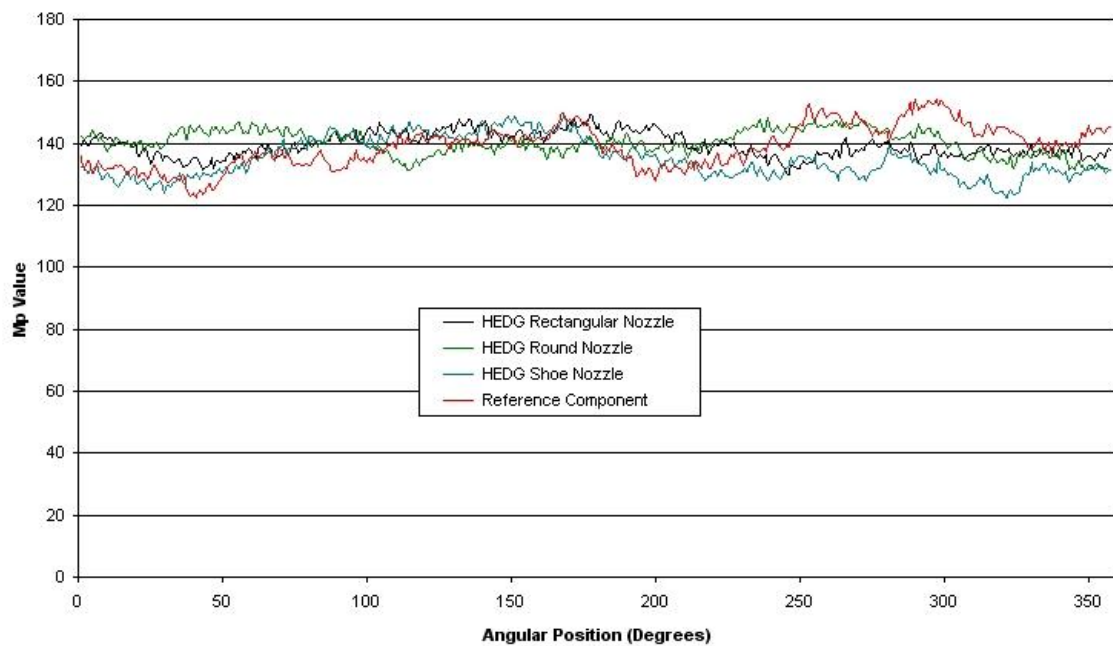


Figure 6-14 Results of Barkhausen noise measurements of cylindrical components traverse ground in the HEDG regime using different nozzle designs.

The significance of these results is that despite working in the HEDG regime where very high contact temperatures are a characteristic of the process, the finish surface temperatures did not exceed the temperature threshold, approximately 400⁰C for 51CrV4 (Stephenson and Jin, 2002), at which metallurgical changes within the material would occur.

These results show that despite the very high contact temperatures associated with HEDG, coupled with the fact that there would have been little or no cooling of the grinding zone by the cutting fluid (a consequence of fluid burn out), HEDG can be used to machine components at very high material removal rates without causing thermal damage to the work piece, if the grinding parameters, and in particular the workpiece feed rate, are properly selected such that most of the thermal energy is removed by the grinding chips.

6.4 Summary

The grinding wheel, and more specifically, the grinding wheels rotational speed, is the primary source of mist generation within the machine canopy. Nozzle design has only a minor influence on the total amount of mist generated within the machine. This said, spray nozzles should not be used for cutting fluid application due to the disproportionately high levels of mist generated within the machine canopy associated with their use, and the subsequent increase in the fire hazard. However it is clear that cutting fluid nozzles should not be selected solely on their mist performance.

Fluid flow rates and delivery pressures should be minimised in order to minimise the oil mist density within the machine canopy, whilst still maintaining an adequate supply for lubrication and, in the creep feed regime, cooling of the grinding zone.

Shoe nozzles should be used for creep feed grinding due to the lower specific grinding energy witnessed when using this type of nozzle. Consequently there will be a reduction in the grind zone temperature which reduces the risk of thermal damage to the workpiece and reduces the potential fire hazard. Shoe nozzles also offer low mist levels at grinding wheel speeds typically associated with creep feed grinding.

Coherent round or coherent rectangular nozzles are more suitable for the cylindrical traverse grinding in the HEDG regime as the use of these nozzles resulted in the lowest levels of specific grinding energy with the subsequent reduction on grind zone temperature.

7 Validation of Cutting Fluid Application Strategy

7.1 Introduction

The aim of this thesis was to produce a cutting fluid application strategy for the cylindrical HEDG regime, or the SATURN process as it is sometimes known, based upon the thermal characteristics of the cutting fluid in order to produce a coherent and robust strategy suitable for industrial applications. The strategy has two key elements, the first being cutting fluid selection, the second being cutting fluid application. The strategy developed in this thesis therefore answers the fundamental question of “what is the most appropriate cutting fluid for the cylindrical HEDG regime based on the thermal characteristics of the fluid, and how do we best apply this cutting fluid”.

In chapter one, the formation of this coherent fluid application strategy was split up into several distinct stages, and it is important to review these elements before moving on to the discussion of the actual work carried out in to develop the strategy.

- a. To establish the properties of the cutting fluid which have a thermal impact on the grinding process.
- b. To develop a standardised test program aimed at measuring the above properties.
- c. Use the data from the standardised test program to select the most effective cutting fluid for the cylindrical HEDG process.
- d. To investigate different nozzle designs typically used for fluid application in grinding operations to determine the most effective and efficient method of fluid application.
- e. To minimise the volume of cutting fluid used in the cylindrical grinding process
- f. To reduce the environmental impact of the grinding process attributable to the use of cutting fluids.
- g. To propose a best practice fluid application strategy for the cylindrical HEDG regime.

The first stage of developing a cutting fluid application strategy based on the thermal characteristics of the cutting fluid was, obviously, to establish exactly which characteristics of the cutting fluid had a thermal impact on the grinding process. The literature presented in chapter two shows there are four areas where the cutting fluid has a thermal impact on the grinding process. These are:

Cooling
Lubrication
Ignition
Misting

The first item in this list is self evident, but lubrication is also a key thermal characteristic when one considers that with the “notable exception of creep feed grinding, cooling by grinding fluids appears to be generally ineffective in lowering the peak temperature within the grinding zone. With improved lubrication and reduced wheel dulling, the grinding forces are reduced thereby lowering the grinding zone temperature and the tendency for thermal damage”. (Malkin, 1989)

Once these thermal characteristics, the second stage of the program was to develop a testing regime that could evaluate all the different thermal characteristics that impact on the grinding process. This testing regime could then be used to fairly compare and contrast the performance of different cutting fluids.

Furthermore, it was also important to consider some of the practical experience gathered when operating in the HEDG regime, most notably in respect of machine fires that were experienced during the course of this project, and these will also be discussed in this chapter. This practical experience combined with the results presented in chapters 3 to 6 will also be used to develop the cutting fluid application strategy.

7.2 Cutting Fluid Selection

Chapter three focussed on the convection coefficient of the cutting fluids, which is a measure of a cutting fluid's ability to cool the grinding zone. The results shown in table 3-5 clearly show water based cutting fluids have a significantly higher convection coefficient than their neat oil counterparts, typically one order of magnitude greater. Typical values for a water based cutting fluid (Hysol XH for example) $258911 \text{ W/m}^2\text{K}$ contrasts greatly with the $97728 \text{ W/m}^2\text{K}$ for a typical neat oil cutting fluid (Castrol Ilogrind 600SP). The results presented in chapter three clearly showed water based cutting fluids were far more effective at removing heat from the grinding zone.

This result was, however, expected. The literature presented in chapter 2 showed that a number of different researchers working in this field had found similar findings. Jin and Stephenson (2003a) predicted values of up to $180000 \text{ W/m}^2\text{K}$ and $60000 \text{ W/m}^2\text{K}$ for water based and neat oil cutting fluids respectively. Furthermore, even the most crude of models, the “fluid wheel” model shown in equation 2.2 (Rowe, 2001a; Jin and Stephenson, 2002) showed that the convection coefficient of the cutting fluid was proportional to the thermal property of the cutting fluid. With water based cutting fluids having a far higher thermal property, no least attributable to their very high values of thermal conductivity made these results almost inevitable.

Cooling, as stated previously, is not the only characteristic of the cutting fluid to have a thermal impact on the grinding process, fluid lubricity, ignition and misting characteristics of the fluid are also vitally important. Chapter four focused on these

other three thermal characteristics, but the results in chapter five meant the conclusions drawn from these tests would be far more significant.

Chapter five presented the results of investigations onto the performance of different cutting fluids under real grinding conditions, both in the HEDG regime and in the creep feed grinding regime for comparison purpose. The results clearly show that neat oil cutting fluids were superior to water based cutting fluids when used in the HEDG regime, the principal area of interest for this thesis.

The use of neat oil cutting fluids in the HEDG regime resulted in significantly lower levels of specific grinding energy (see figure 5-3), lower grinding forces (see figure 5-4) and grinding powers (see figure 5-5), both the total and the grind power, than when water based cutting fluids were employed under similar grinding conditions.

Despite significantly lower levels of convection coefficient (see table 3-5), neat oil cutting fluids, samples ground using a neat oil cutting fluid were subjected to significantly lower contact zone temperatures (see figure 5-6) and consequently the depths of thermal damage as witnessed by a layer of untempered martensite or white layer below the ground surface (see figure 5-6)

The apparent contradiction of water based cutting fluids giving rise to the highest grind zone temperatures despite having far better cooling characteristics is easily explained if one considers the relationship between the specific grinding energy and the total thermal energy entering the system (refer to equation 2-5). For any given set of process parameters (wheel speed, depth of cut etc.), the total thermal energy generated by the grinding process is proportional to the specific grinding energy.

For any given set of process parameters, the specific grinding energy is proportional to the tangential grinding force (see equation 2-4), and that good lubrication of the grinding zone reduces the grinding forces (Brinksmeier and Heinzl, 1999), the use of neat oil cutting fluids will result in less thermal energy entering the system.

Furthermore, the aggressive nature of the HEDG regime, mean high contact temperatures (but not necessarily finish surface temperatures, there is an important distinction between the two) are characteristic of the process, fluid burnout is almost inevitable. Consequently, the cooling action of the fluid is automatically reduced almost to zero (Andrew and Howes, 1985; Ohishi S. Furukawa, 1985; Howes, 1990). It is therefore vital, for any given set of process parameters, to select a cutting fluid with high lubricity to ensure the grind zone is sufficiently lubricated, thus reducing the frictional forces and consequently the total thermal energy generated by the process. With neat oil cutting fluids offering the highest levels of lubrication, a fact shown with the presented in chapter 5 and supported by the results of the torque force tests presented in section 4.2.2, neat oil cutting fluids are the most appropriate for the HEDG regime.

This is a key finding, but one that was not surprising when once considers that, as previously stated, with the “notable exception of creep feed grinding, cooling by grinding fluids appears to be generally ineffective in lowering the peak temperature within the grinding zone” (Malkin, 1989). Furthermore, Malkin (1989) continues “With

improved lubrication and reduced wheel dulling [wear of the abrasive grains], the grinding forces are reduced thereby lowering the grinding zone temperature and the tendency for thermal damage. These considerations would seem to weigh heavily on favour of cutting oils as opposed to soluble oils [water based cutting fluids]”. This passage was not written with particular reference to the HEDG regime, but it perfectly summarises the experimental findings for HEDG presented in chapter five.

Since water based cutting fluids are not best suited for the HEDG regime, despite the obvious benefit of being non flammable, due to their poor lubricity attributable to the fact that these fluids cannot develop the necessary elastohydrodynamic separating films needed in the high pressure contact conditions associated with all grinding regimes (Marinescu and Rowe, 2004), elimination of the potential fire hazard is virtually impossible. The consequence of this is that the other two thermal characteristics of the grinding fluid, the misting and the ignition characteristics, suddenly become vitally important if a robust fluid application strategy is to be developed. In order to produce a strategy robust enough for industrial applications, steps must be taken to significantly reduce the potential fire hazard.

Empirically, the first step on reducing the potential fire hazard is to select a cutting fluid that was the most resistant to ignition, as the option of selecting a non-flammable water based cutting fluid is not available. The results of the fluid ignition trials showed high viscosity ester based cutting fluids were the most difficult fluids to ignite, as in both the tests performed to ignite any cutting fluid evaporate presented in section 4.4.2, and the fluid mist ignition tests presented in section 4.4.3, the high viscosity ester based fluid needed to be raised to the highest temperature before ignition would occur.

Secondly, as the literature showed that fluid mists can be readily ignited, sometimes at temperatures below the base fluids flashpoint (Bowen and Shirvill, 1994; Bowen and Shirvill, 1994a; Maragkos and Bowen, 2002) so the reduction of the mist level in the machine canopy by selecting a cutting fluid that produces comparatively low levels of mist will further reduce the potential fire hazard. The results from the cutting fluid misting trials presented in chapter four (section 4.3.3) again show that high viscosity ester based cutting fluids were the best in this respect, producing the lowest levels of cutting fluid mist of all the different cutting fluids evaluated.

For ignition of a cutting fluid, whether it is the cutting fluid evaporate or the cutting fluid mist (the bulk fluid will not ignite as demonstrated by the fluid ignition tests presented in section 4.4.1), an ignition source or heat source must be present. In grinding, this heat source is effectively the grinding process itself. The grinding process generates all the thermal energy responsible for the high contact temperatures, the ejection of hot grinding chips (or swarf) from the grinding zone and possibly, depending on the exact process parameters, bulk heating of the workpiece resulting in the lighter, more volatile fractions contained within the grinding fluid being released by evaporation.

Any reduction in the grinding zone temperature would therefore have a commensurate effect of reducing the potential fire hazard. As previously stated, a cutting fluid exhibiting very high levels of lubricity reduces the grinding forces, thereby reducing the

total thermal energy produced by the process. For any given set of process parameter, the partitioning of the total thermal energy remains constant, that is to say, the proportion or ratio of heat energy distributed to the grinding wheel, workpiece, cutting fluid and that removed by the ejected grinding chips will remain the same.

In HEDG, the high contact temperatures characteristic of the process exceed the boiling point of the cutting fluid, and consequently the thermal energy partitioned to the cutting fluid is effectively zero. The thermal energy is therefore divided between the wheel, the workpiece and the grinding chips. Since the wheel work partition ratio (R_{ws}) remains constant for any given set of grinding parameters (see equation 3-7), so must the chip partition ratio (R_{ch}), as the sum of the partition ratios must equal one. If the total thermal energy of the grinding process is reduced by improved lubrication, then not only must the thermal energy entering the workpiece reduce, with the obvious result of reduced contact temperature and reduced thermal damage as seen in figure 5-6, but the thermal energy removed by the grinding chips must also be reduced, with the commensurate effect on the average chip temperature.

It is useful at this juncture, to put these findings in to the wider context of the coherent fluid application strategy. In chapter one, the key aim of producing a cutting fluid application based on the thermal characteristics of the cutting fluid was split up into a number of key steps or “objectives”. These steps are so important, that they were repeated at the beginning of this chapter. This discussion thus far has centred on the first three steps (steps A through C), with perhaps step C, the selection of the cutting fluid itself, being perhaps the most critical of all of these from a perspective of actually producing a coherent strategy. The results and subsequent discussion clearly show that the most appropriate cutting fluid for use in the HEDG regime is to be a high viscosity ester based cutting fluid, because of its high lubricity, low misting characteristics coupled with its high resistance to ignition.

The selection of the most appropriate cutting fluid for the HEDG regime, does not satisfy all the requirements of a fluid application strategy, nor does the use of a high viscosity ester based cutting fluid completely eliminate the potential fire hazard. It is therefore important to fully understand some of the causes of real cutting fluid fires experienced on real machine tools to ascertain whether any lesson can be learned which may have an impact on the application of the cutting fluid.

During the course of this body of work, two separate machine fires were experienced on the Edgetek machines at Cranfield, and both these were thoroughly investigated in an attempt to establish the actual cause of the fire. These investigations are detailed in the next section.

7.3 Sources of Ignition

The first machine fire occurred whilst performing the HEDG trials on the Edgetek SAM machine detailed in chapter five. During the course of these trials the cutting fluid ignited, and consequently, the fire extinguisher system fitted to the machine was immediately activated. This activation was performed manually as this proved

significantly quicker in reacting to the fire than the thermal sensors fitted to the machine which trigger the fire extinguisher system automatically. As the fire extinguisher system is interlocked with the machines' emergency stop control circuit, the machine stops (almost instantaneously) once the system is activated. The machine is therefore stopped, quite literally milliseconds after cutting fluid ignition occurred, the time difference being the human reaction time (from seeing the fire to activating the fire extinguisher) and the reaction time of the emergency stop circuit and the servo control systems controlling the axes. This is extremely important, as the grinding process is effectively held at the point the cutting fluid ignition occurred, and this is extremely valuable when attempting to ascertain the most likely cause of the fire.

When investigating the first fire, the source of ignition was most likely to be a build up of grinding swarf that was trapped between the workpiece and the shoulder of the right hand coolant nozzle. This arrangement can be seen in figure 7-1, with a close-up of the swarf ball shown in figure 7-2.

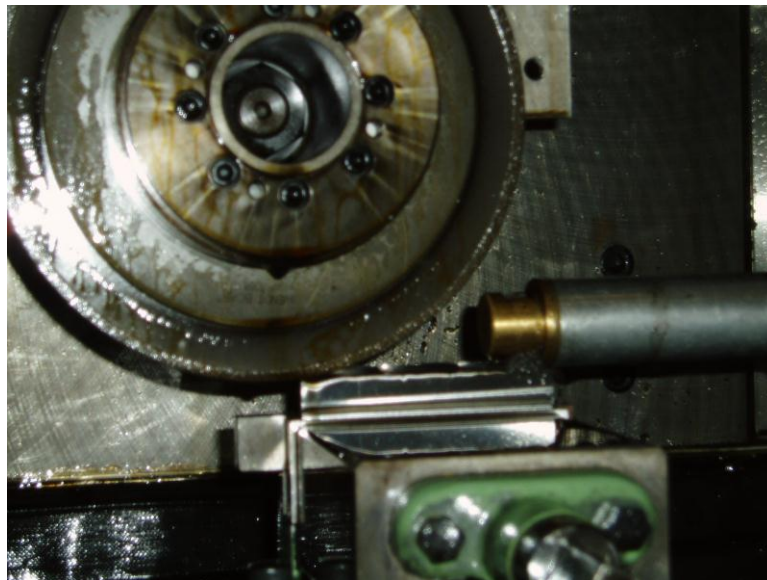


Figure 7-1 Ball of swarf trapped between right hand coolant nozzle and workpiece.

The right hand nozzle was used to extinguish the sparks exiting the grinding zone. Note, during operation workpiece traverses from left to right and grinding wheel rotates counter clockwise.

This swarf ball, observed during the test just prior to ignition, glowed incandescent. It was significantly brighter and was therefore hotter than any other area of the plume of grinding sparks that exits the grinding zone. The cutting fluid passing this swarf ball was mainly mist and fine spray at it too had just exited the grinding zone.



Figure 7-2 Close-up of ball of swarf that was trapped between right hand nozzle and the workpiece.

Note: Grinding wheel and nozzle retracted for a clearer view.

The most likely explanation for the swarf ball being significantly hotter than the surrounding area is the fact that as the swarf ball developed, the volume of the ball increased in a cubic relationship with its nominal diameter. The surface area of the ball however would only increase in a squared relationship to the diameter.

The result would be that whilst the heat energy contained within the ball grew in a cubic relationship to the diameter, the effective cooling area would only increase in a squared relationship, as cooling only would only occur on the surface. The entrapped heat energy within the swarf ball would therefore grow faster than it cooled and thus remained significantly hotter than the surrounding plume of grinding sparks that were being cooled in the usual way.

The problem was compounded by the fact that the test was almost complete, and the wheel was nearing the end of the workpiece. This gives rise to a fluid application problem whereby insufficient fluid enters the grind zone, as there is no “nip” at the end of the workpiece to help focus the fluid into the grind zone, a problem encountered in creep feed grinding and discussed in chapter 2. This problem will be covered in more detail in later in this section, however at this point it is sufficient to say that this would have exacerbated the situation.

To prevent a reoccurrence of this problem two simple modifications were made to the right hand fluid nozzle as it was clear poor nozzle positioning and a lack of cleaning or flushing by the cutting fluid had allowed a build up of hot material in close proximity to flammable mixture of cutting fluid mist and fine spray.

The first measure was to raise the right hand nozzle slightly in order to remove the trap point. The angle of the nozzle was then adjusted to aim the fluid into the nip of the wheel and workpiece as before. The second measure was to add a tapered collar over

the right hand nozzle, thus allowing a smooth flow of material past the shoulder of the right hand coolant nozzle. This revised arrangement can be seen in figure 7-3.

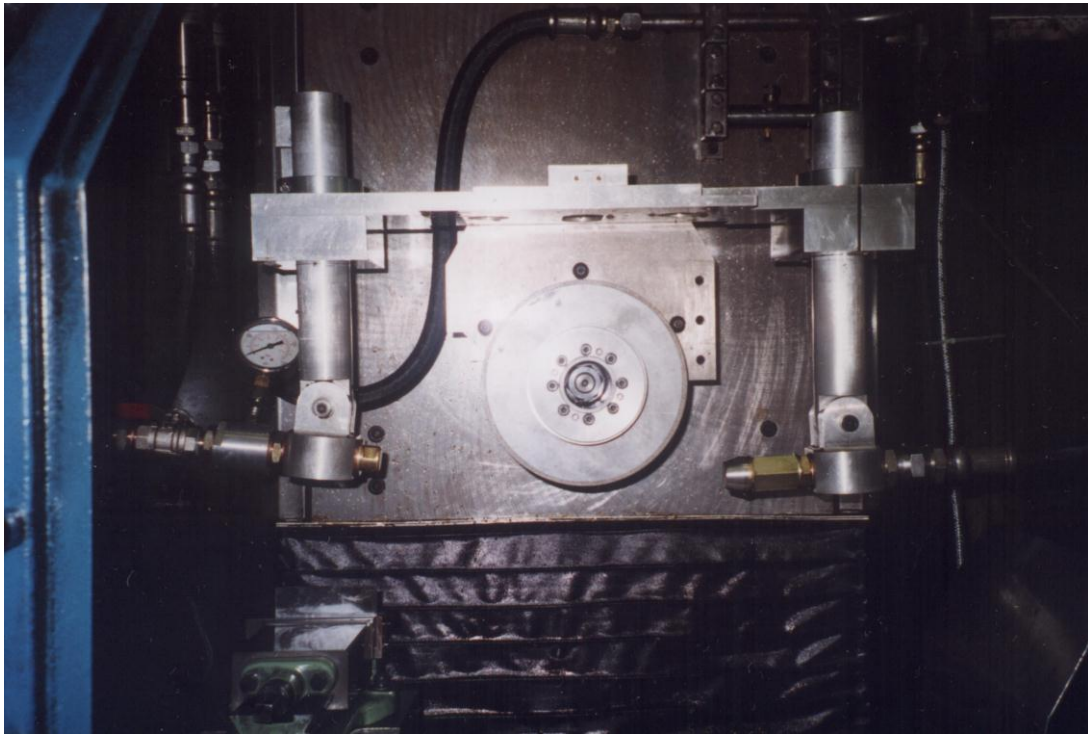


Figure 7-3 New fluid application set-up on the Edgetek SAM machine.

Note the left hand nozzle is unchanged, but the right hand nozzle has been adjusted to remove trap point for hot grinding sparks. Note also the tapered collar over the right hand nozzle.

The investigation of this fire revealed some important points.

- The use of a high flashpoint cutting fluid is no guarantee against ignition. The Fuchs 40SR cutting fluid has a closed cup flashpoint of 216°C (Fuchs Lubricants, 2004) in comparison to a neat mineral oil of 130°C. (Castrol, 1999)
- The importance of careful machine design and set-up to prevent the localised accumulation of hot debris from the grinding zone.
- The importance of chip removal in HEDG to help prevent localised accumulation of debris.

This last point is important as the chip removal action of a cutting fluid is often considered to be of secondary importance to cooling and lubrication (Sheng and Oberwalleney, 1997) and is often overlooked. In HEDG however fluid film boiling can occur, and the fluid no longer cools the grinding zone (Andrew and Howes, 1985; Ohishi and Furukawa, 1985). Even bulk cooling of the workpiece for dimensional consistency loses its importance, as HEDG is predominantly used for roughing operations. Therefore as long as the component is within tolerance for any subsequent

finishing operation, dimensional consistency can be a secondary consideration, whereas flushing away of hot grinding debris to prevent accumulation is vitally important.

This is not to say that the cooling ability of the fluid is irrelevant in HEDG, and its importance increases on machines where roughing and finish operations are carried out on a single machine. In these circumstances the requirements of both processes must be considered, but on machines dedicated to HEDG, cooling can be of secondary importance.

The investigation of the cutting fluid fire presented in the previous paragraphs also highlighted the problem poor cutting fluid application at the end of the workpiece resulting in excessive workpiece temperature, and this was also an issue in the second fire experienced at Cranfield during the course of this work. The problems revolves around the workpiece geometry, and the consequent loss of the “nip” that can occur at the end of the workpiece, which helps to focus the fluid into the grind zone.

This effect is most graphically shown in figure 7-4. Photographs were taken at different stages throughout a single grinding cycle. For most of the grinding cycle sufficient quantities of cutting fluid enters the grinding zone to allow effective cooling and lubrication. This prevents an excessive number of sparks being ejected from the grinding zone. However, when the grinding wheel approaches the end of the workpiece, cutting fluid tends to hit the end face of the component and get diverted away from the grinding zone. Consequently insufficient cutting fluid enters the grind zone for adequate cooling and lubrication and the result is a significant increase in the number of grinding sparks being ejected from the grinding zone.

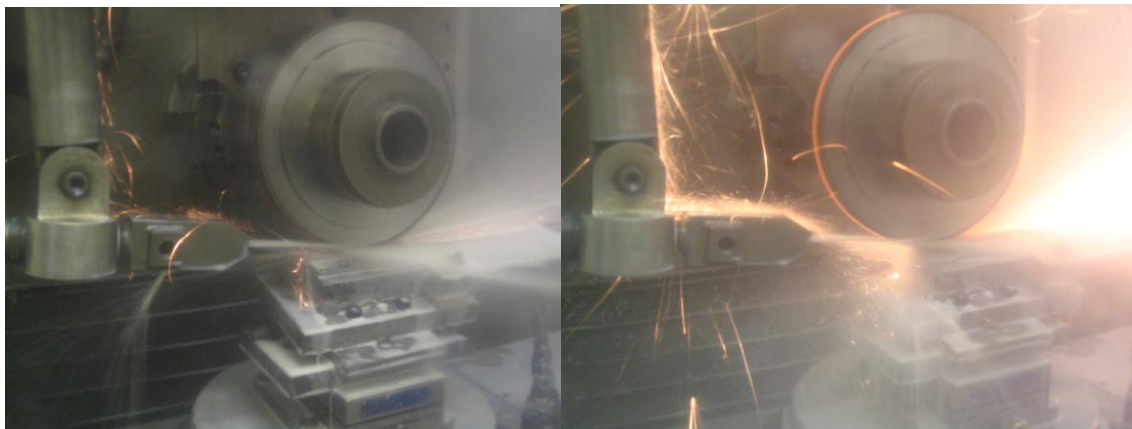


Figure 7-4 Comparison of the grind cycle at different points within the cycle.

The two photographs were taken during the same grinding cycle. In the picture, the workpiece traverses from left to right under the grinding wheel. On the left, the photograph shows the conditions within the grinding machine midway through the grinding cycle. On the right, the photograph shows a massive increase in the number of grinding sparks ejected from the grinding zone. This is attributable to the fact that insufficient cutting fluid is entering the grinding zone due to the loss of the “nip” at the end of the workpiece.

When grinding steels such as 51CrV4, it is clear from both workpiece appearance (see figure 7-5) and from the metallurgy that there has been a substantial increase in workpiece temperature attributable to fluid starvation. The problem is consistent between work pieces and affects not only HEDG but also other grinding modes such as creep and high speed grinding.

What is not clear is the exact mechanism of the ignition process, as there are two possible scenarios. The first is that the elevated body temperature ignites the fluid. The second is grinding swarf ejected from the grinding zone, which like the workpiece body is at an elevated temperature, ignites the fluid mist and vapour within the machine canopy. What is clear however is the need to apply the cutting fluid in such a way as to prevent the problem irrespective of workpiece geometry.



→
Direction of traverse

Figure 7-5 Burn at the left hand end of the workpiece caused by fluid starvation.

The fluid fails to penetrate the grinding zone correctly due to the end face of the workpiece resulting in an area of burn at the left hand end on the workpiece.

In order to alleviate this problem experiments have been conducted with some 30mm long “nip” blocks (dummy work pieces) mounted to the left hand end of the inclined thermocouple test rig shown in figure 3-4, in order to provide an additional land of material which provides the necessary wedge to focus the cutting fluid into the contact zone. This arrangement is shown in figure 7-6.

The use of fluid support or “nip” blocks is frequently used in surface grinding to overcome workpiece burn at the end of components in conventional grinding operations (Andrew and Howes, 1985; Marinescu and Rowe, 2004, Silliman and Perich, 1992), though a similar problem exists in certain cylindrical grinding operations, such as

helical gear and thread form grinding where the traverse feedrate to rotational speed ratio is very high.

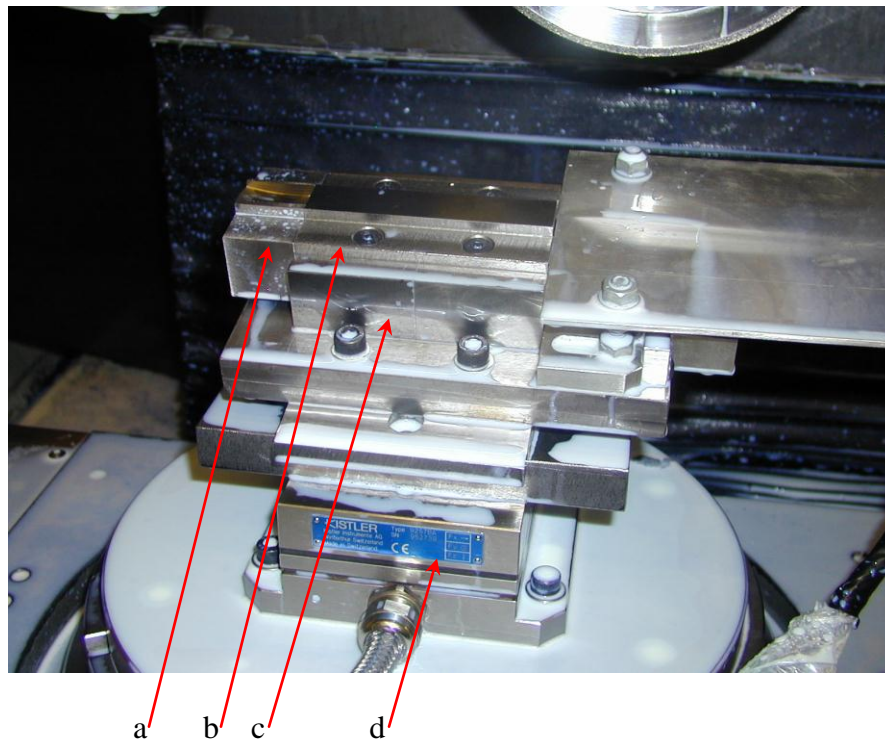


Figure 7-6 Nip block bolted to the left hand end of the workpiece.

The fluid fails to penetrate the grinding zone correctly due to the end face of the workpiece resulting in an area of burn at the left hand end on the workpiece.

- a) Nip Block
- b) Workpiece
- c) Inclined Thermocouple Test Rig
- d) Dynamometer

Figure 7-7 shows the results of these tests, with workpiece burn clearly visible at the end of the component where no additional nip block was used in comparison to a component ground with the use of a nip block. What was not clear was whether this was attributable to improved coolant application, or that the nip block simply acted as heat-sink, with the excessive heat generated at the end of the workpiece being conducted away into the nip block and thus preventing the thermal damage to the workpiece.

A further test was therefore carried out where an insulating material (20micron plastic shim) was placed between the workpiece to prevent the conduction of heat energy into the nip block. Again, the effect of the nip block is clearly visible, with no thermal damage on the ends of the workpiece or the insulating material, suggesting that the elevated temperatures which caused the workpiece burn and consequently increase the potential fire hazard are the result of poor fluid application.

Unfortunately, burn was visible on both the nip blocks, indicating that the problem of high contact temperatures caused by poor lubrication, and thus the potential fire hazard

still remained. Consequently, some longer nip blocks, 60mm long, were manufactured to allow further tests to be performed where there is a longer land of material in front of the wheel when it is taken away from the workpiece at the end of the grinding cycle.

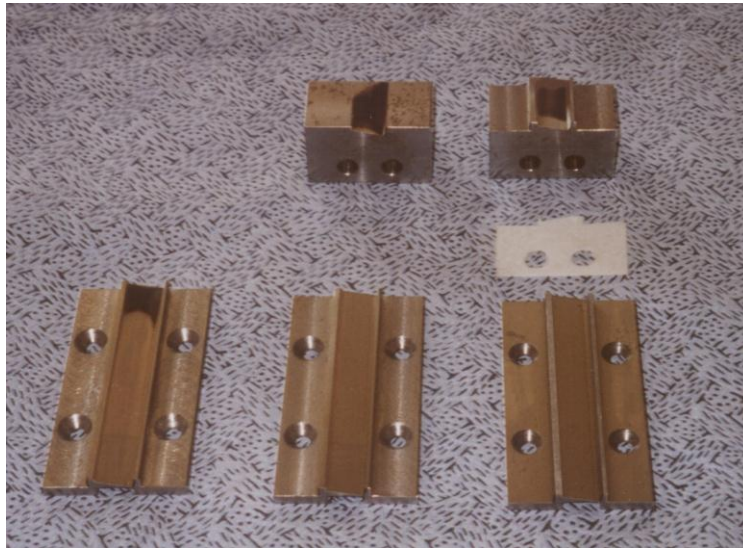


Figure 7-7 *The use of nip blocks to eliminate burn at the end of the workpiece, and thus remove a potential source of ignition.*

The workpiece on the left ground with no nip block, middle ground with 30mm long nip block, right ground with a 20micron white plastic shim sandwiched between 30mm long nip block and workpiece

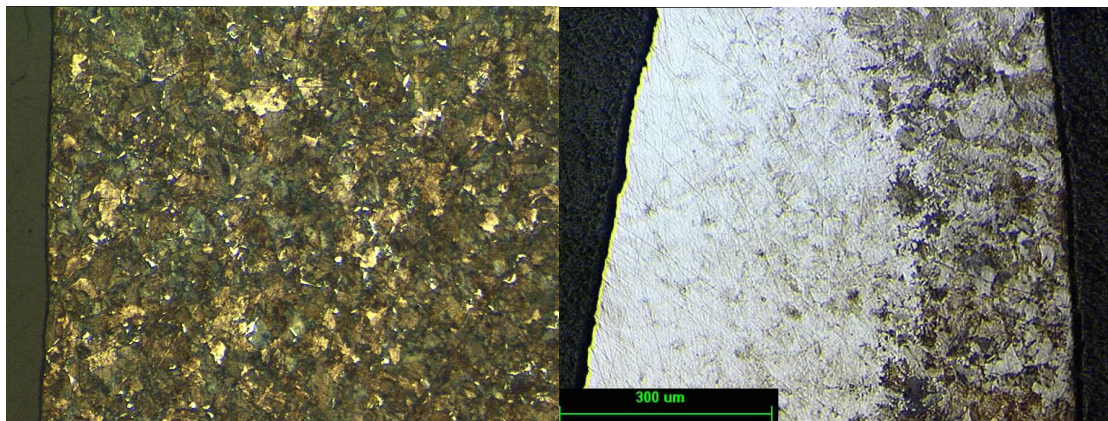


Figure 7-8 *Microstructures from workpiece ground without the use of a nip block.*

Sample taken 50mm from end of workpiece shows no sign of thermal damage (left), whereas sample taken 10mm from end of workpiece (right) has a thick white layer characteristic of elevated surface temperatures.

The main similarity between both these fires was the fact that they occurred at the end of the workpiece where the workpiece geometry prevented proper fluid application to the grinding zone. This, as it has been shown, would have resulted in a significant

increase in the workpiece temperature and a significant increase in the number of hot sparks ejected from the grinding zone.

The actual ignition mechanism is open to conjecture. It could have been a hot grinding spark mixing igniting the fluid mist in the machine canopy, a mechanism simulated by the fluid ignition tests detailed in section 4.4.3. Alternatively, the ignition could have been caused by a hot grinding spark igniting the cutting fluid evaporate released due to the elevated workpiece temperature. In circumstances such as these, an unplanned, unexpected, and to a large extent uncontrolled fluid ignition, the exact mechanism is almost impossible to determine, and it could be argued, that it is largely academic. The most important observation is to apply the cutting fluids in such a way as to prevent fluid starvation in the contact zone, to ensure the machine is set-up in such a way as to prevent accumulations of hot grinding debris, and possibly most importantly, to stop the hot grinding sparks mixing with either the cutting fluid mist or any cutting fluid evaporate.

7.3.1 Cutting Fluid Application

This last point made in the previous paragraph, that of stopping the hot grinding sparks mixing with either the cutting fluid mist or any cutting fluid evaporate, touches on another important aspect of the cutting fluid application strategy, that of the actual application itself. When one considers of cutting fluid application, one traditionally thinks of nozzle design, nozzle positioning, delivery pressures, pumping power and the rest. Important as these are, the fluid application strategy must also ensure that the cutting fluid is delivered to the grinding zone in sufficient quantities under all conditions.

In terms of surface grinding modes, this may mean the inclusion of nip blocks (see figure 7-6) for example, to ensure sufficient cutting fluid enters the grinding zone to ensure adequate lubrication regardless of workpiece geometry. Whilst the surface grinding mode is strictly beyond the scope of this thesis, whose primary focus is on the cylindrical grinding mode, the use of nip blocks in surface grinding modes is a useful example to illustrate the point that the fluid application strategy needs take a more holistic approach to fluid application rather than simply concentrating on the more traditional aspects of the subject.

The investigations into the cause of the machine fires experienced at Cranfield highlighted the fact that the grinding sparks are a likely source of ignition. The fluid application strategy must therefore consider how to stop hot grinding sparks and both fluid mist and any cutting fluid evaporate coming into contact with one another within the machine canopy.

One possible way of achieving this may be to totally submerge the component in cutting fluid, and in fact this was an idea that the author investigated, all be it for other reasons, several years ago when working as a Machine Tool Design Engineer for a leading grinding machine manufacturer. The idea was dismissed due to practical considerations, as submerging the workpiece has serious implications on the design of the machine tool.

For instance, how would an operator load and unload the machine, not just from an ergonomics perspective of weight and reach, but also due to the fact that few operators would want to stick their hands into an oil fluid bath to load and unload the component. Would you therefore need to drain the machine after each cycle and how would this impact on cycle time? What would be the economic knock on effect? How do you seal the main machine mechanisms?, how do you stop the cutting oil from contaminating any hydrostatic systems on the machine?, how do you set the machine up if the component is obscured from view by virtue of it being submerge in cutting oil ?. In fact the list was almost endless and for these, and many other practical considerations, the idea was dropped.

Another possible solution may have been to pump an inert gas, say nitrogen or argon in to the machine canopy. Whilst this would not have stopped hot grinding sparks mixing with either the fluid mist or any cutting fluid evaporate, it would have prevented any machine fires, as the combustion process would have been starved of that vital ingredient – oxygen. However, this again was dismissed due to practical considerations. How would you load and unload the component? Would you need to re-pressurise the system every time the component was loaded? Would the operator need special breathing equipment? Clearly, preventing all contact between hot grinding sparks and any cutting fluid mist or evaporate would be virtually impossible, but it would be possible to minimise the potential fire risk hazard by reducing the number of grinding sparks and the amount of mist within the machine canopy.

With these limitations in mind, a new method of controlling and cooling the sparks ejected from the grinding zone needed to be found. Conventionally, a secondary cutting fluid nozzle would be used to aim cutting fluid at the grinding swarf exiting the grinding zone, a set-up that can be seen in figure 7.3. In cylindrical grinding modes, this spark arresting nozzle, as it is sometimes called, would be positioned under the grinding zone, and would be referred to as the bottom nozzle. An example of such a nozzle can be seen in figure 7-9



Figure 7-9 Bottom Spark Extinguisher Nozzle Mounted Below the Grinding Zone on the SAT Machine

The mass of ejected grinding sparks clearly visible in figure 7-10 show this was inadequate. Figure 7-10 shows a real test grind conducted using a neat oil cutting fluid

(Castrol Ilogrind 600SP) and the underside of the grinding zone is illuminated by a white hot mass of grinding chips. The problem is that normally, the bottom nozzle is mounted relatively close to the grinding zone, as there is limited space between the wheel head and the work table. Grinding sparks being ejected from the grinding zone at, or very close to grinding wheel speed, are in contact with the stream of cutting fluid being supplied from the bottom nozzle, for insufficient time to allow the grinding chips to adequately cool. Consequently the grinding sparks remain very hot.

Furthermore, by virtue of the fact that the grinding chips are incandescent, they are clearly in the presence of oxygen. There is also a large amount of cutting fluid mist in this region, as can be seen in figure 6.2, hardly surprising when as the grinding wheel is responsible for generating the vast majority of the cutting fluid mist found in the machine canopy, as demonstrated in section 6.2.4.3.



Figure 7-10 Mass of Hot Grinding Sparks being Ejected From the Grinding Zone

The sparks are clearly not being controlled or cooled sufficiently despite the presence of a bottom spark extinguisher nozzle mounted below the grinding zone on the SAT machine.

7.3.1.1 Cutting Fluid Trough

A cutting fluid trough was therefore designed by the author to resolve this problem which can be seen in figure 7-11. The actual detailed design of the coolant trough can be seen in appendix 6, but the cutting fluid trough is essentially a tank filled with cutting fluid fitted below the grinding zone in order to catch and quench the ejected grinding chips. This allows the hot grinding sparks to be control and cooled them before they mix with the cutting fluid mist.

Inside the cutting fluid trough is a series of angled plated or baffles, fitted to help split up the stream of hot grinding chips being ejected from the grinding zone, so as to help hasten their quenching. The baffles were based on the idea of arc chutes used in many high rupturing capacity electrical circuit breakers, such as oil blast electrical circuit breakers.

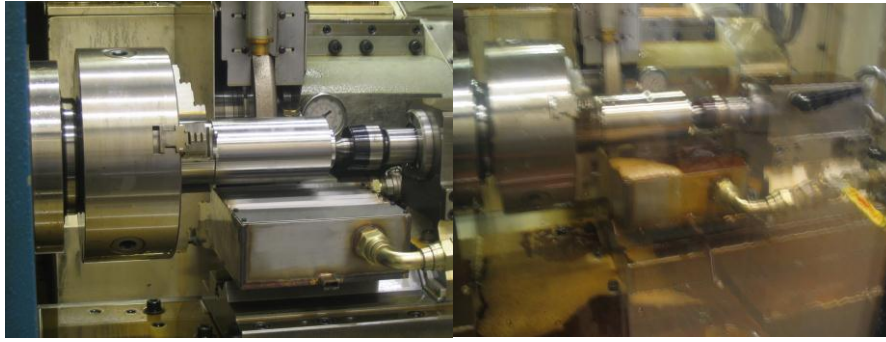


Figure 7-11 Cutting Fluid Trough Fitted below the Grinding Zone on the SAM Machine

The picture on the left shows the cutting fluid trough prior to being filled with cutting fluid. The right hand picture shows the trough filled with cutting fluid.

The cutting fluid trough, being essentially an open topped tank, operates at very low pressure, as opposed to the high pressure required when using a spark extinguisher nozzle. For the purpose of these tests, the cutting fluid was supplied from the high pressure pump fitted to the coolant clarifier system, and the flow was controlled by means of a ball valve installed in the fluid supply line. This ball valve is just visible in the right hand photograph in figure 7-11 (yellow handle), but potentially, the cutting fluid trough could be supplied from the low pressure, “bed wash” system installed on the machine. This is important, as high pressure pumping capacity is expensive to install and costly to run, so if the required capacity can be reduced, this has important economic benefits.

When using the cutting fluid trough, the flow of cutting fluid was adjusted so that the cutting fluid constantly trickled out of the top of the trough to ensure that it was constantly topped up with fluid. A series of tests were then conducted to ascertain the effectiveness of the cutting fluid trough in reducing the number of hot grinding chips. A digital camcorder was mounted outside the grinding machine to video the grinding chips being ejected from the grinding zone. The video footages could then be split up into individual still photographs to so as to allow comparisons to be made.

Figure 7-12 compares the amount of grinding sparks underneath the grinding zone when grinding trials were conducted using similar grinding parameters with the exception of how the cutting fluid was supplied to the underside of the grinding zone. In the left hand photograph, a Ø3mm jet nozzle was used, and on the right, the cutting fluid trough was used. Despite the fact that a lot of cutting fluid “splattered” onto the window when the coolant trough was used thus impairing the visibility into the machine, it can be clearly seen from these photographs, there was a significant reduction in the number of hot grinding sparks, in the area directly below the grinding wheel when the cutting fluid trough was used. The white hot mass of grinding chips seen in the left hand photograph has been eliminated, and what sparks remain, a not as bright indicating they are not as hot. This reduction in both the number and temperature of the grinding chips below the grinding zone obviously reduces the potential fire hazard.

Test Conditions	
Grinding Machine	Edgetek SAT – 3 Axis Cylindrical Grinding Machine
Grinding Mode	Up Grinding
Workpiece	Dimensions : Ø79mm Material : 51CrV4 Hardness : 59Rc
Grinding Parameters	Wheel speed : 150m/s Workpiece Speed : 1000rpm Depth of Cut : 1mm Cross Traverse Speed : 100mm/min Specific Removal Rate : 4000mm ² /s
Grinding Wheel	Electroplated CBN wheel, B213 grit Diameter : 350mm Width : 30mm Wheel Drawing : 300 HP 700-350-30 (see appendix 3)
Fluid Delivery	Pump Pressure: 15 bar Top Nozzle: Ø6.5mm coherent jet nozzle. 70l/min Bottom Nozzle: Ø3mm jet nozzle. 16l/min Fluid Trough : 13l/min
Grinding Fluids	Castrol Ilogrind 600SP Neat Mineral Oil
Number of Repeats	3

Table 7-1 Grinding Parameters used for to assess the performance of the cutting fluid trough



Figure 7-12 Comparison of the hot grinding chips underneath the grinding zone

The left hand photograph shows a white hot mass of grinding chips under the grinding zone when a bottom high pressure nozzle is used. The right hand photograph show a significant reduction in the number of grinding sparks under the grinding zone when the cutting fluid trough. The area under the grinding zone is visibly a lot darker as there are significantly fewer grinding chips, as many are captured and quenched by the cutting fluid trough.

The design on the cutting fluid trough used for these tests was an initial design aimed at testing the idea. It was found that the trough performed best, in terms of reducing the number of hot grinding chips visible below the grinding zone, when the trough was

mounted as close as possible to the grinding wheel. Furthermore, it was clear that the trough only captured the grinding sparks being ejected vertically from the grind zone.

Refining the design of the cutting fluid trough, by “moulding” or shaping it around the profile of the grinding wheel, and then attaching it to the wheel head so as to maintain a constant gap between the grinding wheel and the cutting fluid trough regardless of depth of cut, would reduce the number of grinding sparks further.

7.4 The Cutting Fluid Application Strategy

The results and subsequent discussion presented thus far show that when grinding in the cylindrical HEDG regime, a high viscosity, fully saturated, neat ester based cutting fluid is the cutting fluid that should be used, due to their excellent lubricity, low misting and high resistance to ignition in comparison to conventional neat oil cutting fluids.

Furthermore, these fluids should be applied to the grinding zone using a coherent jet nozzle on the leading edge of the grinding wheel (see figure 6-7), and the hot grinding sparks need to be controlled and quenched using a cutting fluid trough mounted below the grinding zone.

In order to test the validity of this strategy, some validation tests needed to be performed, but first, a series of benchmark tests were needed against which the success of the new strategy could be measured.

7.4.1 Benchmark Tests

An important first stage in evaluating the new cutting fluid application strategy was to establish the performance of the existing fluid application system used on the Edgetek SAT machine. Figure 7-13 shows the original fluid application set-up along with typical nozzle sizes with the bottom spark extinguisher nozzle shown in greater detail in figure 7-9. The grinding parameters used for the benchmark tests are shown in table 7-2

Performing benchmark tests, and taking measurements of mist level in the machine canopy, the grind power to allow the specific grinding energy to be calculated allowing a baseline to be established. This can be then be used to evaluate the performance of any modifications made to the cutting fluid application system and establish whether the changes had a beneficial or detrimental effect on the measurands.

The results from these tests will be presented in the next section, where they will be compared with the results from the validation tests performed after the implementation of the new cutting fluid application strategy.

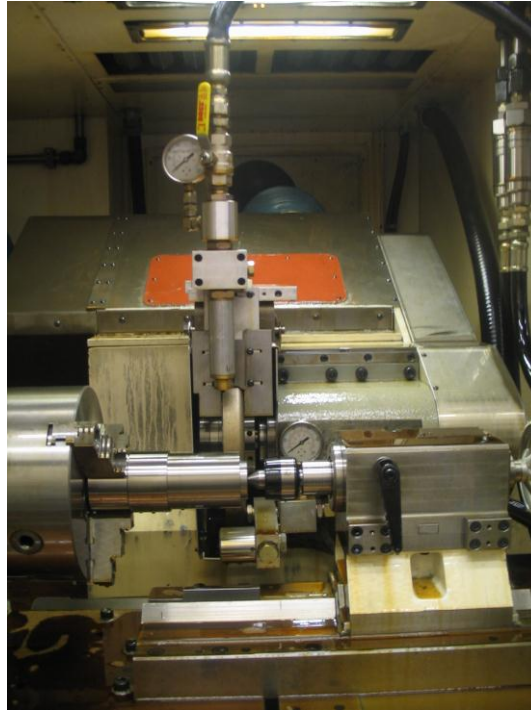


Figure 7-13 Original Cutting Fluid Application Set-up on the Edgetek SAT Machine.

A Ø6.5mm diameter coherent Jet Nozzle is used above the grinding zone, with a 3mm diameter nozzle is used below the work piece to help extinguish the grinding sparks. Also note the use of an air scraper to remove the air barrier around the grinding wheel.

HEDG Test Conditions	
Grinding Machine	Edgetek SAT – 3 Axis Cylindrical Grinding Machine
Grinding Mode	Up Grinding
Workpiece	Dimensions : Ø79mm Material : 51CrV4 Hardness : 59Rc
Grinding Parameters	Wheelspeed : 150m/s Workpiece Speed : 1000rpm Depth of Cut : 1mm Cross Traverse Speed : 100mm/min Specific Removal Rate : 4000mm ² /s
Grinding Wheel	Electroplated CBN wheel, B213 grit Diameter : 350mm Width : 30mm Wheel Drawing : 300 HP 700-350-30 (see appendix 3)
Fluid Delivery	Pump Pressure: 15 bar Top Nozzle: Ø6.5mm coherent jet nozzle. 70l/min Bottom Nozzle: Ø3mm jet nozzle. 16l/min
Grinding Fluids	Castrol Ilogrind 600SP Neat Mineral Oil
Number of Repeats	3

Table 7-2 Grinding Parameters used for the Cutting Fluid Benchmark Tests.

7.4.2 Validation Tests

In order to bring all the different elements of this project together with a view to proving the coherent cutting fluid application strategy, a series of tests were conducted using all the “best” cutting fluid based on the thermal characteristics for the given application and then applying the said cutting fluid in the most appropriate manner.

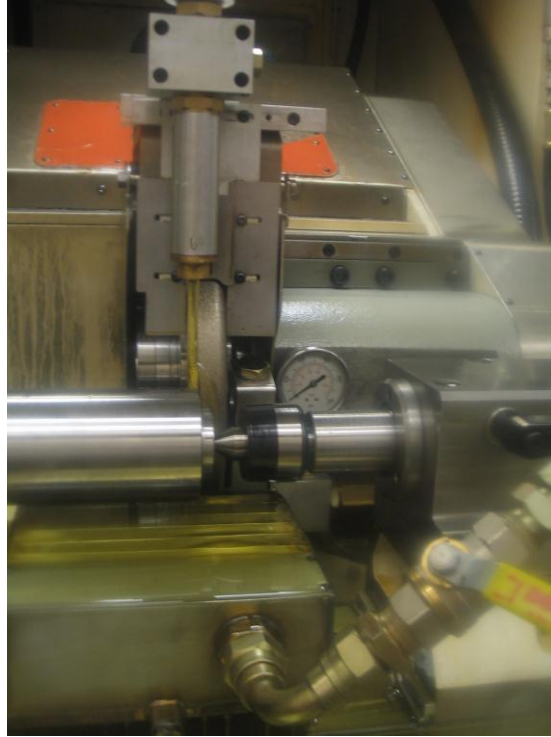


Figure 7-14 Revised Cutting Fluid Application Set-up on the Edgetek SAT Machine.

A Ø4mm diameter coherent Jet Nozzle is used above the grinding zone, with the cutting fluid trough mounted below the grinding zone to capture and control the hot grinding sparks. Also note the use of an air scraper to remove the air barrier around the grinding wheel. Cutting fluid: Fuchs 40SR HEDG.

The first stage of the validation process was to establish the optimum nozzle size for the high viscosity ester based cutting fluid. A series of tests were performed using coherent jet nozzles with different size orifices. The coherent jet nozzle was selected, as in the tested presented in section 6.3.3, this type of nozzle, along with the coherent rectangular nozzle, performed the best in reducing the specific grinding energy of the process when operating in the HEDG regime. However, as the coherent jet nozzles are easier to manufacture than the coherent rectangular nozzles, the coherent jet nozzles were selected.

The results presented in figure 7.15 show that a 4mm coherent jet nozzle produced the lowest levels of specific grinding energy. The decision use the specific grinding energy to optimise the nozzle size was taken as it is a very good indicator not only of the grinding forces, as can be seen in the mathematical relationship shown in equation 2.4, but also because it is a very good indicator of the amount of thermal energy being generated by the process, due to the mathematical relationship presented in equation

2.5. Comparatively low levels in specific grinding energy indicate that there has been a comparative reduction in the tangential grinding forces and comparative reduction in the thermal energy generated by the process, for a given set of process parameters.#

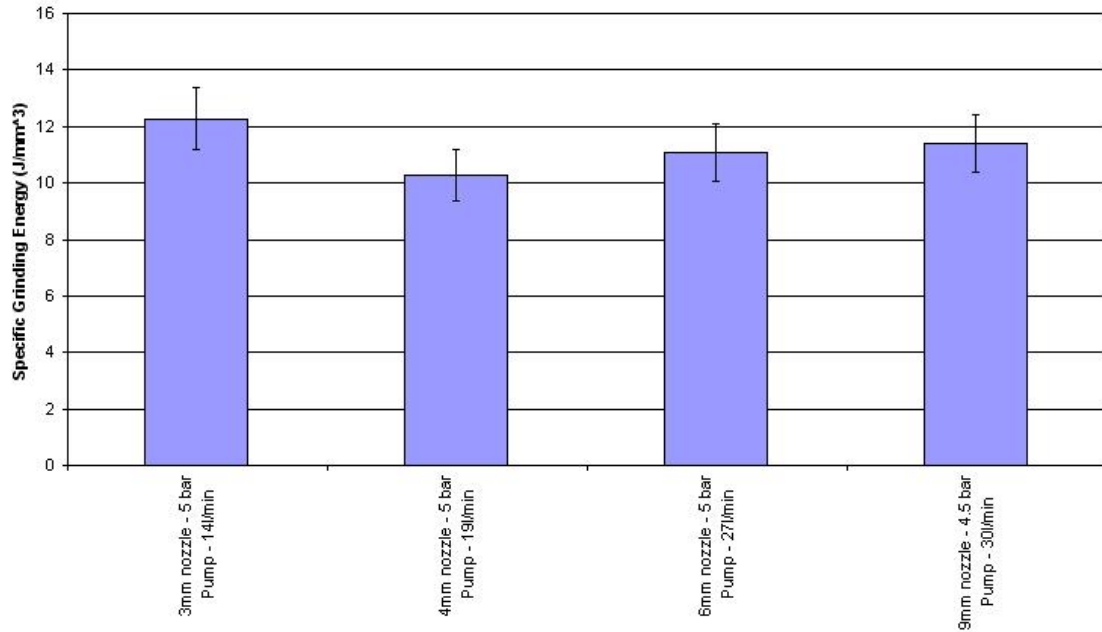


Figure 7-15 The Effect on the Specific Grinding Energy of Nozzle Size when Operating in the HEDG Regime.

Tests performed in the HEDG. 150m/s wheel speed, 1000rpm workpiece, 79mm diameter 51CrV4, 100mm/min cross traverse, 0.5mm DOC. $Q' \approx 2000$. Fuchs Plantocut 40 HEDG

Once the optimal nozzle size had been established a series of tests were conducted using the same grinding parameters used for the benchmark tests, but with the revised cutting fluid application set-up, and the high viscosity ester based cutting fluid. A new high viscosity ester based fluid, Fuchs 40SR HEDG, was used for these tests. This particular fluid was manufactured specifically for these tests, and made using a fully synthetic ester base fluid, rather than the partially saturated base fluid used in Fuchs 40SR. The higher quality base fluid used in the Fuchs 40SR HEDG allowed the elimination of the polymer anti-misting additives, in line with the recommendations made in chapter 4. Keeping all the other grinding parameters constant allowed fair comparisons to be made.

The results shown in figure 7-16 show a significant reduction on the specific grinding energy when the high viscosity ester based cutting fluid was used, dropping from an average of 12.3 J/mm^3 to an average of 9.5 J/mm^3 . This reduction was achieved with a significant reduction in the cutting fluid flow rate and delivery pressure. The high viscosity ester based fluid was delivered at a maximum pressure of 5 bar in comparison to 15 bar typically used prior to the implementation of the new cutting fluid application strategy. This fluid flow rate dropped from 70l/min to 19 l/min: a 72.8% reduction in the fluid flow rate.

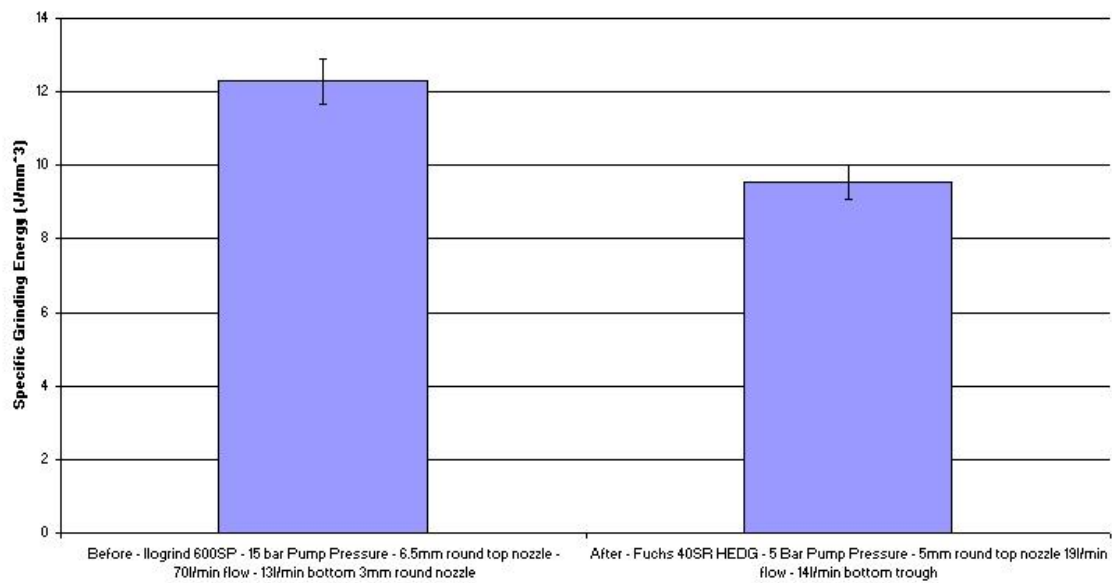


Figure 7-16 Comparison of the Specific Grinding Energy when using the New Cutting Fluid Application Strategy

Tests performed in the HEDG. 150m/s wheel speed, 1000rpm workpiece, 79mm diameter 51CrV4, 100mm/min cross traverse, 1.0mm DOC. $Q'=c.4000$. Fuchs Plantocut 40 HEDG

The results shown in figure 7-17 show a significant reduction in both the total and net grind powers when using the high viscosity ester based cutting fluid was used. The total grind powder dropped from an average of 13.8kW to an average of 9.2kW, a 33.3% reduction in the total grinding power, which again was achieved with a 72.8% reduction in the fluid flow rate.

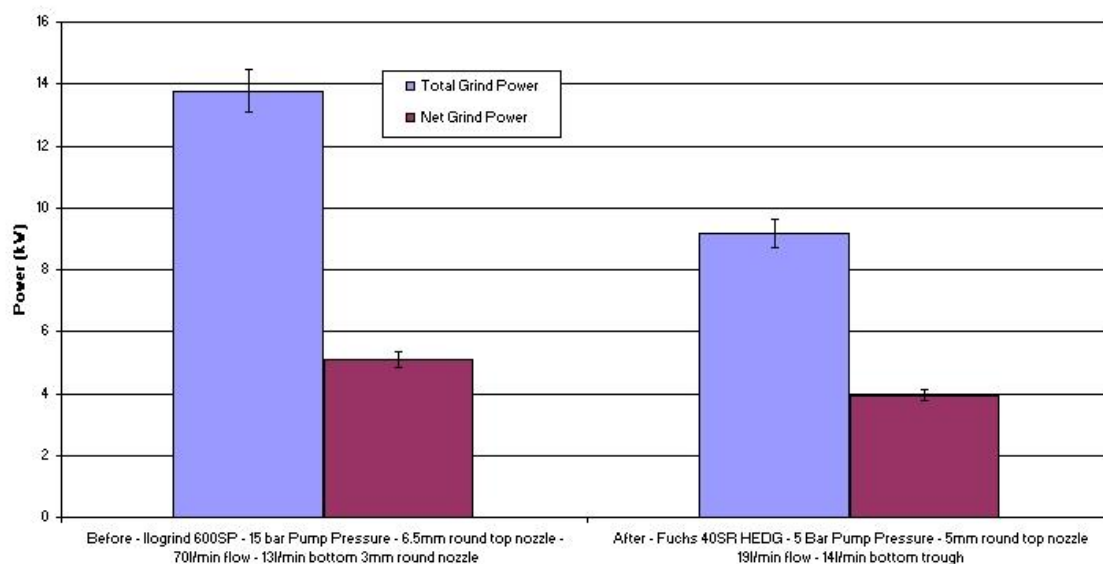


Figure 7-17 Comparison of the Total and Net Grind Powers when using the New Cutting Fluid Application Strategy

Tests performed in the HEDG. 150m/s wheel speed, 1000rpm workpiece, 79mm diameter 51CrV4, 100mm/min cross traverse, 1.0mm DOC. $Q'=c.4000$. Fuchs Plantocut 40 HEDG

The relative mist level in the machine canopy was also measured using the same technique described in section 6.2.2 for both the Castrol Ilogrind 600SP cutting fluid and the high viscosity ester based cutting fluid. The results are presented in figure 7-18, and show a significant reduction in the relative mist levels when the high viscosity ester based cutting fluid was used. The relative mist level after 70 seconds dropped from 30.36mg/m³ to 6.45mg/m³. This equates to a 65.8% reduction in the mist level in the machine canopy.

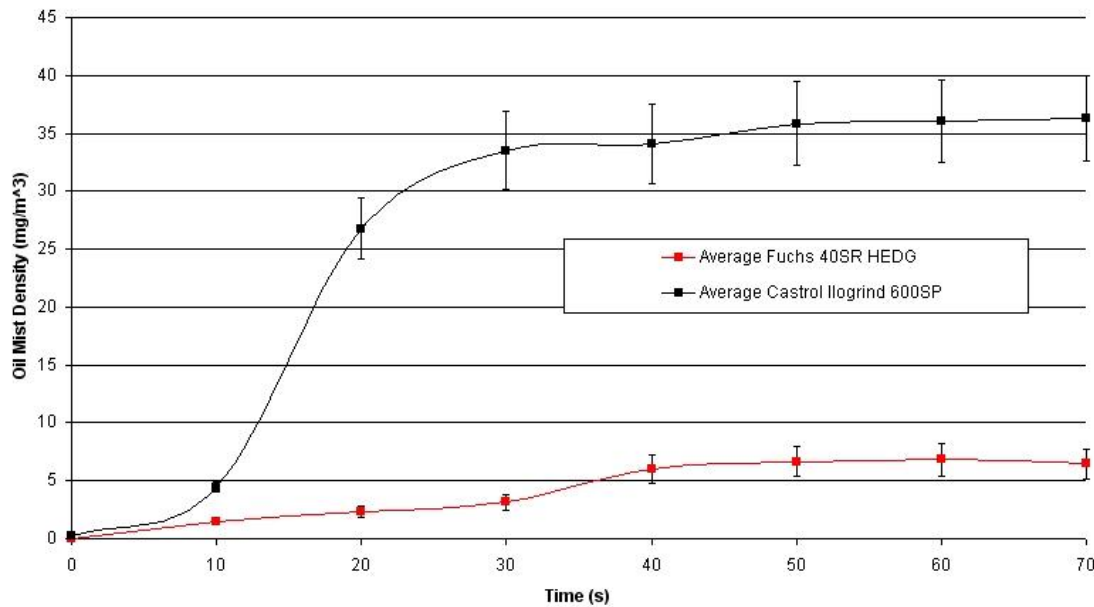


Figure 7-18 Comparison the relative mist levels in the machine canopy.

Comparative machine canopy misting performance for Fuchs 40SR HEDG and Castrol Ilogrind 600SP Results for 30m/s wheel speed, 10rpm work speed, 7.5bar Pump Pressure, 5mm round Nozzle.

This reduction in the mist level within the machine, coupled with a significant reduction in the number of hot grinding chips associated with the use of the cutting fluid trough can only result in a significant reduction in the potential fire hazard in the machine. Furthermore, the high viscosity ester based cutting fluid is much more difficult to ignite (as seen by the results presented in chapter 4) than the standard neat mineral cutting fluid used for the benchmark tests presented earlier in this chapter. Again, this can only further reduce the potential fire hazard within the machine canopy. When this is coupled with a significant reduction in the thermal energy generated by the grinding process, there can be only one result, a significant reduction in the potential fire hazard even though the random nature of the ignition process makes it virtually impossible to statistically quantify this reduction. All this was achieved using 72.8% less cutting fluid and a 33.3% reduction in the total grinding power.

8 Conclusions and Recommendations

8.1 Conclusions

The aim of this thesis was to produce a cutting fluid application strategy for the cylindrical HEDG regime, or the SATURN process as it is sometimes known, based upon the thermal characteristics of the cutting fluid in order to produce a coherent and robust cutting fluid application strategy suitable for industrial applications. The strategy has two key elements, the first being cutting fluid selection, the second being cutting fluid application.

The work conducted during this project has shown that when operating in the cylindrical HEDG regime a high viscosity, fully saturated, neat ester based cutting fluid is the cutting fluid should be used, and that the fluid should be applied to the grinding zone using a coherent jet nozzle on the leading edge of the grinding wheel. Furthermore, to control and quench the hot grinding sparks a cutting fluid trough should be mounted below the grinding zone. The cutting fluid trough should be fitted as close as possible to both the grinding wheel and the workpiece in order to capture as many hot grinding sparks as possible.

This strategy is based upon the main conclusions to be drawn from the work conducted during the project which are:

- Lubrication is of fundamental importance in HEDG.
- Non-flammable water based cutting fluids are totally inadequate for the HEDG regime, due to their poor lubricity.
- Neat oil cutting fluids offer far higher levels of lubrication and this reduces the frictional forces in the grind zone and consequently the contact temperatures in the grinding zone are reduced for any given set of grinding parameters.

Since it is impossible to totally eliminate the potential fire hazard when using neat oil cutting fluids in conjunction with HEDG, a number of different measures, both in terms of the choice of cutting fluid and the manner in which the fluid is applied must be taken to significantly reduce the potential fire hazard.

- A high viscosity ester based cutting fluids not only offer high levels of lubrication, they also exhibit low misting characteristics and offer higher levels of resistance to ignition when compared to other neat oil cutting fluids.
- When a high viscosity ester based fluid was used there was a 65.8% reduction in the fluid mist within the machine canopy in comparison to the standard neat mineral oil used at Cranfield. Consequently, there was significantly less “fuel” in the grinding machine atmosphere for ignition by grinding sparks, and what “fuel” there is, is significantly more difficult to ignite.

- The cutting fluid should be applied using a coherent jet fluid nozzle when operating in the HEDG regime.
- A cutting fluid trough is superior to conventional spark extinguisher nozzle mounted below the grinding zone in controlling and quenching the hot grinding sparks ejected from the grinding zone. The result was visibly fewer grinding sparks and what grinding sparks remained, were visibly cooler.
- With fewer grinding sparks in the machine canopy, a reduction in the contact temperature within the grinding zone coupled with less cutting fluid mist in the machine canopy which is less volatile and less flammable, this only result in a significant reduction in the potential fire hazard.

When this cutting fluid application strategy was applied, the following improvements were seen.

- A significant reduction in the specific grinding energy of a standardised test grind is comparison to the conventional cutting fluid application strategy in use on the Edgetek SAM machine. The specific grinding energy was reduced by 22.4%, a result that was achieved using 72.8% less cutting fluid.
- The total powder used by the process dropped by 33.3%, and since the high viscosity ester based cutting fluid is biodegradable, the result is a cutting fluid delivery strategy that delivers real reductions in the environmental impact of the cylindrical HEDG process.
- Furthermore, the reduction in grinding power (both total and net) and the reduced pumping power as a result of the reduction in cutting fluid flow-rates reduces the carbon footprint of the process.
- Finally, when applying the cutting fluid, it is important to ensure sufficient cutting fluid is applied to the grinding area, not only to provide adequate lubrication to the grinding zone, but to allow sufficient cleaning to prevent any build up of hot grinding sparks.

8.2 Contribution to Knowledge

The major contributions to knowledge presented in this thesis are:

- 1) A cutting fluid strategy has been for the cylindrical HEDG grinding regime based on the thermal characteristics of the grinding fluid.
- 2) It has been shown that high viscosity ester based cutting fluids are the most appropriate for the HEDG regime, due to their low misting, high lubricity and high resistance to ignition.

- 3) It has been shown that coherent jet cutting nozzles are the most appropriate method of applying cutting fluids in the cylindrical HEDG regime.
- 4) A novel method of testing the ignition characteristics of cutting fluids has been developed which is more representative than standard fluid ignition tests.
- 5) A novel method of reducing the hot grinding chips in the machine canopy when grinding in the cylindrical HEDG regime has been demonstrated.
- 6) A novel method of testing the misting performance of grinding fluids has been demonstrated, though the author must acknowledge the contribution of Fuchs Petrolub UK in this area.
- 7) A novel method of measuring the convection coefficient of different cutting fluids has been established, based on recent published work. (Jin and Stephenson, 2006)

8.3 Further Work

All the validation tests presented in section 7.4.2 were performed with a single nozzle directing cutting fluid to the leading edge of the grinding wheel. The author designed a two nozzle set-up which would allow two nozzles to be used to direct cutting fluid to both the leading edge and the face of the grinding wheel independently. The design of this cutting fluid application set-up is shown in appendix 7, and whilst the components were manufactured ready for trials, time constraints prevented them being used.

It was hoped that this new cutting fluid application set-up would apply the cutting fluid to the grinding zone even more effectively than the one nozzle set-up used so successfully in section 7.4.2, allowing even further reductions in the grinding power, specific grinding energy and cutting fluid flows to be achieved.

To test this new cutting fluid application set-up, a statistically based experiment would need to be performed to establish the optimal setting for this new arrangement. Once an optimal set-up was achieved, then comparative tests grinds should be undertaken to test the effectiveness of the new design, this time using the results presented in section 7.4.2 as the benchmark.

Secondly, as stated in section 7.3.1.1 the design on the cutting fluid trough used for these tests was an initial design aimed at testing the idea. Designing a profiled cutting fluid trough, one that was attached to the wheel head so as to maintain a constant gap between the grinding wheel and the cutting fluid trough regardless of depth of cut, should not only reduce the number of grinding sparks further, possibly even eliminating them all together, but would make the system easier to set-up and more flexible for industrial applications, where a number of different depths of cut may well be used on a single workpiece in a single set-up.

REFERENCES

- Andrew C. and Howes T. et al (1985) Creep Feed Grinding. Rinehart and Winston, New York.
- Bartz WJ. (1998) Lubricants and the Environment, Tribology International, Vol.31 No.1-3, p35-47
- Bartz WJ. (2001) Ecological and Environmental Aspects of Cutting Fluids, Lubrication Engineering, Vol.57, No. 3, p13-16
- Batako AD and Rowe WB et al. (2005) Temperature Measurement in High Efficiency Deep Grinding, International Journal of Machine Tools and Manufacture, Vol. 45, p1231-1245
- Battersby N (2004) Base Fluids for Environmentally Acceptable Lubricants- What Does Biodegradable Really Mean?, 14th International Colloquium Tribology, 13th-15th January 2004. Ostfildern, Germany, p735-742
- Belluco W and DeChiffre L (2001) Testing of Vegetable-Based Cutting Fluids by Hole Making Operations, Lubrication Engineering, Vol.57, No.1, p12-16
- Bell. A (2005) Cranfield University, Unpublished work
- Bennett JM and Ballal DR (2003) Ignition of Combustible Fluids by Heated Surfaces, 41st Aerospace Sciences Meeting and Exhibit, 6th-9th January 2003, Reno, Nevada. p1-14
- Blanchard PM and Syrett RJ (1974). Mechanical Testing of Cutting Fluids, Lubrication Engineering, Vol. 30, No 2, p62-71
- Balart MJ and Bouzina A et al (2004) The Onset of Tensile Residual Stresses in Grinding of Hardened Steels, Materials Science and Engineering, Vol. A367, p132-14
- Black SCE and Rowe WB et al. (1995) Temperature Measurements in Grinding, 31st International Machine Tool Design and Research Conference (MATADOR), 20-21st April 1995, Manchester, England, p409-413
- Bock W (2004) Biodegradable lubricants – Market Demands in Germany and Europe, The Environmental Impact of Today's Lubricants : Their Use, Abuse and Disposal. Solihull, Birmingham. 7th December 2004.
- Bowen PJ and Shirvill L.C (1994) Combustion Hazards Posed by the Pressurized Atomization of High-Flashpoint Liquids, Journal of Loss Prevention in the Process Industries, Vol.7, No. 3, p233-241

Bowen PJ and Shrivill LC (1994) Pressurised Atomisation of High Flashpoint Liquids – Implications for Hazardous Area Classification, Proceedings of the Conference on Hazards XII: European Advances in Process Safety, April 19th-21st 1994, Manchester, England, p27-41

Brinksmeier E and Brockhoff T. et al (1997) Minimum Quantity Lubrication in Grinding. 2nd International Machining and Grinding Conference, 8th 11th September 1997, Dearborn, MI, Society of Manufacturing Engineers, Dearborn, Michigan. SME Report No MR97-230 p1-14

Brinksmeier E and Heinzel C. et al (1999). Friction, Cooling and Lubrication in Grinding, Annals of CIRP, Vol. 48, No2, p581-598

Brinksmeier E and Heinzel C. et al (2000) Visualisation of Coolant Flow in Shoe Nozzles and their Effect on the Residual Grinding Stresses, Production Engineering, Vol. 7, No 1, p9-12

Brundle CR and Evans CA Jr et al (1992) Encyclopaedia of Materials Characterization - Surfaces, Interfaces, Thin Films, Elsevier 1992.

Byrne G and Dornfeld D et al. (2003) Advancing Cutting Technology, Annals of CIRP, Vol.52, No2, p483-507

BS 1157 (1975) Recommendations for Tapping drill sizes for use with fluted taps

BS 2000-313 (2001) Methods of Test for Petroleum and its Products, Determination of Air Release of Lubricating and Hydraulic Oils.

Campbell JD (2001). Fluid Comparison for Superabrasive Grinding of Titanium. 33rd International SAMPE Technical Conference, 5th 8th Nov 2001, Seattle, WA, USA: p175-192

Carius AC (1990) Effects of Grinding Fluid Type on CBN Wheel Performance, Abrasive Engineering Society Magazine, Vol.29, No2, p22-27

Castrol (UK) Ltd (1999). Variocut G600SP Safety Data Sheet. Code 7470-UK. 30/03/1999

Castrol (UK) Ltd (2005) Private Correspondence – Chris Poole, 2005. Unpublished.

Challis H and Stanton C (1982) Research on the Problems of Grinding Technology, (1st Ed). Science and Research Engineering Council, Swindon, England.

Chen Z and Liang SY et al.(2002) Predictive Modeling of Cutting Fluid Aerosol Generation in Cylindrical Grinding. NAMRC XXX, West Lafayette, Indiana, 21st-24th May 2002. Society of Automotive Engineers, Report SAE MR02-160, p1-8.

- Chen X. and Rowe W.B et al (2000) Analysis of the Transitional Temperature for Tensile Stress in Grinding, *Journal of Materials Processing Technology*, Vol. 107, p216-221
- Cholakov GS and Rowe GW (1992) Lubricating Properties of Grinding Fluids Part 1. Comparison of Fluids on Four Ball Tribometer Tests, *Wear*, Vol. 55, No.2, p331-342
- Comley P and Stephenson DJ et al (2004) High Efficiency Deep Grinding and the Effect on Surface Integrity, *Key Engineering Materials*, Vol. 257-258, p207-212
- Coughlin RW and Williams D et al (1992) Enumeration of Micro-organisms in Metalworking Fluids using Photometric Methods, *Annals of CIRP*, Vol.41 No.1, p357-360
- Cui C (1995) Experimental Investigation of Thermo-Fluid Effects in the Grinding Zone. PhD Thesis. University of Connecticut.
- Dasch JM and Ang CC et al (2001) The Influence of the Base Oil on Misting in Metal Removal Fluids, *Lubrication Engineering*, Vol.57, No5, p14-19.
- Dasch JM and Ang CC et al (2002) Variables Affecting Mist Generation from Metal Removal Fluids, *Lubrication Engineering*, March 2002, p10-17
- De Chiffre L. (1978) Testing the Overall Performance of Cutting Fluids, *Lubrication Engineering* Vol.34, No.5, p244-251
- De Chiffre L and Belluco W (2000) Comparison of Methods for Cutting Fluid Performance, *Annals of CIR*, Vol.49, No1, p57-60
- Dowdell RL, Jerabek HS. et al (1943) *General Metallography*. J Wiley and Sons, New York.
- Fisher FA. (2000) Some Notes on Sparks and Ignition of Fuels. NASA Report, NASA/TM-2000-210077.
- Fuchs Lubricants (UK) Plc (2004). Plantocut 40SR Safety Data Sheet. Issue Date : 29th April 2004.
- Graham W and Whiston MG (1978) Some Observations of Through-Wheel Coolant Application in Grinding, *International Journal of Machine Tool Design and Research*. Vol.18, p9-18
- Granet I. (1996) *Fluid Mechanics* (4th Ed.), Prentice Hall, New Jersey.

Gulari E and Manke CW et al (1995). Polymer Additives as Mist Suppressants in Metalworking Fluids: Laboratory and Plant Studies, Metalworking Fluids Symposium I. The Industrial Metalworking Environment: Assessment and Control. 13th -16th November 1995, Dearborn, Michigan. American Automobile Manufacturers Association, Washington, p294-300

Gunter KL and Sutherland JW (1999). An Experimental Investigation into the Effect of Process Conditions on the Mass Concentration of Cutting Fluid Mist in Turning, Journal of Cleaner Production, Vol. 7, p341-350.

RS Hahn (1962) On the Nature of the Grinding Process. 3rd International Machine Tool Design and Research (M.T.D.R.) Conference. University of Birmingham UK, 1962 p129-154

Hallet JF (1998) Process Improvement for Crankshaft Grinding Using BNA. 1st International Conference on Barkhausen Noise and Micro-Magnetic Testing. 1st -2nd September 1998, Hannover, Germany, p67-75

Hearn,G (2003) Static Electricity – Guidance for Plant Engineers, Wolfson Electrostatics, University of Southampton, unpublished.

Heindlhofer K (1948). Evaluation of Residual Stress. McGraw-Hill, New York.

Howes T (1990) Assessment of the Cooling and Lubricative Properties of Grinding Fluids, Annals of CIRP, Vol. 39, No 1, p313-316

Howes TD and Gupta H (1990) Avoiding Thermal Damage in Grinding. 28th Abrasive Engineering Society Conference, 16-18th May 1990. Cleveland, OH, USA, p2-8

Howes TD and Tonshoff HK et al (1991). Environmental Aspects of Grinding Fluids, Annals of CIRP, Vol. 40, No.2, p623-630.

Health and Safety Executive (2002). Working Safely with Metalworking Fluids. Good Practice Guide. ISBN 0 7167 2544 3.

Horner D (2003) Modern Grinding Fluids-Can Highly Sophisticated Base Stocks Improve Significantly Grinding Performance. 1st European Conference on Grinding, 6-7th November 2003, Aachen, Germany, p9.1-9.26

Hunz RP (1984) Water-Based Metalworking Lubricants. Lubrication Engineering, Vol. 40, No 9, p549-553.

Hwang J and Chandrasekar S et al (2002). Direct Measurement of Workpiece Temperature Field in Surface Grinding, Abrasives Magazine, April/May 2002, p15-18

Irani RA and Bauer RJ et al (2005). A Review of Cutting Fluid Application in the Grinding Process, International Journal of Machine Tools and Manufacture, Vol.45, p1696-1705

IP34/82 : BS2000: Part 34: (1982) Standard Method of Test for Flash Point by Pensky-Martens Closed Tester.

IP36/84 : BS4689 (1971). Standard Method of Test for Flash and Fire Points by Cleveland Open Cup

Jackson A. (1989) Synthetic versus Mineral Fluids in Lubrication, Transactions of the Australian Institute of Mechanical Engineers, Vol.14, No. 1, p47-56

Jarleton L. (2003) Solid Lubricants: A Novel Answer to the Elimination of Grinding Fluids. MSc Thesis, Cranfield University

Jin T and Rowe WB (2001). Heat Transfer and Partitioning in High Efficiency Deep Grinding (HEDG), Abrasives Magazine, April May 2001, p16-18

Jin T and Rowe WB et al (2001) Temperatures in Deep Grinding of Finite Workpieces, International Journal of Machine Tools and Manufacture, Vol.42, p53-59

Jin T and Stephenson DJ et al (2002) Burn Threshold of High-Carbon Steel in High Efficiency Deep Grinding. Proceedings of the Institute of Mechanical Engineers Part B: Journal of Engineering Manufacture, Vol.216, p357-364

Jin T and Stephenson DJ (2003) Investigation of the Heat Partitioning in High Efficiency Deep Grinding, International Journal of Machine Tools and Manufacture, Vol. 43, p1129-1134

Jin T and Stephenson DJ et al (2003) Estimation of the Convection Heat Transfer Coefficient of Coolant within the Grinding Zone, Proceedings of the Institute of Mechanical Engineers Part B, Journal of Engineering Manufacture, Vol.217, p397-407

Jin T and Stephenson DJ. (2006) Heat Flux Distributions and Convective Heat Transfer in Deep Grinding, International Journal of Machine Tools and Manufacture, Vol.46, No14, p1862-1868

Jones AM (2004). The Influence of Chemical Additives in Metalworking Fluids Used on Metal Cutting Operations. 14th International Colloquium Tribology, Ostfildern, Germany. 13-15th January 2004. p245-253

Johnston WJ and White DW (1995) Machine Enclosure Consideration for Oil Mist Control, The Industrial Metalworking Environment, 13th -16th November 1995, Dearborn, Michigan, p278-283

Kajdas C (1989) Additives for Metalworking Lubricants – A Review, Lubrication Science, Vol.1, No. 4, p 385-409

Kalhan S and Twining S et al (1998) Polymer Additives as Mist Suppressants in Metalworking Fluids Part IIa: Preliminary Laboratory and Plant Studies – Water Soluble Fluids. International Congress and Exposition,. 23-26th February 1998. Detroit, Michigan, Society of Automotive Engineers Report No 980097, p1-5

Kalhan S and Twining S (2000) Shear Stable Mist Suppressants for Aqueous Metalworking Fluids. Development and Field Evaluation, Lubrication Engineering, Vol.56, No. 9, p27-33

Kato T and Fujii H (1997) Temperature Measurement of Workpiece in Surface Grinding by PVD Film Method, Journal of Manufacturing Science and Engineering, Vol.119, p689-694

Kato T and Fujii H (2000) Temperature Measurement of Workpieces in Conventional Grinding, Journal of Manufacturing Science and Engineering, Vol.122, p297-303

Khudobin L.V. (1970) Wheel Clogging and the Lubrication effect of Cutting Fluid during Grinding, Russian Engineering Journal, Vol.50, No6, p66-70

Kim NK and Guo C et al (1997) Heat Flux Distribution and Energy Partitioning in Creep-Feed Grinding, Annals of CIRP, Vol.46, No.1, p227-232

Klocke F and Brinksmeier E et al (1997) High Speed Grinding – Fundamentals and State of the Art In Europe, Japan and the USA, Annals of CIRP, Vol.46 No2, p715-724

Klocke F and Eisenblatter G (1997) Dry Cutting, Annals of CIRP, Vol.46, No.2, p519-526

Klocke F and Baus F et al (2000) Coolant Induced Forces in CBN High Speed Grinding with Shoe Nozzles, Annals of CIRP, Vol. 49 No.1, p241-244

Klocke F and Beck T et al (2000) Minimal Quantity of Lubrication (MQL) – Motivation, Fundamentals, Vistas, 12th International Colloquium Tribology. 11-13th January 2000. Osfildern, Germany, p929-942

Komanduri R and Hou ZB (2001) A Review of the Experimental Techniques for the Measurement of Heat and Temperatures Generated in Some Manufacturing Processes and Tribology, Tribology International, Vol.34, p653-682

Lavine A.S.(1988) A Simple Model for Convective Cooling During the Grinding Process, Journal of Engineering for Industry, Vol.110, p1-6

Liu ZC and Abe S (1994) The Influence of Grinding Oil Viscosity on Grinding Heat and Burn Damage in Creep Feed Grinding, Lubrication Engineering, Vol. 51, No8, p647-651

<http://www.maden.hacettepe.edu.tr/dmmrt/dmmrt660.html>. (2006) Accessed 30th June 2006

Malkin S (1989) Grinding Technology, theory and applications of machining with abrasives, Society of Manufacturing Engineers, Dearborn, USA.

Marinescu I and Rowe WB. et al (2004) Tribology of Abrasive Machining Processes. William Andrew Inc. Norwich, New York, USA

Maragkos A and Bowen PJ (2002) Combustion Hazards due to Impingement of Pressurised Releases of High-Flashpoint Liquid Fuels. 29th International Symposium on Combustion. 21-25th July 2002. Sapporo, Japan, p305-311

McCormack DF and Rowe WB. et al (2001) Controlling the Surface Integrity of Ground Components. 4th International Machining and Grinding Conference, 7-10th May 2001, Troy, Michigan. Society of Manufacturing Engineers Technical Paper MR01-236

National Institute for Occupational Safety and Health (NIOSH) (1998). Report No. 98-102, January 1998.

Okuyama S and Nakamura Y et al (1993) Cooling Action of Grinding Fluid in Shallow Cut Grinding, International Journal of Machine Tools and Manufacture. Vol.33, No.1, p13-23

Ohishi S and Furukawa Y (1985). Analysis of Workpiece Temperature and Grinding Burn in Creep Feed Grinding, Bulletin of Japan Society of Mechanical Engineers, Vol. 28, No242, p1775-1781

http://www.osti.gov/energycitations/product.biblio.jsp?osti_id=6442985. (2007)
Accessed 27th August 2007

Paul S and Chattopadhyay AB (1995) A Study of Effect of Cryo-Cooling in Grinding, International Journal of Machine Tools and Manufacture, Vol.35, No.1, p109-117

Ramesh K and Yeo SH et al. (2001) Coolant Shoe Development for High Efficiency Grinding, Journal of Materials Processing Technology, Vol.114, p240-245

Ratoi M and Spikes HA (1999). Lubricating Properties of Aqueous Sufactant Solutions, Tribology Transactions, Vol.42, No3, p479-486

Rowe WB (2001) Temperature Case Studies in Grinding Including an Inclined Heat Source Model, Proceedings of the Institute of Mechanical Engineers Part B, Journal of Engineering Manufacture, Vol.215, p473-491

Rowe WB (2001) Thermal Analysis of High Efficiency Deep Grinding, International Journal of Machine Tools and Manufacture, Vol.41, p1-19

Rowe WB and Jin T (2001) Temperatures in High Efficiency Deep Grinding (HEDG), Annals of CIRP, Vol. 50, No 1, p205-208

Rowe WB and Morgan MN (1991) An Advance in the Modelling of Thermal Effects in the Grinding Process, Annals of CIRP, Vol.40, No1, p339-342

Salmon SC (2000) Customise your Grinding Fluids, Manufacturing Engineering, Vol. 124, No 2, p42-49

Shaji S and Radhakrishnan V (2002) An Investigation on Surface Grinding using Graphite as a Lubricant, International Journal of Machine Tools and Manufacture, Vol.42, p42-49

Shaji S and Radhakrishnan V (2003) Application of Solid Lubricants in Grinding : Investigations on Graphite Sandwiched Grinding Wheels, Machining Science and Technology, Vol. 7, No.1, p137-155

Shaw MC (1996) Principles of Abrasive Processing. Oxford University Press, Oxford.

Shaw M.C and Vyas A (1994) Heat Effected Zones in Grinding. Annals of CIRP. Vol.43, No1, p279-282

Sheng PS and Oberwalleney S (1997) Life Cycle Planning of Cutting Fluids – A Review, Journal of Manufacturing Science and Engineering. Vol. 119, p791-800

Silliman JD and Perich R Cutting and Grinding Fluids: Selection and Application (2nd Ed). Society of Manufacturing Engineers, Dearborn, Michigan.

Snoeys R and Leuven KU et al (1978) Thermally Induced Damage in Grinding, Annals of CIRP, Vol.27, No.2, p571-581

Sreejith PS and Ngoi BKA (2000) Dry Machining : Machining of the Future, Journal of Materials Processing Technology, Vol.101, p287-291

Stephenson DJ (2004) Trends in Fluid Application Strategy for Machining Processes. The Environmental Impact of Today's Lubricants: Their Use, Abuse and Disposal. 7th December 2004, Solihull, Birmingham, UK.

Stephenson DJ and Jin T (2003). Physical Basics in Grinding. 1st European Conference on Grinding, 6th -7th November 2003, Aachen, Germany.

Stephenson DJ and Jin T et al (2002) High Efficiency Deep Grinding of a Low Alloy Steel with Plated CBN Wheels, Annals of CIRP, Vol.51, No1, p241-244

Stephenson DJ and Laine E. et al (2001). Burn Threshold Studies for Superabrasive Grinding using Electroplated CBN Wheels. 4th International Machining and Grinding Conference, 7th 10th May 2001 Troy, MI, Society of Manufacturing Engineers Technical Paper MR01-219.

Sutherland JW and Kulur VN (2000). An Experimental Investigation of Air Quality in Wet and Dry Turning, Annals of CIRP, Vol.49, No 1, p61-64

Suda S and Yokota H et al (2002) A Synthetic Ester as an Optimal Cutting Fluid for Minimum Quantity Lubrication Machining, *Annals of CIRP*, Vol. 51, No1, p 95-98

Sun F.H and Xu H.J (2002) A New Technology on Enhancing Heat Transfer at Grinding Zone Through Jet Impingement During Creep Feed Grinding, *Machining Science and Technology*, Vol. 6, No.1, p43-52

Suzuki J and Morita K (1992) An Experimental Study on Ignitability of Gasoline by Friction Sparks. International Congress and Exposition, 24-28th February 1992 Detroit, Michigan. Society of Automotive Engineers Technical Paper 920392.

Tawakoli, T. (1993). High efficiency deep grinding (English Ed.), VDI-Verlag and Mechanical Engineering Publications.

Thornburg J and Leith D (2000) Mist Generation during Metal Machining, *Journal of Tribology*, Vol.122, p544-549

Turchin H and Byers JP (2000) Effect of Oil Contamination on Metalworking Fluid Mist, *Lubrication Engineering*, Vol.56, No 7, p21-25

Ueda T and Hosokawa A et al (1986) Measurement of Grinding Temperature using Infrared Radiation Pyrometer with Optical Fibre, *Journal of Engineering for Industry*, Vol.108, p247-251

Ueda T and Tanaka H et al (1993) Measurement of Grinding Temperature of Active Grains Using Infrared Radiation Pyrometer with Optical Fibre, *Annals of CIRP*, Vol.42 No.1, p405-408

Walton IM and Stephenson DJ et al (2006) The Measurement of Grinding Temperatures at High Specific Removal Rates, *International Journal of Machine Tools and Manufacture*, Vol. 46, No.12-13, p1617-1625

Webster J.A. and Cui C (1995) Grinding Fluid Application System Design, *Annals of CIRP*, Vol. 44, No 1, p333-338

Werner G, (1979) Application and Technical Fundamentals of Deep and Creep Feed Grinding, Society of Manufacturing Engineers Technical Paper MR 79-319

Williams JA and Tabor D (1977) The Role of Lubricants in Machining, *Wear*, Vol. 43, No. 3, p275-292

Xu X and Malkin S (2001) Comparison of Methods to Measure Grinding Temperatures, *Journal of Manufacturing Science and Engineering*, Vol. 123, p191-195

Yamanaka Y and Hayama M et al (1998) Development of a New Grinding Fluid for CBN Grinding Wheels: Part 3: Study of the Concentration of Metalworking Additives on Grinding Performance, *Lubrication Engineering*, Vol. 54, No.8, p24-30

Yasui H and Tsukuda S (1983) Influence of Fluid Type on Wet Grinding Temperature, Bulletin of Japan Society of Precision Engineers, Vol.17, No.2, p133-134

Ye N.E and Pearce T.RA (1984) A Comparison of Oil and Water as Grinding Fluids in the Creep Feed Grinding Process, Proceedings of the Institute of Mechanical Engineers, Part B, Vol. 198, No. 14, p229-237

Yue Y and Michalec DJ. et al (1999). An Examination of Cutting Fluid Mist Formation in Turning. NAMRC XXVII, 25-28th May 1999. Berkeley, California. USA. Society of Manufacturing Engineers Technical Paper MR99-180.

Bibliography

Asseal M.J. et al (1996) Thermophysical Properties of Fluids. An Introduction to their Prediction.. Imperial College Press, London.

Beitz W and Küttner K. H (Editors) (1994) Dubbel Handbook of Mechanical Engineering. English Edition. Springer-Verlag, London.

Bird BR. et al (1960) Transport Phenomena.. J Wiley and Sons, New York, USA.

Brooks CR (1996) Principles of the Heat Treatment of Plain Carbon and Low Alloy Steels, ASM International, Ohio, USA.

Challis H and Stanton C (1982) Grinding. Research on the Problems of Grinding Technology, The Science and Engineering Research Council, Swindon UK. 1982.

Goodger EM (1975) Hydrocarbon Fuels. Production, Properties and Performance of Liquids and Gases, Macmillan Press, London.

Granet I (1996) Fluid Mechanics (4th Edition), Prentice Hall, New Jersey, USA

Johnson N.L and Leone F.C (1964) Statistical and Experimental Design in Engineering and the Physical Sciences. Vol.II.. J Wiley and Sons. New York, USA.

Keith F (1973) Principles of Heat Transfer (3rd Edition) Harper and Row, New York, USA.

Montgomery DC (2001) Design and Analysis of Experiments (5th Edition), J Wiley and Sons, New York, USA

Sachanen A.N (1975) The Chemical Constituents of Petroleum, Reinhold Publishing Corporation, New York, USA.

Welty J.R (1974) Engineering Heat Transfer, J Wiley and Sons, New York.

Williams J.A (1994) Engineering Tribology, Oxford University Press, Oxford.

APPENDICES

Appendix 1: Cutting Fluid Data Sheets

- Fuchs Plantocut SR Series Cutting Oils
- Castrol Carecut ES1 Ester Based Cutting Oil
- Castrol Carecut ES2 Ester Based Cutting Oil
- Castrol Ilogrind 600SP Cutting Oil
- Castrol Hysol X Water Soluble Cutting Oil
- Quaker Quakercool 2772 Water Soluble Cutting Oil
- Prolong Ultracut 1 Water Soluble Cutting Oil
- Prolong Anti Friction Metal Treatment

Appendix 2: Load Controls Universal Power Cell – Hall Effect Transducer

Appendix 3: CBN Grinding Wheel Drawings

Appendix 4: Hund TM Data Tyndallometer

Appendix 5: Stanhope Seta Air Release Value Apparatus

Appendix 6: Cutting Fluid Trough - Drawing

Appendix 7: SAT Two Nozzle Fluid Application Design - Drawings

Appendix 8: Shoe Nozzle - Drawings

Appendix 9: Cutting Fluid Ignition Test Rig - Drawings

Appendix 10: Cutting Fluid Mist Ignition Test Rig - Drawings

Appendix 11: G Hearn. Static Electricity – Guidance for Plant Engineers

Appendix 1 – Cutting Fluid Data Sheets

PLAN

Cut

Des

The

for

with

PLA

min

and

App

PLA

mach

PLA

high

PLA

room

break

As

Good

Spe

• PLA

to

to

to

to

to

to

to

to

to

to

to

to

to

to

to

to

to

to

to

to

to

to

to

to

to

to

to

to

to

to

to

Product INFORMATION

FUCHS (UK) PLC.
New Century Street
Hanley
GB-Stoke-on-Trent,
Staffordshire, ST1 5HU



PLANTOCUT SR-SERIES

Cutting Oil Based On Natural Raw Materials

Description

The PLANTOCUT SR-SERIES of oils are based on modified vegetable-based raw materials and are suitable for a broad range of applications. PLANTOCUT SR oils contain carefully selected and matched chlorine-free EP additives and are remarkably copper-inactive.

Application

PLANTOCUT SR oils are recommended for all tool-machining operations because of their EP additives.

PLANTOCUT 10 SR is especially suitable for deep hole drilling where as PLANTOCUT 22 SR, PLANTOCUT 32 SR and PLANTOCUT 40 SR are recommended for turning, milling, thread cutting and broaching operations.

As regards application, please observe VDI Guidelines 3035 and 3397, Sections 1-3.

Specifications

- PLANTOCUT SR is >90% biodegradable according to CEC-L-33-T-82.

Advantages / Benefits

- PLANTOCUT SR is extremely low evaporating.
- PLANTOCUT SR has long-lasting low-misting characteristics achieved by the use of shear-stable anti-misting additives.
- Has a lower health impact on users than traditional products used in similar applications.
- PLANTOCUT SR is oxidation stable.



March 2004 GDUK Page 1 of 2

The above information is supplied to the best of our knowledge and belief on the basis of the current state-of-the-art and our own development work. Subject to amendment.

FUCHS LUBRICANTS (UK) PLC.
New Century Street, Hanley
GB-Stoke-on-Trent, Staffordshire, ST1 5HU

Tel: +44-8701 -20 04 00
Fax: +44-1782 -20 20 73
contact-uk@fuchs-oil.com
<http://www.fuchslubricants.com>

Product INFORMATION

FUCHS (UK) PLC.
New Century Street
Hanley
GB-Stoke-on-Trent,
Staffordshire, ST1 5HU



Typical Data: PLANTOCUT SR-SERIES

PLANTOCUT		10 SR	22 SR	32 SR	40 SR	
Characteristics	Unit					Test Method
Density at 15°C	g/ml	0.863	0.926	0.910	0.923	DIN 51 757
Colour	ASTM	1	0.5	0.5	0.5	DIN ISO 2049
Viscosity						DIN 51 562
at 20°C	mm ² /s	18	49	-	91	
at 40°C	mm ² /s	10	23	32	40	
Flashpoint COC	°C	206	212	220	216	DIN ISO 2592
Neutralization number	mgKOH/g	0.3	0.6	0.5	0.9	DIN 51 558
Saponification number	mgKOH/g	158	236	173	190	DIN 51 559
Corrosive effect on copper	degree of corr.	1-100A3	1-100A3	1-100A3	1-100A3	DIN EN ISO 2160
Pour point	°C	-3	-42	-	-39	DIN ISO 3016
Four ball apparatus	N	2400	3000	3000	3000	DIN 51 350
Reichert wear test (RVT)	mm ²	6.4	3.4	3.8	3.2	FLV-R 3 *)
Evaporation loss	%	18.5	12.0	-	7.0	DIN 51 581
Oil mist index						FLV-N 5 *)
Diocetylphthalate DOP =	100	14.0	4.0	-	2.0	

*) FLV - Internal Laboratory Directive

March 2004 GDUK Page 2 of 2

The above information is supplied to the best of our knowledge and belief on the basis of the current state-of-the-art and our own development work. Subject to amendment.

FUCHS LUBRICANTS (UK) PLC.
New Century Street, Hanley
GB-Stoke-on-Trent, Staffordshire, ST1 5HU

Tel: +44-8701 -20 04 00
Fax: +44-1782 -20 20 73
contact-uk@fuchs-oil.com
<http://www.fuchslubricants.com>

SAFETY DATA SHEET



1. IDENTIFICATION OF THE SUBSTANCE/PREPARATION AND COMPANY

NAME OF MANUFACTURER/SUPPLIER:

FUCHS LUBRICANTS (UK) PLC

Sheet 1 of 4

Revision Number

2

Last revision

12 March 2004

Issue date

12/03/2004

ADDRESS:

New Century Street, Hanley, Stoke-on-Trent ST1 5HU

Business Telephone: 08701 200400 Fax: 01782
2072

PRODUCT NAME:

Product Code: 7762

PLANTOCUT 22 SR

APPLICATION:

Industrial cutting oil based on natural raw materials.

3. COMPOSITIONAL INFORMATION:

Blend of biodegradable ester compounds with multifunctional additives.

Hazardous ingredient

Risk codes

% range

Organic polysulphide

R53

<5%

HAZARDS IDENTIFICATION:

The product is not dangerous when handled with care and according to its determined use. Skin irritation is possible, however, due to prolonged direct exposure.

Special hazards of
product after use:

Products which have become contaminated might present more serious health effects.

PRODUCT NAME:
PLANTOCUT 22 SR

Sheet 2 of 4
Revision Number 2
Last revision 12 March 2004
Issue date 12/03/2004

4. FIRST AID MEASURES:

Eyes: Wash immediately with copious quantities of water. If irritation persists, seek medical attention.

Skin: Wash thoroughly with soap and water. Obtain treatment by a Doctor if symptoms persist.

Inhalation: Remove to fresh air. If effects persist, seek treatment by a Doctor.

Ingestion: DO NOT INDUCE VOMITING. Wash mouth out with water. Obtain immediate treatment by a Doctor and provide a copy of this sheet.

Pressure injection: ALWAYS OBTAIN IMMEDIATE MEDICAL ATTENTION EVEN THOUGH THE INJURY MAY APPEAR MINOR.

5. FIRE FIGHTING MEASURES

Flammability: Combustible

Flash point (°C, PMCC): 215

Extinguishing media: Use foam, dry powder, CO2. Never use water.

Products of combustion: Carbon dioxide, carbon monoxide, together with dense smoke.

6. ACCIDENTAL RELEASE MEASURES.

Personal precautions: Plastic or rubber gloves

Environmental precautions: Prevent spills from entering waterways. Collect absorbent material for disposal.

Decontamination: Contain spilled product with sand or earth. Bulk material can be land dumped at appropriate site in accordance with local regulations. Clean spillage area to avoid slip hazard.

7. HANDLING AND STORAGE.

Keep containers tightly closed. Store under cover. Keep away from food and drink. Compatible with most common metals; may soften certain rubbers - use resistant seals. Avoid sources of ignition. A bunded area may be required.

Storage temperature: Ambient

8. EXPOSURE CONTROLS/PERSONAL PROTECTION.

Occupational exposure limits	Substance	LTEL	STEL	Source/other information
	None assigned			
Engineering control measures	Material of low volatility			
Personal protection	Select PPE appropriate for the product properties/operations taking place. No eating, drinking or smoking in the work area. Wash before breaks and at end of shift/day. Do not keep contaminated cloths in pockets. Launder coveralls at regular intervals.			

PRODUCT NAME:**PLANTOCUT 22 SR**

Sheet 3 of 4

Revision Number 2

Last revision 12 March 2004

Issue date 12/03/2004

9. PHYSICAL AND CHEMICAL PROPERTIES

Appearance:	Yellow fluid	Odour:	Mild
Specific gravity @ 15.6°C:	0.895	pH:	
Vapour pressure (mm Hg)@ 20°C:		Vapour density (air=1)	
Boiling point (°C):		Pour point/Melting point (°)	
Flash point (°C, PMCC):	215	Autoignition temperature, °	
Flammability limit in air, % by volume:	LEL:	UEL:	
Volatile organic compounds, %:			
Kinematic viscosity(cSt) @ 40°C:	22		
Solubility:	Insoluble in water		

PLEASE NOTE: THESE PROPERTIES ARE FOR GUIDANCE ONLY. THEY DO NOT CONSTITUTE A SPECIFICATION

10. STABILITY AND REACTIVITY

Stability:	The product is stable and not subject to polymerisation
Conditions to avoid:	Avoid exposure to extreme heat.
Materials to avoid:	Incompatible with strong oxidising agents
Hazardous decomposition products:	Oxides of carbon and water vapour with unidentified organic compounds dense, white, irritating smoke.

11. TOXICOLOGICAL INFORMATION

The following toxicological assessment is based on a knowledge of the toxicity of the product's components

Estimated oral LD50 Rat, >2000mg/Kg.

HEALTH EFFECTS

In eyes:	May cause temporary irritation and discomfort
In skin:	Generally non-irritant on incidental contact. Excessive or prolonged contact may give rise to slight irritation.
Inhalation:	Harmful concentrations of vapour do not normally arise except under high temperature or high atomisation. High concentrations of mist may give rise to respiratory irritation.
Ingestion:	Low order of acute oral toxicity. Ingestion of this product is not regarded as a significant health hazard likely to arise in normal use.
Chronic:	None anticipated
Other:	None determined

12. ECOLOGICAL INFORMATION

Biodegradability:	Inherently biodegradable	Chemical oxygen demand (mgO2/l):	Not determined.
-------------------	--------------------------	----------------------------------	-----------------

The lubricant is 96% biodegradable after the standard 21 day test period of the CEC L-33-T82 test.

13. DISPOSAL CONSIDERATIONS

Used, degraded or contaminated product may be classified as special waste. Anyone classifying hazardous waste and determining its fate must be qualified in accordance with state and international regulations.

PRODUCT NAME**LANTOCUT 22 SR**

Sheet 4 of 4

Revision Number

2

Last revision 12 March 2004

Issue date 12/03/2004

4. TRANSPORT INFORMATION

Classification for transport: Not classified for transport

Shipping name: n.a.

UN number: n.a.

Packing Group: n.a.

Hazard Class: n.a.

Marine pollutant: No

RID: n.a.

EmS number:

ADR/ATA: n.a.

MFAG number:

5. REGULATORY INFORMATION

Hazard label data Not classified as hazardous for supply.

Phrases None assigned

None assigned

Directives Framework waste directive, 91/156/EEC

Regulatory information HASWA. Control Of Substances Hazardous to Health Regulations. Chemicals (Hazard Information and Packaging) Regs., as amended (CHIP3). Environmental Protection Act. Waste Management Duty of Care Regs. Special Waste Regs.

European Waste Catalogue No: 13 01 07

6. OTHER INFORMATION

The data and advice given apply when the product is sold for the stated application(s). The product is not sold as suitable for any other application. Use of the product for applications other than as stated in this sheet may give rise to risks not mentioned in this sheet. You should not use the product other than for the stated application or applications without seeking advice from us.

If you have purchased the product for supply to a third party for use at work, it is your duty to take all necessary steps to secure that any person handling or using the product is provided with the information in this sheet.

If you are an employer, it is your duty to tell your employees and others who may be affected of any hazards described in this sheet and any precautions which should be taken.

Approved Codes of Practice**Reference notes**

Guidance Note EH 40. "Occupational Exposure Limits" Guidance Note EH 58. "The Carcinogenicity of Mineral Oils" IND (G) 165-169: Metalworking fluids. SHW 397 Effects of Mineral Oil on the Skin. MS/B/5 "Skin cancer caused by oil" MS 24: Health surveillance

SAFETY DATA SHEET



1. IDENTIFICATION OF THE SUBSTANCE/PREPARATION AND COMPANY

NAME OF MANUFACTURER/SUPPLIER:

FUCHS LUBRICANTS (UK) PLC

Sheet 1 of 4

Revision Number

1

Last revision

28 April 2004

Issue date

29/04/2004

ADDRESS:

New Century Street, Hanley, Stoke-on-Trent ST1 5HU

Business Telephone: 08701 200400 Fax: 01782
02072

PRODUCT NAME:

Product Code: A017

PLANTOCUT 40 SR

APPLICATION:

Industrial neat cutting oil.

2. COMPOSITIONAL INFORMATION:

blend of biodegradable components with multifunctional additives.

hazardous ingredient	Risk codes	CAS Number	EEC Number	% range
thiol sulphides, di-tert-dodecyl	R53	068425-15-0		<5%

3. HAZARDS IDENTIFICATION:

The product is not dangerous when handled with care and according to its determined use. Skin irritation is possible, however, due to prolonged direct exposure.

Special hazards of
product after use:

Products which have become contaminated might present more serious health effects.

PRODUCT NAME:**LANTOCUT 40 SR**

Sheet 2 of 4

Revision Number

1

Last revision

28 April 2004

Issue date

29/04/2004

FIRST AID MEASURES:

- es:** Wash immediately with copious amounts of water/eyewash, holding the eyelids open. Obtain treatment by a Doctor if symptoms persist.
- in:** Wash thoroughly with soap and water. Obtain treatment by a Doctor if symptoms persist.
- halation:** Remove to fresh air. If effects persist, seek treatment by a Doctor.
- gestion:** DO NOT INDUCE VOMITING. Wash mouth out with water. Obtain immediate treatment by a Doctor and provide a copy of this sheet.
- essure injection:** ALWAYS OBTAIN IMMEDIATE MEDICAL ATTENTION EVEN THOUGH THE INJURY MAY APPEAR MINOR.

FIRE FIGHTING MEASURES

- mmability:** Combustible
- ash point (°C,PMCC):** 216
- tinguishing media:** Use foam, dry powder, CO2. Never use water .
- oducts of combustion:** Carbon dioxide, carbon monoxide, together with dense smoke.

ACCIDENTAL RELEASE MEASURES.

- sonal precautions:** Plastic or rubber gloves
- vironmental precautions:** Prevent spills from entering waterways. Collect absorbent material for disposal.
- contamination:** Contain spilled product with sand or earth. Bulk material can be land dumped at appropriate site in accordance with local regulations. Clean spillage area to avoid slip hazard.

HANDLING AND STORAGE.

ep containers tightly closed. Store under cover. Keep away from food and drink. Compatible with most common metals; may soften
tain rubbers - use resistant seals. Avoid sources of ignition. A bunded area may be required.

- rage temperature:** Ambient

EXPOSURE CONTROLS/PERSONAL PROTECTION.

- | Occupational exposure | Substance | LTEL | STEL | Source/other information |
|-----------------------|---------------|------|------|--------------------------|
| its | None assigned | | | |

- ineering control** Material of low volatility
- asures**

- onal protection** Select PPE appropriate for the product properties/operations taking place. No eating, drinking or smoking in the work area. Wash before breaks and at end of shift/day. Do not keep contaminated cloths in pockets. Launder coveralls at regular intervals.

PRODUCT NAME:**PLANTOCUT 40 SR**

Sheet 3 of 4

Revision Number

1

Last revision

28 April 2004

Issue date

29/04/2004

9. PHYSICAL AND CHEMICAL PROPERTIES

Appearance:	Clear fluid	Odour:	Mild
Specific gravity @ 15.6°C:	0.920	pH:	
Vapour pressure (mm Hg)@ 20°C:		Vapour density (air=1)	
Boiling point (°C):		Pour point/Melting point (°)	-39
Flash point (°C, PMCC):	216	Autoignition temperature, °	>250
Flammability limit in air, % by volume:	LEL:	UEL:	
Volatile organic compounds, %:			
Kinematic viscosity(cSt) @ 40°C:	37		
Solubility:	Insoluble in water		

PLEASE NOTE: THESE PROPERTIES ARE FOR GUIDANCE ONLY. THEY DO NOT CONSTITUTE A SPECIFICATION

10. STABILITY AND REACTIVITY

Stability:	The product is stable and not subject to polymerisation
Conditions to avoid:	Avoid exposure to extreme heat.
Materials to avoid:	Incompatible with strong oxidising agents
Hazardous decomposition products:	Oxides of carbon and water vapour with unidentified organic compounds dense, white, irritating smoke.

11. TOXICOLOGICAL INFORMATION

The following toxicological assessment is based on a knowledge of the toxicity of the product's components

Estimated oral LD50 Rat, >2000mg/Kg.

HEALTH EFFECTS

Eyes:	May cause temporary irritation and discomfort
Skin:	Generally non-irritant on incidental contact. Excessive or prolonged contact may give rise to slight irritation.
Inhalation:	Harmful concentrations of vapour do not normally arise except under high temperature or high atomisation. High concentrations of mist may give rise to respiratory irritation.
Ingestion:	Low order of acute oral toxicity. Ingestion of this product is not regarded as a significant health hazard likely to arise in normal use.
Toxic:	None anticipated
Other:	None determined

12. ECOLOGICAL INFORMATION

Biodegradability:	Inherently biodegradable	Chemical oxygen demand (mgO2/l):	Not determined.
The lubricant is 96% biodegradable after the standard 21 day test period of the CEC L-33-T82 test.			

13. DISPOSAL CONSIDERATIONS

Used, degraded or contaminated product may be classified as special waste. Anyone classifying hazardous waste and determining its disposal must be qualified in accordance with state and international regulations.

PRODUCT NAME	Sheet 4 of 4
	Revision Number 1
	Last revision 28 April 2004
	Issue date 29/04/2004
4. TRANSPORT INFORMATION	

Classification for transport:	Not classified for transport		
Shipping name:	n.a.		
UN number:	n.a.	Packing Group:	n.a.
UN Class:	n.a.	Marine pollutant:	No
ADR/RID:	n.a.	EmS number:	
AO/ATA:	n.a.	MFAG number:	

5. REGULATORY INFORMATION

Hazard label data	Not classified as hazardous for supply.
Signal Phrases	None assigned
	None assigned
Directives	Framework waste directive, 91/156/EEC
Regulatory information	HASWA. Control Of Substances Hazardous to Health Regulations. Chemicals (Hazard Information and Packaging) Regs., as amended (CHIP3). Environmental Protection Act. Waste Management Duty of Care Regs. Special Waste Regs.
European Waste Catalogue No:	13 01 07

6. OTHER INFORMATION

<p>The data and advice given apply when the product is sold for the stated application(s). The product is not sold as suitable for any other application. Use of the product for applications other than as stated in this sheet may give rise to risks not mentioned in this sheet. You should not use the product other than for the stated application or applications without seeking advice from us.</p> <p>If you have purchased the product for supply to a third party for use at work, it is your duty to take all necessary steps to secure that any person handling or using the product is provided with the information in this sheet.</p> <p>If you are an employer, it is your duty to tell your employees and others who may be affected of any hazards described in this sheet and any precautions which should be taken.</p>	
Approved Codes of Practice	
Guidance notes	<p>Guidance Note EH 40. "Occupational Exposure Limits" Guidance Note EH 58. "The Carcinogenicity of Mineral Oils" IND (G) 165-169: Metalworking fluids. SHW 397 Effects of Mineral Oil on the Skin. MS/B/5 "Skin cancer caused by oil" MS 24: Health surveillance</p>

Product Data

Carecut ES1

Biodegradable Ester Based Cutting Fluid

DESCRIPTION

Castrol Carecut ES1 is a biodegradable cutting fluid and has been formulated using specially selected advanced biodegradable esters.

APPLICATION

Castrol Carecut ES1 is primarily designed for heavy duty machining applications where the highest quality surface finish is required. This product has also been successfully used to improve productivity by increasing machine feeds. On selected applications, productivity increases have been improved by over 70% compared with traditional products without any loss of tool-life.

FEATURES

- ◆ Chlorine free biodegradable
- ◆ Low misting
- ◆ Low smoking
- ◆ High Flash Point
- ◆ Pale Colour
- ◆ Low odour
- ◆ Improved surface finish
- ◆ Improved tool life

BENEFITS

- ◆ Environmentally friendly
- ◆ H & S friendly
- ◆ H & S / User friendly
- ◆ User friendly
- ◆ Improved engineering and productivity
- ◆ Improved engineering and productivity

Carecut ES1
27/04/2004

All reasonable care has been taken to ensure that the information contained in this publication is accurate at the date of printing. It should be noted however that the information may be effected by changes subsequent to the date of printing in the blend formulation or methods of application of any of the products referred to or in the requirements of any specification approval relating to any such Products

Castrol International
Pipers Way
Swindon
SN3 1RE
United Kingdom
Tel +44 (0)1793 452111
Fax +44 (0)1703 486083

Product Data

TYPICAL PHYSICAL CHARACTERISTICS

Colour	-	Pale (almost colourless)
Odour	-	Mild
Density @ 20°C kg/m ³	-	0.930
Viscosity @ 40°C cSt	-	28
Viscosity Index	-	160
Air release value @ 50°C	-	less than 30 secs
Flash Point	-	280°C

Castrol International
Pipers Way
Swindon
SN3 1RE
United Kingdom
Tel +44 (0)1793 452111
Fax +44 (0)1703 486083

Carecut ES1
27/04/2004

All reasonable care has been taken to ensure that the information contained in this publication is accurate at the date of printing. It should be noted however that the information may be effected by changes subsequent to the date of printing in the blend formulation or methods of application of any of the products referred to or in the requirements of any specification approval relating to any such Products

Product Data

Carecut ES2

Biodegradable Ester Based Machining & Grinding Fluid

DESCRIPTION

Castrol CareCut ES2 has been formulated using advanced biodegradable ester based technology and is intended for use in grinding machines and for deep hole drilling.

APPLICATION

Castrol CareCut ES2 can be used with all types of grinding media, but is especially effective with CBN grinding. It is suitable for severe grinding, form grinding and gear grinding on machines such as: Niles, Kapp Reishauer. It is suitable for all ferrous and non-ferrous metal machining but is particular suitable for boring operations in general deep hole drilling, boring and trepanning where pressurised coolant systems are used to clear swarf quickly.

FEATURES

- ◆ Very high lubricity
- ◆ Biodegradable
- ◆ Chlorine free
- ◆ Pale colour and low odour
- ◆ Low misting
- ◆ High flash point

BENEFITS

- ◆ Improved tool life, surface finish and productivity (increased G ratio)
- ◆ Environmentally friendly
- ◆ Environmentally friendly
- ◆ Pleasant to use
- ◆ Improved health and safety

Castrol International
Pipers Way
Swindon
SN3 1RE
United Kingdom
Tel +44 (0)1793 452111
Fax +44 (0)1703 486083

Carecut ES2
17/04/2004

Reasonable care has been taken to ensure that the information contained in this publication is accurate at the date of printing. It should be noted however that the information may be effected by changes subsequent to the date of printing in the blend formulation methods of application of any of the products referred to or in the requirements of any specification approval relating to any such products.

Product Data

TYPICAL PHYSICAL CHARACTERISTICS

Colour	-	Light Straw
Odour	-	Mild
Density at 20°C kg/m ³	-	0.865
Viscosity at 40°C, cSt	-	8.8
Flash point °C	-	200

Castrol International
Pipers Way
Swindon
SN3 1RE
United Kingdom
Tel +44 (0)1793 452111
Fax +44 (0)1703 486083

Carecut ES2
27/04/2004

Reasonable care has been taken to ensure that the information contained in this publication is accurate at the date of printing. It should be noted however that the information may be effected by changes subsequent to the date of printing in the blend formulation or methods of application of any of the products referred to or in the requirements of any specification approval relating to any such products

Product Data

Castrol Ilogrind[®] 600

High Performance Cutting & Grinding Oil

Description

Castrol Ilogrind 600 is a chlorine-free high performance cutting and grinding oil based on specially selected, thermally stable base oils. This allows Castrol Ilogrind 600 to provide a consistent level of grinding performance as well as guaranteeing excellent wetting, lubrication and cooling. Castrol Ilogrind 600 performs well for high-speed-surface, creep-feed, and form grinding. Castrol Ilogrind 600 provides excellent grind ratios in CBN applications.

Application

- Belt grinding
- Centerless grinding
- Creep feed grinding
- Flute grinding
- Form grinding
- Gear making

Advantages

- Chlorine free
- Good wetting and load carrying capabilities.
- Lowest possible mist generation; good air release.
- Low foaming propensity.
- Improved lubrication at point of grind; retains form longer, longer wheel life, greater stock removal with the same power, less heat in the cut zone.
- Machine friendly; does not affect painted surfaces on machine tools.
- Excellent operator acceptance; skin compatibility, mild odor.
- Low drag-out propensity; lower product usage.
- Maintains surface finish; even in high stock removal metal cutting operations.
- Maintains the accuracy of grinding wheels; fewer dresses, less wheel wear, lower scrap rates.
- Kapp Grinder approval (Variocut G600 German product, Castrol Ilogrind 600 International brand name).

Characteristics

	Unit	Test Method	Value
Appearance		Visual	Clear, Yellow Color
Specific Gravity	@ 60 °F (16 °C)		0.862
Viscosity	SUS @ 100 °F (38 °C)	CN-TM-101	66
Viscosity	cSt @ 40 °C (104 °F)	CN-TM-101	12
Flash Point	COC °F/°C	CN-TM-039	176.67 °C (350 °F)
Bulk density	lbs/gal		7.2
Copper Corrosion		ASTM 130	4c
Chlorine		CN-TM-012	No
Fat		MW-TM-321	Yes
Sulfur		CN-TM-096	Yes
Active Sulfur		CN-TM-151	Yes

User advice

Consult your Castrol Sales Engineer for questions regarding compatibility.

Machine Tool Approvals

Castrol Ilogrind 600 is approved by the following manufacturers:

Blohn

Huffman CNC Grinders

Kapp Grinders

Castrol Ilogrind 600

03.09.2005, Version Number 2.0

Ilogrind 600 and the Castrol logo are trademarks of Castrol limited.

All reasonable care has been taken to ensure that the information contained in this publication is accurate as of the date of printing. However, such information may, nevertheless, be affected by changes in the blend formulation occurring subsequent to the date of printing. Material Safety Data Sheets are available for all Castrol Ltd products. The MSDS must be consulted for appropriate information regarding storage, safe handling and disposal of a product.

Castrol Industrial North America Inc.

150 W. Warrenville Road

Naperville, IL 60563

Tel (877) 641 1600

Fax (877) 648 9801

www.castrol.com/Industrial

Product Data

Hysol X

Premium Quality Chlorine Free Soluble Cutting Fluid

DESCRIPTION

Castrol Hysol X has been formulated using chlorine-free high performance additives to ensure exceptional cutting characteristics where the cutting process is particularly arduous eg. broaching and where the metal is difficult to machine eg. Stainless Steel, nimonics etc.

APPLICATION

Castrol Hysol X contains specially developed extreme pressure and lubricity additives that are equal to the demands of creep feed grinding and may other arduous operations. It has such exceptional cutting properties that in some instances it is possible to replace some neat oil applications with it. The high performance additives also allow the product to be used for general purpose applications such as cutting of steel. Castrol Hysol X incorporates advanced additive technology to control fungal and bacterial growth ensuring exceptional bath life and means the product can be used equally well in central systems or single sump machines and reduces the need for fluid maintenance.

FEATURES

- ◆ High performance synthetic lubricity additives
- ◆ Optimised surfactant package
- ◆ Advanced additive technology
- ◆ Chlorine free

BENEFITS

- ◆ Exceptional tool-life and surface finish
- ◆ Can replace neat oils in some applications
- ◆ Inherently low foam
- ◆ Long bath life
- ◆ Reduced need for maintenance
- ◆ Environmentally acceptable

Hysol X
30/04/2004

All reasonable care has been taken to ensure that the information contained in this publication is accurate at the date of printing. It should be noted however that the information may be effected by changes subsequent to the date of printing in the blend formulation or methods of application of any of the products referred to or in the requirements of any specification approval relating to any such Products

Castrol International
Pipers Way
Swindon
SN3 1RE
United Kingdom
Tel +44 (0)1793 452111
Fax +44 (0)1703 486083

Product Data

For maximum service life, coolant systems should be cleaned and sterilised by treatment with Castrol System Cleaner before changing to Hysol X. Treatment entails the addition of approximately 1% System Cleaner to the previous charge of coolant the day before it is due to be discarded.

TYPICAL PHYSICAL CHARACTERISTICS

Concentrate		
Appearance	-	Dark Amber
Density at 20°C kg/m ³	-	0.990
Emulsion		
Appearance	-	Milky emulsion
pH at 3% Concentration	-	9.0 - 9.5
Refractometer Correction Factor	-	1.02

RECOMMENDED CONCENTRATIONS

Material	Mild and Low Carbon Content Steels	Stainless Steels	Nimonic Alloys	Heat Resistant
Operation				
Multi-Tool Lathes	4%	5%	5%	5%
Gear Cutting	4%	5%	6%	6%
Deep Hole Drilling	5%	7%	7%	7%
Creep feed grinding	5%	5%	5%	5%
Broaching	5%	6-7%	8%	8%
General Machining	4%	5%	5%	5%

ADDITIONAL INFORMATION

Note that if the concentration of Hysol X should become too high, above a maximum of 10% not only will the emulsion become unstable but there is also the possibility of skin complaints among operators.

Hysol X
30/04/2004

All reasonable care has been taken to ensure that the information contained in this publication is accurate at the date of printing. It should be noted however that the information may be effected by changes subsequent to the date of printing in the blend formulation or methods of application of any of the products referred to or in the requirements of any specification approval relating to any such Products

Castrol International
Pipers Way
Swindon
SN3 1RE
United Kingdom
Tel +44 (0)1793 452111
Fax +44 (0)1703 486083



TECHNICAL DATA

QUAKERCOOL 2772

High performance, mineral oil free dilution

Description

QUAKERCOOL 2772 is a high performance dilution developed for machining operations and drawing applications where a high level of lubrication is required. It is specially recommended for the machining and grinding of cast iron, steel, stainless steel and light machining operations on aluminium alloys. It has been especially formulated as neat oil replacement in conventional grinding and other traditional neat oil operations.

Operations & Materials

- Machining and grinding operations on steel, cast iron and stainless steels.
- Concentration range: 5 to 20%, depending on the type of operation.
- Light machining on aluminium alloys.
- Water hardness: suitable for all waters.

Advantages

- Mineral oil free
- Ensures a good surface finish
- Excellent bio-resistance
- Good anti-corrosion properties on all metals.
- Pleasant odour.

Properties	Units	Data
Appearance (concentrate)	[-]	Clear, colourless liquid
Appearance (emulsion)	[-]	Clear translucent
pH, 5%, 10 dH/180ppm	[-]	8.8
Kinematic viscosity at 20° C	[mm ² /s]	32-39
Density at 15° C	[kg/m ³]	1072
Pour point	[° C]	< 4
Alkalinity pH 5.0	[mg KOH/g]	94.5
Refraction index factor	[°Brix/%]	0.55
Chlorine content	[% wt]	< 0.01
Sulphur content	[% wt]	< 0.01

The information contained and the recommendations made in this data sheet are based upon data collected and believed by us to be correct. However, no guarantee or warranty of any kind, expressed or implied, is made herein with respect to the products described and the buyer must assume full responsibility for the results, from the use thereof.

Storage, Safety & Disposal

Quaker Chemical can supply this quality product in drums, in containers and in bulk. The drum is our standard package. Other packages can be made available by Quaker Chemical or by distributors upon request.

As with all metalworking products, **QUAKERCOOL 2772** should be stored in dry conditions and protected from extreme temperatures: 4 - 35° C is the recommended storage temperature.

QUAKERCOOL 2772 is unlikely to present any significant health or safety hazard when used as recommended by Quaker Chemical. Good standards of personal and industrial hygiene are to be maintained by the user (see Material Safety Data Sheet).

In order to protect the environment, the product used should be safely disposed by a licensed contractor. The packaging material should be handled by a recognised drum reconditioning firm.



**MATERIAL SAFETY DATA SHEET**

Page 1 of 5

MSDS Code: UC

Date Issued: 10/28/04

Replaces Issue: 01/05/04

SECTION 1 - PRODUCT AND COMPANY IDENTIFICATION**PRODUCT NAME:**
(As Used on Label and List)**PROLONG ULTRA CUT 1 WATER SOLUBLE CUTTING FLUID****PRODUCT CODE:** UC**MANUFACTURER NAME AND ADDRESS:**
Prolong Super Lubricants, Inc.
6 Thomas
Irvine, CA 92618**MANUFACTURER PHONE NUMBERS:**
800.201.7599 or 949.587.2700
FAX: 949.587.2701**FOR HEALTH OR HAZMAT EMERGENCY:**
CHEM-TEL (US & Canada) 800.255.3924

CHEM-TEL (International)

813.248.0585 (collect)

SECTION 2 - COMPOSITION/INFORMATION ON INGREDIENTS**PRODUCT DEFINITION:** Mixture (Preparation)**CHEMICAL NATURE:** Petroleum Hydrocarbon

PRODUCT	CAS # OF COMPONENTS	LIMITS	EXPOSURE GUIDELINES	
			AGENCY	TYPE
Hydrotreated Naphthenic Distillate	64742-53-6		None Established	
Oil Mist, if generated	None	5mg/m ³ 10mg/m ³ 5mg/m ³	ACGIH ACGIH OSHA	TLV / TWA TLV / STEL PEL / CEILING: NONE
1- NP	108-03-2	25 ppm 25 ppm	ACGIH ACGIH	TLV / TWA TLV / STEL
Morpholine	110-91-8	20 ppm 20 ppm	ACGIH ACGIH	TLV / TWA TLV / STEL
Triethanolamine	102-71-6	5/m ³	ACGIH	TLV / TWA

Please note that the chemical identity of some or all of the above ingredients is confidential information and may be withheld as permitted by 29CFR 1910.1200 and Various State Right To Know Laws

SECTION 3 - HAZARDS IDENTIFICATION

- Health Hazards:** Avoid contact with eyes, skin and clothing. Wash thoroughly after handling. Use in well-ventilated area. Avoid breathing Mist. (See Section 11.)
- Physical Hazards:** Avoid incompatible materials. Hydrogen sulfide gas may be present in the headspace of the product container. Exposure to intense heat can cause containers to rupture.



MATERIAL SAFETY DATA SHEET

Page 2 of 5

MSDS Code: UC

Date Issued: 10/28/04

Replaces Issue: 01/05/04

SECTION 4 - FIRST AID MEASURES

Eye: Flush with water. If irritation occurs call for medical assistance.

Skin: Remove contaminated clothing. Wash with soap and water. Call for medical attention if symptoms prevail.

Ingestion: DO NOT induce vomiting. Get medical assistance.

Inhalation: Remove person to fresh air. Call for medical attention if needed.

SECTION 5 - FIRE FIGHTING MEASURES

Flash Point: >320 deg. F **Method:** ASTM-92

Flammable Limits (% by volume in air): **Lower:** ND **Upper:** ND

Extinguishing Media: Dry chemical, carbon dioxide, water fog, foam.

NFPA Ratings: **Health:** 1 **Flammability:** 1 **Reactivity:** 0 **Specific Hazard:** None

HMS Ratings: **Health:** 1 **Flammability:** 1 **Reactivity:** 0 **Specific Hazard:** Personal Protection Index -C

Fire Fighting Instructions: Wear protective clothing and self-contained breathing apparatus. Extinguish with foam, dry chemical. Carbon dioxide.

Combustion or Decomposition Properties: May cause dense smoke, oxides of carbon, nitrogen, sulphur and chlorides.

SECTION 6 - ACCIDENTAL RELEASE MEASURES

Chem-Tel Emergency Number (24 hrs): (800) 255.3924

U.S. Coast Guard National Response Center: (800) 424.8802

Spill Procedures: Protective personal equipment must be worn; see section 8 for recommendations. Ventilate area if spill in confined space or poorly ventilated areas. Prevent entry into sewers and waterways. Pick up free liquid for recycle and/or disposal. Residual liquid can be absorbed on inert material. Check under Transportation and Labeling (DOT/CERCLA) and Other Regulatory Information Section (SARA) for hazardous substances to determine regulatory reporting requirements for spills.

SECTION 7 - HANDLING AND STORAGE

Handling and Storage: Avoid eye and prolonged skin contact as with all industrial materials. Wash thoroughly after handling. Follow all MSDS/Label precautions after container is emptied because they may retain product residues. Store in a cool, dry place. Keep containers closed when not in use.



MATERIAL SAFETY DATA SHEET

Page 3 of 5

MS Code: UC

Date Issued: 10/28/04

Replaces Issue: 01/05/04

SECTION 8 - EXPOSURE CONTROLS / PERSONAL PROTECTION

Eye/Face Protection:	Use chemical goggles or face shield.
Skin Protection:	Contact may be minimized by wearing protective clothing and oil resistant gloves.
Respiratory Protection:	Under normal use conditions respirator is not usually required. Use self-contained breathing apparatus for entry into confined space, for other poorly ventilated areas and large spill clean-up sites.
Engineering Controls:	Good general ventilation should be sufficient to control airborne levels below exposure limits. A local exhaust is recommended in enclosed areas.
Clothing Recommendation:	Long sleeve shirt is recommended. Wear a chemically protective apron when contact with material may occur. Do not wear rings, watches or similar apparel that could entrap the material and cause a skin reaction.

SECTION 9 - PHYSICAL AND CHEMICAL PROPERTIES

SPECIFIC GRAVITY: 1.00 @ 15.6C (TYPICAL)	VAPOR PRESSURE: NOT DETERMINED
% VOLATILE BY VOLUME: NOT DETERMINED	VAPOR DENSITY (AIR=1) NOT DETERMINED
SOLUBILITY IN WATER: 100%	EVAPORATION RATE (n-BUTYL ACETATE =1) NOT DETERMINED
BOILING POINT: NOT DETERMINED	% SOLID NIL
DENSITY OF PRODUCT: 8.2 LBS/GAL (TYPICAL)	VOLATILE ORGANIC COMPOUND (VOC) LBS/GAL: NOT DETERMINED
pH: NOT DETERMINED	VISCOSITY: 7.10 cSt @ 100C (TYPICAL)
APPEARANCE: CLEAR, BLUE LIQUID	ODOR: SWEET ODOR

SECTION 10 - STABILITY AND REACTIVITY

Hazardous Decomposition Products:	May cause dense smoke, oxides of carbon, nitrogen, sulphur and chlorides.
Chemical Stability:	Material is normally stable at room temperature and pressure. See the Handling and Storage section for further details.
Conditions to Avoid:	Excessive heat or flames.
Incompatibility with other Materials:	Oxidizing or acidic materials.
Hazardous Polymerization:	Will not occur.



MATERIAL SAFETY DATA SHEET

Page 4 of 5

MSDS Code: UC

Date Issued: 10/28/04

Replaces Issue: 01/05/04

SECTION 11 - TOXICOLOGICAL INFORMATION

No Information Available at Present Time.

Chronic Effects: Not Listed as a Human Carcinogen by OSHA, IARC, or NTP.

Variable among Individuals: Health studies have shown that many petroleum hydrocarbons and synthetic lubricants pose potential human health risks which may vary from person to person. As a precaution, exposure to liquids, vapors, mists or fumes should be minimized.

Refer to section 13 for further information.

SECTION 12 - ECOLOGICAL INFORMATION

No data are available on the adverse effects of this material on the environment. As a precaution, product should be kept out of sewage and drainage systems and bodies of water.

SECTION 13 - DISPOSAL CONSIDERATIONS

All components are listed on the TSCA inventory.

Any disposal practice must be in compliance with local, state and federal laws and regulations. Empty containers must be handled with care due to the product residue.

SECTION 14 - TRANSPORTATION INFORMATION

DOT Shipping Name: Not regulated.

DOT Hazard Class: Not regulated.

DOT Packaging Group: NA

DOT/UN Identification: NA

SECTION 15 - REGULATORY INFORMATION

TSCA Status: All Components are listed in TSCA inventory.

CERCLA Reportable Quantity: This product does not contain any RQ substances.

SARA Title III: Title III Superfund Amendments and Reauthorization Act of 1986:

Section 302 Extremely Hazardous Substances: Not an extremely hazardous substance.

Section 311/312 Hazardous Categories:

Immediate: (Acute) Health Effects: No

Delayed: (Chronic) Health Effects: No

Fire Hazard: No

Sudden Release of Pressure: No

Reactivity Hazard: No

Carcinogenicity Status: Constituents not listed by: IARC, NTP, OSHA

Section 313 Toxic Chemical Release Reporting:

This product does not contain greater than 1.0% (greater than 0.1% for carcinogenic substance) listed under SARA Section 313.

California Proposition 65 Status: N/A



MATERIAL SAFETY DATA SHEET

Page 5 of 5

MSDS Code: UC

Date Issued: 10/28/04

Replaces Issue: 01/05/04

SECTION 16 - OTHER INFORMATION

The information and recommendation herein are, to the best of our knowledge and belief, accurate and reliable as of the date issued. Prolong Super Lubricants, Inc. does not warrant or guarantee their accuracy or reliability, and shall not be liable for any loss or damage arising out of the use thereof. The information and recommendations are offered for the user's consideration and examination, and it is the user's responsibility to satisfy itself that they are suitable and complete for its particular use.

Since the conditions for use, handling, storage and disposal of this product are beyond Prolong Super Lubricants' Inc. control, it is the responsibility of the user both to determine safe conditions for use of this product and to assume liability for loss, damage or expense arising out of the improper use from any statement or omission in this MSDS.

Various government agencies, (e.g. DOT, EPA, FDA, etc.) may have specific policies concerning the transportation, handling, storage, use or disposal of this product which may not be reflected in this MSDS. The user should review these regulations to insure full compliance.

The recipient of a MSDS is responsible for acting in accordance with a risk assessment in regard of the conditions of product use and for taking necessary precautionary measures in a given work situation, and has the responsibility to keep the users informed about the hazards relevant to their individual workplace. The recipient of a MSDS is responsible for choosing the appropriate way of informing the users. When formulating the specific instructions for the workplace, the recipient should consider the general recommendations of the relevant MSDS. Since a MSDS is merely product-related, it cannot take into account all the possible situations that may arise at any given workplace.¹

This MSDS is generated using an ISO 11014-1:994(E) Safety data sheet for chemical products International Standards, PART 1: Section 4 - General Aspects.

¹ Reference from ISO 11014-1:994(E), PART 1: Section 4.



MATERIAL SAFETY DATA SHEET

Page 1 of 6

MSDS Code: TRAN

Date Issued: 05/19/99

Replaces Issue: 10/08/98

SECTION 1 - PRODUCT AND COMPANY IDENTIFICATION

PRODUCT NAME:
(As Used on Label and List)

PROLONG TRANSMISSION TREATMENT

PRODUCT CODE: TRAN

MANUFACTURER NAME AND ADDRESS:

Prolong Super Lubricants, Inc.
6 Thomas
Irvine, CA 92618

MANUFACTURER PHONE NUMBERS:

800.201.7599 or 949.587.2700
FAX: 949.587.2701

FOR HEALTH OR HAZMAT EMERGENCY:

CHEM-TEL (US & Canada)

800.255.3924

CHEM-TEL (International)

813.248.0585 (collect)

SECTION 2 - COMPOSITION/INFORMATION ON INGREDIENTS

PRODUCT DEFINITION: Mixture (Preparation)

CHEMICAL NATURE: Petroleum/Chemical Mixture

PRODUCT	CAS # OF COMPONENTS	LIMITS	EXPOSURE GUIDELINES AGENCY	TYPE
Aromatic Petroleum Distillates	64742-94-5		None Established	
Aliphatic Naphtha	64742-88-7	100ppm	Supplier	TWA
Hydrotreated Light Naphthenic Distillate	64742-53-6		None Established	
Oil Mist, if generated	None	5mg/m ³ 10mg/m ³ 5mg/m ³	ACGIH ACGIH OSHA	TLV / TWA TLV / STEL PEL / CEILING: NONE
Proprietary Additives	Mixture		None Established	

Please note that the chemical identity of some or all of the above ingredients is confidential information and may be withheld as permitted by 29CFR 1910.1200 and Various State Right To Know Laws

SECTION 3 - HAZARDS IDENTIFICATION

HEALTH HAZARDS: May be harmful if inhaled repeatedly for prolonged periods of time. Do not ingest. May cause eye and skin irritation. May cause chronic health effects.

PHYSICAL HAZARDS: Keep away from all sources of ignition. Avoid contact with strong oxidizers and reducers. Protect against decomposition products.

SECTION 4 - FIRST AID MEASURES

INHALATION: Remove exposed person to fresh air if adverse effects are observed. If breathing is labored, administer oxygen. If breathing has stopped apply artificial respiration. If irritation persists or if toxic symptoms are observed, seek medical attention.

SKIN CONTACT: In case of skin contact, remove any contaminated clothing and wipe excess off. Wash skin with soap and water or a waterless hand cleaner followed by soap and water. Launder 205 dry clean clothing before reuse and discard shoes and other leather articles saturated with the material. Seek medical attention if irritation persists or develops.



MATERIAL SAFETY DATA SHEET

Page 2 of 6

Date Issued: 05/19/99

Replaces Issue: 10/08/98

MSDS Code: TRAN

EYE CONTACT:

Immediately flush eyes with large amounts of clear, cool water for at least 15 minutes, while holding eyelids open. Seek medical attention.

INGESTION:

Do not induce vomiting. This material can be an aspiration hazard. If vomiting occurs spontaneously, keep head below hips to prevent aspiration of liquid into the lungs. Seek medical attention immediately.

NOTE TO PHYSICIANS:

This material can enter lungs during swallowing or vomiting and can cause lung inflammation and/or damage.

SECTION 5 - FIRE FIGHTING MEASURES

EXTINGUISHING MEDIA:

CO₂, Dry chemical, foam or water fog. Water spray can be used to cool and protect containers exposed to heat and flame.

SPECIFIC HAZARDS:

Toxic fumes, gases or vapors may evolve on burning. Vapors are heavier than air and may travel along the ground or be moved by ventilation and ignited by heat, pilot lights, other flames and ignition sources at locations distant from material handling point. Protect against decomposition products.

Thermal decomposition products are highly dependent on the combustion conditions. A complex mixture of airborne, solid, liquid, particulates, various hydrocarbons, and gases will evolve when this material undergoes combustion or pyrolysis. The following may be formed: Fumes, smoke, oxides of carbon, hydrogen chloride, oxides of calcium, oxides of sulfur, and other unidentified organic compounds.

SPECIFIC METHODS/

PROTECTION OF FIREFIGHTERS: Positive-pressure self contained breathing apparatus should be used. Product can burn upon heating to temperatures at or above the flashpoint. Do not enter any enclosed or confined area without proper protective equipment or self-contained breathing apparatus.

SECTION 6 - ACCIDENTAL RELEASE MEASURES

PERSONAL PRECAUTIONS:

Personnel protective equipment must be worn (See Section 8). Minimize contact with skin and clothing.

ENVIRONMENTAL PRECAUTIONS:

Keep product out of sewers and watercourses by diking or impounding. This product is an oil under 49 CFR (DOT) Part 130. If shipped by rail or highway in a tank with a capacity of 3,500 gallons or more, it is subject to the requirements of Part 130. Advise authorities if product has entered or may enter sewers, water courses, or extensive land areas. Assure conformity with applicable governmental regulations. Contact the coast guard national response center (800) 424-8802 if a spill or any amount is made into or upon U.S. navigable waters, the contiguous zone or adjoining shorelines.

METHODS FOR CLEANING UP:

Remove all sources of ignition. Prevent contact with strong oxidizers and reducers. Ventilate spill area if confined or poorly ventilated. Recovery should be performed by picking up free liquid with explosion proof or hand pump for recycle and/or disposal. Residual material can be absorbed or inert material.

SECTION 7 - HANDLING AND STORAGE

HANDLING

TECHNICAL MEASURES:

Avoid generating oil mists while handling. Excessive misting may cause slippery floors. Proper footwear is required. Keep containers closed when not in use. Maintain minimal handling temperatures. Avoid excessive heat, open flame or ignition sources, or heating product above flash point. (275°F COC [Min]) - Do not smoke -



MATERIAL SAFETY DATA SHEET

Page 3 of 6

MSDS Code: TRAN

Date Issued: 05/19/99

Replaces Issue: 10/08/98

PREVENTION OF USER EXPOSURE: Avoid contact with eyes. Avoid prolonged or repeated contact with skin and clothing. Wash thoroughly after handling. Remove contaminated clothing and launder before reuse. Avoid inhalation of fumes. Handle in well-ventilated area. Do not take internally. Keep out of the reach of children. (See Sections 3, 5, 6 & 8.)

PREVENTION OF FIRE AND EXPLOSION: Liquid or vapor may ignite. Keep away from all sources of ignition. Protect against contact with strong oxidizers, reducers, and decomposition products. (See Sec. 3, 5 & 6.)

PRECAUTIONS: Handle in a well-ventilated area.

SAFE HANDLING ADVICE: See Section 10.

STORAGE

TECHNICAL MEASURES: Avoid generating oil mists while handling. Excessive misting may cause slippery floors. Proper footwear is required. Keep containers closed when not in use. Maintain minimal handling temperatures. Avoid excessive heat, open flame or ignition sources, or heating product above flash point. (275°F COC [Min]) - Do not smoke -

STORAGE CONDITIONS: Store in a cool, dry location. Keep away from all sources of ignition. Heating of non-vented container may cause container to rupture. Keep containers tightly closed and upright when not in use. See Section 13, Disposal Considerations, regarding disposition of empty containers.

INCOMPATIBLE PRODUCTS: Protect against contact with strong oxidizers, reducers, and decomposition products.

PACKAGING MATERIALS: The original Prolong Container is the recommended storage material for this product.

SECTION 8 - EXPOSURE CONTROLS / PERSONAL PROTECTION

ENGINEERING MEASURES

CONTROL PARAMETERS: Not Required

PERSONAL PROTECTIVE EQUIPMENT

RESPIRATORY PROTECTION: Under normal use conditions, respirator is not usually required. Use NIOSH / MSHA approved air-purifying respirator for organic vapors and particulates if the recommended exposure limit is exceeded. Use self-contained breathing apparatus for entry into confined space, for other poorly ventilated areas, and for large spill clean-up sites.

HAND PROTECTION: Use chemical resistant gloves to avoid prolonged or repeated skin contact. Nitrile or Neoprene gloves are recommended.

EYE PROTECTION: Wear safety spectacles with unperforated side-shields.

SKIN AND BODY PROTECTION: Use chemical resistant gloves to avoid prolonged or repeated skin contact. Nitrile or Neoprene gloves are recommended. Use of clothing that completely covers limbs, and chemical resistant apron or other impervious clothing is recommended. Launder clothing before reuse. Chemical resistant boots are recommended.

HYGIENE MEASURES: Minimize breathing vapor, mist or fumes. Avoid prolonged or repeated contact with skin. Remove contaminated clothing and launder or dry clean before reuse. Remove contaminated shoes and thoroughly clean before reuse. Cleanse skin thoroughly after contact, before breaks and meals, and at the end of working period.



MATERIAL SAFETY DATA SHEET

Page 4 of 6

MSDS Code: TRAN

Date Issued: 05/19/99

Replaces Issue: 10/08/98

SECTION 9 - PHYSICAL AND CHEMICAL PROPERTIES

APPEARANCE: Clear, light orange liquid

PHYSICAL STATE: Liquid

MELTING POINT (°C): Not Applicable

BOILING POINT: Not Determined

SPECIFIC GRAVITY (H₂O = 1): 1.01 @ 15.6°C (Typical)

% VOLATILE BY VOLUME: Not Determined

VOC (lbs/gal): Not Determined

FLASHPOINT (°C): 135 COC (Typical)

ODOUR: Characteristic petroleum odor

SOLUBILITY IN WATER (20°): Negligible

DENSITY (g/ml): 8.4 (Typical)

pH @ 25°C: Not Determined

VAPOR PRESSURE (mm Hg): Not Determined

VAPOR DENSITY (AIR = 1): Not Determined

VISCOSITY (cPs): 41.6 @ 40°C (Typical)

EVAPORATION RATE (Butyl Acetate = 1): Not Determined

SECTION 10 - STABILITY AND REACTIVITY

STABILITY: Stable under normal conditions of storage and handling.

CONDITIONS TO AVOID: Avoid heating to decomposition.

MATERIALS TO AVOID: Strong oxidizing and reducing agents, acids and heat.

HAZARDOUS POLYMERIZATION: Will not occur.

SECTION 11 - TOXICOLOGICAL INFORMATION

PRIMARY ROUTES OF ENTRY OR EXPOSURE: Skin absorption, eye contact and inhalation.

INHALATION: If material is misted or if vapors are generated from heating, exposure may cause irritation of mucous membranes in the upper respiratory tract. High concentrations may cause headaches, dizziness, nausea, behavioral changes, weakness, drowsiness and stupor based on data from components or similar products.

SKIN: May cause skin irritation, including redness, burning, drying and cracking, and skin burns based on data from components or similar products.

EYE: May cause eye irritation. Direct contact with liquid or exposure to vapors may cause stinging, tearing and redness based on data from components or similar products.

INGESTION: Ingestion may cause irritation of the mouth, esophagus and stomach. Aspiration (breathing of vomitus into the lungs) must be avoided as even small quantities may result in aspiration pneumonitis. Ingestion may cause CNS depression based on data from components or similar products.

ACUTE TOXICITY: Pre-existing skin and respiratory disorders may be aggravated by exposure, based on data from components or similar products. Health studies have shown that many petroleum hydrocarbons and synthetic lubricants pose potential human health risks, which may vary, from person to person. As a precaution, exposure to liquids, vapors mists or fumes should be minimized.

CHRONIC TOXICITY: Repeated overexposure to petroleum naphtha can cause nervous system damage. Based on data from components or similar products.

SPECIAL EFFECTS: Symptoms of overexposure include: Gastrointestinal irritation (nausea, vomiting, diarrhea), irritation (nose, throat, respiratory tract), central nervous system depression (dizziness, drowsiness, weakness, fatigue, nausea, headache, unconsciousness, effects on hearing.)



MATERIAL SAFETY DATA SHEET

Page 5 of 6

MSDS Code: TRAN

Date Issued: 05/19/99

Replaces Issue: 10/08/98

SECTION 12 - ECOLOGICAL INFORMATION

STEPS TO BE TAKEN IF MATERIAL IS RELEASED OR SPILLED: Ventilate and remove with inert absorbent.

SECTION 13 - DISPOSAL CONSIDERATIONS

WASTE DISPOSAL METHODS: Comply with all Federal, state and local laws.

NOTE: Waste disposal should be in compliance with all Federal, state and local laws.

SECTION 14 - TRANSPORTATION INFORMATION

DOT CLASSIFICATION: Not applicable

SECTION 15 - REGULATORY INFORMATION

THE FOLLOWING INFORMATION MAY BE USEFUL IN COMPLYING WITH VARIOUS STATE AND FEDERAL LAWS AND REGULATIONS UNDER VARIOUS ENVIRONMENTAL STATUTES:

THRESHOLD PLANNING QUANTITY (TPQ), EPA REGULATION 40 CFR 355 (SARA SECTIONS 301-304): No TPQ for product or any constituent greater than 1% or 0.1% (carcinogen) for SARA Section 302.

TOXIC CHEMICAL RELEASE REPORTING, EPA REGULATION 40 CFR 372 (SARA SECTION 313): This product contains the following substances subject to the reporting requirements of SARA III Section 313 1986 and 40 CFR part 372:
None known

REPORTABLE QUANTITY (RQ), EPA REGULATION 40 CFR 302 (CERCLA SECTION 102): No RQ for product known to be greater than 1% or 0.1% (carcinogen).

CALIFORNIA PROP 65: This product contains chemicals known to the state of California to cause birth defects, and/or reproductive harm.

TSCA INVENTORY: All components are listed on the TSCA inventory.

NOTE: State and local regulatory requirements may be more restrictive or otherwise different from US Federal regulations. Consult state and local regulations regarding other regulatory requirements.

SECTION 16 - OTHER INFORMATION

The information and recommendation herein are, to the best of our knowledge and belief, accurate and reliable as of the date issued. Prolong Super Lubricants, Inc. does not warrant or guarantee their accuracy or reliability, and shall not be liable for any loss or damage arising out of the use thereof. The information and recommendations are offered for the user's consideration and examination, and it is the user's responsibility to satisfy itself that they are suitable and complete for its particular use.

Since the conditions for use, handling, storage and disposal of this product are beyond Prolong Super Lubricants' Inc. control, it is the responsibility of the user both to determine safe conditions for use of this product and to assume liability for loss, damage or expense arising out of the improper use from any statement or omission in this MSDS.

Various government agencies, (e.g. DOT, EPA, FDA, etc.) may have specific policies concerning the transportation, handling, storage, use or disposal of this product which may not be reflected in this MSDS. The user should review these regulations to insure full compliance.

The recipient of a MSDS is responsible for acting in accordance with a risk assessment in regard of the conditions of product use and for taking necessary precautionary measures in a given work situation, and has the responsibility to keep the users informed about the hazards relevant to their individual workplace. The recipient of a MSDS is responsible for choosing the appropriate way of informing the users. When formulating the specific instructions for the workplace, the recipient should consider the general recommendations of the relevant MSDS. Since a MSDS is merely product-related, it cannot take into account all the possible situations that may arise at any given workplace.¹



MATERIAL SAFETY DATA SHEET

Page 6 of 6

Date Issued: 05/19/99

Replaces Issue: 10/08/98

MSDS Code: TRAN

This MSDS is generated using an ISO 11014-1:994(E) Safety data sheet for chemical products International Standards, PART 1: Section 4 - General Aspects.

¹ Reference from ISO 11014-1:994(E), PART 1: Section 4.

Appendix 2 – Load Controls Universal Power Cell

ECOLOGICAL PARK
PO BOX 100
BRIDGE, MA 01846
TEL: 347-2808
FAX: 308-347-2064

NEW UNIVERSAL POWER CELL

Gives You Valuable Information About Machine and Process Performance
by Monitoring Motor Load

- Mixture Viscosity
- Tool Condition
- Optimum Feedrate
- Pump or Fan Flow
- Beginning or End of Process
- Obstructions
- Overloads
- Loss of Load

The Universal Power Cell Senses True Motor Power—
Three Phase, Variable Frequency, Single Phase or DC.

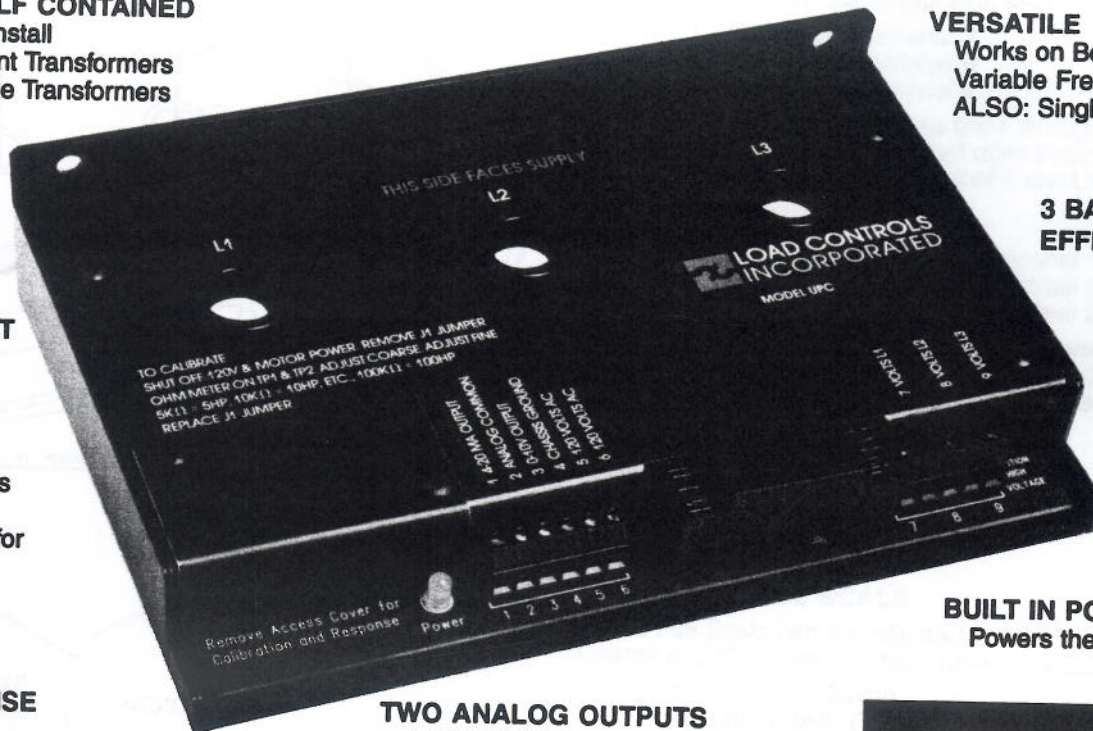


FULLY SELF CONTAINED

- Easy to Install
- No Current Transformers
- No Voltage Transformers

VERSATILE

Works on Both Fixed and
Variable Frequency Power
ALSO: Single Phase & DC



**3 BALANCED HALL
EFFECT SENSORS**

**SAMPLE
VOLTAGE
DIRECTLY**
Up to 600 Volts

BUILT IN POWER SUPPLY
Powers the Analog Signals

TWO ANALOG OUTPUTS

4-20 Milliamps
0-10 Volts DC
Electrically Isolated

FACT
x 5 1/8" x 8"

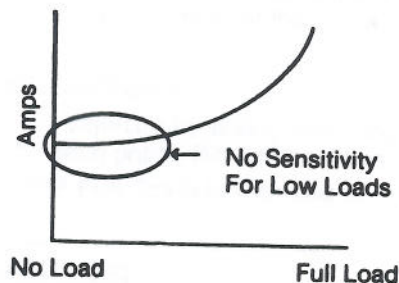
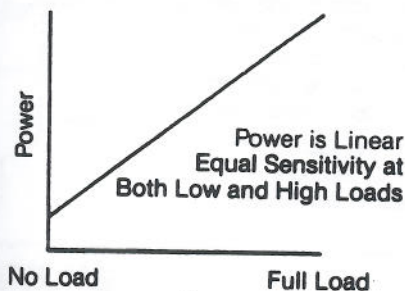
CAN ADJUST
SCALE TO
YOUR

Use and Fine
Adjustment Pots
to 150HP
Extra Turns for
Small Motors

IN RESPONSE
STMENT

You slow the Response of the
Cell to average the readings.

Why Monitor Power Instead of Just Amps?



LOAD CONTROLS INCORPORATED

Vydas International Marketing
Swan House Passfield Bus Ctr
Lynchborough Road Passfield
Surrey GU30 7SB United Kingdom
Tel: 01428 751822 Fax: 01428 751833

TECHNOLOGY PARK
10 PICKER ROAD
STURBRIDGE, MA 01566
508-347-2606
FAX 508-347-2064

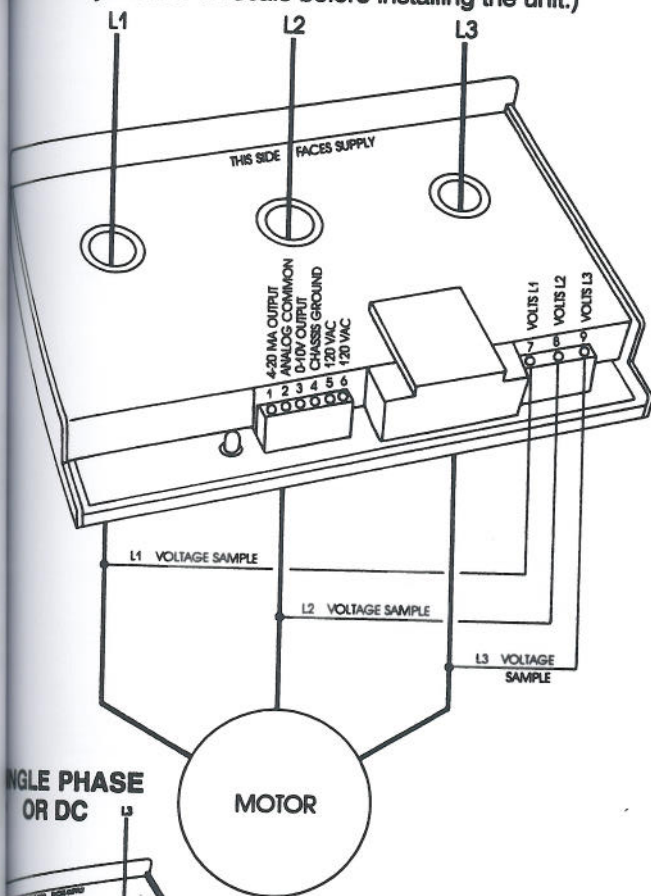
UNIVERSAL POWER CELL MODEL UPC

The Universal Power Cell is a Motor Load Sensor that monitors power (HP or KW). It works on both fixed frequency and variable frequency power and has 2 analog outputs. It also works on single phase, DC and brushless DC. The Universal Power Cell has 3 balanced Hall Effect devices, each with a flux concentrator. Each phase passes through a window. A voltage sample for each phase is also taken. The Hall Effect semiconductor does a vector multiplication of the current flow and voltage and also calculates the power factor. The output is proportional to power (HP or KW).

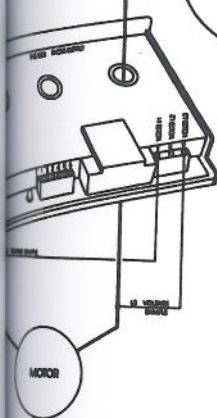
INSTALLATION

MOUNTING

The Universal Power Cell is direction sensitive. Locate the Power Cell so that the motor electrical supply lines can be passed through the Cell. The TERMINAL side of the Cell faces the SUPPLY. (It is convenient to adjust the Full Scale before installing the unit.)



SINGLE PHASE
OR DC



RESPONSE ADJUSTMENT

In some cases, the average power signal may be more useful than instantaneous power. The Response Adjustment slows the response of the Universal Power Cell.

Pot is located under Access Cover.
Clockwise is fastest.

INPUT CONNECTIONS

Pass each of the phases through the L1, L2, L3 holes in the Cell. Be certain that DIRECTION is correct. The TERMINAL side of the Cell faces the SUPPLY.

Provide a voltage sample for each phase with 20 gauge or larger wire. When a variable frequency drive is being used, locate the Power Cell on the output side of the drive. Take the voltage samples on the output side also.

L1 Volts to Terminal 7
L2 Volts to Terminal 8
L3 Volts to Terminal 9

It doesn't matter which phase goes through each hole. But, the Voltage sample from the wire that goes through the L1 hole must go to Terminal 7, L2 hole to Terminal 8 and L3 hole to Terminal 9.

ANALOG OUTPUTS

4-20 Milliamp Terminal 1
0-10 Volt DC Terminal 3
Analog Common Terminal 2

The Analog Output is powered by the Power Cell. Use shielded cable 20 gauge or larger for the analog output. Shield is ungrounded at Power Cell. Grounded at device.

120 VOLT SUPPLY

Terminals 5 & 6

GROUND

Terminal 4

TO ADJUST FULL SCALE

The Full Scale can be adjusted to match your motor with the Coarse and Fine Pots located under the access cover.

Convenient Scaling
5K ohm = 5HP (This is the minimum setting)
10K ohm = 10HP
Etc.
150K ohm = 150HP (This is the maximum setting)
(KW = HP x .746)

- 1) Turn off 120 Volt power AND motor power.
- 2) Remove Access Cover.
- 3) Remove J1 Jumper.
- 4) Ohmmeter leads on Test Points TP1 & TP2.
- 5) Adjust Full Scale Coarse Pot then Fine 20 Turn Pot.
- 6) Replace J1 Jumper.

FOR SMALL MOTORS

Reduce the capacity by taking additional "TURNS" through each hole for each phase (Mount the Power Cell on Standoffs).
Example: 5HP Full Scale is reduced to 1HP with 5 Turns.

SPECIFICATIONS

FREQUENCY
1KHz

RESPONSE - ADJUSTABLE
Responds to 3 Seconds

ANALOG OUTPUT

4-20 Milliamp - 500 Ohm Maximum connected impedance
0-10V DC - 2000 Ohm Minimum load

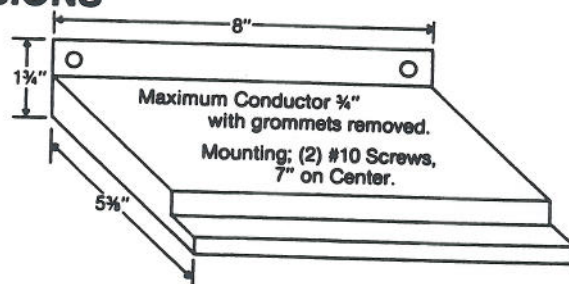
ACCURACY

.5% Full Scale

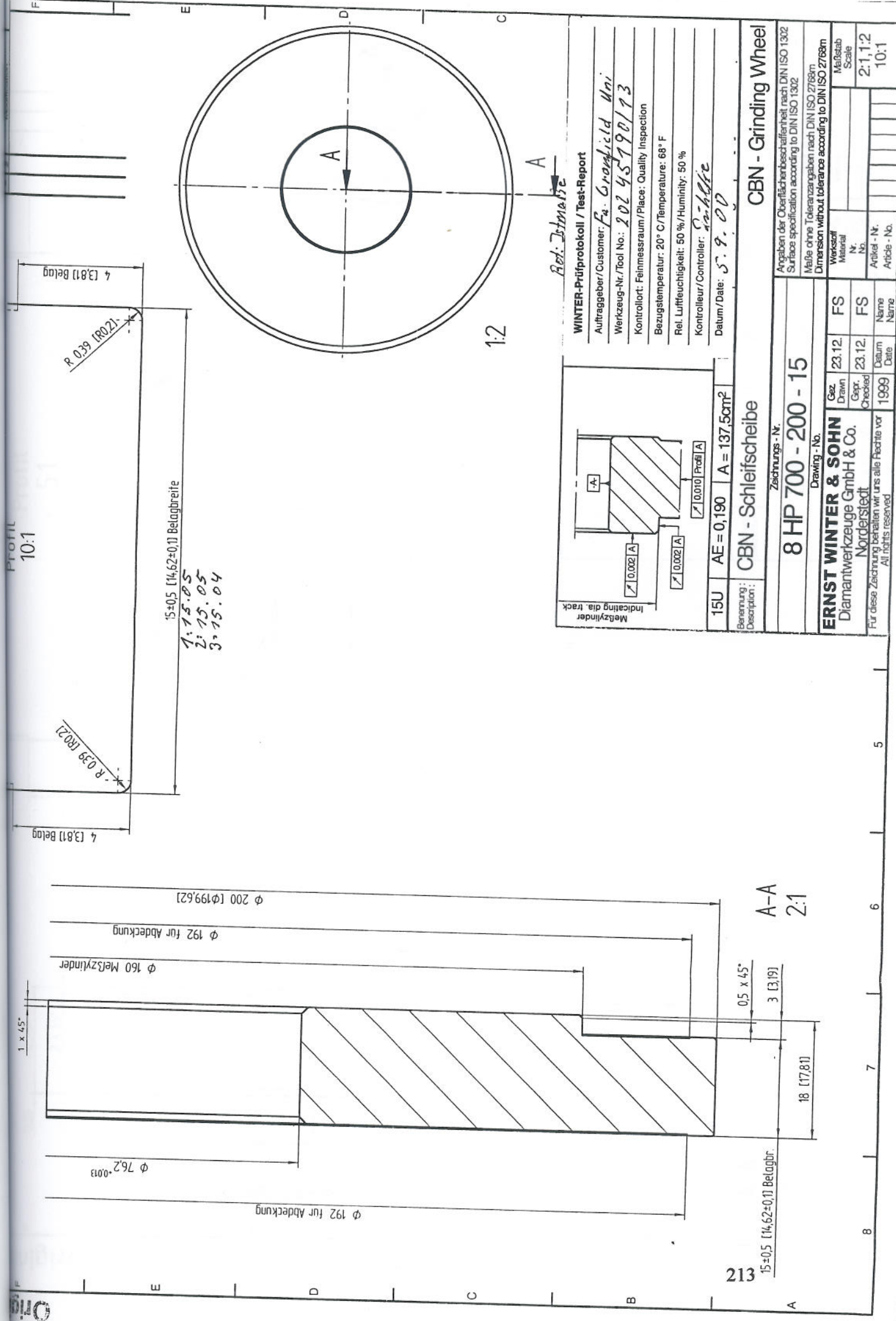
TEMPERATURE

60°C Maximum

DIMENSIONS

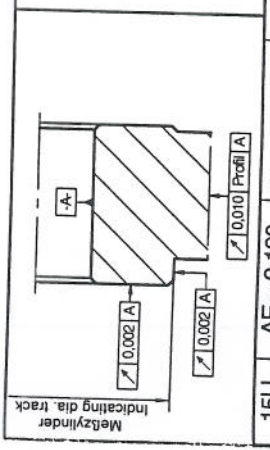


Appendix 3 – CBN Grinding Wheel Drawings

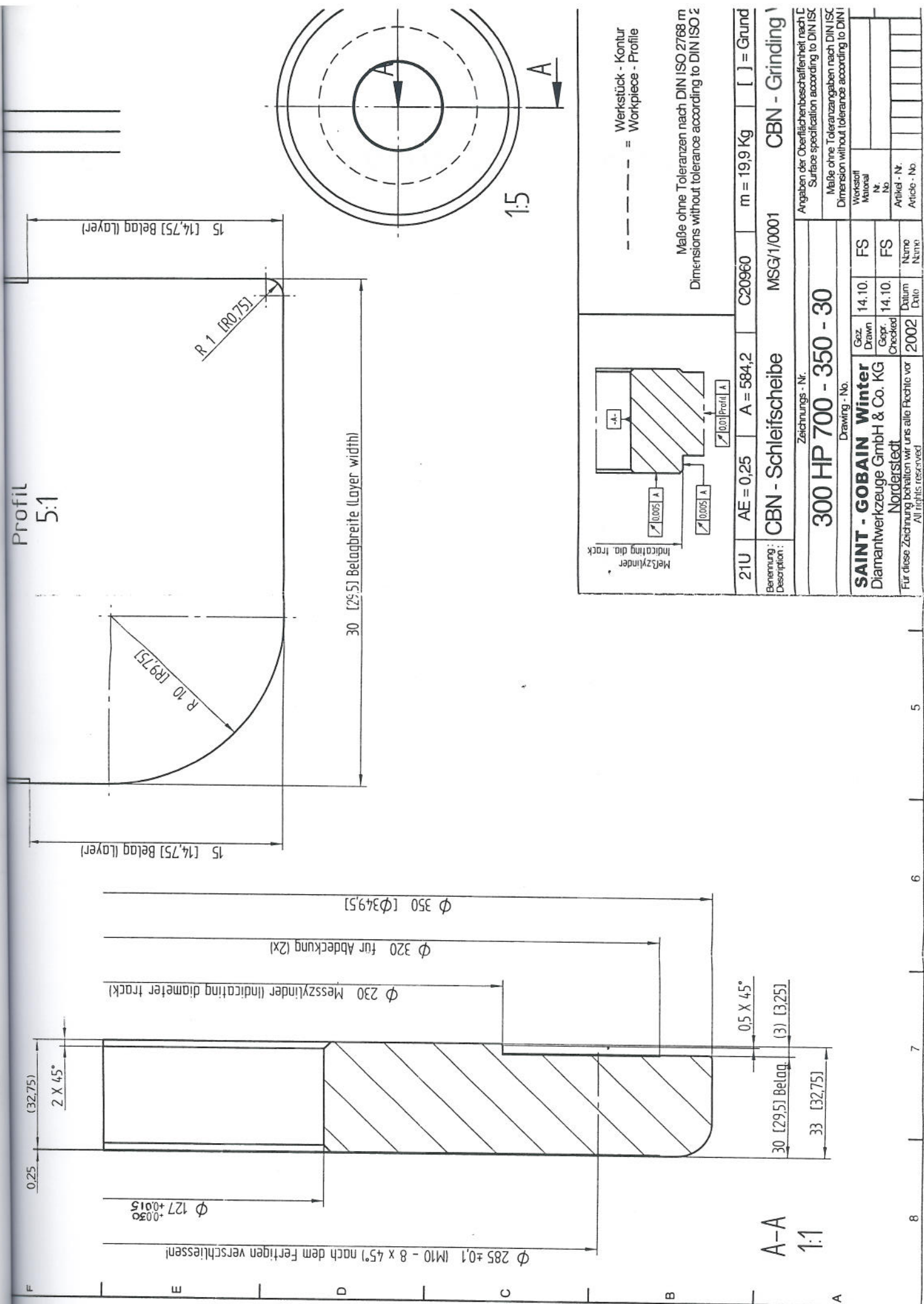


Red: J. J. J. J.

WINTER-Prüfprotokoll / Test-Report
Auftraggeber/Customer: *Fa. Grayfield Uni*
Werkzeug-Nr./Tool No.: *202 45190/13*
Kontrollort: Feinmessraum/Place: Quality Inspection
Bezugstemperatur: 20° C/Temperature: 68° F
Rel. Luftfeuchtigkeit: 50 %/Humidity: 50 %
Kontrollleur/Controller: *Schiffle*
Datum/Date: *5.9.00*



Benennung : Description :		CBN - Schleifscheibe		CBN - Grinding Wheel	
Zeichnungs - Nr. Drawing - No.		8 HP 700 - 200 - 15		Angaben der Oberflächenbeschaffenheit nach DIN ISO 1302 Surface specification according to DIN ISO 1302	
ERNST WINTER & SOHN Diamantwerkzeuge GmbH & Co. Norderstedt		Gez. Drawn	23.12.	FS	Maßstab Scale
Für diese Zeichnung behalten wir uns alle Rechte vor All rights reserved		Gepr. Checked	23.12.	FS	
		1999	Datum Date	Name Name	Maße ohne Toleranzangaben nach DIN ISO 2768m Dimension without tolerance according to DIN ISO 2768m



Appendix 4 – Hunt TM Data Tyndallometer

TM-data - Respirable Dust measuring instrument

Title:

TM-data - Respirable Dust measuring instrument

General Task:

Emission monitoring, workplace monitoring

Use:

portable

Measuring Principle:

Scattered light, passive

Standards/Approvals:

EEKial, intrinsically safe, in comply with EN 50014-50020, Johannesburg Convention, ACGIH Respirable dust

Measuring Range:

0 - 100 mg/m³

Lower detection:

ca. 10 µg/m³ for DEHS-particles

Output:

0 - 4 V, Digital Interface

Weight:

Miscellaneous:

Untertage-Zulassung weltweit, integrierter Datenspeicher u. EDV-Anschluß

Application:

Measurement of respirable dust in the mining industry, Localizing and assessing of emission sources, Emission monitoring of air ducts at filter plants, Evaluating of dust reduction measures, Quality control, Personal workplace monitoring, Area workplace monitoring

Article no:

001.0008.000



Appendix 5 – Stanhope Seta Air Release Value Apparatus

AIR RELEASE VALVE

1. Connect and Purge

2. Set pressure
3. Set temperature
4. Set flow rate

5. Set the hydraulic flow rate
6. Set the air flow rate
7. Set the pressure gauges, and connect
8. Set the air flow rate
9. Set the air flow rate
10. Set the air flow rate

11. Set the air flow rate
12. Set the air flow rate
13. Set the air flow rate
14. Set the air flow rate
15. Set the air flow rate

16. Set the air flow rate
17. Set the air flow rate
18. Set the air flow rate



15850-3 and 15880-5 Balance

15850-3 SETA AIR RELEASE VALUE APPARATUS

ASTM D3427; IP 313; BS 2000 Part 313;
DIN 51 381; ISO 9120; NF T60-149

- Ambient to 75°C temperature range
- 200kPa maximum air pressure
- 23l/min maximum flow rate
- Optional automated density monitoring

Determines the time taken for hydraulic fluids and lubricating oils to release entrained air and gases.

The main unit comprises an air heater, fine control pressure regulator, pressure gauge, and mounting clip for the test vessel. An interlocked 3 pin socket provides power to an external air pump when the heater is on. The digital temperature controller is housed in a separate unit. The instrument is protected by an overtemperature cut-out.

A density balance (15880-5) comprising an electronic balance, Seta-ARV software, sinker and platinum wire, is available as an accessory. The output of the balance is monitored by the software, calculating the density of the sample prior to and during the test, and the time taken for the sample to reach target density to be determined automatically. End point values can be output to a printer or stored on disk.

SUPPLIED WITH: connection tubing, digital temperature control unit and instruction manual.

Note: Requires connection to a suitable air supply



Max. Air Temperature:	65°C
Sample Temp. Range:	Ambient to 75°C
Voltage:	110/120V, 50/60Hz
or:	220/240V, 50/60Hz
Power consumption:	170W max
Size (HxWxD):	46 x 38 x 35cm
Weight:	8.5kg

ACCESSORIES

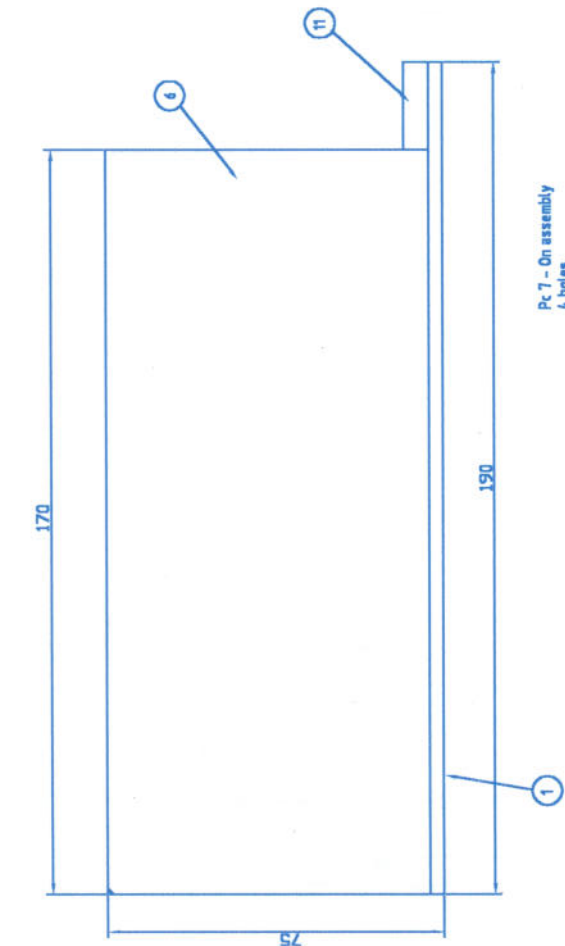
REQUIRED

15870-4	CIRCULATING WATER BATH, 10 l/min flow rate. Maintains test cell at 25°, 50° or 75°C (77°, 122° or 167°F).
	Voltage: 110/120V, 50/60Hz
	or: 220/240V, 50/60Hz
	Power: 1.6kW
	Size (HxWxD): 36 x 60 x 30cm
	Weight: 9kg
20290-2	AIR PUMP, (for details see page 130).
15860-0	SETA TEST VESSEL, glass, comprises a jacketed sample tube, matched air inlet capillary, baffle plate and air outlet tube.
15865-0	DIGITAL THERMOMETER AND THERMOCOUPLES, for monitoring sample temperature.
16125-2	TEMPERATURE PROBE AND INDICATOR, for measuring air inlet temperature before the test.
15880-5	DENSITY BALANCE, electronic, with digital display ± 0.001 g/ml and computer interface. Supplied with stand, 10ml sinker, 123mm platinum wire, cable and Seta ARV software for analysing, data logging and printing. Requires an IBM compatible Personal Computer.
	Voltage: 110/120V or 220/240V, 50/60Hz
	Size (HxWxD): 7 x 24 x 27cm
	Weight: 7kg
99200-2	OVEN, for warming test sample, (see page 131).

OPTIONAL

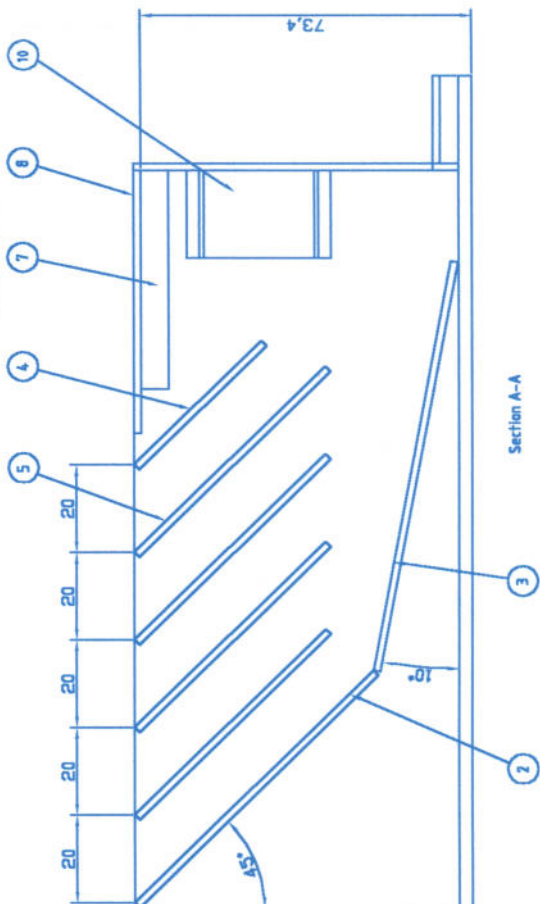
45000-0	SETAPLUS EXTENDED 12 MONTH WARRANTY
---------	-------------------------------------

Appendix 6 – Cutting Fluid Trough – Drawings

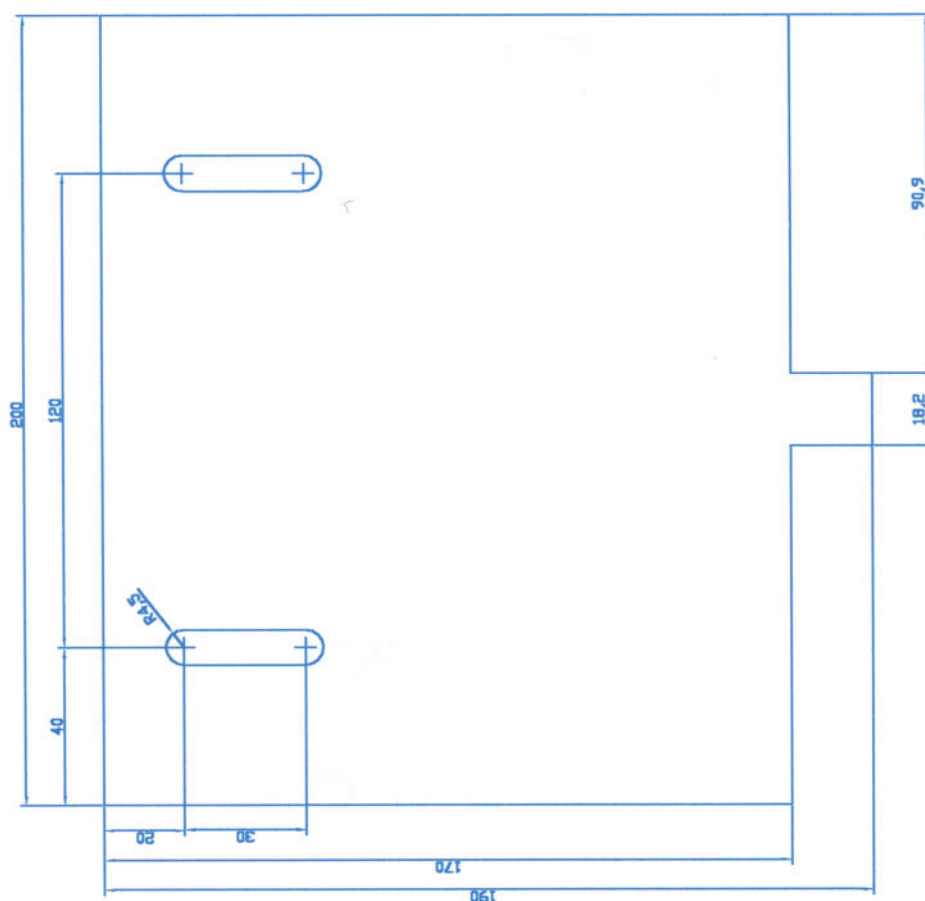


Welded Construction.

- Pc2 75 x 196.8 x 1.6 stainless sheet
Pc3 95 x 196.8 x 1.6 stainless sheet
Pc4 40 x 196.8 x 1.6 stainless sheet
Pc5 60 x 196.8 x 1.6 stainless sheet (5 off)
Pc6 170 x 72 x 1.6 stainless sheet (2 off)
Pc7 6 x 6 x 50 stainless steel rect bar (2 o
See sheet 2 for details of Pc 1, Pc 8, Pc 9,

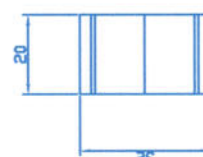


Item#ref	Quantity	Title/Name, designation, material, dimension etc	Article No./Reference
Designed by MM	Checked by MM	Approved by - date MM'18 Feb 2004	Date Coolant Trough 18 Feb 2004
Cranfield University SIMS			Scale NTS
Coolant Trough			Sheet 1 of 2

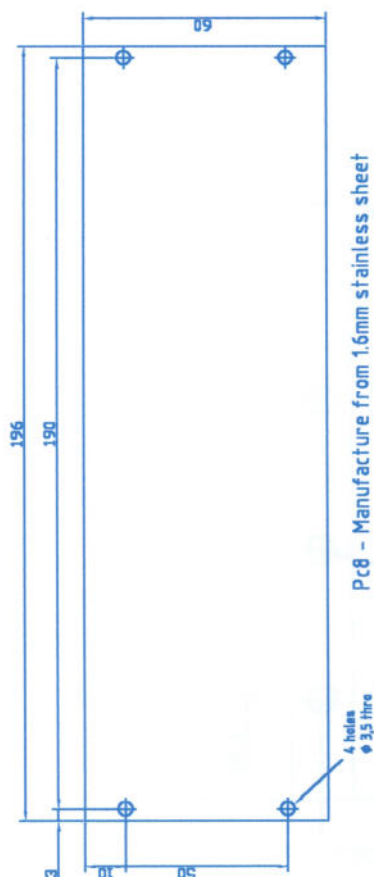
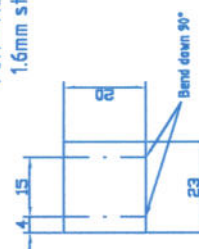


Pc1 - Manufacture from 3mm Stainless Sheet

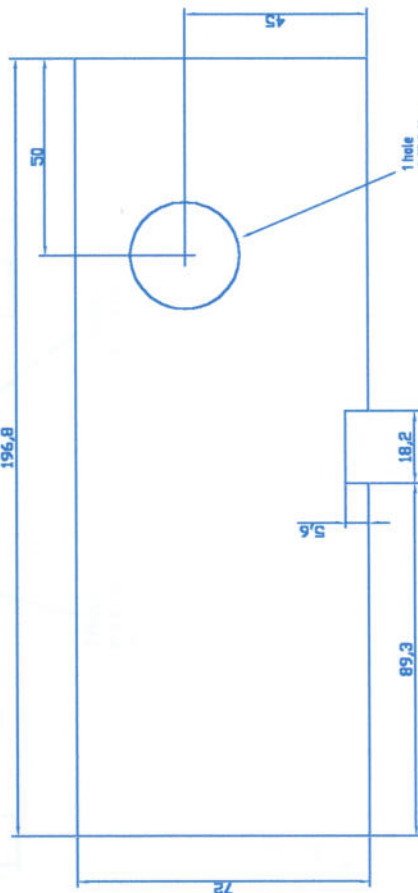
Pc10 Manufacture from
 ø32mm stainless steel bar



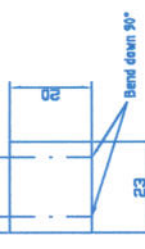
Pc11 - Manufacture from
 1.6mm stainless sheet



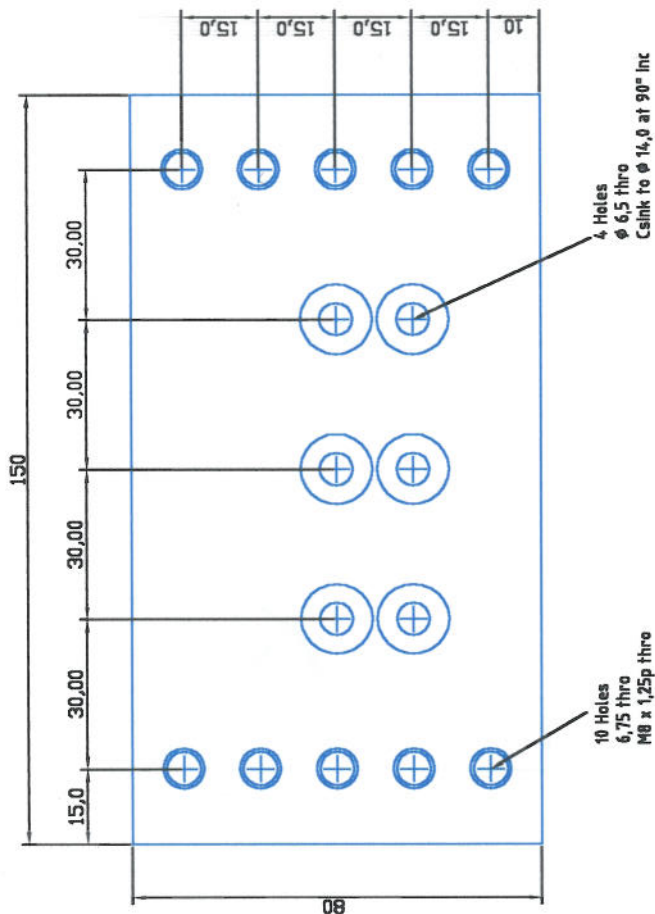
Pc8 - Manufacture from 1.6mm stainless sheet



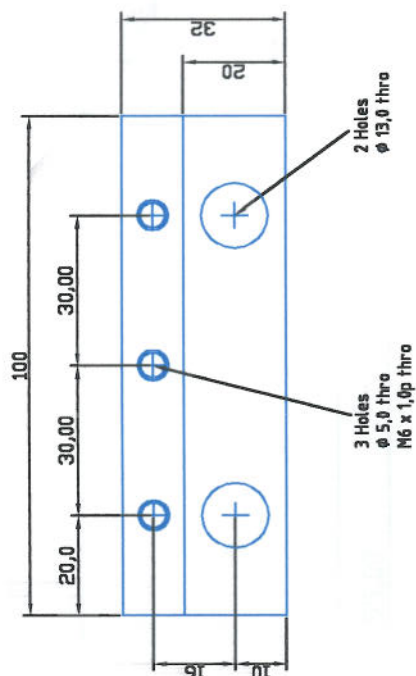
Pc9 Manufacture from 1.6mm stainless sheet



Itemref	Quantity	Title/Name, designation, material, dimension etc	Article No./Reference
Designed by MM	Checked by MM	Approved by - date MM 18 Feb 2004	Date Coolant Trough 18 Feb 2004
		File name Coolant Trough 18 Feb 2004	Scale NTS
Cranfield University SIMS			
Coolant Trough			
Edition 1			
Sheet 2 of 2			



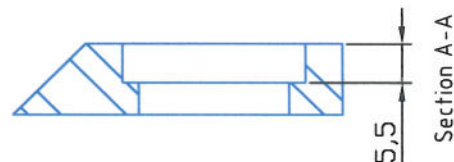
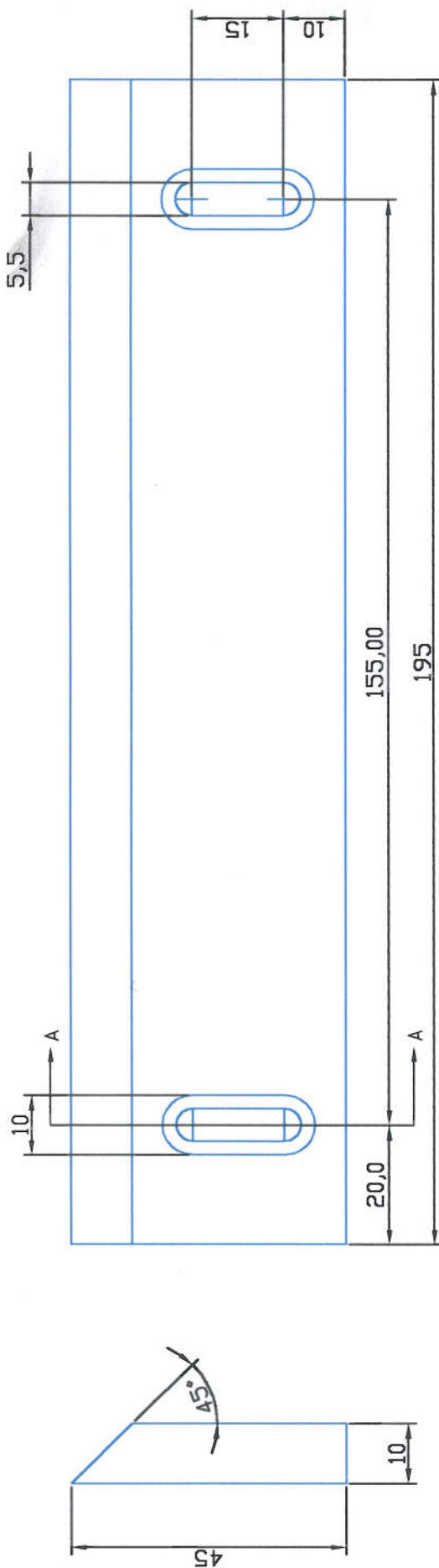
Piece 1
 Mild Steel (RSP), Stock size 150 x 80 x 12.5



Piece 2
 Mild Steel, Stock Size 25 x 40 x 100



Itemref	Quantity	Title/Name, designation, material, dimension etc	Article No./Reference
Designed by MH	Checked by MH	Approved by - date MH 2 Mar 05	Date 2 Mar 05
		File name	Scale NTS
Bracket Coolant Trough			
Cranfield University SIMS			Edition 1
			Sheet 1



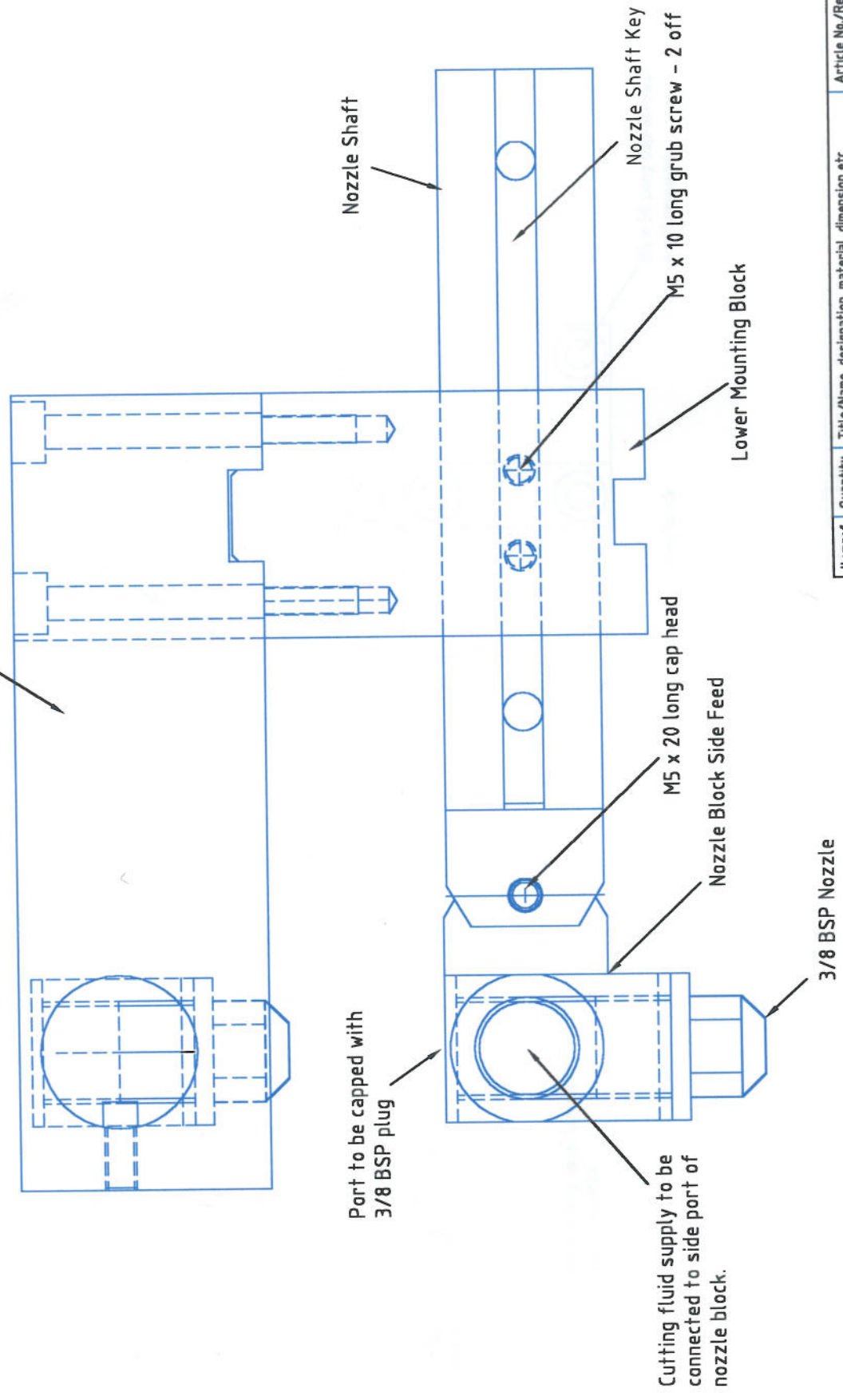
Material : Graphite
 Stock Size: 195mm x 45mm x 10mm thick
 2 off Required

Itemref	Quantity	Title/Name, designation, material, dimension etc	Article No./Reference
Designed by MM	Checked by MM	Approved by - date MM 19 Dec 05	File name Date 19 Dec 05
Cranfield University SIMS		Scrapers Coolant Trough	
		Edition 1	Scale NTS
		Sheet 1 of 1	

Appendix 7 – SAT Two Nozzle Fluid Application

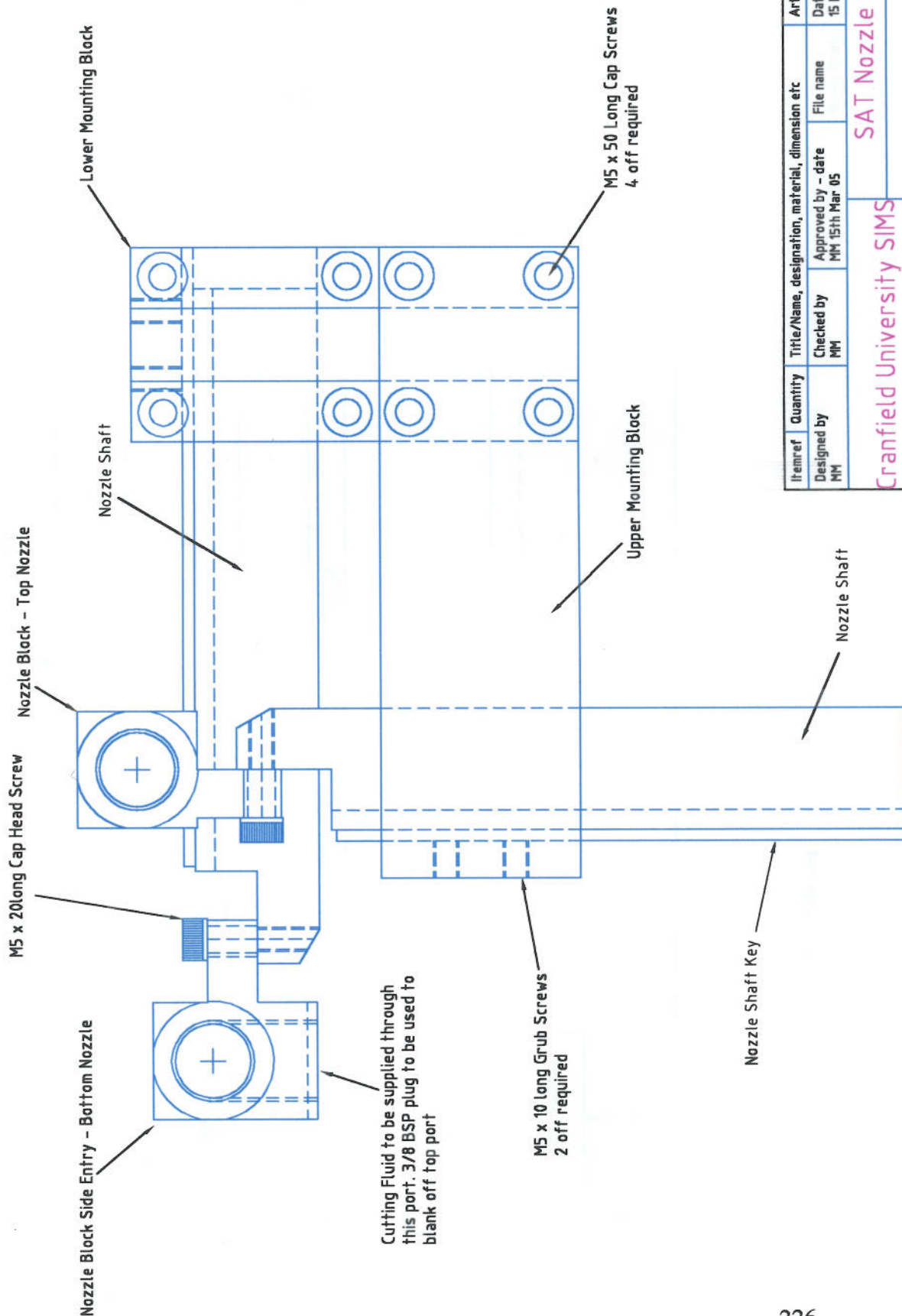
SIDE ELEVATION

Upper Mounting Block



Item/ref	Quantity	Title/Name, designation, material, dimension etc	Article No./Reference
Designed by MM	Checked by MM	Approved by - date MM 15th Mar 05	Date 15th Mar 05
		File name	Scale NTS
SAT Nozzle Assembly			
Cranfield University SIMS			Edition 1
			Sheet 1 of 2

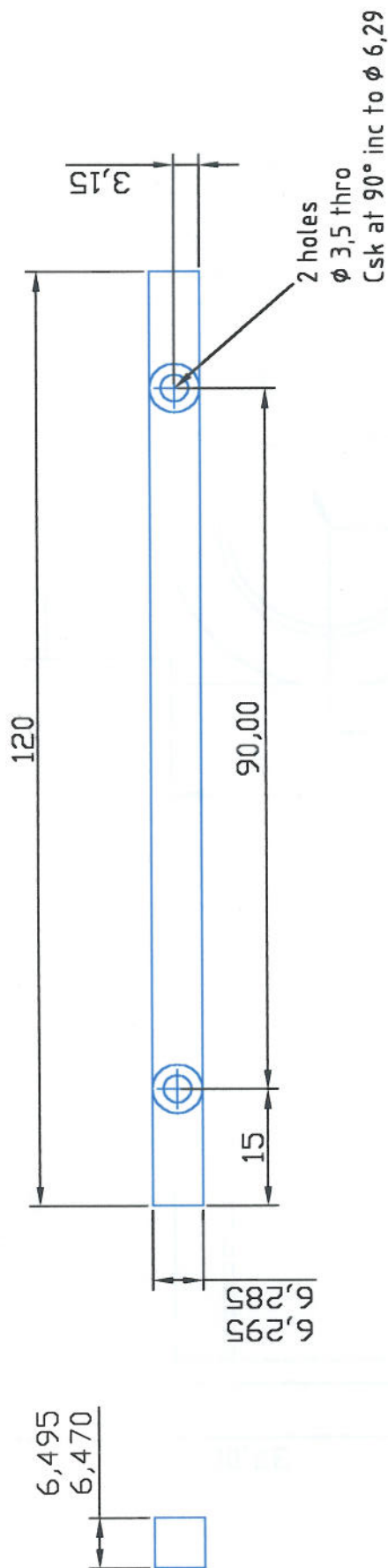
PLAN VIEW - BOTTOM NOZZLE SHOWN 60MM FURTHER FORWARD THAN SIDE ELEVATION FOR CLARITY



Item ref	Quantity	Title/Name, designation, material, dimension etc	Article No./Reference
Designed by MM	Checked by MM	Approved by - date MM 15th Mar 05	Date 15 Mar 05
Cranfield University SIMS			Scale NTS
SAT Nozzle Assembly			Edition 1
			Sheet 2 of 2



Item ref	Quantity	Title/Name, designation, material, dimension etc				Article No./Reference	
Designed by MM	Checked by MM	Approved by - date MM 30 Jan 05	File name Nozzle Shaft	Date 30 Jan 05	Scale NTS		
Cranfield University SMS					Nozzle Shaft		
					Edition 1		Sheet 1

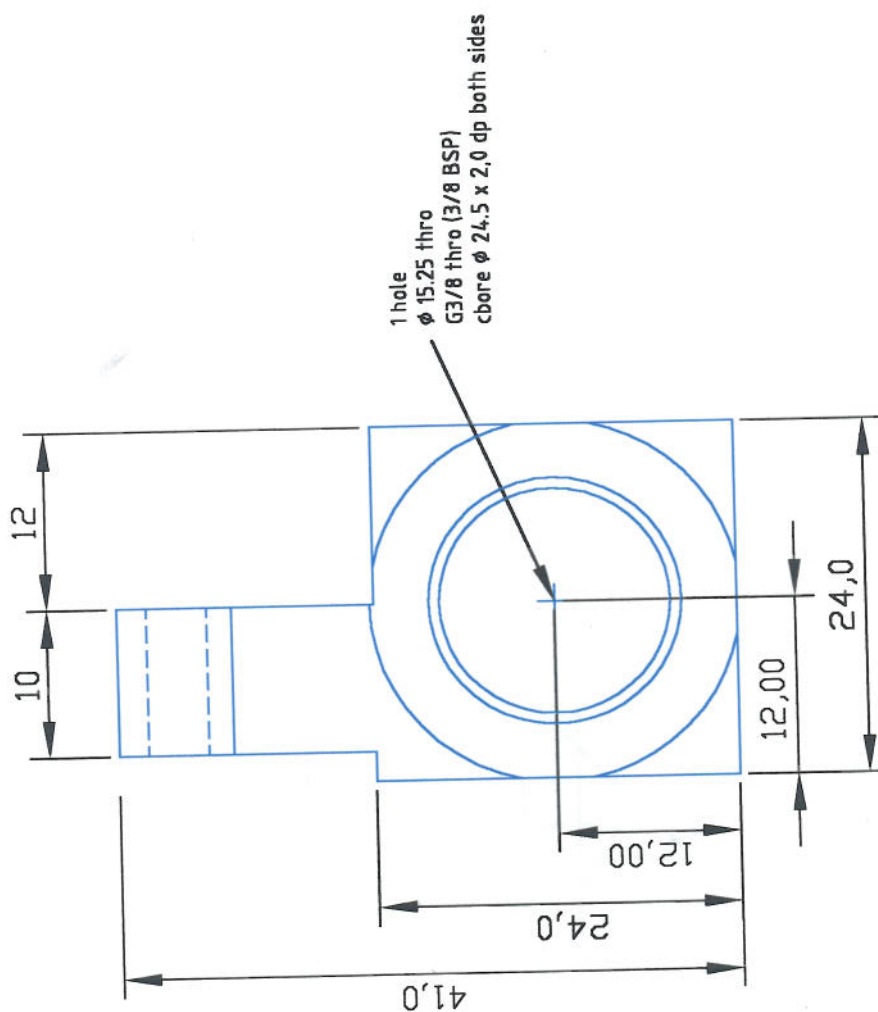
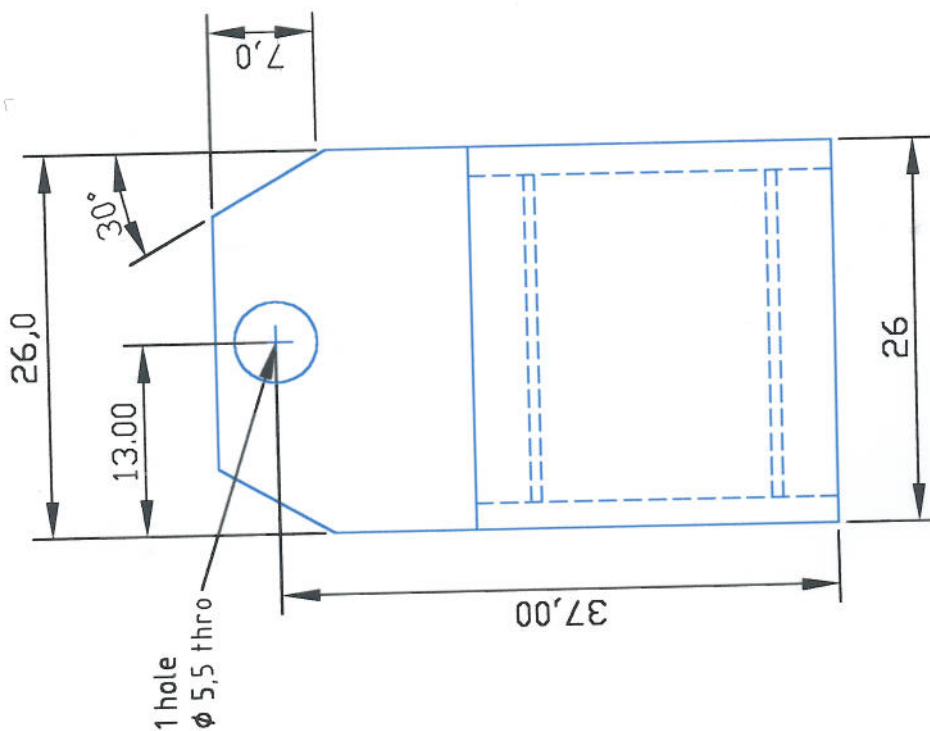


Material : 1/4" Key Steel, 120mm long
 2 off Required

Itemref	Quantity	Title/Name, designation, material, dimension etc	Article No./Reference
Designed by MM	Checked by MM	Approved by - date MM 26 Apr 05	Date 25 Apr 05
		File name	Scale NTS
Cranfield University SIMS		Nozzle Shaft Key	
		Edition 1	Sheet 1 of 1

ALL DIMENSIONS IN MM
 MACHINED WHOLE NUMBER DIMENSIONS ± 0.5
 MACHINED 1 PLACE DIMENSIONS ± 0.2 MM
 MACHINED 2 PLACE DIMENSIONS ± 0.1 MM

MACHINED SURFACES
 $3.2/\sqrt{R}$
 3RD ANGLE PROJECTION



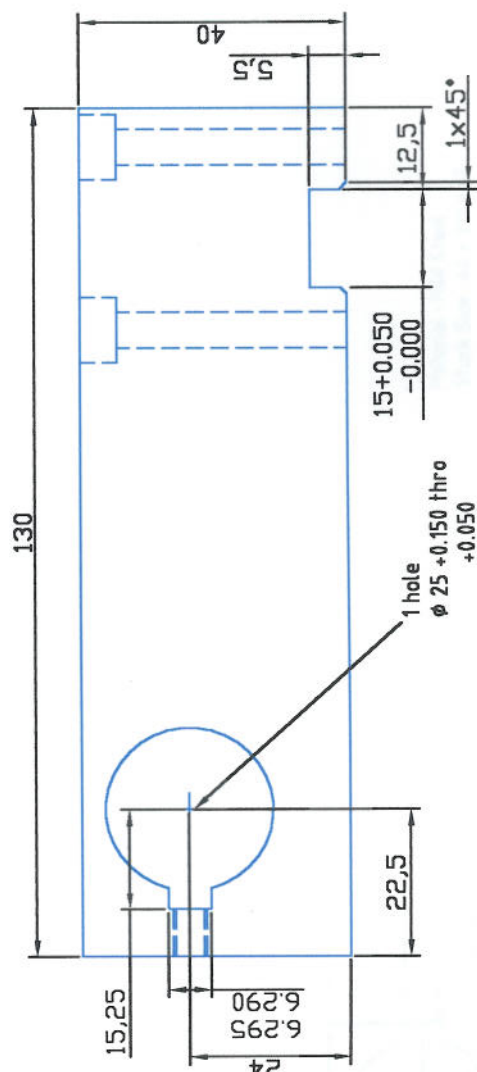
Material : Mild Steel
 Stock Size : 50 x 30 x 25
 1 off required

Itemref	Quantity	Title/Name, designation, material, dimension etc	Article No./Reference		
Designed by MM	Checked by MM	Approved by - date MM 29 Jan 05	File name Nozzle Block	Date 29 Jan 05	Scale NTS
Cranfield University SMS			Nozzle Block		
			Edition 1	Sheet 1	8

Itemref	Quantity	Title/Name, designation, material, dimension etc	Article No./Reference
Designed by MM	MM	Checked by MM	Approved by - date MM 11 Mar-05
		File name	Date 11 Mar-05
			Scale NTS

Nozzle Block Side Feed

<h2 style="color: #800080;">Cranfield University SIMS</h2>	<h2 style="color: #800080;">Nozzle Block Side Feed</h2>
	<div style="display: flex; justify-content: space-between;"> <div>Edition 1</div> <div>Sheet 1 of 1</div> </div>



Material : Mild Steel
Stock Size : 40 x 40 x 130
1 off required

Upper Mounting Block

ALL DIMENSIONS IN MM
 MACHINED WHOLE NUMBER DIMENSIONS +/- 0,5
 MACHINED 1 PLACE DIMENSIONS +/- 0,2MM
 MACHINED 2 PLACE DIMENSIONS +/- 0,1MM

3.2 / U05

3RD ANGLE PROJECTION

DO NOT SCALE

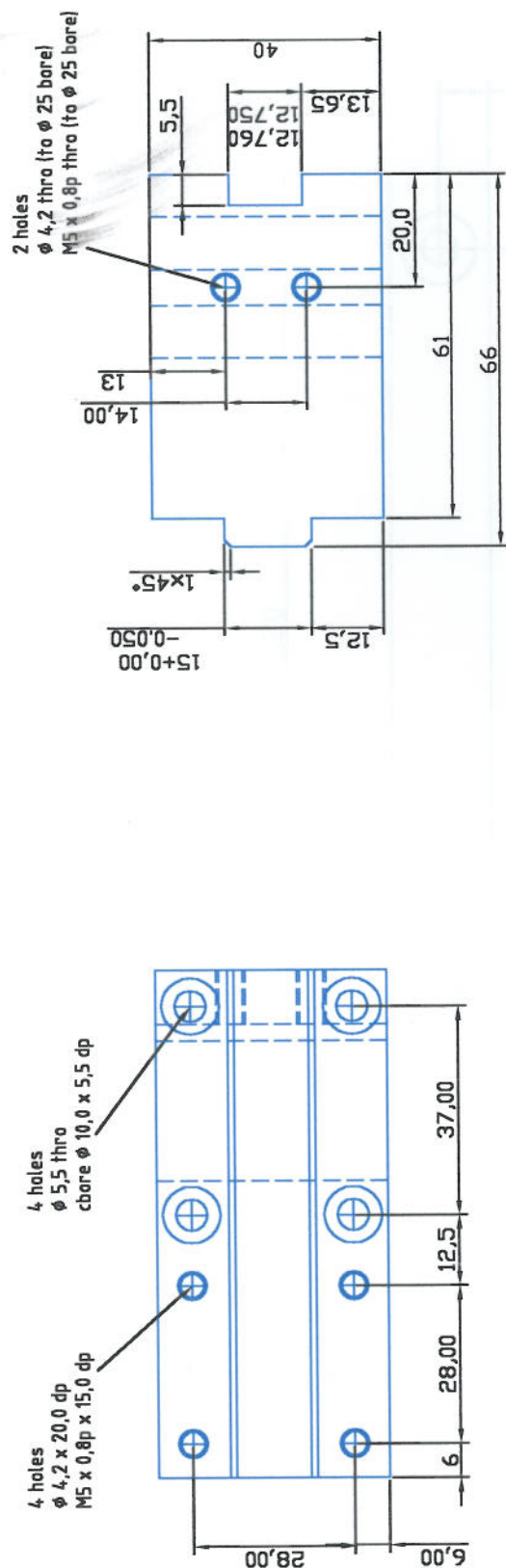
RevNo Revision note

Date

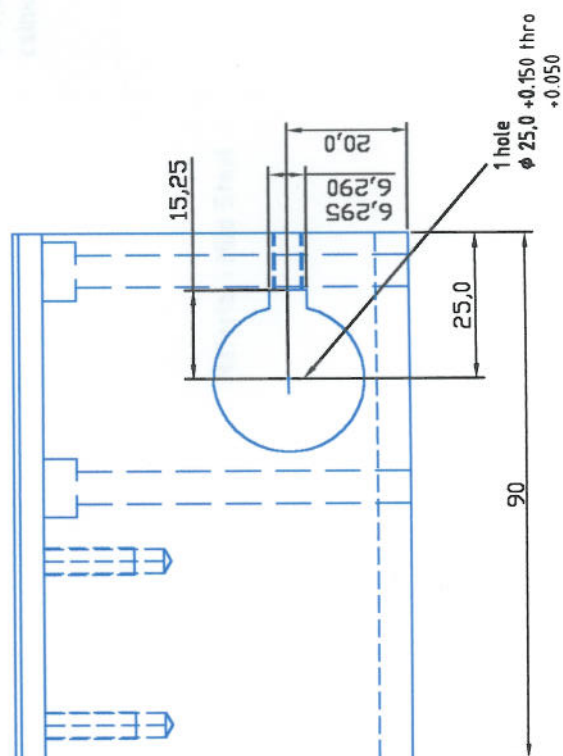
Signature Checked

4 holes
 $\phi 4,2 \times 20,0$ dp
 M5 x 0,8p x 15,0 dp

4 holes
 $\phi 5,5$ thro
 bore $\phi 10,0 \times 5,5$ dp



Material : Mild Steel
 Stock Size : 40 x 100 x 66
 1 off required



Itemref	Quantity	Title/Name, designation, material, dimension etc	Article No./Reference
Designed by MM	Checked by MM	Approved by - date MM 11 Mar 05	Date 11 Mar 05
		File name	Scale NTS
Lower Mounting Block			
Cranfield University SIMS			Edition 1
			Sheet 1 of 1

ALL DIMENSIONS IN MM

MACHINED WHOLE NUMBER DIMENSIONS +/- 0,5

MACHINED 1 PLACE DIMENSIONS +/- 0,2MM

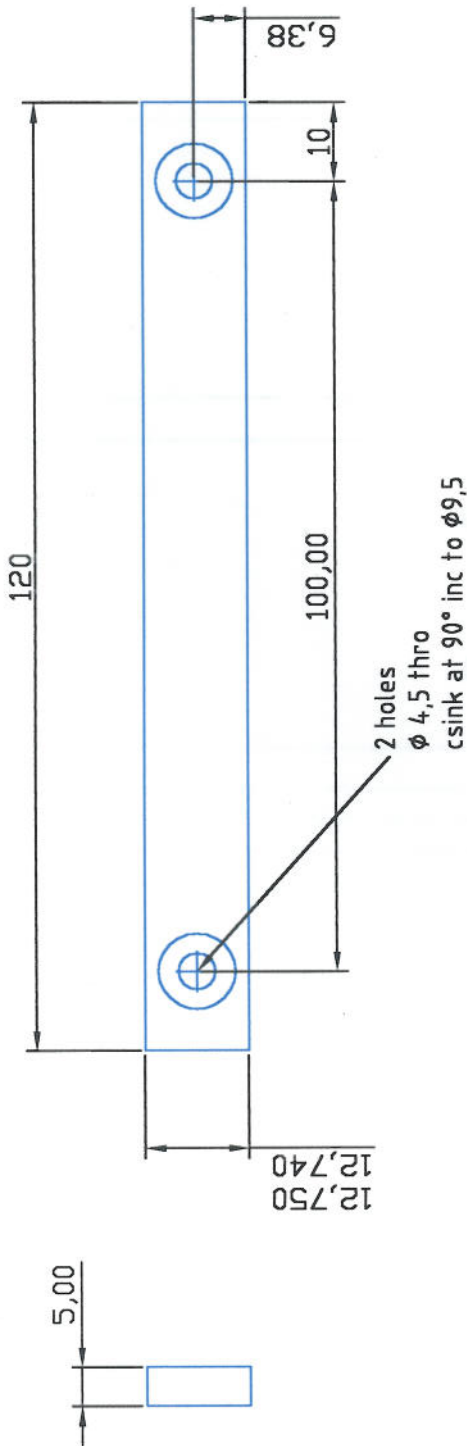
MACHINED 2 PLACE DIMENSIONS +/- 0,1MM

3.2

U05

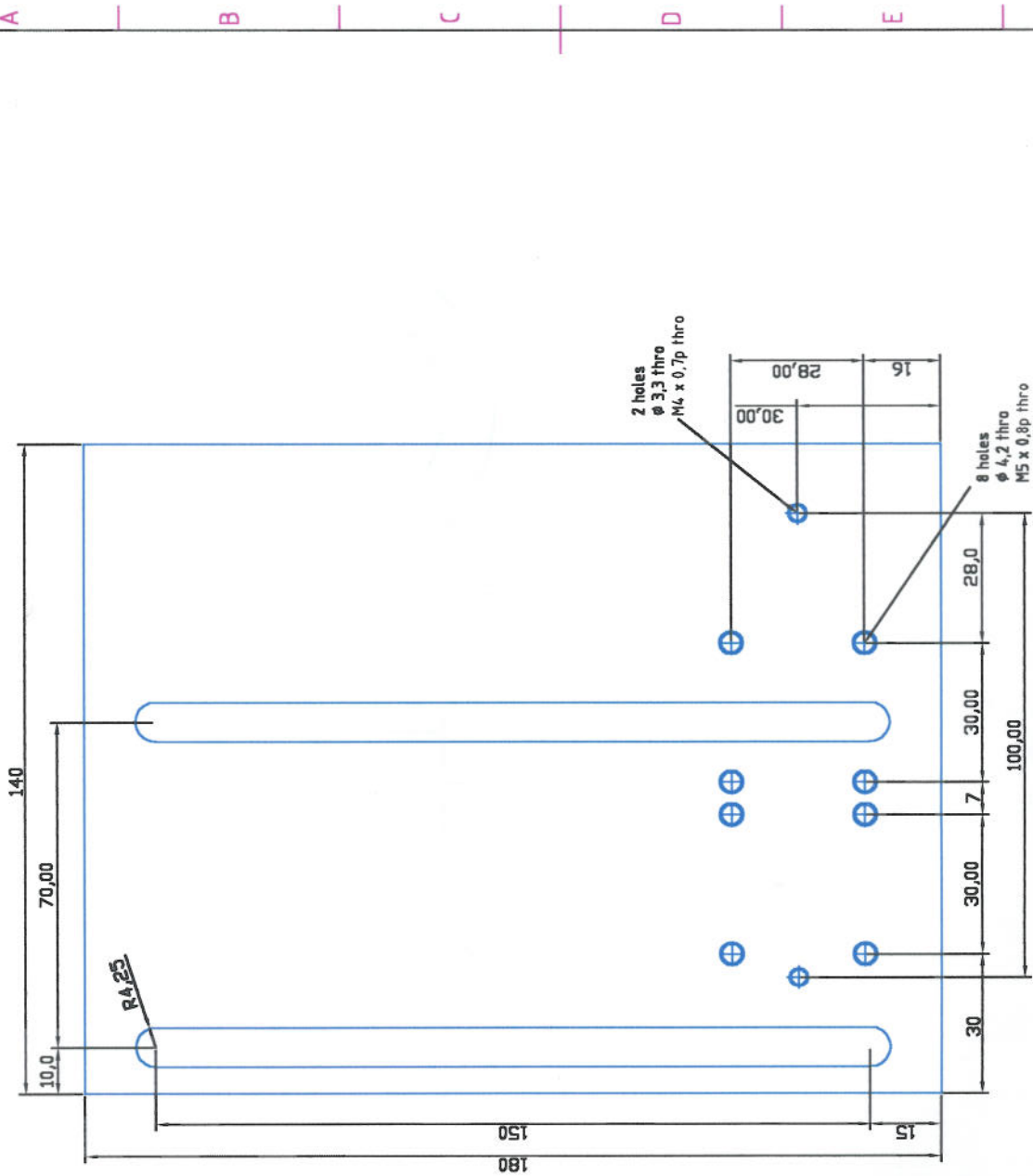
3RD ANGLE PROJECTION

Itemref	Quantity	Title/Name, designation, material, dimension etc	Article No./Reference
Designed by MM	Checked by MM	Approved by - date MM 27 Apr 05	Date 27 Apr 05
		File name	Scale NTS

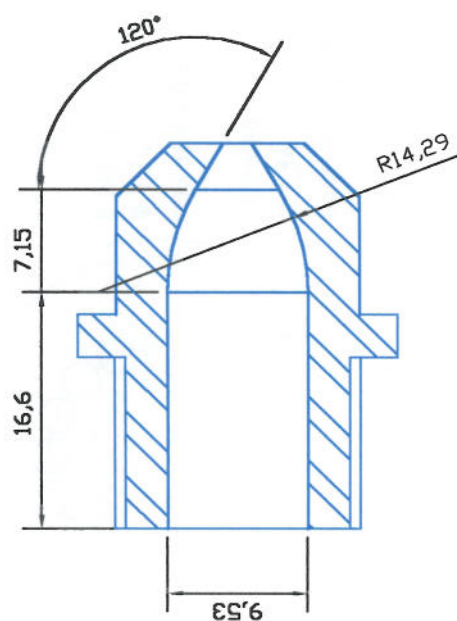
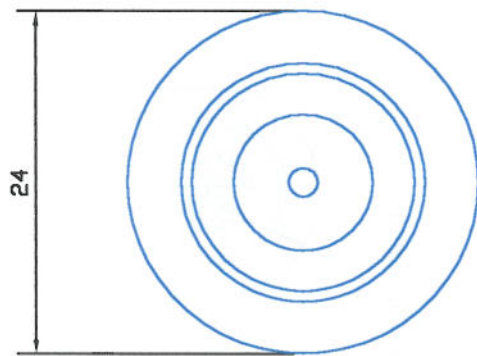
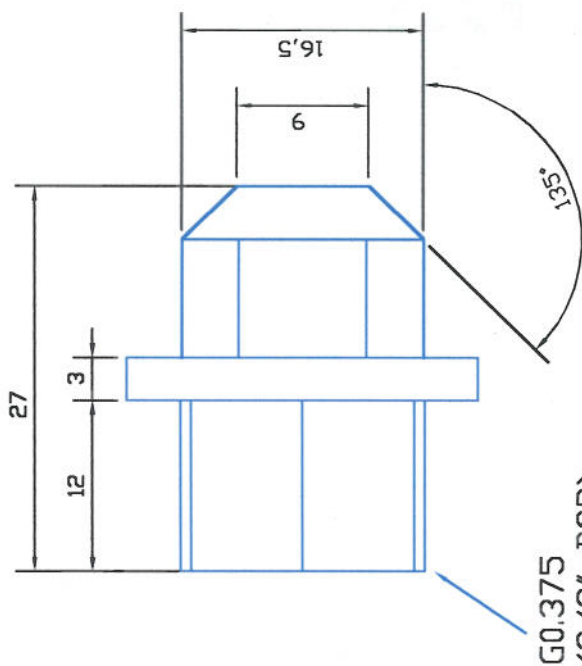
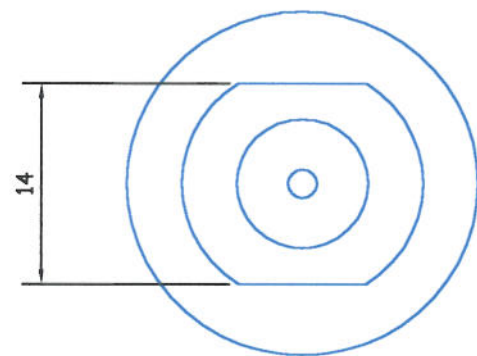


Material : Mild Steel

Itemref	Quantity	Title/Name, designation, material, dimension etc	Article No./Reference
Designed by MM	Checked by MM	Approved by - date MM 27 Apr 05	Date 27 Apr 05
		File name	Scale NTS
Cranfield University SIMS			Edition 1
Key Lower Mounting Block			Sheet 1 of 1

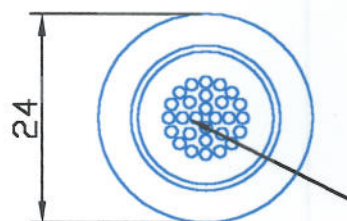


Itemref	Quantity	Title/Name, designation, material, dimension etc	Article No./Reference
Designed by	MM	Checked by	MM
Approved by - date	MM 7 Apr 05	File name	Scale
			NTS
			Date
			7 Apr 05
			Sheet
			1 of 1
			8

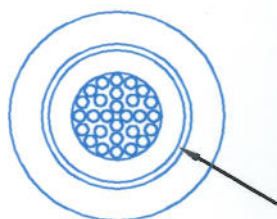
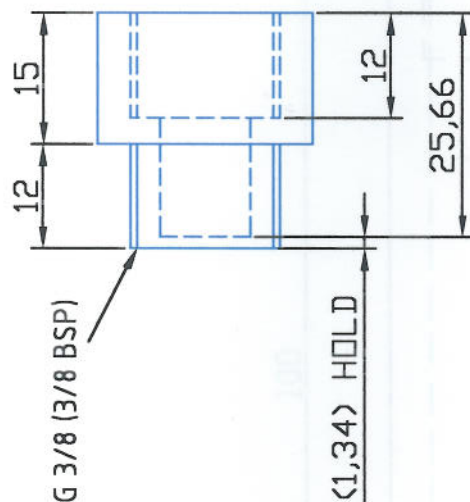


Nominal Aperture Size 1.94mm
 Material : Brass
 Note, Maximum attainable aperture size = 5mm

Item ref	Quantity	Title/Name, designation, material, dimension etc	Article No./Reference
Designed by MM	Checked by MM	Approved by - date MM 18th Feb 2005	Date 18th Feb 2005
		File name	Scale NTS
Cranfield University SIMS		Webster Nozzle G0.375	
		Edition 1	Sheet 1



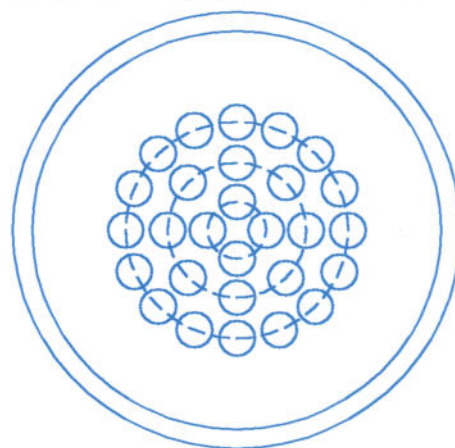
See enlarged view
 for hole details



1 hole

ϕ 10,00 (flat bottom, see detail for depth)
 ϕ 15,25 (flat bottom, see detail for depth)
 G3/8 (3/8 BSP, flat bottom tap, see detail for depth)

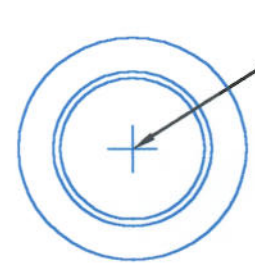
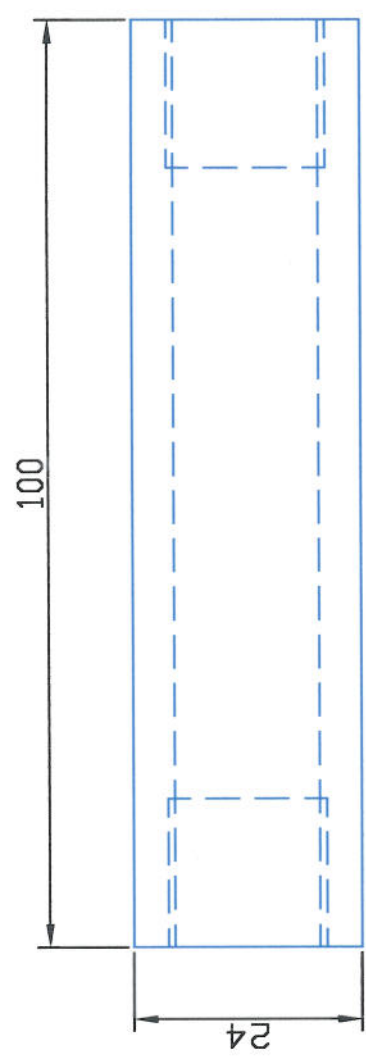
- 4 holes
 ϕ 1,34 thro
 equi-spaced on 2,18 PCD
- 8 holes
 ϕ 1,34 thro
 equispaced on 5,16 PCD
- 16 holes
 ϕ 1,34 thro
 equi-spaced on 8,28 PCD



Enlarged View of Holes

Material : Brass
 2 off required

Itemref	Quantity	Title/Name, designation, material, dimension etc	Article No./Reference
Designed by MH	Checked by MH	Approved by - date MH 21 May 2005	Date 21 May 2005
		File name	Scale NTS
Cranfield University SIMS		Uniform Flow Conditioner	
		Edition 1	Sheet 1 of 1

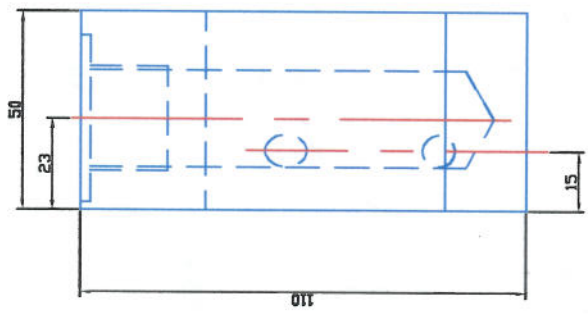
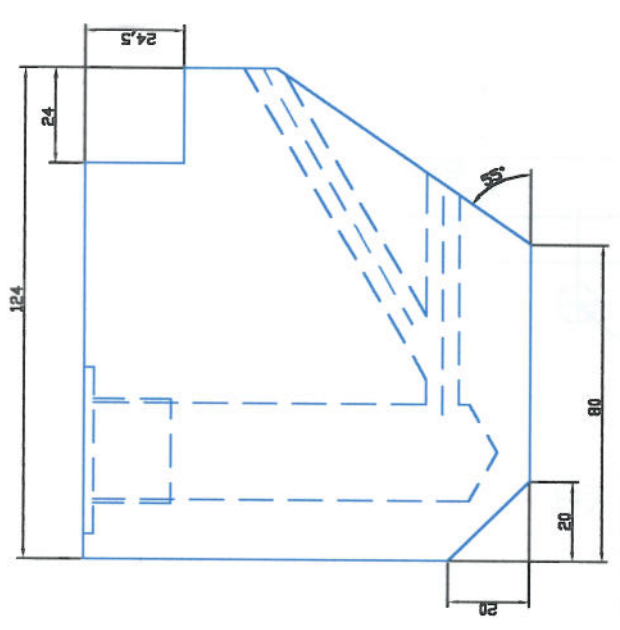


1 hole
Ø 15,25 thro
G3/8 (3/8 BSP) x 16, 0 dp both ends

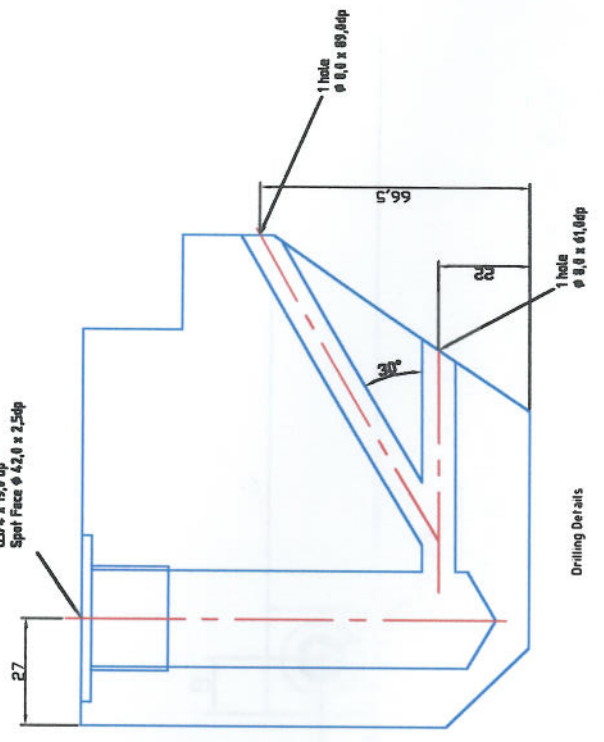
Material : Mild Steel
Stock Size : Ø 25 x 100 long
1 off required

Itemref	Quantity	Title/Name, designation, material, dimension etc			Article No./Reference	
Designed by MM	Checked by MM	Approved by - date MM 13 Mar 05	File name	Date 13 Mar 05	Scale NTS	
Cranfield University SIMS		100mm Extension				
		Edition 1			Sheet 1 of 1	

Appendix 8 – Shoe Nozzle – Drawings

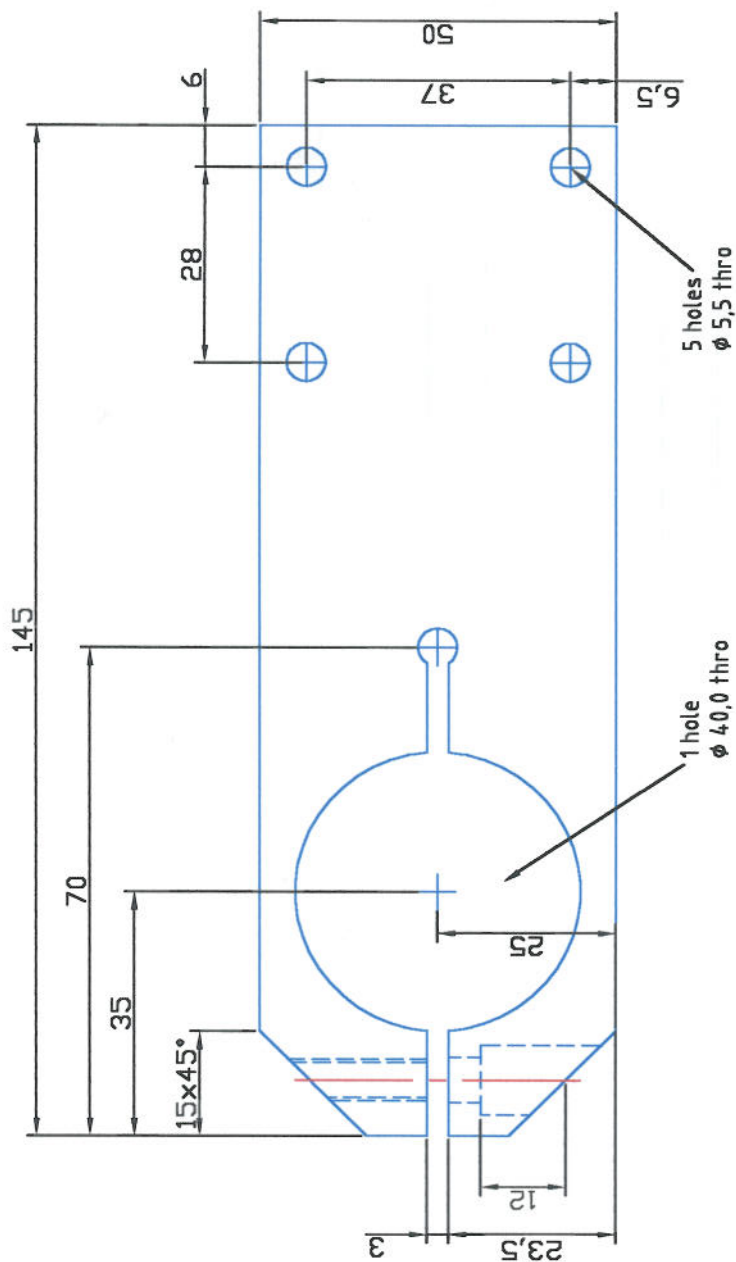


1 hole
 $\phi 24.5 \times 95 \text{ dp}$
 $63/45 \times 19.8 \text{ dp}$
 Spot face $\phi 42.8 \times 2.5 \text{ dp}$



Material : Graphite
 1 off Required

Itemref	Quantity	Title/Name, designation, material, dimension etc	Article No./Reference
Designed by MM	Checked by MM	Approved by - date MM 12 Jan 06	Date 12 Jan 06
		File name	Scale NTS
Cranfield University SMS		Coolant Shoe Offset Holes	
		Edition 1	Sheet 1 of 1



Material : Aluminium

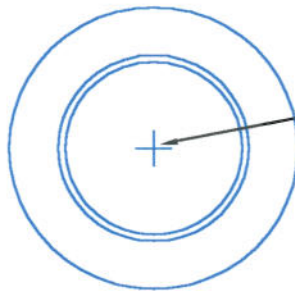
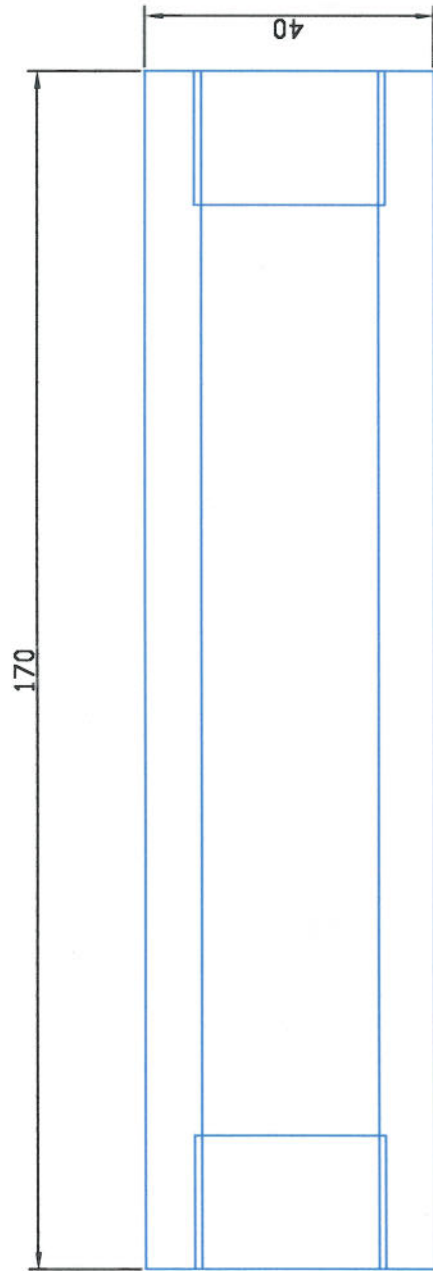
Itemref	Quantity	Title/Name, designation, material, dimension etc	Article No./Reference
Designed by MM	Checked by MM	Approved by - date MM 21 Aug 05	Date 21 Aug 05
		File name	Scale NTS

Coolant Shoe Mounting Bracket

Cranfield University SIMS

Edition 1	Sheet 1 of 1
--------------	-----------------

Core Ø 6,5 thro to slot
Core Ø 11,0 x 12,0dp (on centre line - see detail)

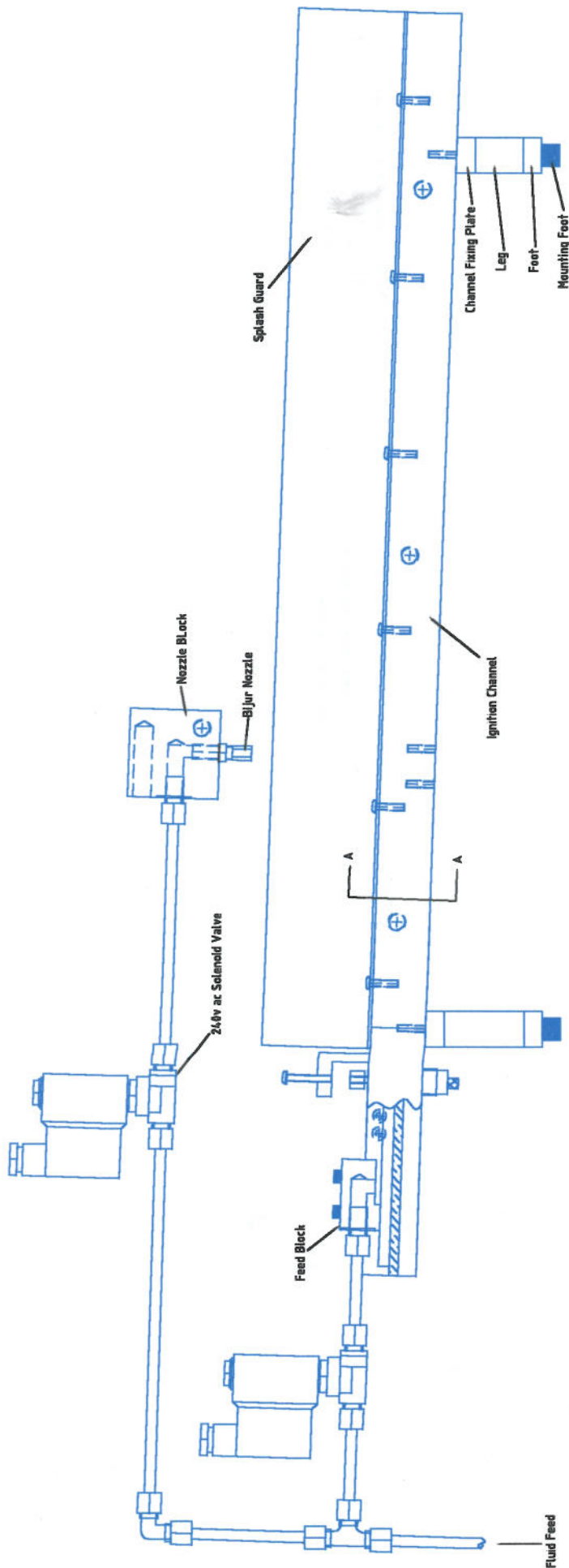


1 hole
 ϕ 24,5 thro
Thread G3/4 x 19,0 dp at both ends

Material : Aluminium

Itemref	Quantity	Title/Name, designation, material, dimension etc	Article No./Reference
Designed by MM	Checked by MM	Approved by - date MM 12 Aug 05	Date 12 Aug 05
Cranfield University SIMS		G3/4 Extension 170mm long	Scale NTS
		1	Sheet 1 of 1

Appendix 9 – Cutting Fluid Ignition Test Rig

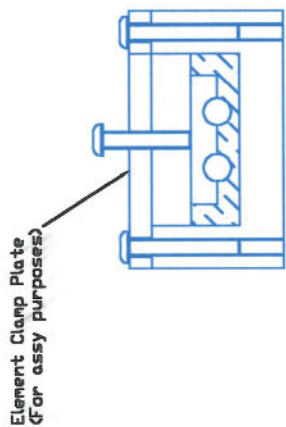
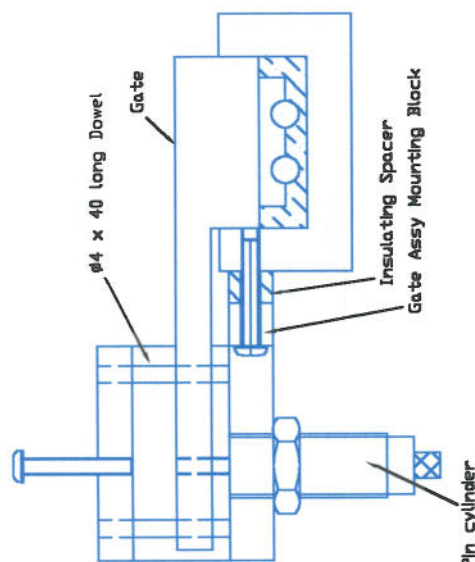
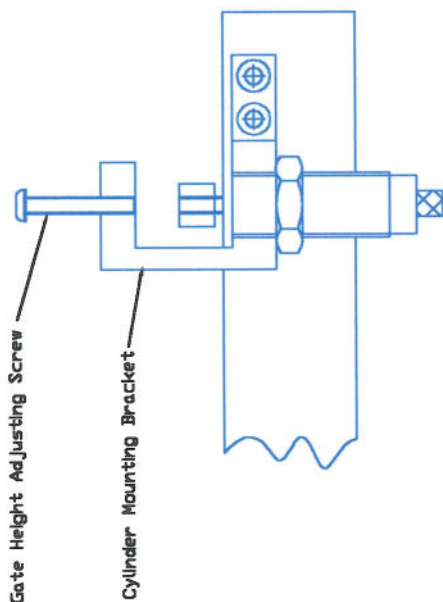


Bought Out Parts

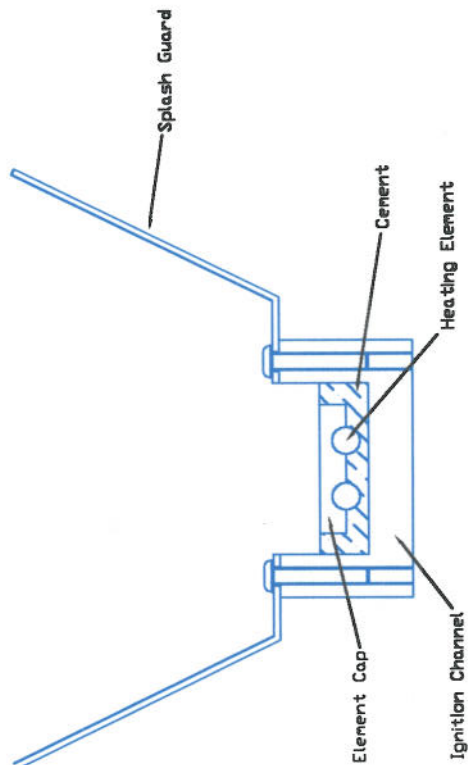
- 6mm s/s equal elbow - 1 off - RS 439-565
- 6mm s/s equal tee - 1 off - RS 439-600
- 6mm s/s tube 2m length - 1 off (pack of 2) - RS 190-866
- 1/8 bsp s/s male stud coupling - 6 off - RS 439-391
- 1/8 bsp s/s plug - 1 off - RS 295-2723
- 1/8 bsp s/s double female sleeve - RS 310-8618 - 1 off
- 10mm bore 15mm stroke single acting pin cylinder - RS 183-3994 - 1 off
- Flawtech F133-10-230 1/8 BSP, 240VAC Solenoid Valve - 2 off
- Bjour Jet Tip B134 - 1 off
- 10 x 40 long 100V Cartridge Heater RS 376-1821 - 1 off
- Type K Adjustable Bayonet Thermocouple RS 290-5042 - 4 off
- 1/8 BSP Thermocouple Adapter RS 150-032 - 4 off

Itemref	Quantity	Title/Name, designation, material, dimension etc	Article No./Reference
Designed by MM	Checked by MM	Approved by - date MM 17 May 2005	Date 17 May 05
		File name	Scale NTS
Cranfield University SIMS		Inclined Channel Test Rig	
		Edition 1	Sheet 1 of 2

View of pneumatically operated gate

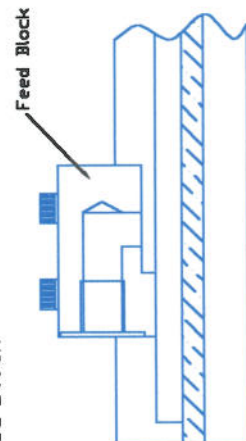
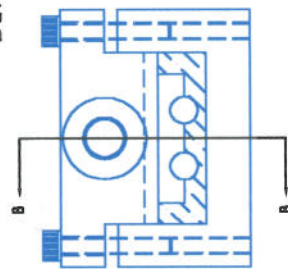


Section A-A
Detail of Element Clamp Plate
used for Assembly



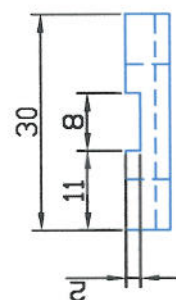
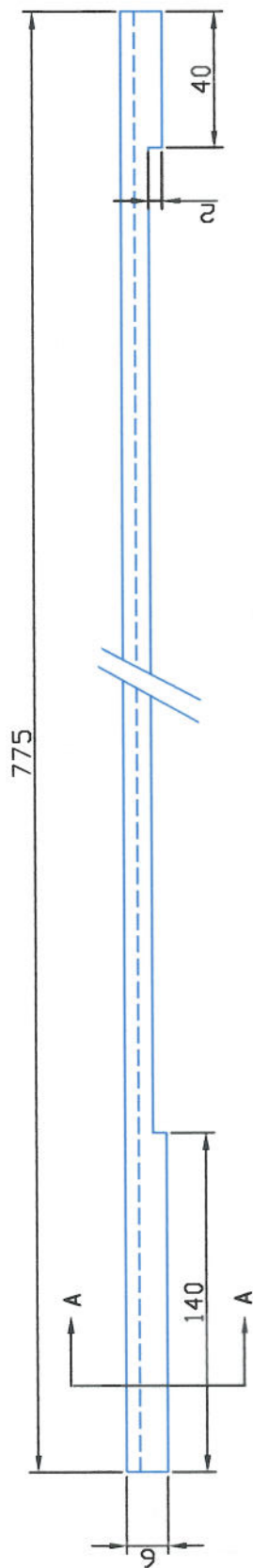
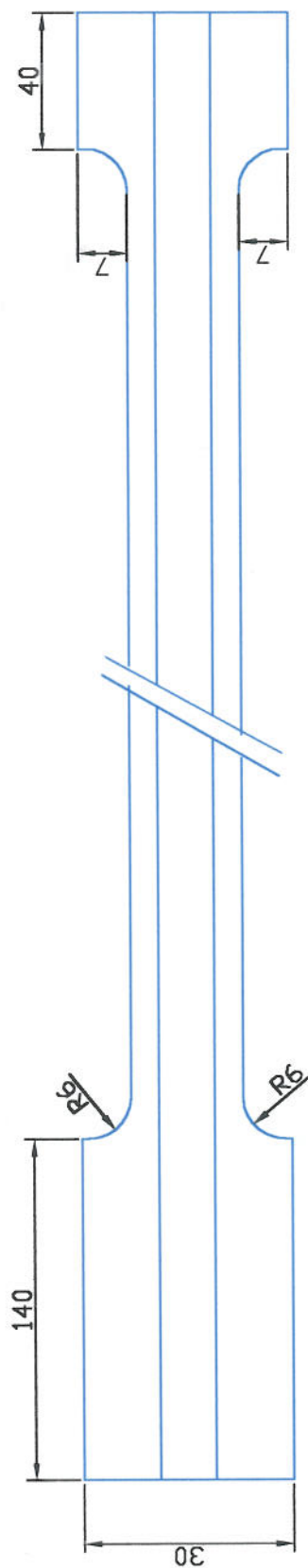
Section A-A

Detail of Feed Block



Section B-B

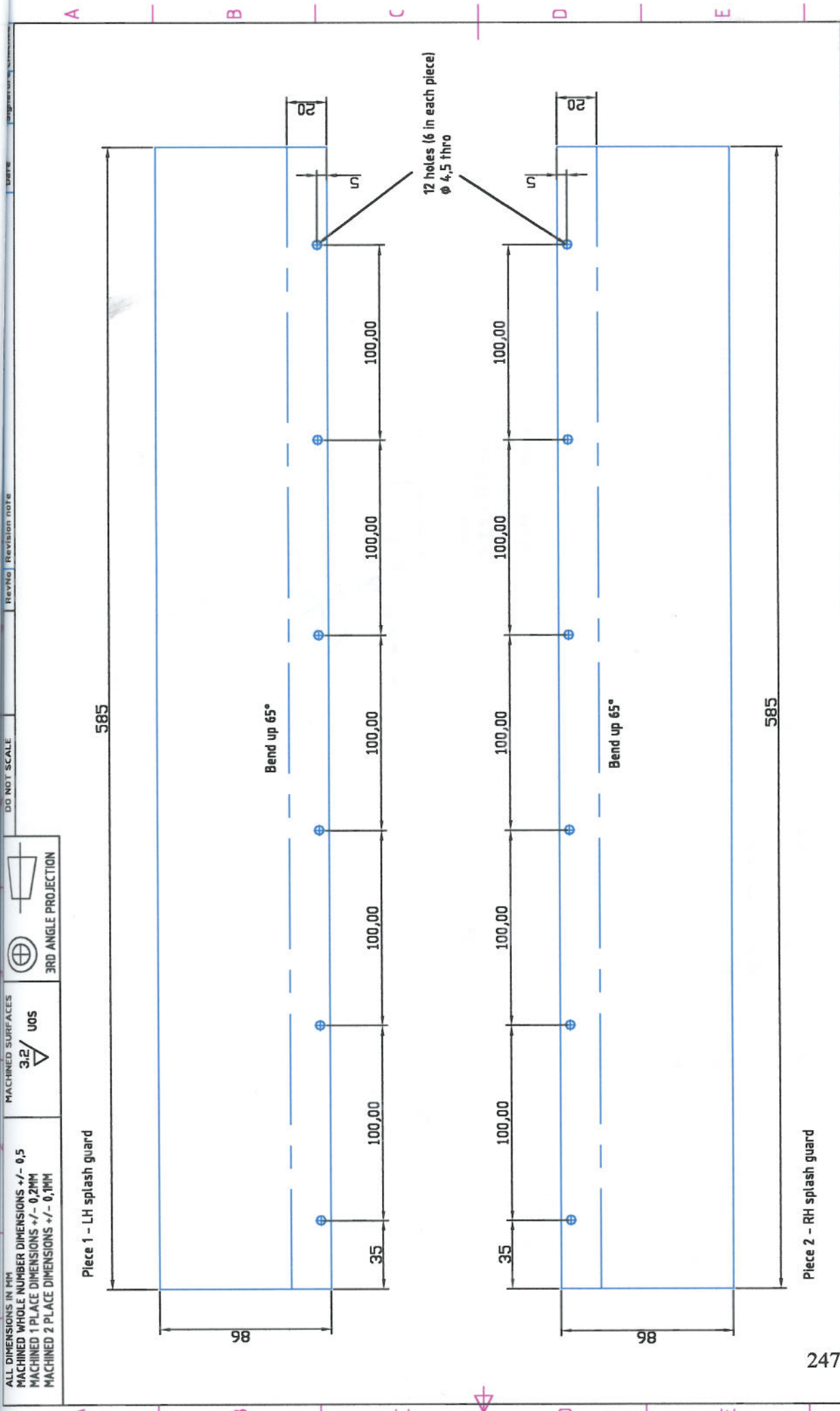
Itemref	Quantity	Title/Name, designation, material, dimension etc	Article No./Reference
Designed by MM	Checked by MM	Approved by - date MM 17 May 05	Date 17 May 05
		File name	Scale NTS
Cranfield University SIMS		Inclined Channel Test Rig	
		Edition 1	Sheet 2 of 2



Section A-A

Material : Stainless Steel
 Stock Size : 30 x 6 x 775

Itemref	Quantity	Title/Name, designation, material, dimension etc	Article No./Reference
Designed by MM	Checked by MM	Approved by - date MM 4, Apr 05	Date 4, Apr 05
		File name	Scale NTS
Stainless Element Cap			
Cranfield University SIMS			Edition 1
			Sheet 1 of 1



ALL DIMENSIONS IN MM

MACHINED WHOLE NUMBER DIMENSIONS +/- 0,5

MACHINED 1 PLACE DIMENSIONS +/- 0,2MM

MACHINED 2 PLACE DIMENSIONS +/- 0,1MM

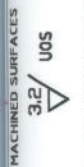
MACHINED SURFACES

3.2 / U05

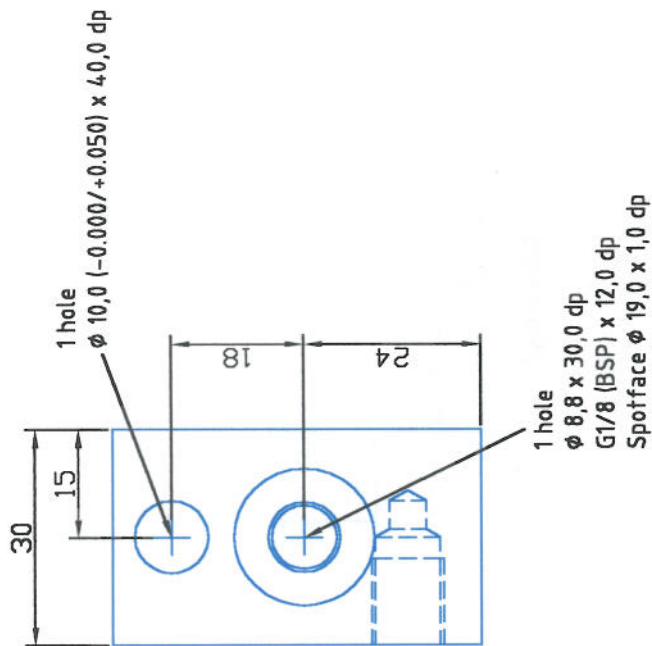
3RD ANGLE PROJECTION

Itemref	Quantity	Title/Name, designation, material, dimension etc	Article No./Reference
Designed by MH	Checked by MH	Approved by - date MH 4 Apr 05	Date 4 Apr 05
		File name	Scale NTS
Cranfield University SIMS		LH and RH Splash Guard	
		Edition 1	Sheet 1 of 1

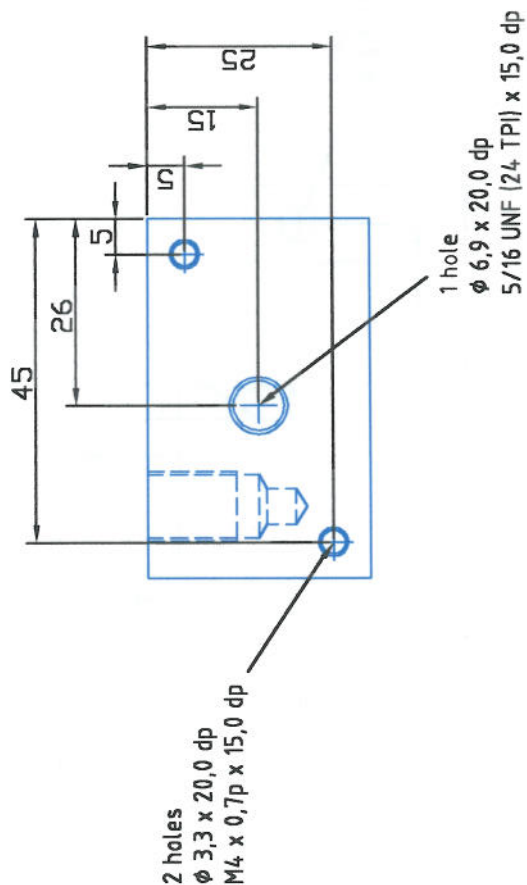
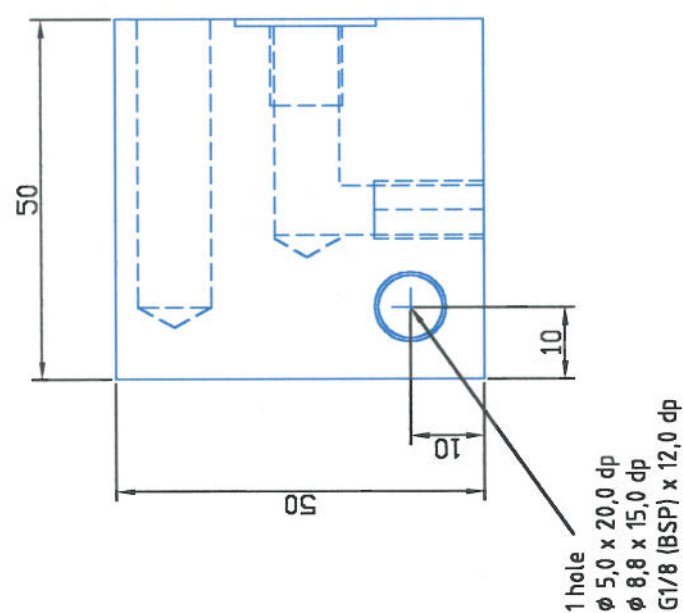
Material : 585 x 86 x 1,6 thick stainless sheet - 2 Pieces



ALL DIMENSIONS IN MM
MACHINED WHOLE NUMBER DIMENSIONS +/- 0,5
MACHINED 1 PLACE DIMENSIONS +/- 0,2MM
MACHINED 2 PLACE DIMENSIONS +/- 0,1MM



Material : Aluminium
Stock Size : 50 x 50 x 30

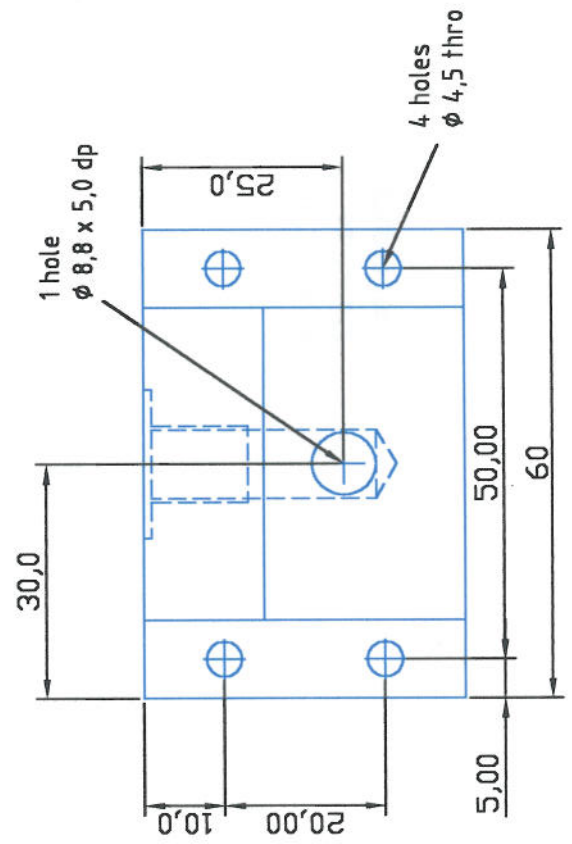
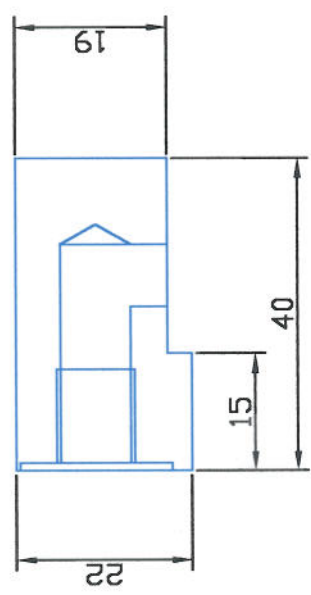
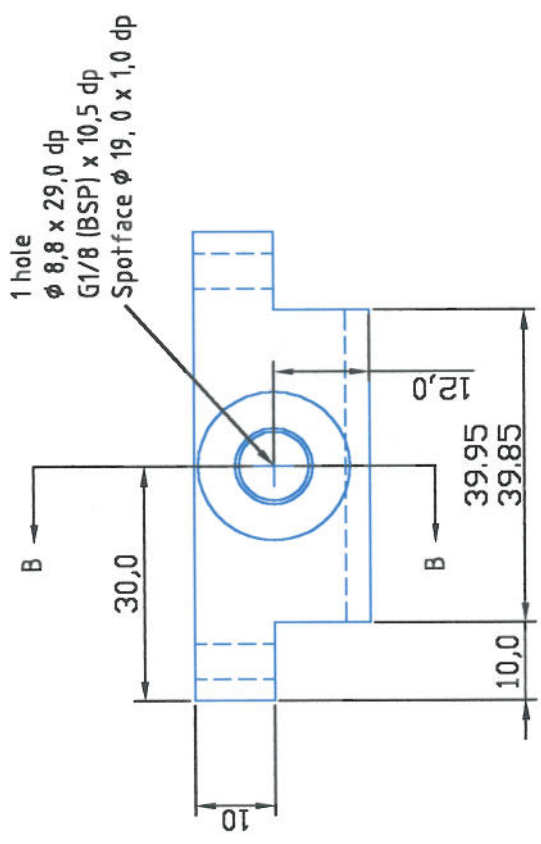


Itemref	Quantity	Title/Name, designation, material, dimension etc	Article No./Reference
Designed by MM	Checked by MM	Approved by - date MM 10 Apr 05	Date 10 Apr 05
		File name	Scale NTS
Nozzle Block			
Cranfield University SIMS			Edition 1
			Sheet 1 of 1

ALL DIMENSIONS IN MM
MACHINED WHOLE NUMBER DIMENSIONS +/- 0,5
MACHINED 1 PLACE DIMENSIONS +/- 0,2MM
MACHINED 2 PLACE DIMENSIONS +/- 0,1MM

MACHINED SURFACES
3.2 / U05

3RD ANGLE PROJECTION



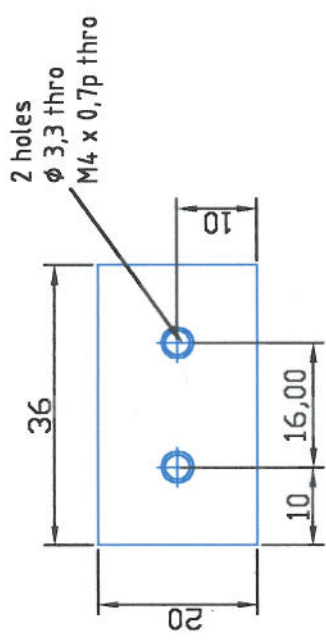
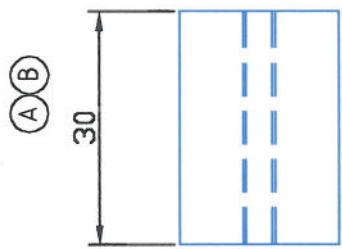
Material : Aluminium
Stock Size : 60 x 40 x 22

Itemref	Quantity	Title/Name, designation, material, dimension etc	Article No./Reference
Designed by MM	Checked by MM	Approved by - date MM 4 Apr 05	Date 4 Apr 05
		File name	Scale NTS
Feed Block			
Cranfield University SIMS			Edition 1
			Sheet 1 of 1

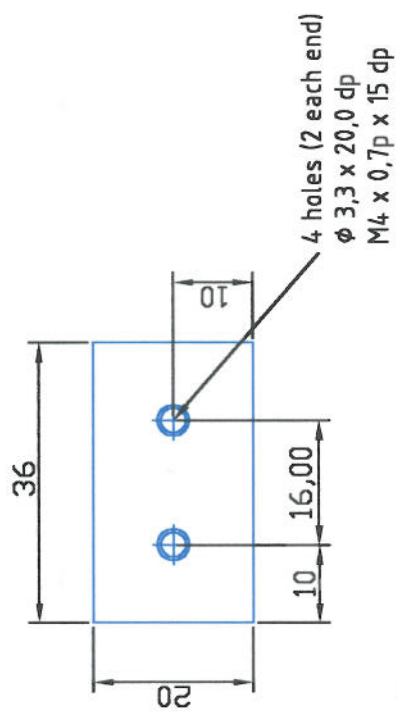
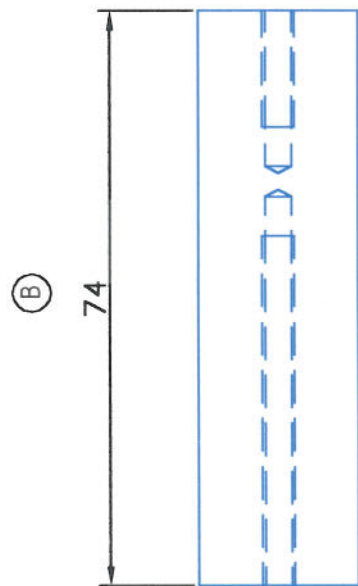


Itemref	Quantity	Title/Name, designation, material, dimension etc			Article No./Reference	
Designed by MM		Checked by MM	Approved by - date MM 10 Apr 05	File name	Date 10 Apr 05	Scale NTS
Cranfield University SIMS Test Rig Feet						

ALL DIMENSIONS IN MM MACHINED WHOLE NUMBER DIMENSIONS +/- 0.5 MACHINED 1 PLACE DIMENSIONS +/- 0.2MM MACHINED 2 PLACE DIMENSIONS +/- 0.1MM	MACHINED SURFACES 3.2 U05	3RD ANGLE PROJECTION	DO NOT SCALE	RevNo Revision note		Date	Signature	Checked
				A	Leg lengthened was 20mm now 26.5mm			
				B	Both Legs lengthened by 30mm			
						16 May 05	MM	MM
						30 Sep 05	MM	MM



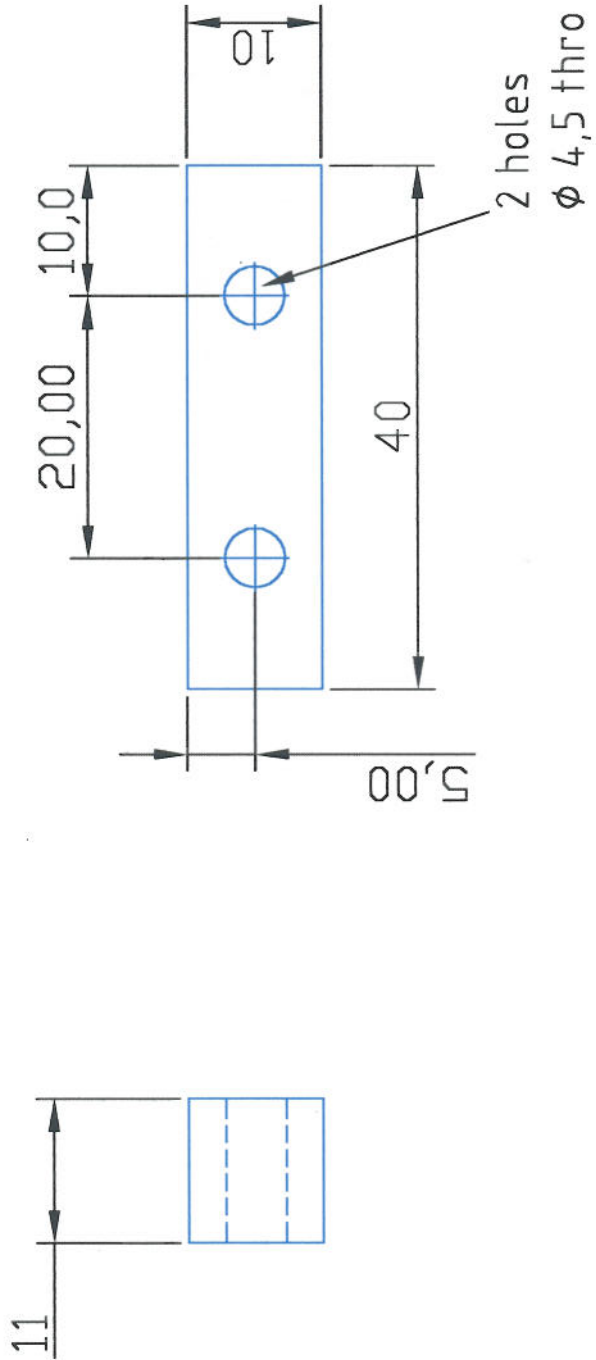
Piece 1



Piece 2

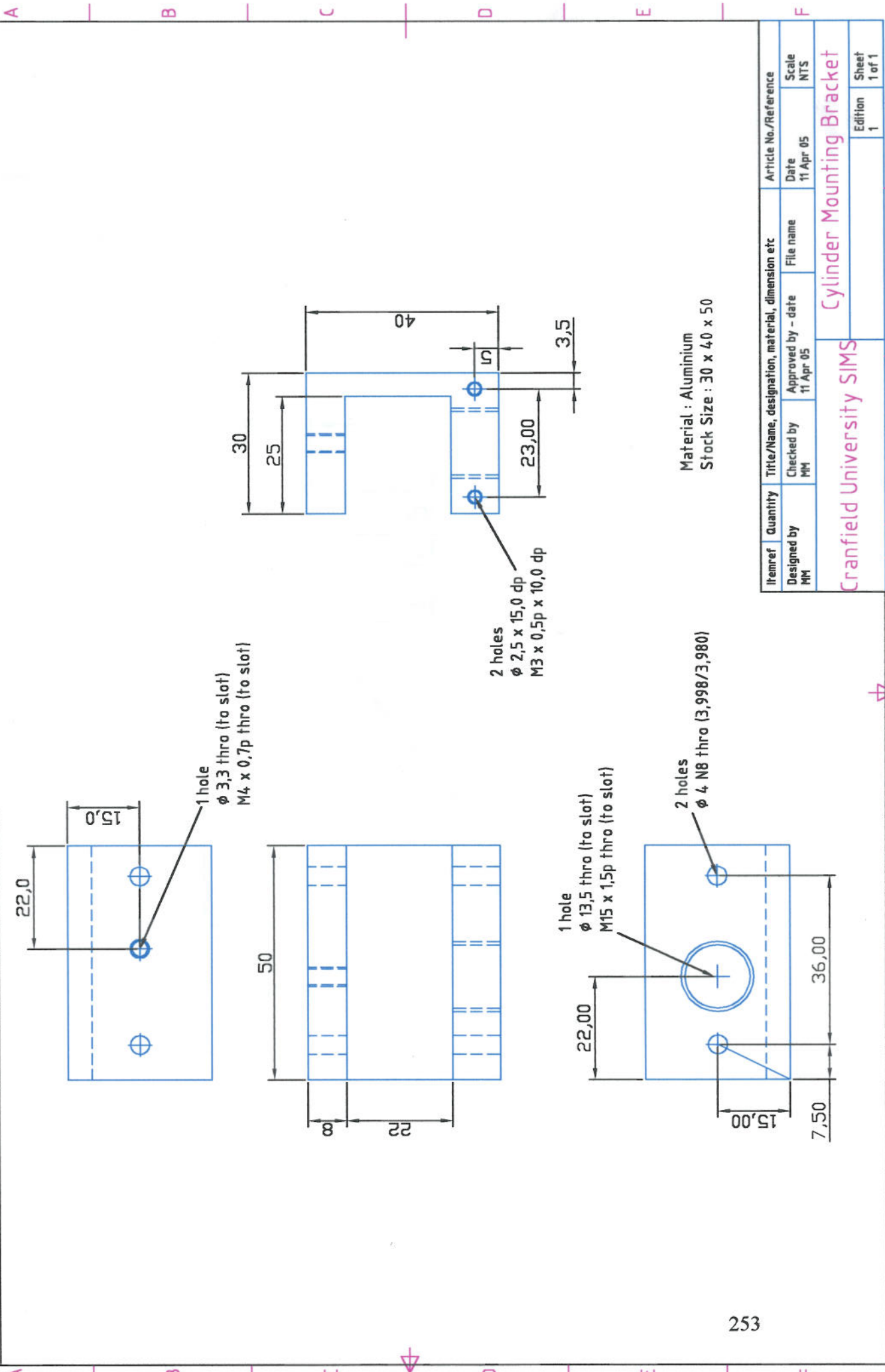
Material : Aluminium
Stock Size : 20 x 20 x 36 (piece 1)
20 x 74 x 36 (piece 2)

Itemref	Quantity	Title/Name, designation, material, dimension etc	Article No./Reference
Designed by MM	Checked by MM	File name	Date 10 Apr 05
	Approved by - date MM 10 Apr 05		Scale NTS
Cranfield University SIMS			Test Rig Legs
			Sheet 1 of 1
			Edition 1

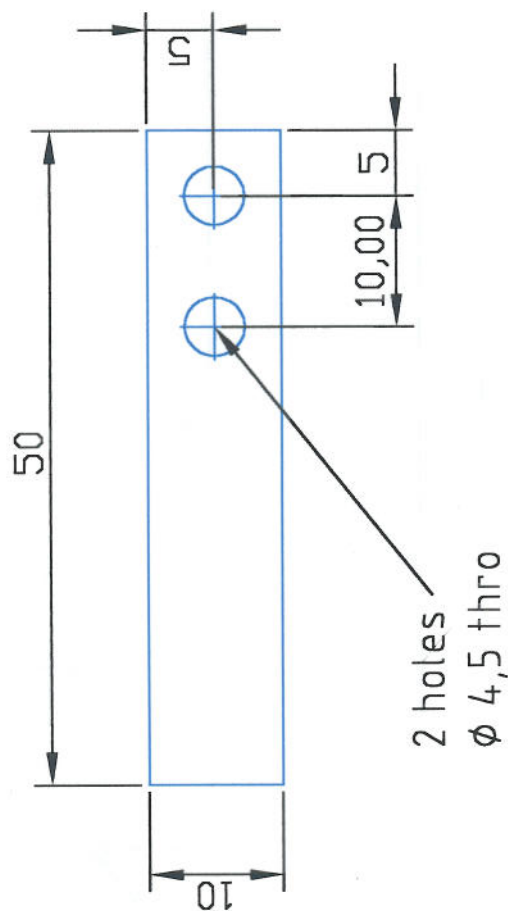


Material : Stainless Steel
2 off required

Itemref	Quantity	Title/Name, designation, material, dimension etc	Article No./Reference
Designed by MM	Checked by MM	Approved by - date MM 4 June 2005	Date 4 Jun 05
		File name	Scale NTS
Cranfield University SIMS		Feed Block Spacer	
		Edition 1	Sheet 1 of 1



Itemref	Quantity	Title/Name, designation, material, dimension etc	Article No./Reference
Designed by MM	Checked by MM	Approved by - date 11 Apr 05	Date 11 Apr 05
		File name	Scale NTS
Cylinder Mounting Bracket			
Cranfield University SIMS			Edition 1
			Sheet 1 of 1

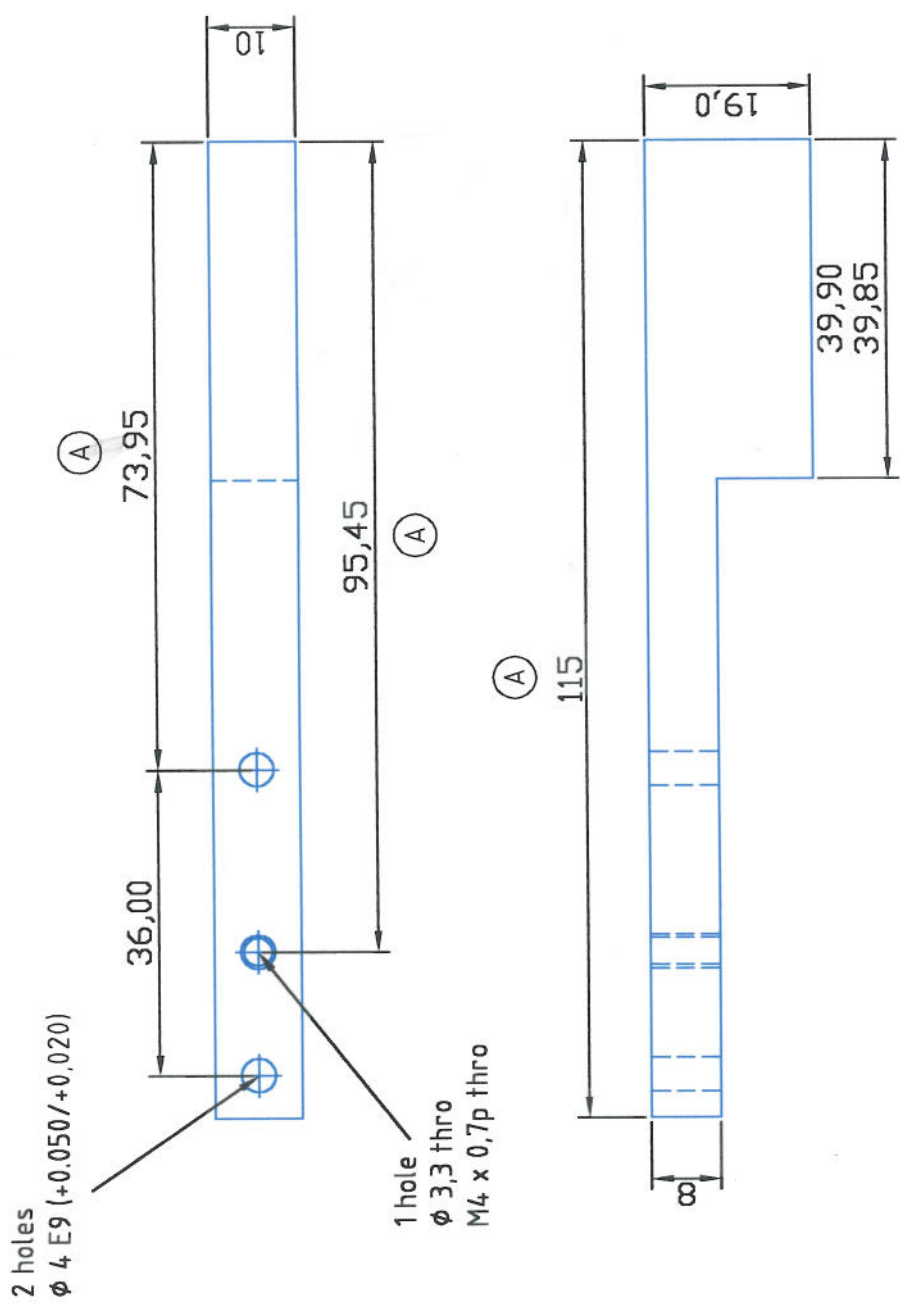


Material : 7,5mm thick Tufnel (9/32")

Itemref	Quantity	Title/Name, designation, material, dimension etc			Article No./Reference	
Designed by MM	Checked by MM	Approved by - date MM 10 Apr 05	File name	Date 10 Apr 05	Scale NTS	
Cranfield University SIMS				Insulating Spacer		
				Edition 1	Sheet 1 of 1	

MACHINED SURFACES
3.2 / U05

3RD ANGLE PROJECTION



Material : Aluminium
Stock Size : 20 x 10 x 115

Itemref	Quantity	Title/Name, designation, material, dimension etc	Article No./Reference
Designed by MM	Checked by MM	Approved by - date MM 11 Apr 05	Date 11 Apr 05
		File name	Scale NTS
Gate			
Cranfield University SIMS			Edition 1
			Sheet 1 of 1

ALL DIMENSIONS IN MM

MACHINED WHOLE NUMBER DIMENSIONS +/- 0,5

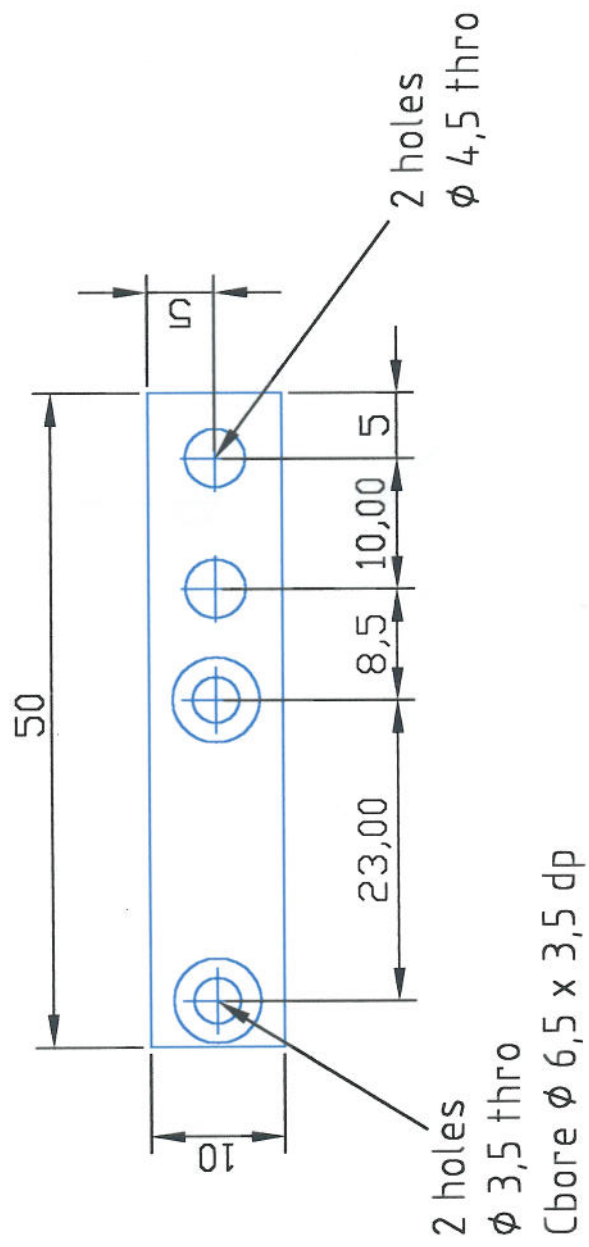
MACHINED 1 PLACE DIMENSIONS +/- 0,2MM

MACHINED 2 PLACE DIMENSIONS +/- 0,1MM

MACHINED SURFACES

3.2 / U05

3RD ANGLE PROJECTION



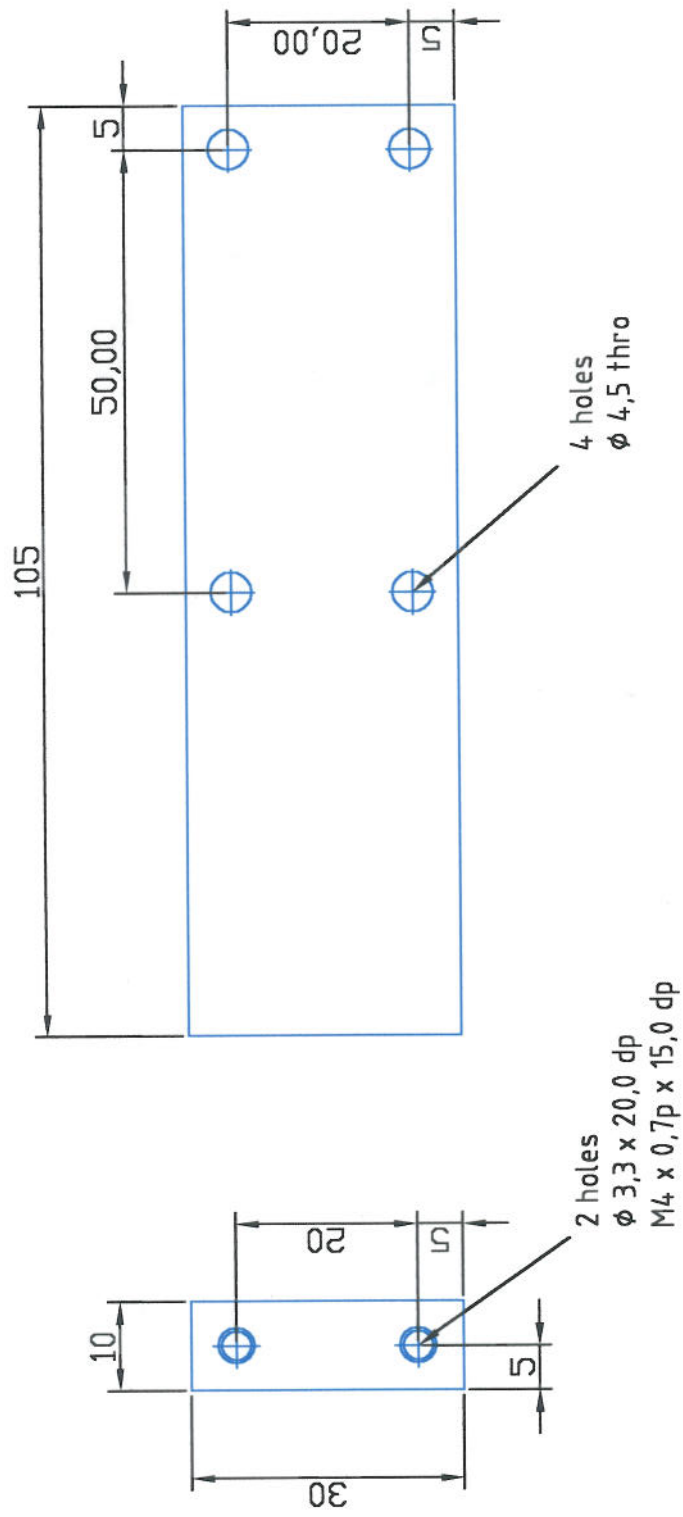
Itemref	Quantity	Title/Name, designation, material, dimension etc		Article No./Reference	
Designed by MM	Checked by MM	Approved by - date MM 10 Apr 05	File name	Date 10 Apr 05	Scale NTS
Cranfield University SIMS			Gate Assy Mounting Block		
		6	7	Edition 1	Sheet 1 of 1
				8	

ALL DIMENSIONS IN MM
MACHINED WHOLE NUMBER DIMENSIONS +/- 0,5
MACHINED 1 PLACE DIMENSIONS +/- 0,2MM
MACHINED 2 PLACE DIMENSIONS +/- 0,1MM

MACHINED SURFACES
3.2 / U05


3RD ANGLE PROJECTION

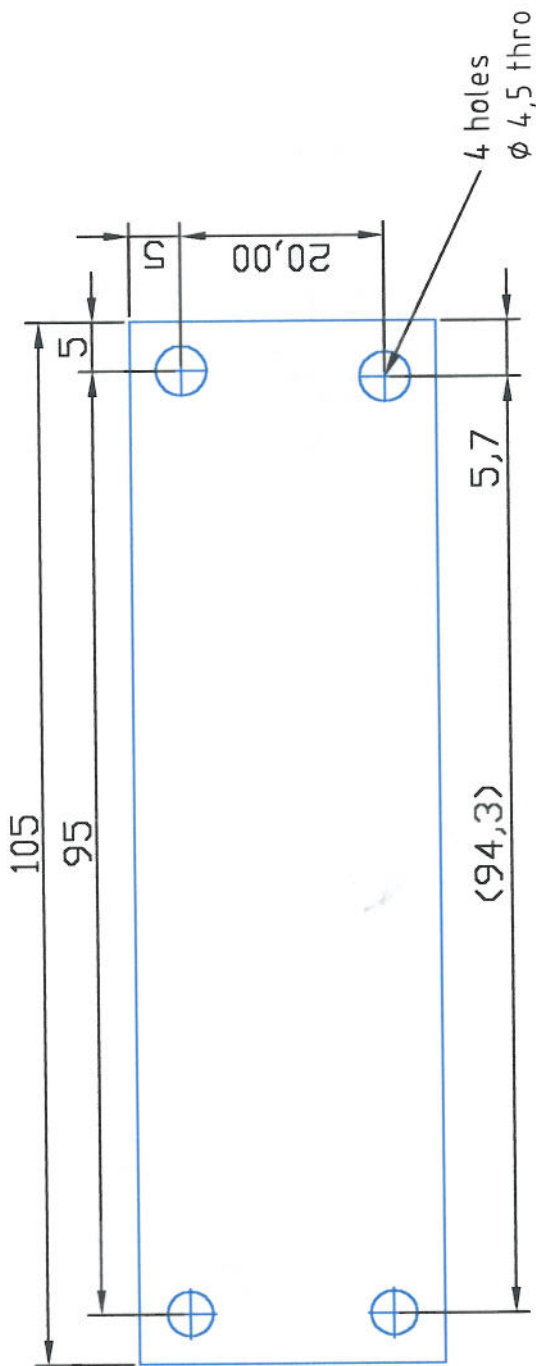
DO NOT SCALE



Material : Aluminium
Stock Size : 30 x 10 x 105

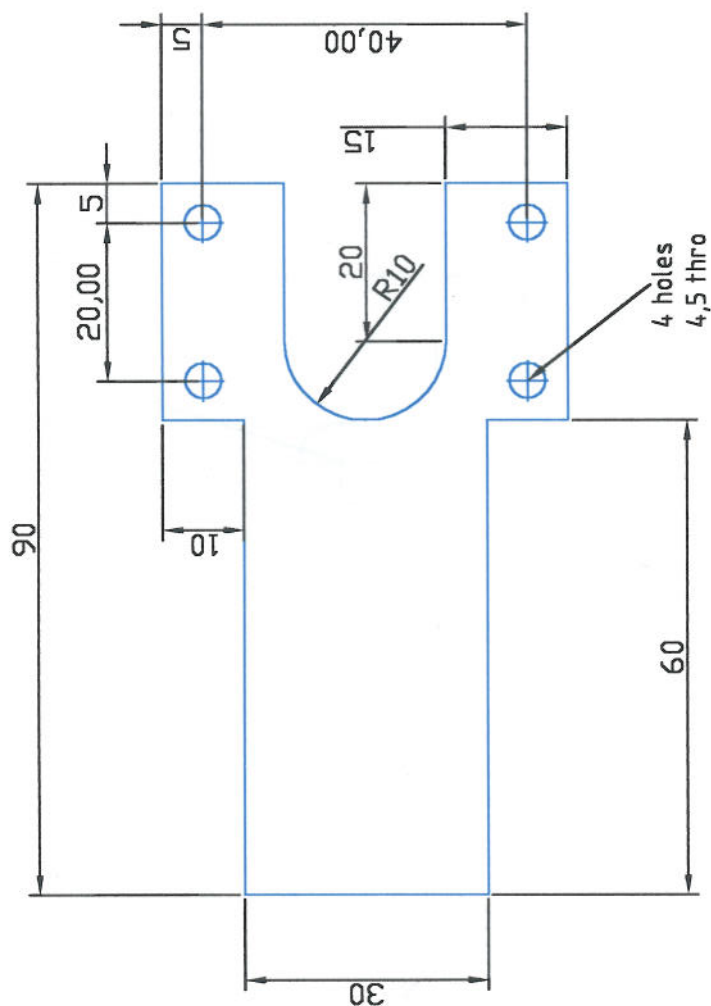
Itemref	Quantity	Title/Name, designation, material, dimension etc	Article No./Reference		
Designed by MM	Checked by MM	Approved by - date MM 11 Apr 05	File name	Date 11 Apr 05	Scale NTS
Cranfield University SIMS			Nozzle Block Bracket Piece 1		
			Edition 1	Sheet 1 of 1	

ALL DIMENSIONS IN MM	MACHINED SURFACES	3RD ANGLE PROJECTION	DO NOT SCALE	RevNo	Revision note	Date	Signature
MACHINED WHOLE NUMBER DIMENSIONS +/- 0,5	3.2/ UOS						
MACHINED 1 PLACE DIMENSIONS +/- 0,2MM							
MACHINED 2 PLACE DIMENSIONS +/- 0,1MM							



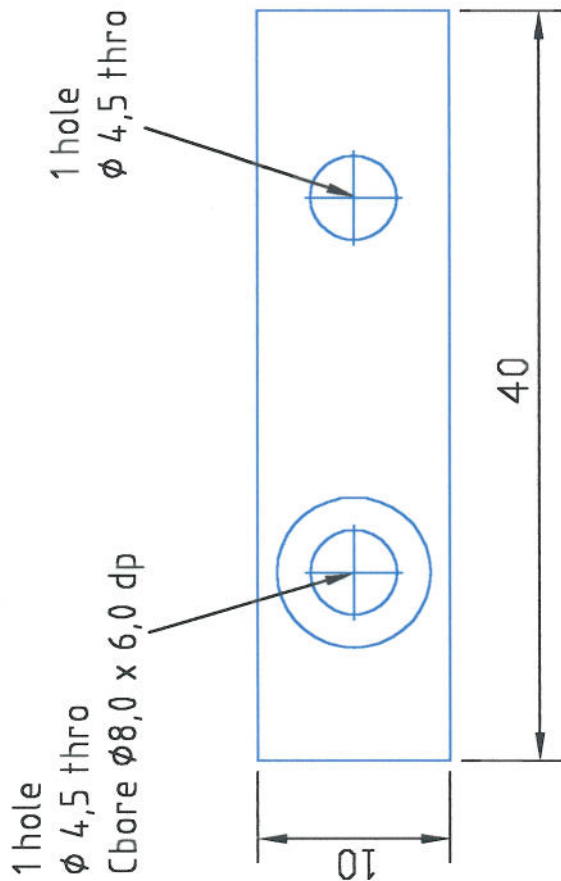
Material : Aluminium
Stock Size : 30 x 6 x 105

Itemref	Quantity	Title/Name, designation, material, dimension etc	Article No./Reference	Scale
Designed by MM	Checked by MM	Approved by - date MM 11 Apr 05	Date 11 Apr 05	Scale NTS
Cranfield University SIMS				Nozzle Block Bracket Piece 2
				Edition 1
				Sheet 1 of 1



Material : Aluminium
Stock Size : 50 x 10 x 90

Itemref	Quantity	Title/Name, designation, material, dimension etc	Article No./Reference
Designed by MM	Checked by MM	Approved by - date MM 11 Apr 05	Date 11 Apr 05
		File name	Scale NTS
Cranfield University SIMS		Nozzle Block Bracket Piece 3	
		Edition 1	Sheet 1 of 1



Material : Cogemica Insulation (supplied) – 10mm thick
6 off required

Itemref	Quantity	Title/Name, designation, material, dimension etc			Article No./Reference	
Designed by MM	Checked by MM	Approved by – date MM 5 Oct 05	File name	Date 5 Oct 05	Scale NTS	
Cranfield University SIMS				Insulator		
				Edition 1	Sheet 1 of 1	

Signature

Date

RevNo

Revision note

DO NOT SCALE



MACHINED SURFACES

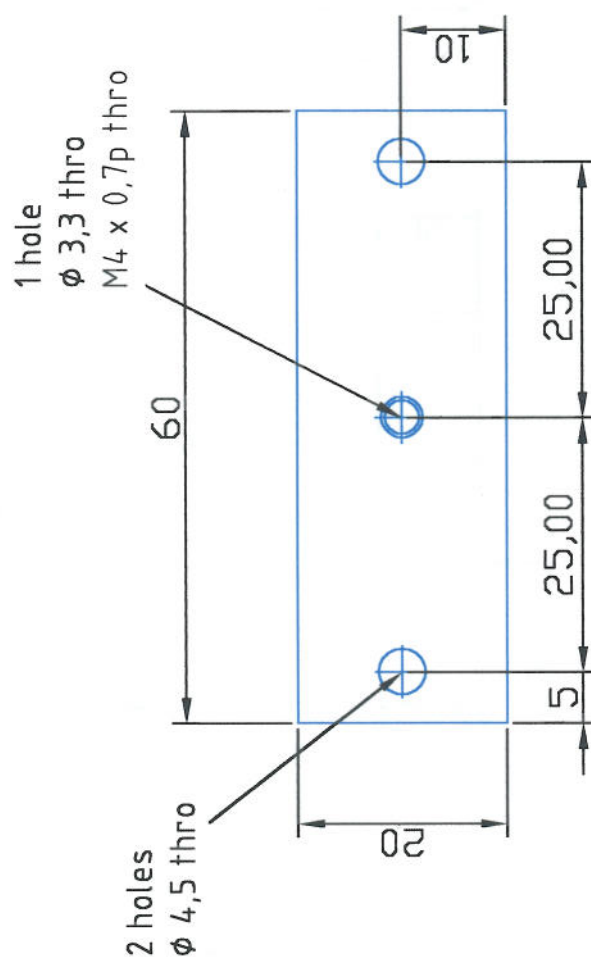
3.2
U05

ALL DIMENSIONS IN MM

MACHINED WHOLE NUMBER DIMENSIONS +/- 0.5

MACHINED 1 PLACE DIMENSIONS +/- 0.2MM

MACHINED 2 PLACE DIMENSIONS +/- 0.1MM



Material : Aluminium
Stock Size : 60 x 20 x 10 thick
3 off required

Itemref	Quantity	Title/Name, designation, material, dimension etc	Article No./Reference
Designed by MM	Checked by MM	Approved by - date MM 14, Apr 05	Date 14, Apr 05
Cranfield University SMS		File name	Scale NTS
		Element Clamp Plate	
		Edition 1	Sheet 1 of 1

ALL DIMENSIONS IN MM
 MACHINED WHOLE NUMBER DIMENSIONS +/- 0,5
 MACHINED 1 PLACE DIMENSIONS +/- 0,2MM
 MACHINED 2 PLACE DIMENSIONS +/- 0,1MM

MACHINED SURFACES
 $\frac{3,2}{\sqrt{u05}}$

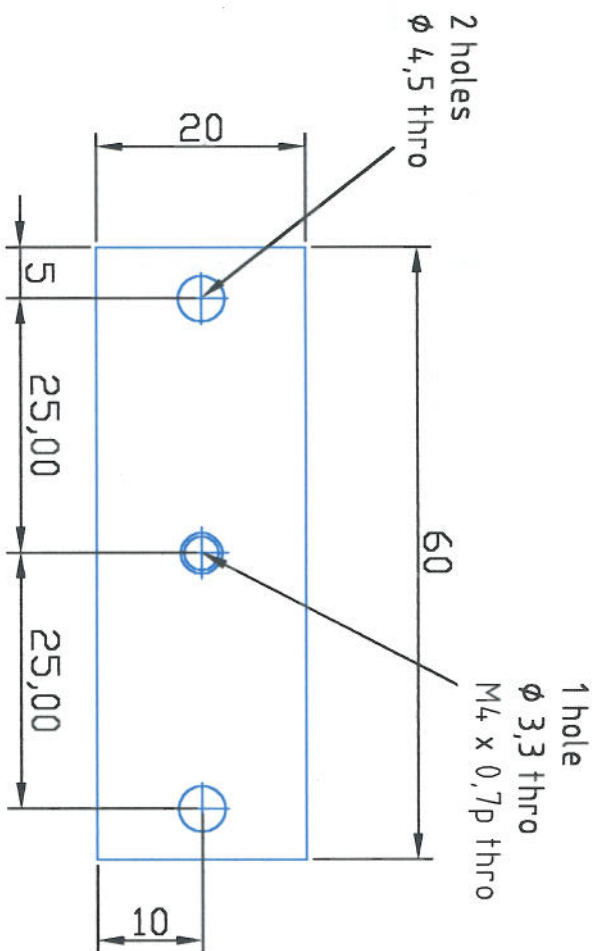


DO NOT SCALE

RevNo Revision note

Date

Signature Checked



Material : Aluminium
 Stock Size : 60 x 20 x 10 thick
 3 off required

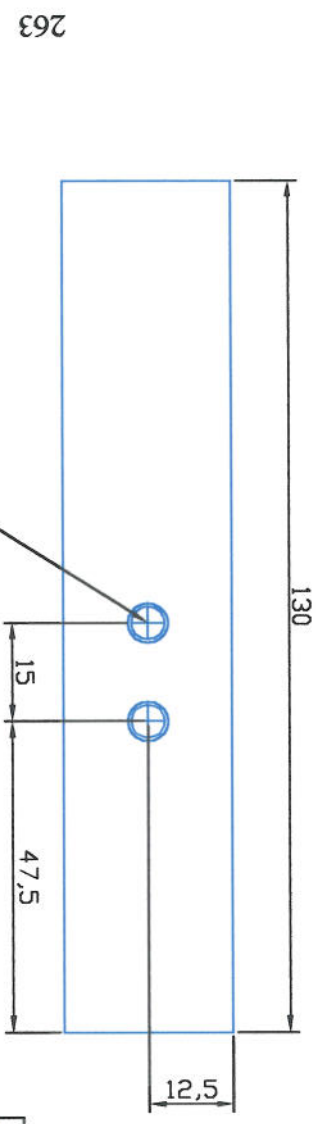
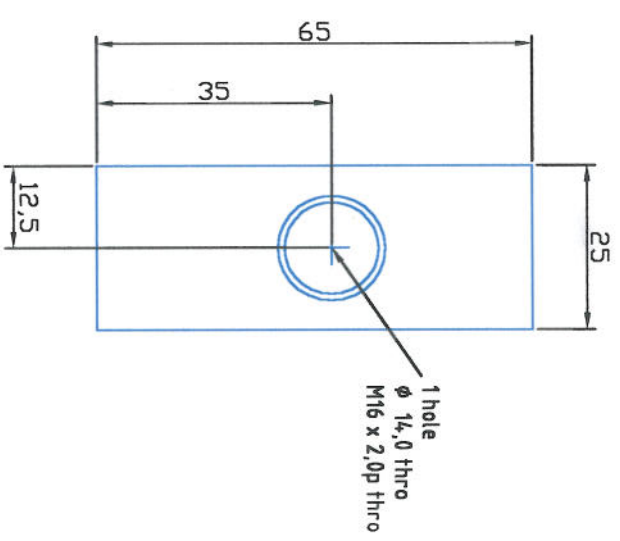
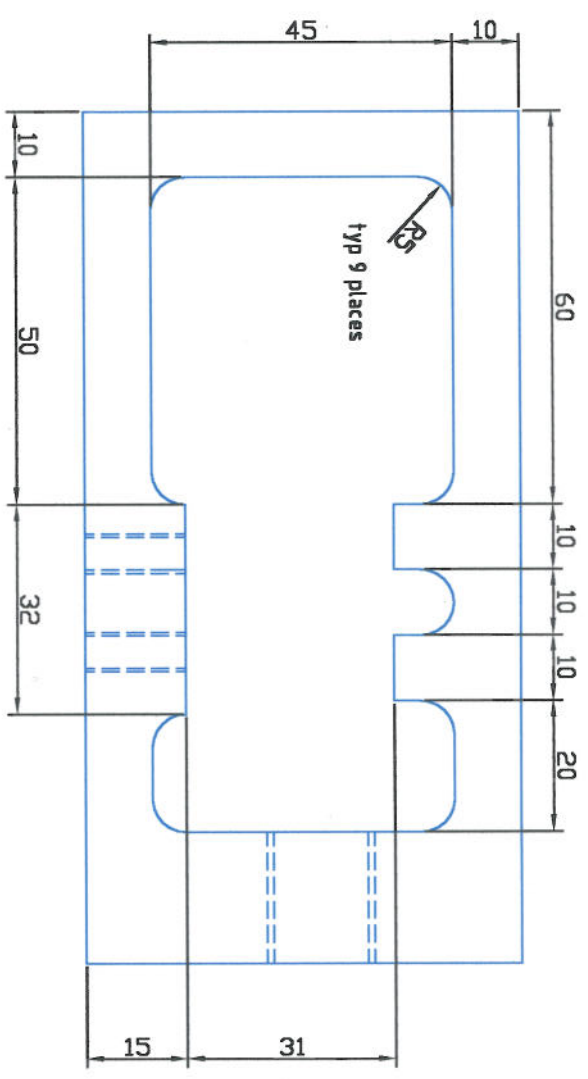
Itemref	Quantity	Title/Name, designation, material, dimension etc	Article No./Reference
MM	MM	MM	MM

Designed by	Checked by	Approved by - date	File name	Date	Scale
MM	MM	MM 14, Apr 05		14, Apr 05	NTS

Cranfield University SIMS

Element Clamp Plate

Edition 1
 Sheet 1 of 1



Material : Brass
 2 off required

Itemref	Quantity	Title/Name, designation, material, dimension etc	Article No./Reference
MM	MM	MM	MM
Designed by	Checked by	Approved by - date	File name
MM	MM	21 Jul 05	25 Jul 05

Cranfield University SIMS

Electrical Contact Clamp

Edition 1

Sheet 1 of 1

Appendix 10 – Cutting Fluid Mist Ignition Rig

ALL DIMENSIONS IN MM

MACHINED WHOLE NUMBER DIMENSIONS +/- 0.5

MACHINED 1 PLACE DIMENSIONS +/- 0.2MM

MACHINED 2 PLACE DIMENSIONS +/- 0.1MM

MACHINED SURFACES

3.2/ U05



3RD ANGLE PROJECTION

680

200

50

10

20

20

360

500

20

20

50

660

10

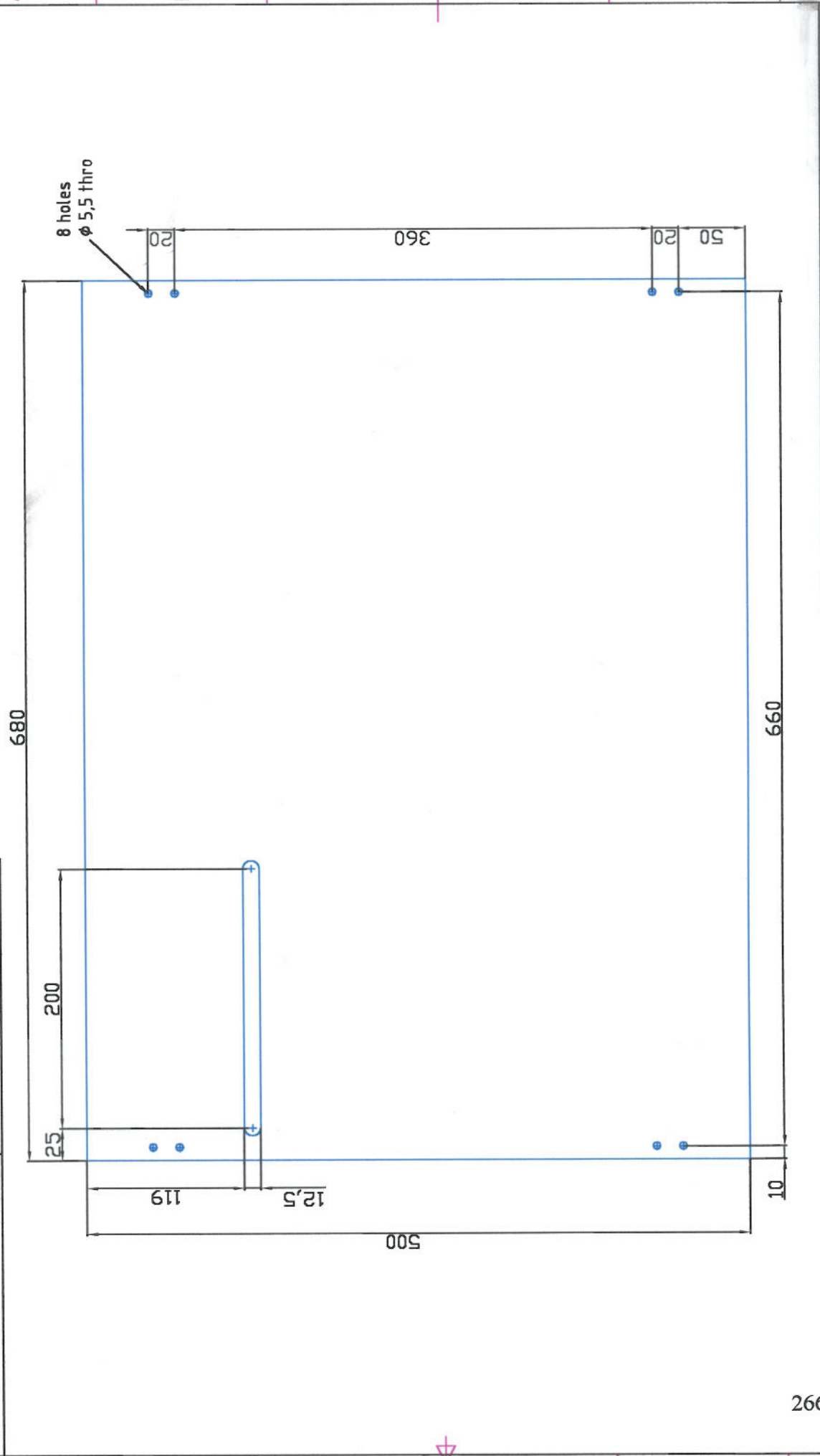
10 holes
Ø 5,5 thro

Material : Aluminium or Stainless Steel
Thickness: 1.6mm to 3mm

Itemref	Quantity	Title/Name, designation, material, dimension etc	Article No./Reference	
Designed by MM	Checked by MM	Approved by - date MM 29 Oct 05	Date 29 Oct 05	Scale NTS
Cranfield University SIMS			Skirt Panel 1	
			Edition 1	Sheet 1 of 1

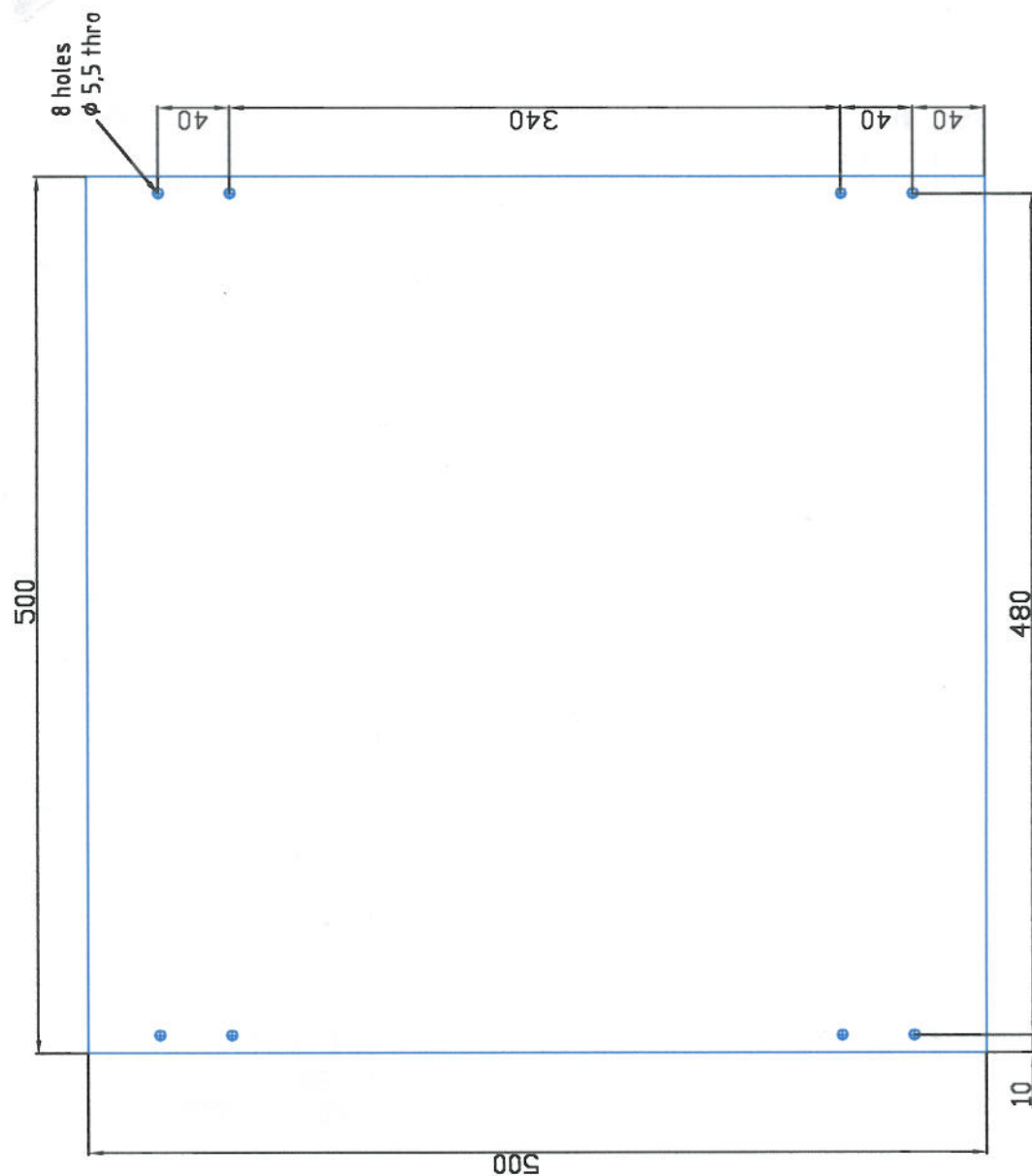
ALL DIMENSIONS IN MM	MACHINED SURFACES	DO NOT SCALE	RevNo	Revision note	Date	Signature	Checked
----------------------	-------------------	--------------	-------	---------------	------	-----------	---------

MACHINED WHOLE NUMBER DIMENSIONS +/- 0.5
 MACHINED 1 PLACE DIMENSIONS +/- 0.2MM
 MACHINED 2 PLACE DIMENSIONS +/- 0.1MM



Itemref	Quantity	Title/Name, designation, material, dimension etc	Article No./Reference
Designed by MM	Checked by MM	Approved by - date MM 29 Oct 05	Date 29 Oct 05
File name			Scale NTS
Cranfield University SIMS			Sheet 1 of 1
Skirt Panel 2			Edition 1

Material : Aluminium or Stainless Steel
Thickness. 1.6mm to 3mm



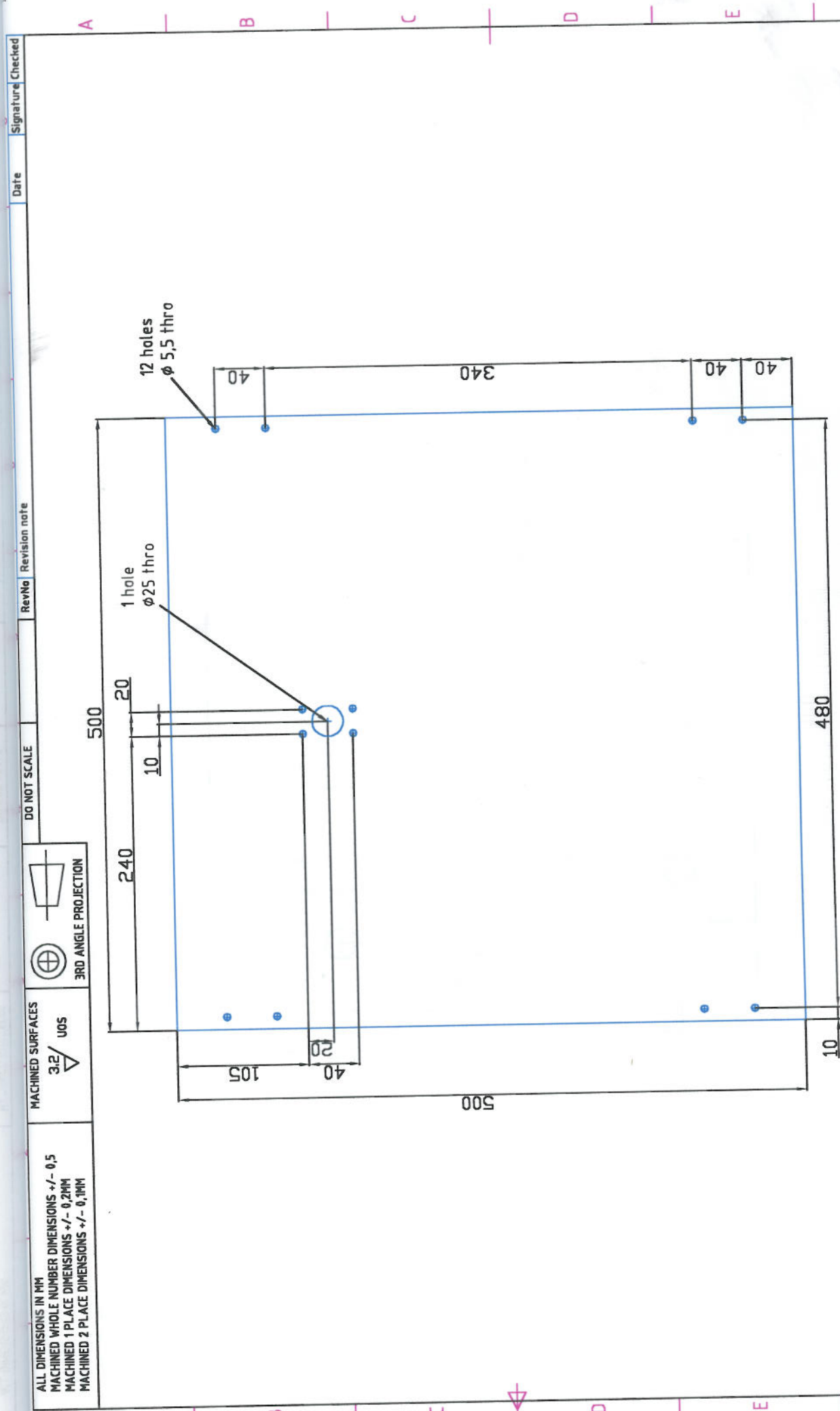
Item#ref	Quantity	Title/Name, designation, material, dimension etc	Article No./Reference
Designed by MM	Checked by MM	Approved by - date MM 29 Oct 05	Date 29 Oct 05
		File name	Scale NTS

Skirt Panel 3

Cranfield University SIMS		Edition 1	Sheet 1 of 1
---------------------------	--	--------------	-----------------

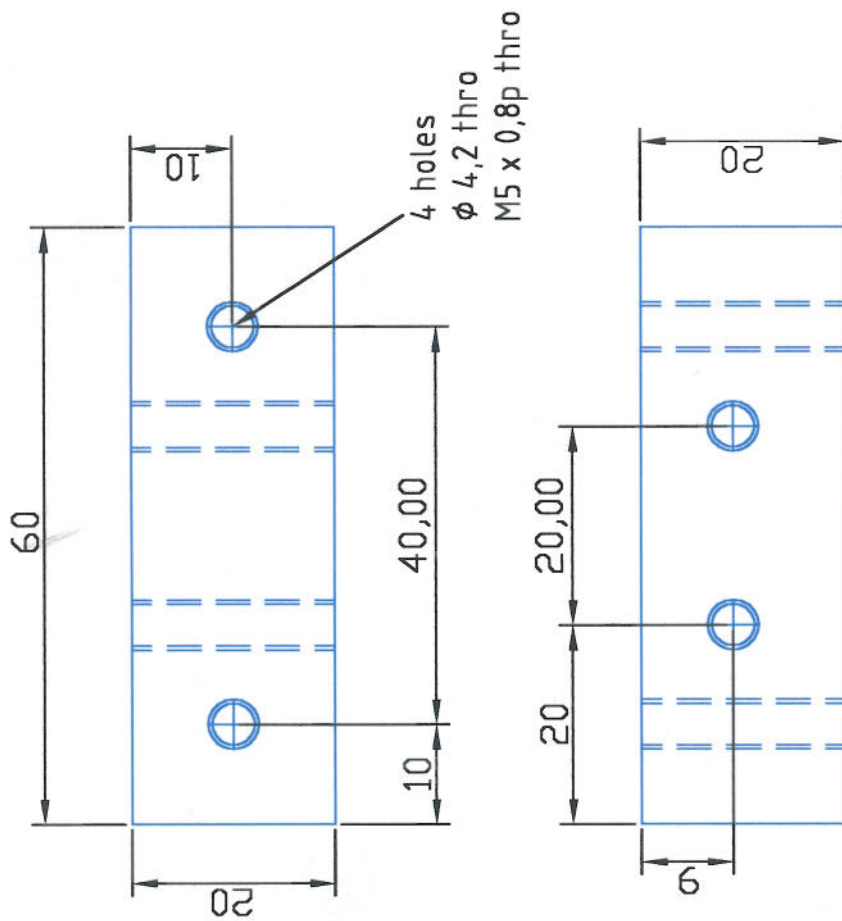
6 7 8

Material : Aluminium or Stainless Steel
Thickness. 1,6mm to 3mm



Itemref	Quantity	Title/Name, designation, material, dimension etc	Article No./Reference
Designed by MM	Checked by MM	Approved by - date MM 29 Oct 05	Date 29 Oct 05
			Scale NTS
Skirt Panel 4			
Cranfield University SIMS			Edition 1
			Sheet 1 of 1

Material : Aluminium or Stainless Steel
Thickness. 1,6mm to 3mm

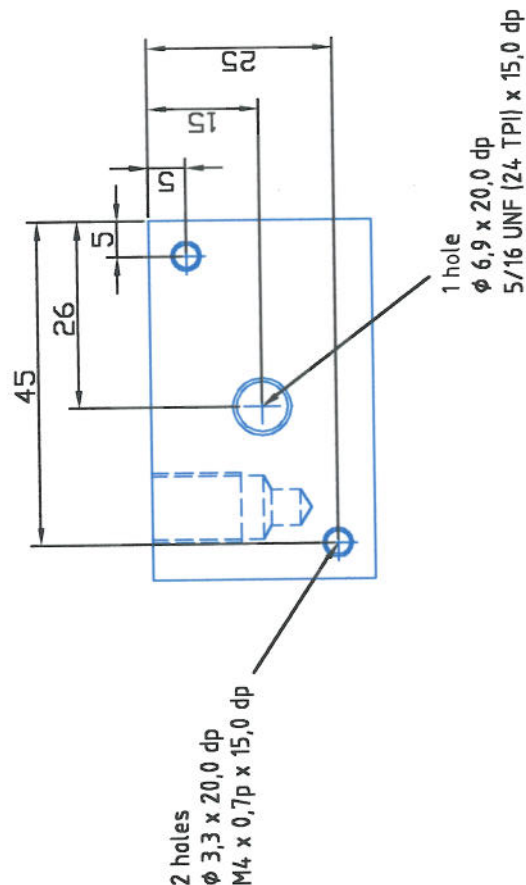
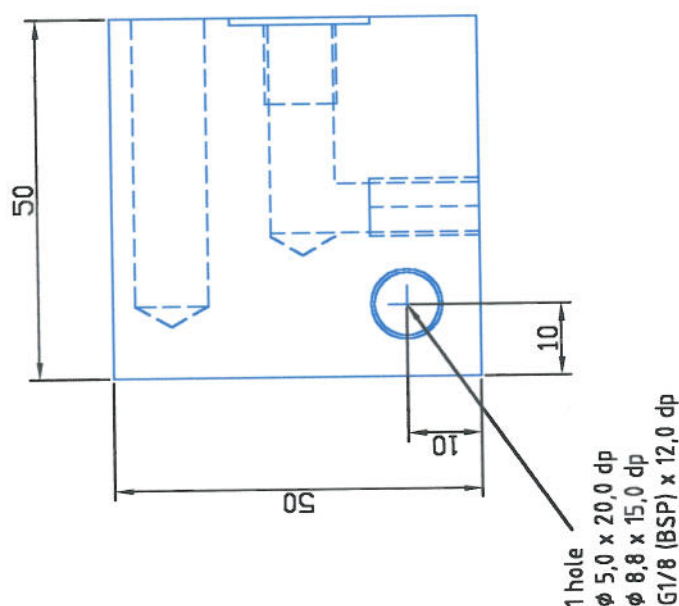
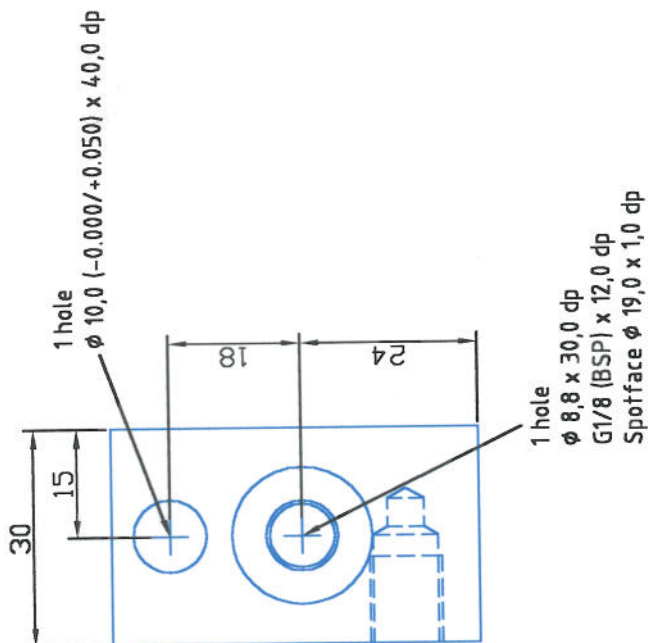


Itemref	Quantity	Title/Name, designation, material, dimension etc	Article No./Reference
Designed by MH	Checked by MH	Approved by - date MH 29 Oct 05	Date 29 Oct 05
		File name	Scale NTS
Fixing Block			
Cranfield University SIMS			Edition 1
			Sheet 1 of 1



MACHINED SURFACES
3.2 / U05

ALL DIMENSIONS IN MM
MACHINED WHOLE NUMBER DIMENSIONS +/- 0.5
MACHINED 1 PLACE DIMENSIONS +/- 0.2MM
MACHINED 2 PLACE DIMENSIONS +/- 0.1MM



Material : Aluminium
Stock Size : 50 x 50 x 30

Itemref	Quantity	Title/Name, designation, material, dimension etc	Article No./Reference
Designed by MM	Checked by MM	Approved by - date MM 10 Apr 05	Date 10 Apr 05
		File name	Scale NTS
Cranfield University SIMS		Nozzle Block	
		Edition 1	Sheet 1 of 1

Appendix 11 – G Hearn, Static Electricity – Guidance for Plant Engineers

Static Electricity

Guidance for Plant Engineers.

Graham Hearn - Wolfson Electrostatics
University of Southampton

Static electricity is one of the most insidious sources of fire and explosion encountered in modern industry. It is by nature unpredictable and therefore difficult to detect. In some industry sectors it is viewed almost as a black art.

Uncontrolled static electricity is a problem in many sectors of manufacturing industry but is of particular concern in operations where sensitive flammable materials are present. Fires and explosions attributable to static may actually be increasing in frequency due increased product purity and faster process speeds.

With the right approach electrostatic ignition hazards can be identified and controlled. This fact sheet looks at the steps taken in a hazard assessment and the key parameters that need to be determined.

Analysis

There are five general conditions necessary for an electrostatic ignition hazard to be present:

1. Sensitive flammable atmosphere
2. Generation of electrostatic charge
3. Accumulation of charge
4. Electrostatic discharge (ESD)
5. Sufficient discharge energy

If all of the above conditions exist, an ignition hazard will be present, if any of the conditions are removed, the hazard is obviated. As a belt and braces approach attempts are often made to remove more than one of these conditions, however the extent to which any mitigating measures can be applied in practice often involve other considerations which may include cost and practicality.

Are Sensitive Flammable Materials Present?

In any investigation, it is usually straightforward to identify the presence of flammable media.

From the point of view of electrostatic ignition hazard it is only necessary to restrict the

investigation of flammable atmospheres to those sensitive enough to be ignited by an electrostatic discharge. In most industrial situations these are flammable gases, solvent vapours, aerosols and fine combustible dusts. Many pyrotechnic materials are also very sensitive to electrostatic ignition.

Gases and vapours

Many common industrial hydrocarbon gases and solvents are flammable in air over the range 1 - 12% by volume. This is referred to as the flammable or explosive range existing between the lower explosive limit (LEL) and the upper explosive limit (UEL). The electrostatic discharge energy required for ignition varies significantly over this range but the minimum ignition energy value is likely to be of the order of 0.2 - 2.0 millijoules (mJ). This energy level is very low and indicates that ignition may result easily.

From Lewis and von Elbe [1] the relationship between the minimum ignition energy of the solvent vapours and their concentration will be similar to that shown by the red U-shaped curve in Figure 2. Note that the solvent is most sensitive to ignition approximately midway between the lower and upper flammable limits and that the spark energy required to ignite the vapour increases rapidly as it approaches these limits.

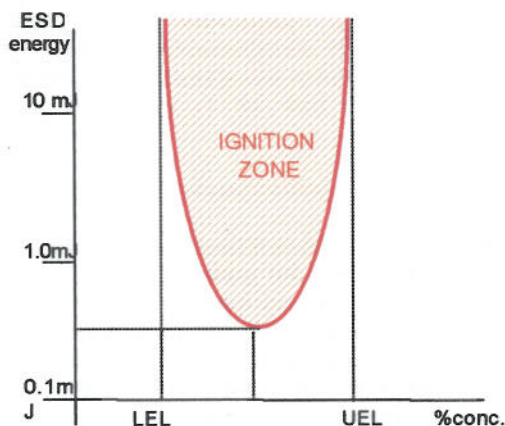


Figure 1. Typical relationship between ignition sensitivity and concentration of fuel vapour in air.

If the atmosphere is oxygen-rich (in excess of normal air), the sensitivity to ignition is significantly increased. This will be in terms of both an extended flammable range and a greatly

reduced minimum ignition energy (MIE). Reduction in pressure below atmospheric may also influence the flammable range and reduce the MIE.

Aerosols and foams

Flammable liquids in the form of a dense mist or aerosol may be ignited easily at temperatures below the liquid flashpoint. Kerosene for example may have a flashpoint in excess of 70°C but can be ignited at room temperature with a low-energy spark [2]. In combustion, mists comprising small droplets below 10 µm tend to behave like a vapour whereas those with droplet diameters above around 40 µm propagate combustion in a similar way to flammable dust clouds[3]. Typical minimum flammable concentrations for aerosols vary from 15 to 50 g.m⁻³.



Figure 2. Electrostatic ignition of kerosene foam at 25°C - fifty degrees below its flashpoint.

The presence of foam, for example on the surface of an agitated solvent, can also result in ignition below the liquid flashpoint (figure 2). Foaming liquid surfaces of non-volatile solvents allow fuel and oxygen to mix more effectively enabling ignition to occur at lower temperatures.

Dust clouds

Most natural and synthetic materials, if subdivided into a fine dust, will easily ignite and burn vigorously. In general, dust clouds are less sensitive to ignition than flammable gases or solvent vapours. They can however produce violent explosions and are more likely to be associated with electrostatic ignition due to their propensity over gases and liquids to generate electrostatic charge through handling.

For a flammable dust to be at risk from electrostatic ignition it must be dispersed to form a cloud. This cloud then exhibits upper and lower explosion limits similar to a flammable gas or vapour. Typical lower and upper explosive limits for a dust cloud are 50 and 1000 g.m⁻³, respectively. The sensitivity to ignition varies with dust concentration also in a similar way to gases and vapours. Even at the lowest extreme of the flammable range the concentration represents an extremely dense dust cloud and is unlikely to be encountered in a normal working environment other than within process equipment (driers, cyclones, silos, etc) or as the result of the temporary disturbance or dispersion of an accumulated dust layer. An innocuous 1mm thick layer of dust on the floor of a room, if partially or totally dispersed throughout the volume of the room, can easily produce a sensitive flammable dust cloud. The physical and chemical nature of the material, its particle size and moisture content, will all influence the ease at which the dust cloud is ignited. Fine dry dusts tend to have a lower ignition energy and are more explosive.

Hybrid vapour-dust mixtures

In many industrial situations, a dispersed flammable dust may coexist with traces of flammable hydrocarbon vapour. In such cases vapour concentrations well below the LEL may significantly reduce the minimum ignition energy of the dust cloud. The presence of propane in the concentration of 1% by volume with air for example can reduce the minimum ignition energy of the dust by 2 orders of magnitude[4].

Hazardous area classification (zoning)

Hazardous area classification is a method often used when undertaking risk management. The classification is based on identifying areas or zones within a plant according to the likelihood of sensitive flammable gas or vapour concentrations being present. For solvents or gases there are generally 3 classifications as follows.

- Zone 0 - in which an explosive gas/air mixture is continuously present, or present for long periods.
- Zone 1 - where an explosive gas/air mixture is likely to occur in normal operation.

- Zone 2 - in which an explosive gas/air mixture is not likely to occur in normal operation and if it does occur will exist only for a short time.

An example of such zones would be a process vessel in which flammable solvents are being mixed within a building located at an industrial site. The inside of the reaction vessel can be classified as Zone 0. The building containing the vessel may be classified as Zone 1 (as the vessel may be opened from time to time and drums of solvent or solvent pipes may be present). The area outside the building would normally be classified as Zone 2 providing sensitive flammable atmospheres could not be generated from other sources.

Hazardous area classification is similarly applied to the presence of flammable dusts, in this case zones 0, 1 and 2 become zones 20, 21 and 22 respectively. Similar limitations apply to equipment and materials used in these areas.

The application of hazardous area classification has advantages from the point of view of general safety standards, in particular, the use of electrical equipment and other potential ignition sources which must be safety certified to the appropriate level before they can be used in certain zones. From the point of view of static electricity, highly insulating surfaces such as plastics are prohibited from use in Zones 0 and 1 if the exposed area exceeds certain limits. (This is interpreted in some detail later in this paper).

Is Static Electricity Generated?

The generation of electrostatic charge is intrinsic to many industrial operations. The rate of charge generation is notoriously difficult to predict, however, operations involving rapid and energetic movement and the contact and separation of surfaces will produce increased charging. Milling of powder, for example, will generate more charge than pouring. In industry charge generation mechanisms are as follows:

- The contact and separation of solid surfaces such as moving webs over rollers.
- The movement of personnel.
- The flow/movement of liquids.
- The production of mist or aerosols.
- The flow or movement of powders.
- Charging by induction in an electric field.

Powder handling

A powder has a large total surface area per unit mass and since electrostatics is a surface phenomenon there is a propensity to generate and store high levels of static. All powder handling operations are likely to generate electrostatic charge.

Studies at the University of Southampton [5,6] and elsewhere [7] have shown that electrostatic charge is generated when particles are transported through pipelines and ducts. The charging process arises from the physical interaction of the particles and the duct wall and occurs whether the pipe is constructed from plastic or metal. Industrial processes such as pneumatic conveying can often suffer from static electricity related problems and occasionally very high levels of potential and energetic sparks can be generated.

Parameters influencing the levels of electrostatic potential generated are:

- The nature of the material comprising the particulate.
- Flow velocity.
- Mass flow rate/density (kg/m^3)
- Particle size
- Composition of duct walls.
- Turbulence due to bends, constrictions etc.
- Temperature and humidity.

General observations are that the charge-to-mass ratio in Coulombs per kilogram (C.kg^{-1}) of particulate matter pneumatically conveyed through a duct increases with increased flow velocity and decreases with increased mass flow density and increased particle size. This can be explained in terms of the collision frequency of particles with the wall. The number of particle-wall collisions per unit mass is increased as mass flow density is decreased. The charge transfer efficiency increases with velocity of impact and separation and hence with flow velocity. Smaller particles can sustain a larger charge-to-mass ratio before leakage to the surrounding gas occurs. It follows that the largest charge-to-mass ratios are observed with small particles conveyed at high velocity and low mass flow density. The presence of electrostatic charge on powders or particles does not normally constitute an ignition hazard until a significant mass of the particles are bulked together.

It is envisaged that a charge generation mechanism will only occur when solid particles or liquid droplets are carried in the gas stream. The movement of gases alone creates little, if any, static electricity [8]. Since it is primarily the number of collisions and the force of each collision between particles and the duct wall, which influence the level of electrostatic charge generation, it follows that an increase in transport velocity will result in higher levels of charge generation. The relationship between the two, however, is complicated due to the influence of the duct geometry and turbulence. This makes it very difficult to set maximum velocity limits as a mitigating measure without performing an empirical study. Naturally, it is better to limit the velocity such that the gas flow is laminar rather than turbulent and this should be considered. It is known, however, that the maximum level of surface charge density for well-dispersed particles cannot exceed a value of approximately $10 \mu\text{C.m}^{-2}$ [9]. This value can be used to estimate maximum levels of charging developed on objects or surfaces onto which the particles impinge and from this determine electrostatic ignition hazard at these points.

Charge generation in liquids

Unlike industrial powders most liquids are in electrostatic terms relatively electrically conductive. For this reason it is non-polar liquids such as paraffin, gasoline, purified aromatics (toluene, xylene, etc), diesel and light oils, which exhibit significant charge generation. This is actually more to do with their charge retention properties but it is appropriate to mention it in this section as electrostatic problems are confined to low conductivity liquids.

It is known that high levels of electrostatic charging occur as the result of high velocity flow in pipelines and agitation in tanks. Pouring, gravity fill and splashing are also charge generators but to a much lesser extent.

Charging of liquids in a pipeline, normally takes place because the moving liquid carries with it a loosely bound layer of charge leaving the other layer attached to the solid surface i.e. the pipe wall. The potential in the fluid at the plain of slip is called the zeta potential.

As the liquid flows through a pipe it carries with it charge from the diffuse layer. If the charging

process is to continue, the charge must be replenished by charge moving through the walls of the pipe. This movement of charge creates an electrical current measured between the pipe wall and ground called the streaming current and is generally in the order of 10^{-14} to 10^{-8} A. With electrically insulating pipe work material such as plastic, the current is reduced. As a consequence, there are large differences in the charging behaviour of liquids in metal and plastic pipes[10].

The amount of charge generated on a liquid flowing in a straight pipe is generally limited by three factors:

- The conductivity of the liquid
- The flow velocity
- The nature of the pipe wall

The rate at which charge on a liquid flows to earth depends on its conductivity. It follows, therefore, that a highly conductive liquid cannot store charge. A perfectly pure insulating liquid will not generate charge because there are insufficient disassociated ions present. It is generally found that the electrostatic activity associated with a liquid flow builds up as the conductivity increases, reaches a maximum when the liquid conductivity is in the range $10\text{--}50 \text{ pS.m}^{-1}$, then decreases with further increasing conductivity as the generated charge flows rapidly to earth.

Volume charge densities in liquids can range from between 10^{-6} to 10^{-2} Coulombs. m^3 which infers that tanks receiving hydrocarbon fuels or solvents from pipeline systems can also store a relatively high level of electrical energy.

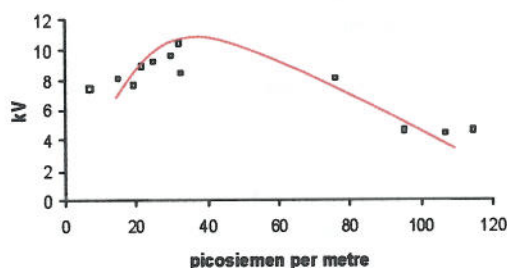


Figure 3. Electrostatic potential in kilovolts developed on an isolated metal valve during solvent flow through a pipeline as a function of solvent conductivity [11].

Although many people associate electrostatic problems with plastics and other insulators, it is metal pipes that give the highest charging rates (with very little difference between different metals)[12]. Naturally, charging also occurs in glass, rubber and plastic pipes. Turbulent flow produces more charge than laminar flow and pipes with rough internal surfaces tend to produce more charge than smooth surfaces, even when the roughness is on too small a scale to affect the state of turbulence.

Can Electrostatic Charge Accumulate?

As electrostatic charge is generated, by the means indicated above, it will either accumulate or dissipate depending of the conductivity of the materials involved and the possible conduction path to earth. Wood, concrete, natural fabrics, water, alcohols and of course metals can be considered conductive in electrostatic terms. Most polymers, on the other hand may retain electrostatic charge for many minutes or even hours. Glass can exhibit wide variations in conductivity.

Electrostatic charge can accumulate on insulating surfaces such as plastics and also on ungrounded conductors. Both of these situations can be potentially hazardous. An example of an ungrounded conductor is a metal solvent drum on an epoxy floor.

Capacitance

Any object or surface that can accumulate electrical charge can be thought of as a capacitor. In most industrial situations, the value of capacitance can be determined either by direct measurement or calculation. Capacitance is often expressed in picofarads (10^{-12} Farads) and in the example above, the ungrounded metal drum could be around 500pF. British Standard BS5958 gives typical capacitance values for various industrial objects including the human body.

It is important to note that objects or surfaces will only acquire and accumulate electrostatic charge if they are subjected to a charging mechanism. Furthermore, the accumulation of low levels of charge does not guarantee the presence of an ignition hazard. It is the magnitude of electrical energy that is stored and then released in a discharge which ultimately influences the degree of ignition hazard present.

Many powders used in industry are electrically insulating. A powder also has a large total surface area per unit volume and consequently, high levels of static electricity can be accumulated. Industrial liquids on the other hand tend to be relatively conductive. Exceptions include fuel oils, petroleum spirit, kerosene and non-polar solvents including toluene, xylene, heptane etc.

Resistivity and charge relaxation

If conductive materials are used, there can be no charge build up on their surface if they are sufficiently conductive and grounded. Standards usually recommend a maximum resistance to ground of between 10^6 and 10^8 ohms. In practice resistance paths of up to 10^{10} ohms may be sufficient for all but the most extreme situations.

Since electrical charge can be conducted across the surface or through the volume of a material, a resistivity value can be assigned to each. Surface and volume resistivity are usually related but have different units. It is often important to measure these parameters during hazard analysis.



Figure 4. Commercially available resistivity meter.

Surface resistivity (ρ_s) is expressed in ohms per square of surface i.e. The electrical resistance between two parallel 'bar' electrodes separated by a distance equal to their length. (This encompasses a square of surface the size of which is unimportant because the resistance value will remain the same. 1 cm^2 will exhibit the same resistance as 1 m^2 provided that the surface is homogeneous). In some standard test methods, the electrode geometry is two concentric rings with the resistance measured between the inner and the outer ring. Figure 4 shows a commercially available instrument.

Volume resistivity (P_V) is the reciprocal of conductivity and is expressed in ohm.metres. It is defined as the resistance through a volume of material of cross-section $1m^2$ and thickness $1m$. Special metering cells are available which enable this parameter to be quantified for both liquids and powders.

Charge relaxation time (T) and resistivity (P_V) are related by the formula $T = \epsilon_0 \epsilon_r P_V$. Where ϵ_0 and ϵ_r are the permittivity of free space and the relative permittivity of the material. Like resistivity, charge relaxation time can be measured directly. This is normally achieved by applying charge to the surface under test using an ion source, grounding the sample and measuring the rate of decay of surface potential. Commercial instruments are also available for this.

Charge on personnel

It is possible for a person to generate charge on his or her body by movement, particularly walking. In many industrial situations however charge is transferred to personnel by proximity to a process. Irrespective of the method of charge generation, the problem is one of accumulation. Electrostatic charge developed on the human body can be a particular problem (a) because a person is mobile and may carry dangerous potentials into hazardous areas and (b) because human skin is conductive in electrostatic terms and can give rise to energetic spark discharges.

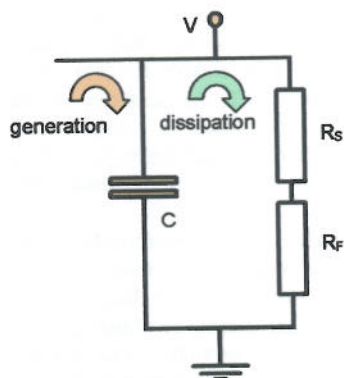


Figure 5. Electrostatic model of the human body. The charge generation mechanism could be walking, movement, powder handling etc.

A person standing can be modelled as a capacitor in parallel with two resistors (Figure 5). The capacitance (C) of the human body is usually in the range $100-300pF$. R_s and R_f respectively represent the footwear and flooring resistance to ground. The time taken for charge on the body to decay is given by the product $(R_s+R_f)C$. If either the footwear or flooring resistance is high, charge will be retained on the body.

Standards recommend a maximum resistance for footwear and flooring of 10^8 ohms. This gives a charge relaxation time of 0.06 seconds or less.

Can Electrostatic Discharges Occur?

There are four common types of electrostatic discharge (ESD) that need be considered from the point of view of ignition hazard. These are sparks, brush discharge propagating brush discharge and cone discharge. (Corona discharges may occur but are considered non-hazardous and are therefore not discussed here).

Sparks

Spark discharges are responsible for the majority of industrial fires and explosions caused by static electricity. Spark discharges will occur from conductive objects, surfaces and personnel, which are ungrounded and have become charged to an electrostatic potential. The energy (E) in a spark is expressed in Joules or more commonly millijoules (mJ) and can be calculated from the formula $E = \frac{1}{2}CV^2$ where C is the capacitance of the object and V is its potential. With the correct equipment both C and V can be measured and E can be calculated.

Flammable hydrocarbon vapours are extremely sensitive to spark ignition. A number of hydrocarbons have minimum ignition energies of 0.2 millijoules. A spark of this energy is often below human perception in terms of sight and sound.

In a plant, sources of spark energy will comprise metal sections including fixtures and fittings, which are ungrounded. They may also include personnel if their footwear and flooring are insulating, mobile and non-fixed items such as trolleys, metal drums, ancillary equipment, gauging equipment and hand tools. Once identified, this hazard can usually be simply remedied by providing a permanent conduction

path to ground. Recommendations for grounding mobile plant etc are repeated in all the relevant international standards.

Brush Discharges

Electrostatic brush discharges occur from charged non-conductive surfaces such as plastics and may even occur from highly charged non-conductive liquids such as hydrocarbon solvents and fuels. The incendivity (igniting power) of a brush discharge depends on a number of factors but energy content is limited to a theoretical maximum of 4 millijoules. Furthermore, since the theoretical limit of 4mJ applies to brush discharges they only represent an ignition hazard with flammable gases and solvents over part of their flammable range (refer to fig. 1).

Generally for brush discharges to present an ignition hazard, the following conditions must apply:

- the charged surface has a potential of 20kV or greater
- the polarity of charge on the surface is negative
- a flammable atmosphere exists at the point of discharge
- the energy content of the brush is greater than the minimum ignition energy of the flammable atmosphere.

The energy content of the brush will be dependant not only on the surface potential but also on the area of surface contributing to the discharge. Normally, since there is a maximum charge density that can be established on any surface, an area in excess of 100 cm² [13] is required to produce an ESD with sufficient energy to ignite a flammable hydrocarbon vapour. It is doubtful that brush discharges can ignite flammable dusts.

Important differences exist between brush discharges and sparks. The first is that since only part of a charged insulator contributes to the brush it is possible to obtain many discharges from a single large charged surface. Secondly, because of the low mobility of charge carriers, in an insulator, it is impossible to remove the charge by simply connecting to ground. The discharges themselves also vary significantly in the way the energy is released with brushes producing lower currents and consequently lower temperatures[14].

Propagating Brush Discharges

Propagating brush discharges (PBD's) can occur when an insulating material of up to around 8mm thickness has become highly polarised with electrostatic charge, i.e. positive charge on one face and negative charge on the opposite face. In industry PBD's may occur where large areas of insulating sheets are subjected to high levels of electrostatic charge generation (*note that both of these conditions are necessary*). More often than not these insulating sheets are in the form of a lining or layer, with an earthed metal backing. An example of this situation is a Teflon or glass-lined reactor vessel.

A photograph of a propagating brush discharge is shown in figure 6. In this case the discharge has occurred during high velocity fuel flow through a plastic pipe. Partial ignition of the fuel can be observed. This type of discharge event is high in energy and dangerous.

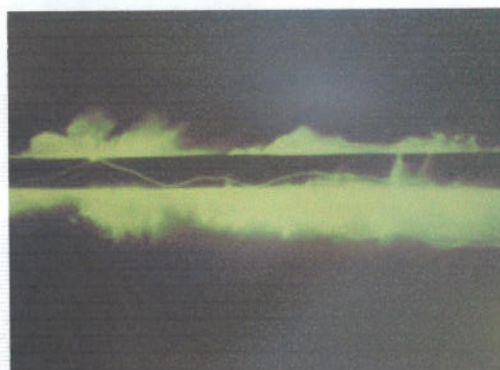


Figure 6. Propagating brush discharge from a plastic pipe conveying diesel fuel (photo courtesy J. F. Hughes, University of Southampton).

Cone discharge

Cone discharges are sometimes referred to as 'bulking brush discharges' and occur across the surface of bulked powder in storage silos, containers and hoppers. They can also occur deep within the powder heap.

Conditions for cone discharges are a charged powder of resistivity exceeding 10^{10} ohms. In grounded metal silos the discharges travel radially towards the silo wall across the surface of the powder cone during filling and may have an effective energy of up to 20mJ. Particle size and charge density will both affect the resultant ESD energy. Large vessels produce higher

energies and cone discharges are not normally observed in volumes below 1m³[15]. In some cases this type of electrostatic discharge has been initiated by adding solvent to a vessel containing charged dry granular product. This practice is clearly dangerous and should not be undertaken unless it is certain that the product is uncharged.

Is The Discharge Energy Sufficient To Cause Ignition?

It is possible for a sensitive flammable atmosphere and electrostatic discharges to coexist without ignition. If the discharge energy is increased, a threshold energy is eventually obtained, at which the discharge becomes incendiary, either partially or wholly through the volume of the flammable medium. This threshold energy is known as a minimum ignition energy (MIE) and is usually expressed in milliJoules (mJ). Typical values for flammable media are given below.

- Hydrogen 0.02mJ.
- Hydrocarbon vapours 0.2-2.0mJ.
- Fine flammable dusts 1-50mJ.
- Coarse flammable dusts 40-1000mJ.

Published MIE values should be used as a guide when undertaking an electrostatic hazard analysis and a margin of safety should always be included. Many flammable hydrocarbons in air have a minimum ignition energy below 1 milliJoule. This is so low that in practice no electrostatic discharges at all can be tolerated in such atmospheres. Hydrogen, carbon disulphide and oxygen-rich hydrocarbon mixtures are particularly sensitive to electrostatic ignition and require special precautions.

Brush discharges, which are limited in energy, will present an ignition hazard in the presence of hydrocarbon gases and vapours and possibly hybrids but are unlikely to ignite dust clouds. Ignition of an industrial dust by an electrostatic brush discharge has yet to be demonstrated despite the fact that some fine dry powders may have a minimum ignition energy as low as 1 mJ.

Due to their higher energy content, propagating brush discharges and cone discharges can ignite dust clouds. Sparks from ungrounded conductors however remain the most common source of electrostatic ignition in industry [16].

Figure 7 shows propane gas from a test probe being ignited by a brush discharge from a flexible intermediate bulk container (FIBC). The charging mechanism in this case is the FIBC being emptied of charged polystyrene pellets.

The ignition probe test has been developed to evaluate antistatic FIBC designs (often denoted as 'Type C or D') for use in potential flammable atmospheres. Since it is impossible to eliminate ESD's completely with these items, emphasis is placed upon limiting the igniting power of the discharge to a safe level.



Figure 7. Propane ignition by brush discharge from an FIBC.

Concluding remarks

Virtually all manufacturing processes which involve sensitive flammable materials will contain some of the elements necessary for an electrostatic ignition hazard to exist. More often than not the process runs trouble free - the generation and accumulation of electrostatic energy is unseen and discharges if they occur may be low in energy and remain unnoticed. A simple change in the properties of the materials, process or operating procedures however may be all that is necessary to complete the chain between charge generation and ignition. The consequences of an ignition are of course often catastrophic.

History has demonstrated that a plant may run trouble free for decades and then for no immediately apparent reason experience a series of fires. In the battle against static electricity it is important to be vigilant and to carefully consider the consequences of any changes to material, plant and process. If in doubt, expert advice should be sought.

References.

1. Lewis B. & von Elbe G., 'Combustion, Flames and Explosions of Gases', ISBN 0 12 446751 2, 1987
2. Hearn G. L., Wolfson Electrostatics Report No.301B/GLH for Western Mining Corporation, July 2002
3. Burgoyne J. H. & Cohen L., Proc. Royal Soc. A225, 375, 1954
4. ANSI/NFPA 68 'Venting of deflagrations' 1988 National Fire Protection Assoc., USA.
5. ANSI/NFPA 77, 'Static Electricity', 1988 National Fire Protection Assoc., USA.
6. Cartwright et al. IEEE Trans. IAS IA-21, 541, 1985
7. Wolfson Electrostatics Unit, 'Guidelines on the Electrostatic Hazards During Pneumatic Conveying and Storage of Powders', J. Loss Prev. Process Ind., Vol. 4, July 1991
8. Kinzing, G.E., 'Electrostatic Effects in Pneumatic Transport: Assessment, Magnitudes and Future Direction', J. Pipelines, 4, 95-102, 1984
9. British Standard 5958 Parts 1 & 2, 1991
10. Felici N. J. Journal of Electrostatics, 15, 291-297 (1984).
11. Hearn G. L., 'Electrostatic ignition hazards arising from fuel flow in plastic pipelines', J. Loss Prev. in the Proc. Ind. 15 (2002) 105-109.
12. Cross J. et al. 'Electrostatic Hazards from Pumping Insulating Liquids in Glass Pipes' Proc. 3rd Int. Conf. on Static Electricity, Grenoble, 1997.
13. Gibson N., & Lloyd F. C., 'Incendivity of Discharges from Electrostatically Charged Plastics', Brit. J. Appl. Phys., Vol. 16, 1965.
14. Smallwood J. & Hearn G. L., 'A wide bandwidth probe for electrostatic discharge measurements' Electrostatics 2003, Ins. Phys Conf. Ser.
15. Britton, G., 'Avoiding Static Ignition Hazards in Chemical Operations', ISBN 0 8169 0800 1, 1999.
16. Cross, J., 'Electrostatics Principles, Problems & Applications', Adam Hilger ISBN 0-85274-589-3, 1987.



Graham Hearn is a senior member of staff in the Electrical Power Engineering Research Group at the University of Southampton and Technical Director of Wolfson

Electrostatics. He directs research projects at the University and acts as consultant to industry in the fields of electrical and electrostatic hazards. Since 1981 he has undertaken professional consulting in 24 countries including Europe, North America, Gulf States, Pacific rim & Australia. Further information on the activities of Wolfson Electrostatics can be found on the web at www.soton.ac.uk/~wolfson

Copyright © G L Hearn 2002. This article must not be reproduced either in full or part without the consent of the author.